


**METAL COMPLEXES OF
5-ARYL-1-PHENYL-4-PENTENE-1,3-DIONES
AND 6-ARYL-5-HEXENE-2,4-DIONES**

*Thesis submitted to the Faculty of Science,
University of Calicut in partial fulfilment of the
requirements for the Degree of **Doctor of Philosophy** in Chemistry*

By

MATHEW PAUL UKKEN

**SEPTEMBER 2002
DEPARTMENT OF CHEMISTRY
UNIVERSITY OF CALICUT
KERALA - 673 635
INDIA**


16/07/02

DECLARATION

I hereby declare that the thesis bound herewith is an authentic record of the research work carried out by me under the supervision of Dr. K. Krishnankutty, Professor, Department of Chemistry, University of Calicut, in the partial fulfilment of the requirements for the Degree of Doctor of Philosophy in Chemistry of the University of Calicut and further that, no part thereof has been presented before for any other Degree.



Mathew Paul Ukken

CERTIFICATE

This is to certify that the Thesis bound herewith is an authentic record of the research work carried out by Mr. Mathew Paul Ukken, under my supervision in partial fulfilment of the requirements for the degree of Doctor of Philosophy in Chemistry of the University of Calicut, and further that no part thereof has been presented before for any other degree.



Dr. K. Krishnankutty
(Supervising Teacher)

ACKNOWLEDGEMENT

I express my heartfelt gratitude and deep indebtedness to my supervising teacher, Dr. K. Krishnankutty, Professor of Chemistry, University of Calicut, for his inspiring and intellectual guidance, healthy criticism, unfailing support, reliable encouragement and whole-hearted co-operation throughout the course of this investigation. I am happy to place on record the love, care and simplicity of the great teacher scholar that made me confident in taking up and completing this investigation.

Doing research in the Department of Chemistry has benefited from the helpful advice and inspiration of Dr. M.P. Kannan, Head of the Department of Chemistry, University of Calicut. I gratefully acknowledge all the support that has extended to me in my project. I sincerely appreciate the whole hearted co-operation and help extended by the teaching and non-teaching staff, Department of Chemistry, University of Calicut.

I wish to extend my thanks to Dr. A.D. Joy, Agricultural University, Mannuthy, for the instrumental facilities extended to me for analysis. I am grateful to Dr. Sasikumar of Schering-Plough Research Institute, New Jersey for providing spectral data. I am extremely thankful to Dr. Balakrishnan K.V. of the Chemistry Department, Calicut University for valuable suggestions and help in thermogravimetric studies.

My thanks are due to RSIC, CDRI, Lucknow, RSIC, IIT, Mumbai, RSIC IIT, Madras and RRL Thiruvananthapuram.

I am extremely thankful to a host of friends and fellow research scholars at Calicut University, especially to Sri. V.D. John, Sri. Muhammed Basheer

Ummathur, Smt. Malini P.T., Smt. Preeji Ranjith and Smt. Sayudevi, P. for their timely help and co-operation.

I express my sincere thanks to the Principal and Manager, Christ College, Irinjalakuda for deputing me for the research work and also to UGC for providing me teacher fellowship under FIP. I would like to acknowledge my gratitude to my teachers and colleagues of Chemistry Department, Christ College, Irinjalakuda for their valuable advice and timely help during the tenure of my study.

I am also grateful to my mother, wife and son for their enthusiastic support in my career advance.

My sincere thanks to M/s Bina Photostat and Microtech Computer Centre, Chenakkal for their wonderful job in processing the manuscript.

Finally a word of thanks to the Almighty God for his blessings during this investigation.

Mathew Paul Ukken

P R E F A C E

Coordination Chemistry is one of the fascinating and rewarding field of modern chemical science. Realisation of the involvement of metal complexes in biological systems has also helped immensely to sustain a live interest in metal chelates of multidentate ligands. The β -dicarbonyls and their metal complexes still serves as the starting material for the design and synthesis of numerous important compounds having diverse applications. Recently, the pharmacological importances of several naturally occurring β -dicarbonyl compounds have been discussed. One of the best known examples is curcuminoids, the active chemical constituent of turmeric. In curcuminoids the diketo function is directly attached to olefinic groups. Metal complexes of curcuminoids are also known to possess several biological properties. However, such biologically important β -dicarbonyl compounds and their metal complexes have not received as much attention as they deserve. In the present investigation two new types of unsaturated 1,3-diketones and their metal complexes are considered. A series of 6-aryl-5-hexene-2,4-diones (6-arylhexanoids) and 5-aryl-1-phenyl-4-pentene-1,3-diones (5-aryl-1-phenyl-4-pentanoids) and their metal complexes have been synthesised and characterised using various analytical and spectral techniques. Certain biological properties of some of these compounds have also been examined.

The thesis is divided into three parts.

Part I is a **general introduction** which highlight the importance of various aspects in coordination chemistry of β -diketones. The salient structural characterisations of metal 1,3-diketonates are included. Need for further investigation particularly on structural features of β -diketones have been indicated importance in the present investigation have been stated.

Results of the present study are presented in **Part II**. For convenience this part is divided in two chapters based on the nature of substituents in the aryl ring of the 6-aryl hexanoids and 5-aryl-1-phenyl-4-pentanoids. Each chapter is further divided into section 1 and section 2. Synthesis and characterisation of 6-aryl hexanoids and their metal complexes are presented in **Chapter I** Section 1. Uv, ir, ^1H nmr and mass spectral data clearly indicate the existence of the compounds entirely in intramolecularly hydrogen bonded cis-enol form. The compounds function as monobasic bidentate ligand in their $[\text{ML}_2]$ complexes ($\text{M} = \text{Cu}^{+2}$, Ni^{+2} , Co^{+2} , VO^{+2} and Fe^{+3}) was also established from the spectral data. In these metal complexes the ligand moiety is bonded to metal ion through the dicarbonyl oxygens to form a six membered chelate ring. In Chapter II Section 2 the synthesis and characterisation of 6-aryl hexanoids containing different substituents are considered. Uv, ir, ^1H nmr and mass spectral evidence show that the compounds exist in internally hydrogen bonded enolic form. The direction of enolisation being

towards the cinnamoyl function. In metal chelates, the metal ion replaced the enol proton with the formation of a six membered metal chelate ring in which both oxygens of the dicarbonyl function are involved. The esr studies of some copper complexes are also discussed in this chapter. Thermogravimetric analysis of some metal complexes are also included. The results of the biological studies (antibacterial and antifungal) also presented.

Details on the synthesis and characterisation of the α,β -unsaturated 1,3-diketones, 1-phenyl-5-aryl-4-pentanoids and their metal complexes are considered in **Chapter II Section 1**. The uv, ir, ^1H nmr and mass spectral data of the compounds unequivocally showed the presence of intramolecularly hydrogen bonded enol form. The stoichiometry and nature of bonding of the $[\text{ML}_2]$ chelates are established on the basis of various physicochemical and spectral data. A novel product formed during condensation of pyridine-3-aldehyde with benzoyl acetone has been characterised as a 2,4,6-triketone. The 1:1 metal complexes of the compound have also been synthesised and characterised using uv, ir, ^1H nmr and mass spectral data.

Chapter II Section 2 includes the synthesis and characterisation of 5-(substituted aryl)-1-phenyl-4-pentanoids and their metal complexes. The uv, ir, ^1H nmr and mass spectral data agrees with the $[\text{ML}_2]$ stoichiometry for the complexes. The esr studies of some copper complexes are also given.

Thermogravimetric analysis of some compounds and their Cu^{+2} , Ni^{+2} , Co^{+2} and Fe^{+3} complexes are discussed. The results of the biological studies (antifungal and antibacterial) carried out are also presented in this part of the thesis.

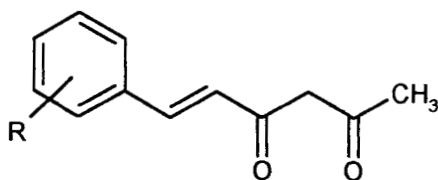
In Part III references are given in serial order.

The work described in this thesis has partially been published/accepted/communicated for publication are listed below.

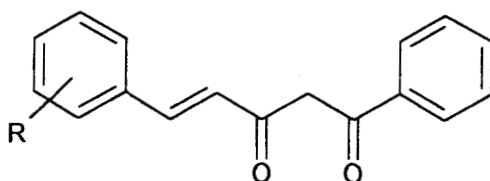
1. "Synthesis and characterisation of Co(II), Ni(II) and Cu(II) complexes of some 6-aryl-5-hexene-2,4-diones". Asian Journal of Chem. Vol. 14, No.2 (2002), 949-956.
2. "Metal complexes of some conjugated 1,3-diketones". Asian Journal of Chemistry, Vol. 14, No.2 (29002), 943-948.
3. "Metal chelates of 5-aryl-1-phenyl-4-pentene-1,3-diones". Asian Journal of Chemistry, Vol. 14, Nos. 3-4 (2002), 1335-1340.
4. "Metal chelates of 5-(aryl substituted)-1-phenyl-4-pentene-1,3-diones" (to be communicated).
5. Synthesis and characterisation of Cu(II), Ni(II) complexes of 4,8-diphenyl-7-(pyridin-3-ylmethylene)-4-octene-2,6,8-trione (to be communicated).

Nomenclature and Abbreviations

In the present investigation both the systematic and trivial names are used wherever necessary. The two types of 1,3-diketones considered in the present study are systematically named as 6-aryl-5-hexene-2,4-diones (**1**) and 5-aryl-1-phenyl-4-pentene-1,3-diones (**2**). For brevity and better readability these compounds are designated generally as 6-arylhexanoids and 5-aryl-1-phenyl-4-pentanoids.



1



2

Important abbreviations used in the thesis are:

Ar	aryl group
A	frequency factor
BM	Bohr Magneton
dmf	dimethylformamide
dmsO	dimethyl sulfoxide
E	activation energy
FAB	Fast atom bombardment
Fig.	figure(s)
h	hour
Hz	Hertz
J	Coupling constant
L	deprotonated ligand
LSM	Least square method
M	Central metal ion in a metal complex
M.P.	Melting point
OAc	acetate
ph	phenyl group
ppm	parts per million
py	pyridine
tlc	thin layer chromatography
TG	Thermogravimetry
ϵ	molar extinction coefficient
μ_{eff}	effective magnetic moment in Bohr magnetus
γ	correlation coefficient
ΔS	entropy of activation

CONTENTS

	Page
<i>Preface</i>	i
<i>Nomenclature and abbreviations</i>	v

PART I GENERAL INTRODUCTION

Coordination chemistry of β-diketones	1
Tautomerism of β -diketones	3
Classification of metal β -diketonates	6
Structural characterisation of metal complexes of 1,3-diketones	19
Application and use of metal complexes of β -diketones	23

PART II METAL COMPLEXES OF 5-ARYL-1-PHENYL-4-PENTENE- 1,3-DIONES AND 6-ARYL-5-HEXENE-2,4-DIONES

Materials, Instruments and Methods	30
------------------------------------	----

CHAPTER I SYNTHESIS AND CHARACTERISATION OF 6-ARYL-5-HEXENE-2,4-DIONES AND THEIR METAL COMPLEXES

Section 1 : Synthesis and characterisation of 6-Aryl-5-hexanoids and their metal complexes

Synthesis of the 6-Aryl-5-hexene-2,4-diones	36
Synthesis of metal chelates	38
Results and discussion	38
Characterisation of 6-aryl-5-hexene-2,4-diones	40
Characterisation of metal chelates of 6-aryl-5-hexene-2,4-diones	50

Section 2 : Synthesis and characterisation of 6-(substituted aryl)-5-hexene-2,4-diones and their metal complexes	
Synthesis of the 6-(substituted aryl)-hexanoids	70
Synthesis of metal chelates	71
Results and discussion	71
Characterisation of 6-(substituted aryl)-hexanoids	73
Characterisation of metal chelates of 6-(substituted aryl)-hexanoids	89
ESR studies	104
Thermogravimetric studies	117
Biological studies	136
CHAPTER II SYNTHESIS AND CHARACTERISATION OF 5-ARYL-1-PHENYL-4-PENTENE-1,3-DIONES	
Section 1 : Synthesis and characterisation of 5-Aryl-1-phenyl-4-pentanoids and their metal complexes	
Synthesis of 5-aryl-1-phenyl-4-pentene-1,3-diones	145
Synthesis of metal complexes	146
Results and discussion	147
Characterisation of the 5-aryl-1-phenyl-4-pentanoids	148
Characterisation of metal chelates	161
Characterisation of the condensation product of pyridine-3-aldehyde with benzoylacetone and its metal complexes	173
Section 2 : Synthesis and characterisation of 5-(substituted aryl)-1-phenyl-4-pentene-1,3-diones and their metal complexes	
Preparation of 5-(substituted aryl)-1-phenyl-4-pentanoids	187
Preparation of metal complexes	188
Results and discussion	188

Characterisation of metal chelates	201
ESR spectra	220
Thermogravimetric studies	230
Biological studies	240

PART III

REFERENCES	245
-------------------	-----

GENERAL INTRODUCTION

Mathew Paul Ukken “Metal complexes of 5-aryl-1-phenyl-4-pentene-1,3-diones and 6-aryl-5-hexene-2,4-diones ” Thesis. Department of Chemistry , University of Calicut, 2002

PART I
GENERAL INTRODUCTION

GENERAL INTRODUCTION

Coordination Chemistry of β -diketones

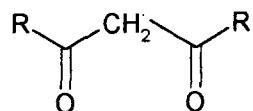
There has been a welcome renaissance in inorganic chemistry after the celebrated coordination theory of Alfred Werner.¹ The Werner's theory has been refined and extended greatly. New Synthetic techniques and convergence of structural methods of investigation, together with great theoretical advances have made coordination chemistry as a self consistent field in modern scientific studies. The growth of interest in coordination chemistry has been further stimulated by far-reaching developments in many fields including chemical analysis, catalysis, metal winning, the technology of dyes and pigments and through the realisation of the vital role of metal complexes in biology where much progress has been made during the last few decades.

As a consequence of the ability of coordinated metal ion to influence many of the complex reactions upon which the vital processes of living organisms depends, coordination compounds of many varieties are found widely distributed in nature. Several synthetic metal complexes which mimic the behaviour of complicated biomolecules are known and at present the study of such compounds are receiving much attention. Although the results obtained so far do not always

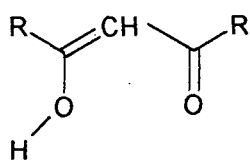
parallel those in nature, a knowledge of the chemistry is being built up and the biochemical role of metal ions in natural systems is beginning to be better understood.

The properties, structure and applications of metal complexes are dependent on the nature of the metal ion and the ligands attached. The variation in metal ions is considerable; on the other hand variation in ligands is virtually limitless, thanks to the ingenuity of synthetic organic chemists. Literature reveals that ligands based on certain important structural types such as azo, azomethines, hydrazones, diketones, etc. have proliferated much during recent years. This trend is evident from the reports of hundreds of ligand systems based on β -dicarbonyl compounds and allied derivatives.²

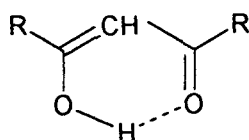
The 1,3-dicarbonyl compounds still serve as the starting material for the design and synthesis of a large number of compounds having wide application in many fields. This is not unexpected of these compounds because proton transfer and hydrogen bonding are two important aspects of the chemistry that governs the behavior and structure of many simple and complex molecules starting from water to DNA.^{3,4,5,6} The 1,3-diketones exhibit both these features and are highly efficient in complex formations with various metal ions. Therefore studies on diverse types of 1,3-diketones and their metal complexes have considerable importance in present day coordination chemistry. **The present investigation is mainly on the synthesis and characteristics of a new series of 1,3-diketones in which the diketo function is directly attached to olefinic groups.** Therefore

Cis conformers

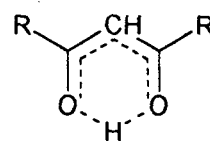
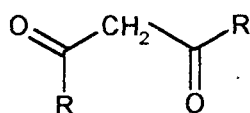
U; cis diketo; Z, Z



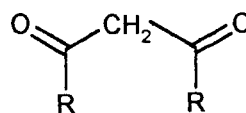
U; open cis enol; Z, Z*



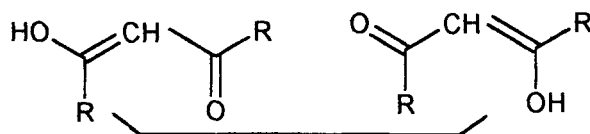
U; cis enol; Z, Z; Cs*

U; cis enol; Z, Z; C_{2v}**Trans Conformers**

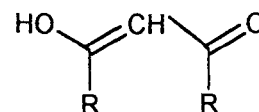
S; trans diketo; E, Z*



W; trans diketo; E, E



S; trans enol; E, Z*



W; trans enol; E, E*

*distinguishable by extra conformers in asymmetric

Fig. 1. The conformers of β -diketones, R-CO-CH₂-CO-R

For an unsymmetrical β -diketone, the nature of possible conformers increases further. There are several ways of naming these various conformers such as U/S/W/ or E/Z. But since in reality only a limited number of conformers exist, the *cis* and *trans* are used to indicate conformers that have an intramolecular hydrogen bond and those that have not. The keto and enol tautomers prefer a *cis* conformation and a *syn (cisoid)* conformation. The presence of a methyl group on the α -carbon destabilizes the *cis* enol relative to the *trans* and the latter can then be observed even in neutral, nonpolar solvents.³

Within the β -diketone system three types of proton transfer can be distinguished.

- i) The relatively slow exchange between the vinylic CH and the enol OH sites, that is the keto \leftrightarrow enol tautomerism, which takes hours, even days, to reach equilibrium.
- ii) The rapid exchange of the labile proton between OH groups on different molecules which is too fast to be distinguishable even by ^1H nmr spectroscopy under normal conditions
- iii) The extremely rapid transfer of the proton from one oxygen of the *cis* enol tautomer to the other, that is, the oscillation of the proton between the two minima of the potential energy well of the OHO hydrogen atom.

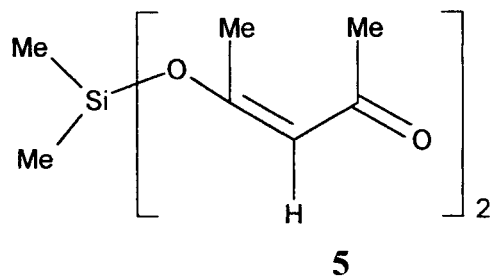
It has been generally accepted that the enolic form is favoured in nonpolar solvents, and simultaneous conjugation and chelation through hydrogen bonding is responsible for the stability of the enol tautomers.

The proportion of the enol tautomers generally increases when an electron withdrawing group for example chlorine is substituted for hydrogen at an α -position in β -diketones. The enolization also increases^{11,12} when the compounds are fluorinated or contain an aromatic ring. Substitution by a bulky group (eg. alkyl) at the α -position tends to produce steric hindrance between R-group protons particularly in the enol tautomer, and this together with inductive effects of the alkyl groups often brings about a large decrease in the enol ratio.¹³⁻¹⁵ No enolization is possible if both the hydrogen atoms of the α -carbon atom are substituted.

Classification of metal β -diketonates

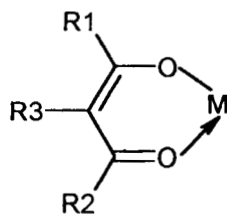
The coordinating ability of 1,3-diketones was recognised as early as in 1887 when Combes⁷ reported the synthesis of beryllium acetylacetonate. This was followed by the pioneering work of Werner¹, Morgan^{8,16,17} and Sidgwick^{18,19} who confirmed the bifunctional chelating characters of β -dicarbonyl compounds. Being powerful chelating agents, the diketonate anions form complexes with virtually all the transition and main group metal and metalloid elements. Literature on 1,3-diketones and metal 1,3-diketonates are so voluminous that even an attempt to

tetrahedral environment. The stability of this complex has been explained on the basis of diffuseness of the d-orbitals of silicon.



b) β -Ketoenolate as bidentate ligand

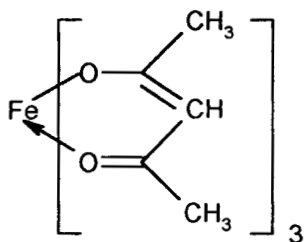
This is the usual mode of bonding of β -diketones. A metal cation replaces the enolic hydrogen with the formation of a six-membered chelate ring **6**. Delocalization of the electron cloud in the resultant chelate ring has been established on the basis of various physico-chemical characteristics, to endow it with a certain amount of aromatic character.



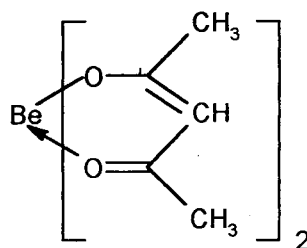
6

Since the enolate ion carries a single negative charge, metal atoms can react with one or more enolate ions to give either neutral or charged molecules depending on the co-ordination number (m) and valency (n) of the central metal atom. This type of bonding give rise to three different types of complexes.

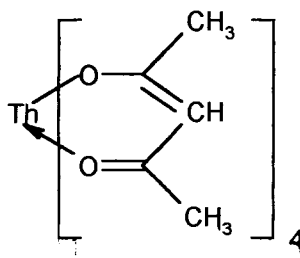
(i) When $m = 2n$, the metal β -diketonate so formed behaves as a neutral molecule. Common examples of this class of compounds^{9,10,26-29} are given in structure as 7-9.



7



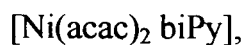
8



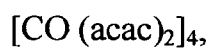
9

In these compounds the metal ions are coordinatively saturated, show predominantly covalent behavior, soluble in common organic solvents and are volatile.

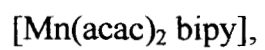
(ii) When $m > 2n$, the complexes so formed behaves as lewis acids and achieve the desired coordination either by polymerization or by adduct formation. For example metal β -diketonates of types given in structures **10-13**.



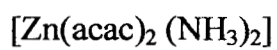
10



11

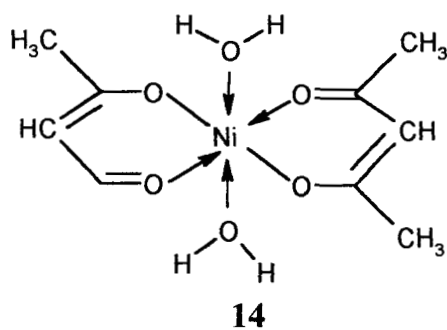


12

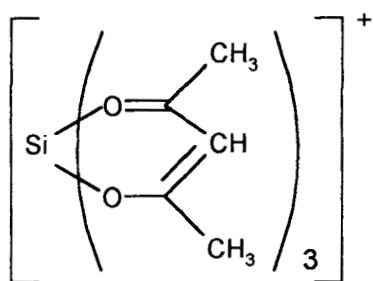


13

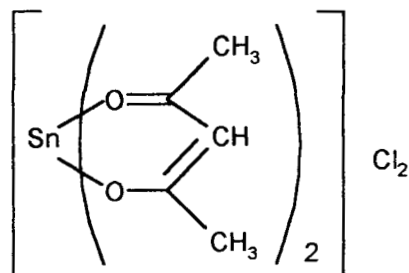
The structure of $\text{Ni}(\text{acac})_2 \cdot 2\text{H}_2\text{O}$ is



(iii) When $m < 2n$, complexes of the type **15-19** are well known in literature.

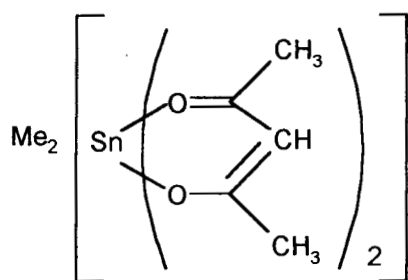


15

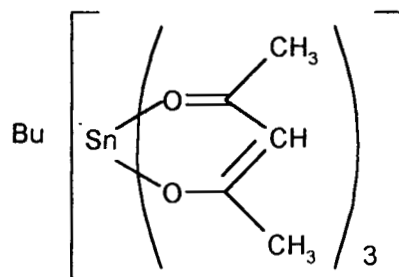


16

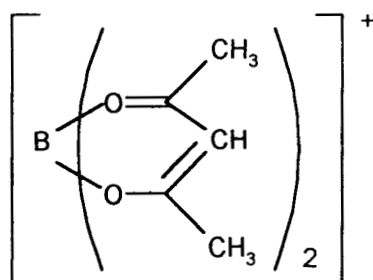
12



17



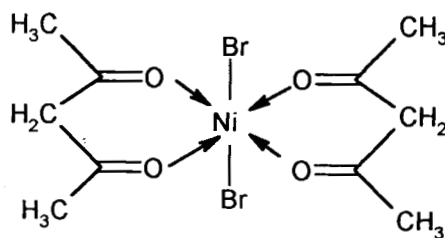
18



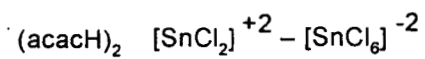
19

c) Neutral bidentate coordination

Although complexes in which both carbonyl groups of the β -diketones act as donor atoms are rather rare, several examples like **20,21** are well known.^{31,32}



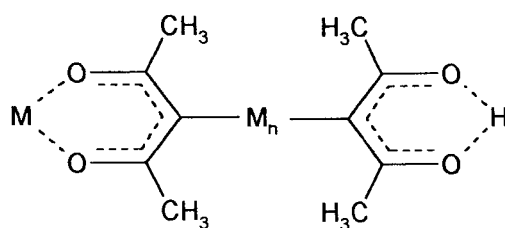
20



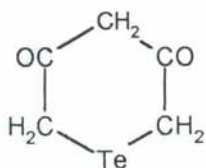
21

2) Carbon bonded complexes

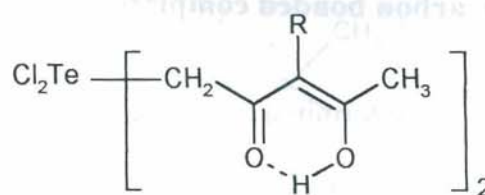
The terminal as well as the central carbon bonded β -diketone complexes are now well established. Elements such as sulphur, selenium, tellurium, gold, etc. form well defined complexes in which the alkyl and methine carbon atoms are involved in bonding. The metal carbon bonds in these complexes are quite stable, as is apparent from their reported methods of preparation. Typical examples³³⁻³⁵ are given in structure 22-25.



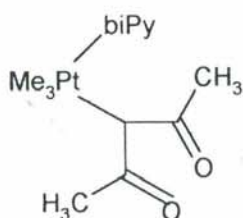
(M = S; n = 1, 2; M = Se, n = 2)



23



24



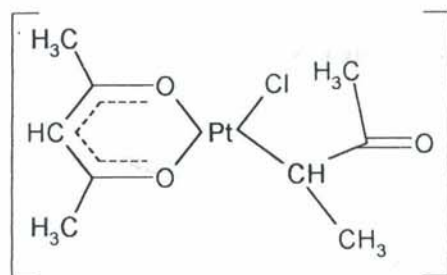
25

 $L_3 A_u (A)$
 $(A = \text{acac}, \text{bzac};$
 $L = \text{Ph}_3\text{P}, \text{Ph}_2\text{EtP}, \text{Et}_3\text{P}$

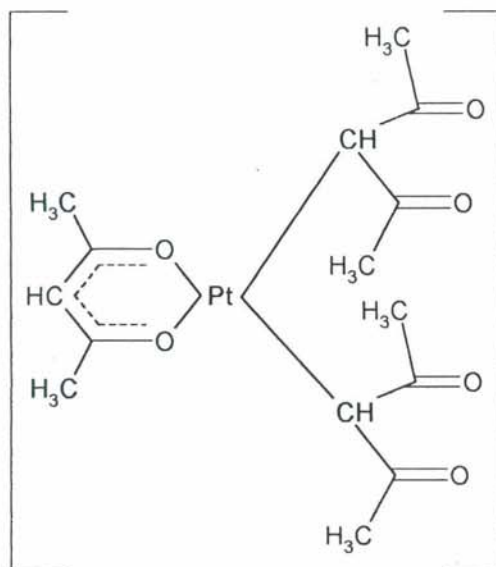
26

3) Both carbon-bonded and oxygen-bonded complexes

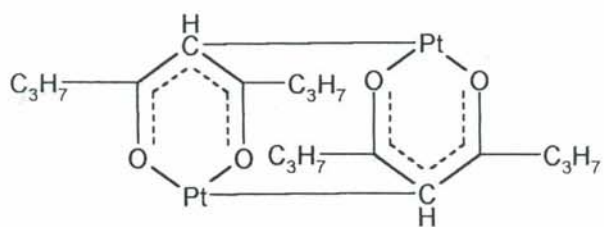
Complexes in which the metal ion is bonded to β -diketone in such a way that one ligand moiety always bonds to the metal through carbonyl oxygens while another β -diketone through the methylene carbon atom are also quite common. Examples of this class of compounds^{33,36} are shown in structures 27-29. These stable complexes are generally coloured and are soluble in common organic solvents.



27



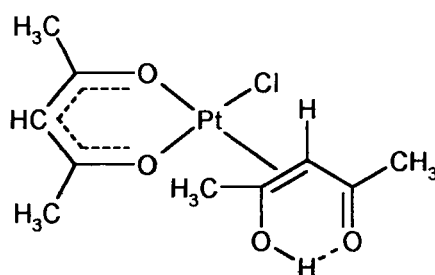
28



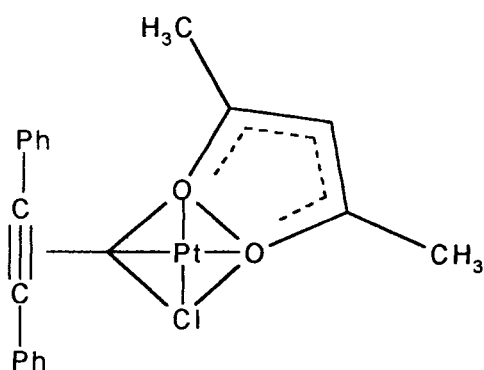
29

4) Olefin bonded complexes

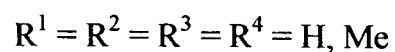
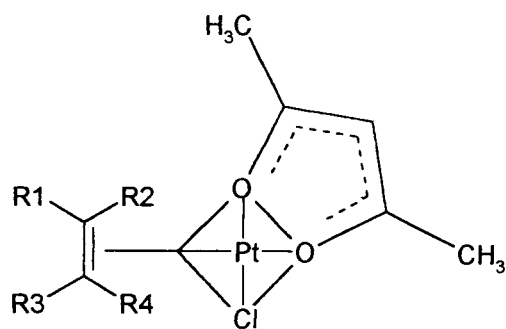
Metal complexes of the β -ketoenol tautomer of 1,3-diketone in which the olefinic $>C=C<$ system bonded to metal ion have also been synthesised and characterised. Typical complexes in this category^{30,37,38} are given in structures 30-32.



30



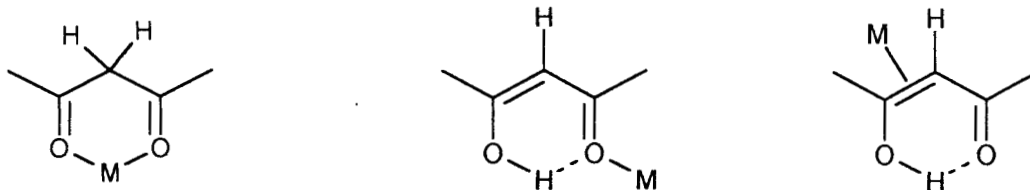
31



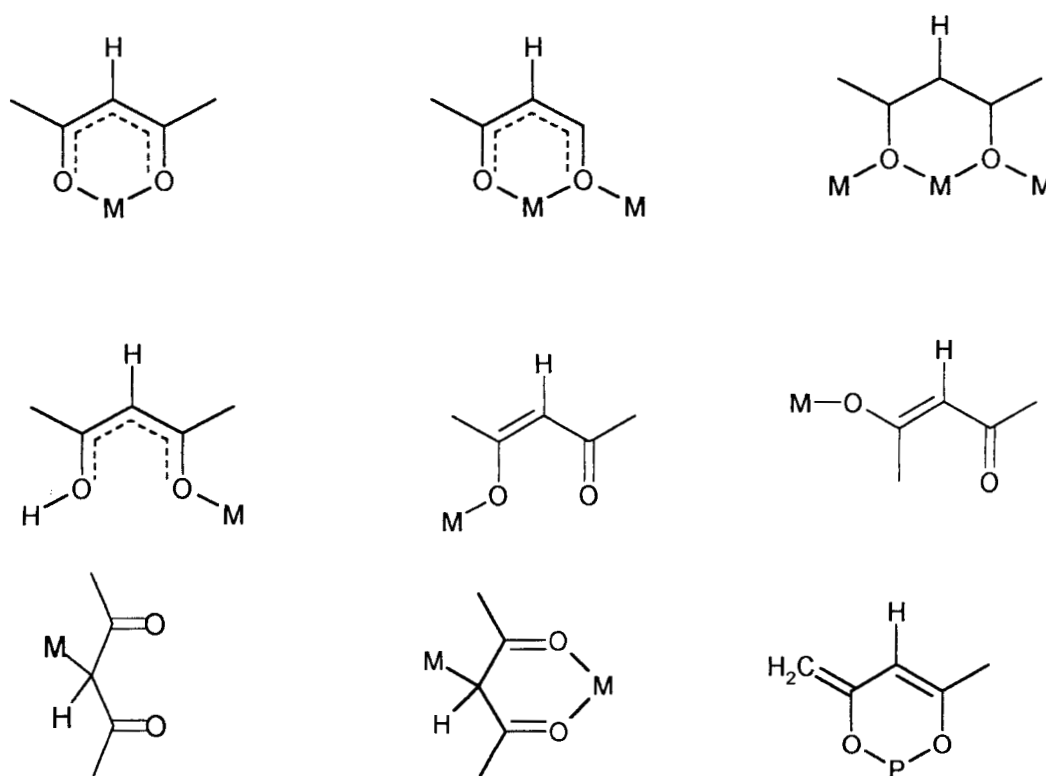
32

The diverse types of coordination modes of this versatile class of ligand systems can also be summarised²² as in figure 2.

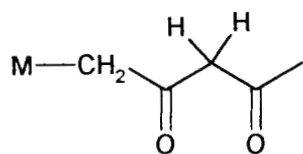
i) Neutral molecule



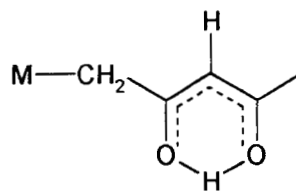
ii) Mono anion



contd....



and



iii) Dianion

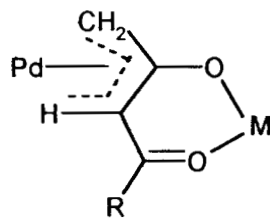
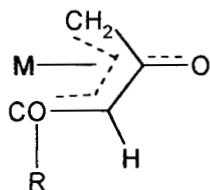
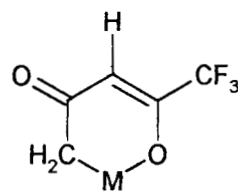
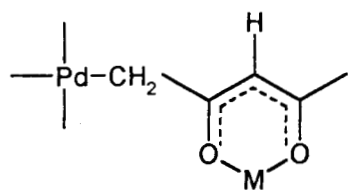
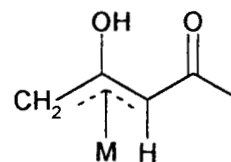
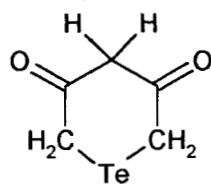
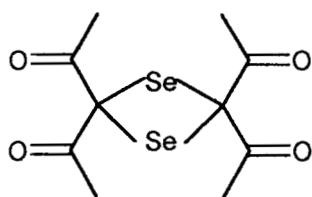


Fig. 2. Different bonding modes of β-diketones

Structural characterisation of metal complexes of 1,3-diketones

Virtually all most all spectral methods apart from the usual physio-chemical techniques have been employed in studying various type metal derivatives of β -diketones. Thus electronic spectral data together with magnetic properties have been extensively used in determining the geometry of the complexes, IR spectral data and NMR chemical shift in determining the nature of bonding, X-ray diffraction studies in fixing the correct disposition of the complexes, mass spectroscopy in the structural elucidation and electron spin resonance studies for a better understanding of the nature of bonding in β -diketone complexes. Thermogravimetric studies have been used for characterising complexes and in evaluating kinetic and thermodynamic parameters; metal ligand formation constants and stability constants for indicating the increase in stability of the enolic form and for identifying the *cis-trans* configuration in chelates. Some of these techniques are briefly mentioned below.

Electronic spectra

An extensive study of the electronic spectra of acetylacetonate complexes was reported by Holm and Cotton.³⁹⁻⁴⁶ The strong absorption band appearing at $\sim 34700\text{cm}^{-1}$ has been assigned to $\pi\text{-}\pi^*$ transition. The SCF and LCAO-MO calculations each place the lowest allowed transition near 33500 cm^{-1} in 1,3-diketonate anion for ionic metal complexes. The second transition occurs near

49500 cm^{-1} in copper(II) 1,3-diketonate complexes.⁵³ This band has been assigned to $\pi_3 \rightarrow \pi_6$ while the SCF result⁵⁴ corresponds to a $\phi_3 \rightarrow \phi_5$ transition.

IR spectra

Vibrational spectroscopy coupled with isotopic labelling has extensively been used to detect the exact tautomeric nature of 1,3-dicarbonyl compounds.⁴⁷⁻⁴⁹ 1,3-diketones such as acetylacetone, benzoylacetone, etc. have been shown by chemical and spectroscopic methods to exist as tautomeric diketo and enol forms related by a 1,3-hydrogen shift.^{67,68} The characteristic carbonyl band of the enol form of acetylacetone appeared at 1613 cm^{-1} and that of diketo form at ~ 1712 and ~ 1725 cm^{-1} . Of the $3n-5$ vibrational modes possible the $\nu_{\text{O-H}}$, $\nu_{\text{C-O}}$ and $\nu_{\text{C-C}}$ are highly significant. The enolic OH stretching absorption is usually seen as a broad band at 2700-3000 cm^{-1} presumably due to its involvement in strong intermolecular hydrogen-bonding.^{51,52} In general, upon complexation, the carbonyl stretching frequency of 1,3-diketones shows a shift (10-50 cm^{-1}) to lower values and additional bands due to $\nu_{(\text{M-O})}$ vibrations appear in the region 400-500 cm^{-1} .

NMR Spectra

The ^1H and ^{13}C nmr spectra of a wide variety of diamagnetic metal 1,3-diketonates have been reported. It has been shown that the position and nature of splitting of the signals depends on the mode of the coordination, nature of the substituents and the extend of delocalisation in the chelate ring.⁵⁵⁻⁶¹ The cis enol

proton chemical shift, δ (OHO)/ppm of β -diketone and β -ketoaldehyde enol tautomers of general formula $R^1COCH(R'')COR^{111}$ have been reported.⁶² Nonhebel⁶³ showed that the bulky substituents on the α and β - sites not only shifted δ (OHO) down field but produced a sharper line. An ingenious proof that the proton of the hydrogen bond was not a double minimum was advanced by Shapet'ko.⁶⁴ The change in the chemical shift between the resonance of hydrogen bonding proton in the 1H nmr spectrum and that of the hydrogen bonding deuteron in the 2H nmr spectrum has been shown to be a good indicator of the type of potential energy well⁶⁵ in which the proton or deuteron is confined.

X-ray and Neutron diffraction studies

Among the first β -diketones to be investigated by X-ray methods were the *m*-chloro and *m*-bromo derivatives of dibenzoyl methane.⁶⁶⁻⁶⁸ More sophisticated x-ray analysis gave a better idea of the position of the proton and several structural determinations carried out using this diffraction method have been able to describe the cis enol hydrogen bond in terms not only of R (O...O) but also of R (O-H) and R (H- - O).

Mass spectra

The potential of mass spectroscopy in the structural elucidation of coordination compounds has been demonstrated.⁶⁹⁻⁷¹ Mass spectra of a series of metal acetylacetonates have been rationalized in terms of ion reaction by

Macdonald and Shammon.⁷² The most intense peaks in the spectra are usually derived from the monomeric forms of the complexes, but in a number of cases ions derived from a dimer or even trimer have been observed. These studies confirm the influence of the odd- or even electron character of an ion on its dissociation reactions (Mac Lafferty⁷³) and provides additional evidence⁶⁹⁻⁷¹ that odd-electron ions can be changed to even electron ions and vice versa, by change of valency of the metal atom in the ions.

Thermogravimetric studies

Thermal analysis is now established as an invaluable and rapid method for the characterisation of materials and evaluation of kinetic and thermodynamic parameters over a wide range of temperatures. This technique can be used to determine the factors such as rate constant, activation energy, order of reaction, frequency factor, phase equilibria, enthalpy of transition, specific heat, etc. Now it has been developed as a primary source of information concerning the solid state thermal decomposition (heterogeneous kinetics).

Eisentraut and Sievers reported that the thermogravimetric technique can be a powerful tool for comparing the relative volatilities of a group of β -diketonates. By examining thermograms, it has been generally possible to gather information regarding volatility changes upon substitution of various groups in β -diketone chelates.

Applications and use of metal complexes of β -diketones

Great interest in the study of metal complexes of β -diketones has been stimulated by their potential application in areas such as nmr, shift reagents,^{13,74} laser technology (laser chelates),⁷⁵⁻⁷⁷ gas chromatography,⁷⁸ polymer industry, chemical catalysis, and in various biochemical fields.⁷⁹ The expected application of 1,3-diketonate chelates in photocatalysis, as "uv stabilizers" and as laser chelates has motivated the study of their photochemical and photophysical properties. The use of sensitizers has opened up a new research area for the study of photochemistry of 1,3-diketonate chelates. Metal complexes of β -diketones have been used as fuel additives,⁸⁰ as supercritical fluids for waste clean up,⁸¹ in super conducting thin film manufacturing⁸² and in production of homogeneous and heterogeneous catalysts.^{83, 84}

The application of certain coordinatively unsaturated lanthanide chelates called "shift reagents" for nmr spectral elucidation has become an extremely useful technique to organic chemists. Use of metal β -diketonate like $\text{Cr}(\text{acac})_3$, $\text{Eu}(\text{fod})_3$, $\text{Pr}(\text{fod})_3$, etc., in ^{13}C nmr spectra of metal carbonyl compounds has been found to be very useful. Rare earth metal β -diketonates are also used as potential laser materials. Metal β -diketonates are useful in the determination of trace metals in biological system by gas chromatography. Fluorinated β -diketones (such as trifluoroacetylacetone and 2-thenoyltrifluoroacetone) are especially useful in the

solvent extraction of metals as the fluoromethyl group increases the acidity of the enol form.

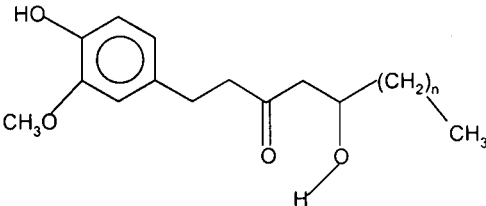
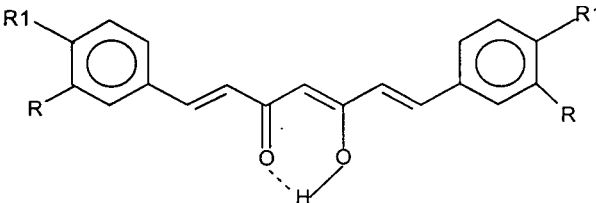
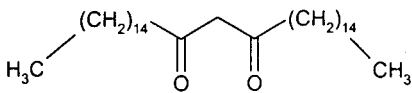
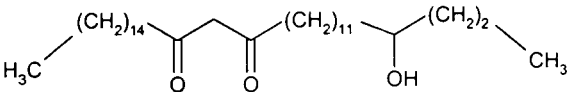
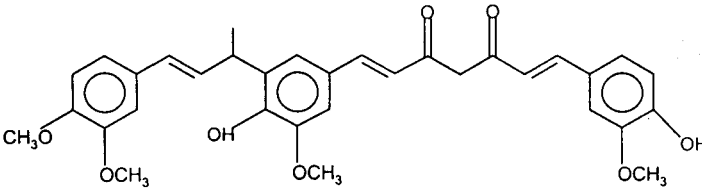
Iron(II) and iron(III) chelates of β -diketone have been proposed as catalysts for the removal of hydrogen sulfide from natural gas.⁸⁵ The use of β -diketonate complexes of scandium, yttrium and some f-block elements in effectively scrubbing H₂S from a gas stream have also been reported.⁸⁵

Extensive literature is available on the synthesis, characterisation and diverse types of applications of 1,3-diketones and their metal complexes. However, most of these studies are on 1,3-diketones in which the carbonyl groups are directly linked to different alkyl/aryl groups. It is to be pointed out that only very few reports¹⁶⁹ are available on such studies based on β -diketones in which the diketo function directly attached to olefinic groups. These types of 'unsaturated' 1,3-diketones are of considerable importance in view of the fact that the active components present in several medicinal plants have this type of structure. Some of these biologically active components of plant origin that contains dicarbonyl group are brought out in table 1.

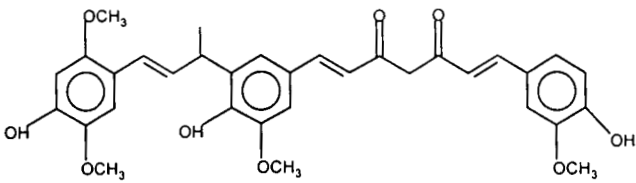
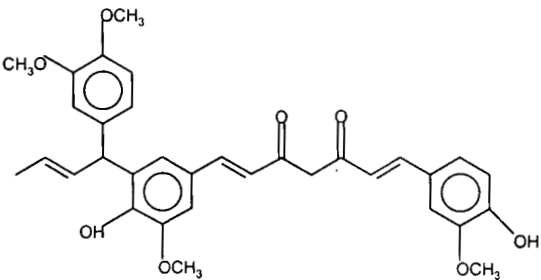
Among compounds given in table I, curcuminoids, the active chemical components present in turmeric possess several interesting aspects which are related to the present study. In the indigenous system of medicine of the orient, turmeric (*Curcuma longa* Linn., *Zingiberaceae* family) has been employed since

Table 1

Active constituents of some common spices and medicinal plants

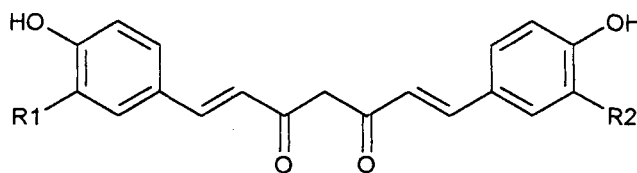
Spice (Plant species)/ Active principle	Structure
Ginger (<i>Zingiber officinale</i>) Gingerols	 <p style="text-align: center;">n = 2, 4, 6 and 8</p>
Turmeric (<i>Curcuma longa</i>) Curcuminoids	
Eucalyptus (<i>Eucalyptus globulus</i>) n-Tritriacontan-16,18-dione	
4-Hydroxy-tritriacontan-16,18-dione	
Indonesian medical ginger (<i>Zingiber cassumunar</i>) Cassumunin A	

contd...

Spice (Plant species)/ Active principle	Structure
Cassumunin B	 <p>The chemical structure of Cassumunin B is a symmetrical polyphenolic compound. It features a central 1,5-diketone chain (heptane-2,6-dione) with two trans-alkene groups at the 3 and 7 positions. Each alkene is substituted with a 3,4,5-trimethoxyphenyl group. The central chain also has a methyl group at the 4 position.</p>
Cassumunin C	 <p>The chemical structure of Cassumunin C is a polyphenolic compound similar to Cassumunin B. It features a central 1,5-diketone chain (heptane-2,6-dione) with two trans-alkene groups at the 3 and 7 positions. Each alkene is substituted with a 3,4,5-trimethoxyphenyl group. The central chain also has a methyl group at the 4 position. Additionally, there is a 3,4,5-trimethoxyphenyl group attached to the 2 position of the central chain via a propyl side chain.</p>

time immemorial.⁸⁶ Turmeric enjoys the reputation as an antiinflammatory agent, as a carminative, diuretic and blood purifier as well as a remedy against jaundice. It is also recommended for use against common cold, cough, leprosy, affections of the liver and among other indications in the treatment of ulcers.^{87,88} These effects are ascribed to the yellow pigment, curcumin isolated from the plant. The active chemical constituent of the pigment has been characterised as curcuminoids.

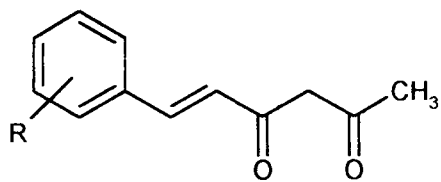
Several recent reports available on the broad spectrum of beneficial physiological activities of curcuminoids and their metal complexes⁸⁹⁻¹⁰² particularly in cancer treatment. A number of synthetic analogues of these curcuminoids and their metal complexes were also reported to possess enhanced activity than the curcuminoids isolated from turmeric. Structurally curcuminoids are group of 1,3-diketones in which the diketo function is directly attached to olefinic groups (33-35). Systematically these compounds are 1,7-diaryl-1,6-heptadiene-3,5-dione.



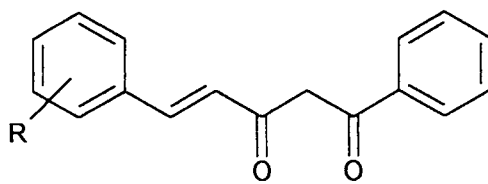
	R1	R2
33	O CH ₃	O CH ₃
34	O CH ₃	H
35	H	H

In these compounds both the carbonyl groups are attached to olefinic groups. The various biological activities of these compounds have been attributed to the highly conjugated dicarbonyl functions as well as on the nature and position of the substituents on the aryl rings. The biochemical activities of the metal complexes are also reported to be dependent on these structural factors apart from the nature of the metal ion. In order to reveal the structural influence of a biologically important compound, it is necessary to synthesis related compounds having restricted structural variations. The present study is an attempt in this direction.

In curcuminoids and allied compounds both the carbonyl groups are linked to olefinic function. The synthesis, structural studies and coordination behaviour of a number of these type of 1,3-diketones have appeared recently. However only one or two reports exist on such unsaturated 1,3-diketones in which only one of the carbonyl group is linked to olefinic groups. These types of studies have tremendous importance in establishing the structural relationship of biologically important molecule. **The present study is an attempt in this direction. Therefore in this investigation a new series of unsaturated 1,3-diketones, in which only one of the keto group linked to an olefinic group and their metal complexes are considered. Thus synthesis, characterisation and biological activity of two series of such unsaturated 1,3-diketones of the type 36, 37 and their metal complexes are considered in this study.**



36



37

SYNTHESIS AND CHARACTERISATION OF 6-ARYL-5-HEXENE-2,4-DIONES AND THEIR METAL COMPLEXES

Mathew Paul Ukken “Metal complexes of 5-aryl-1-phenyl-4-pentene-1,3-diones and 6-aryl-5-hexene-2,4-diones ” Thesis. Department of Chemistry , University of Calicut, 2002

PART II

METAL COMPLEXES OF 5-ARYL-1-PHENYL-4-PENTENE-1,3-DIONES AND 6-ARYL-5-HEXENE-2,4-DIONES

Materials, Instruments and Methods

Materials

All chemicals used were of 'Analar' grade. Commercial solvents were purified by the methods recommended in literature^{104,105} and were used for various physical and physico-chemical measurements.

The metal salts used for the synthesis of metal complexes were nickel(II) acetate tetrahydrate, cobalt(II) acetate tetrahydrate, copper(II) acetate monohydrate, iron(III) chloride and oxovanadium(IV) sulphate.

Only compounds isolated analytically pure are reported in this Thesis. All the compounds reported in this Thesis are stable and have good keeping qualities. Compounds for recording spectra were recrystallised from proper solvents several times till chromatographically pure (tlc) materials were obtained.

Instruments

Instruments used in this investigation are

1. UV-1601 Shimadzu recording spectrophotometer.
2. Shimadzu 8201 PC FTIR spectrophotometer.
3. Jeol 400 nmr spectrometer.
4. Jeol Sx-102(FAB) mass spectrometer.
5. Heraeus Carlo Erba 1108 elemental analyzer.

6. Perkin Elmer 2380/Atomic absorption spectrophotometer.
7. TGA V5.1A Dupont 2100 system.
8. Varian E 112 ESR spectrometer
9. Systronic pH meter
10. Toshniwal conductivity bridge.
11. Gouy type magnetic balance.

Methods

Elemental analysis: Metal percentages of the complexes were analysed by standard methods¹⁰⁶ and by AAS after decomposing them with perchloric acid-nitric acid mixture. Carbon, hydrogen and nitrogen percentages reported are by micro analysis carried out at RSIC, Central Drug Research Institute, Lucknow.

UV-visible spectra were recorded from solution (10^{-3} M) of compounds in ethanol unless otherwise mentioned. Infrared spectra of compounds were recorded with KBr pellets.

¹H nmr spectra were recorded using CDCl₃/dmsO-d₆ as solvents and TMS as internal reference.

FAB mass spectra were recorded at room temperature using Argon (6 KV, 10 mA) as the FAB gas, and *meta*-nitrobenzyl alcohol (NBA) as the matrix. The probable matrix peaks were located at m/z 136, 137, 154, 289 and 307. If metal

ions such as Na^+ are present these peaks may be shifted accordingly. ESR spectra (X-band) were recorded at 77K in glassy state between 8.5-9.5 GHz and calibrated with diphenylpicryl hydrazil (DPPH) free radical for which $g = 2.0036$.

Thermal analysis were carried out in an atmosphere of N_2 , at a constant heating rate of $10^\circ\text{C min}^{-1}$ and $\sim 5\text{mg}$ of sample size were employed for each study.

pH measurements (accuracy ± 0.05) were made after calibrating with potassium hydrogen phthalate solution at $28 \pm 0.1^\circ\text{C}$.

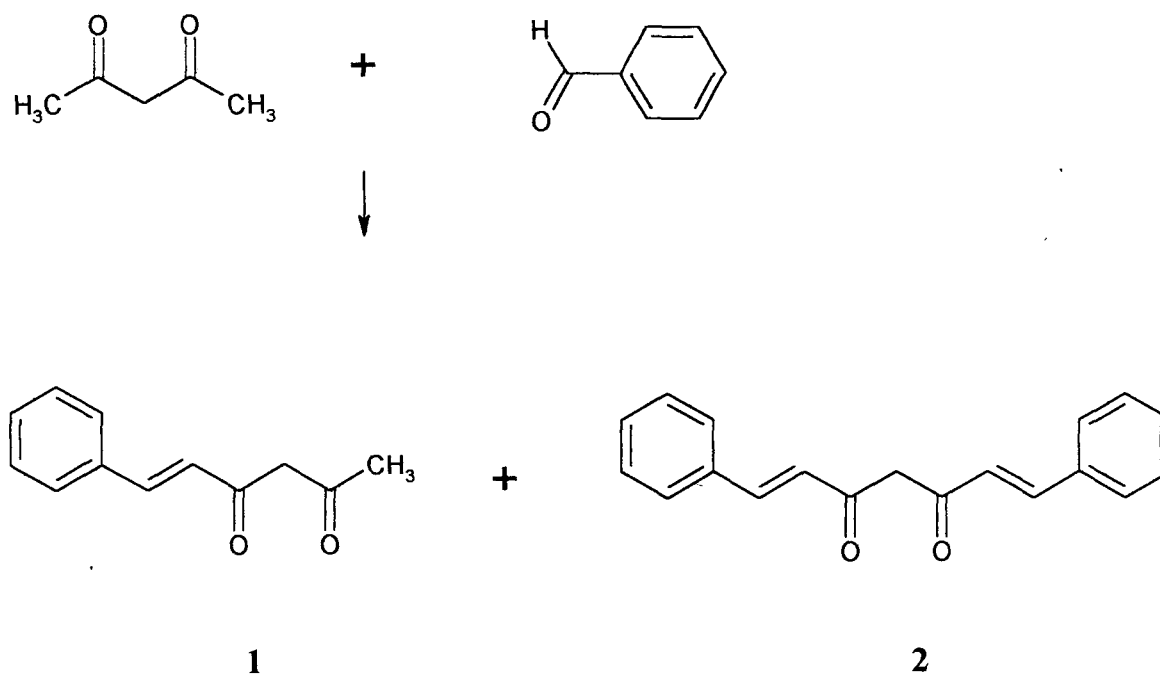
Molar conductance¹⁰⁷ of the complexes were determined in dmf at $28 \pm 1^\circ\text{C}$, using solution of about 10^{-3}M . Magnetic susceptibility was determined at room temperature ($28 \pm 1^\circ\text{C}$) using $\text{Hg}[\text{Co}(\text{NCS})_4]$ as standard on a Gouy type balance.

CHAPTER I

**SYNTHESIS AND CHARACTERISATION OF
6-ARYL-5-HEXENE-2,4-DIONES AND THEIR
METAL COMPLEXES**

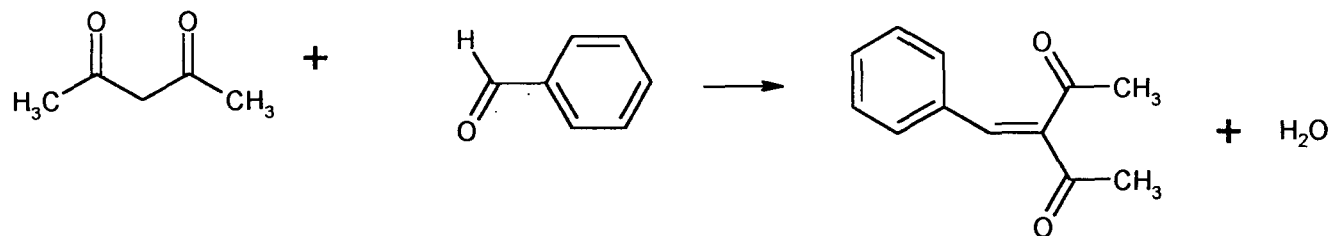
Synthesis and characterization of 6-aryl-5-hexene-2,4-diones and their metal complexes

Reaction of aromatic aldehydes with 1,3-diketones such as acetylacetone in presence of boric oxide, tributyl borate and n-butylamine usually leads to unsaturated 1,3-diketones **1** and **2** as illustrated¹⁰³ in the reaction scheme 1.1.



Scheme 1.1

The use of boric oxide and tributyl borate is to prevent the condensation of the aldehyde at the methylene carbon of the diketone. That is to avoid Knoevenagel type condensation as in scheme 1.2.



Scheme 1.2

The relative yield of formation of **1** and **2** depends to a large extent on the temperature of the condensation reaction. At temperature about 30°C the predominant product is **2**, nearly 50-75% yield. However at ice cold temperatures **1** is the major compound formed together with small amounts of **2**. Though mixture of products are formed, both compounds of the types **1** and **2** are unsaturated 1,3-diketones. This method is an efficient synthetic route for 1,3-diketones in which olefine linkage(s) directly attached to the diketo function. The present investigation is mainly on compounds of the type **2** in which one of the carbonyl group is directly bonded to olefinic linkage. By varying the nature of the aryl groups it is possible to prepare unsaturated 1,3-diketones having diverse properties. In this study a series of such compounds having different aryl groups have been prepared and characterised. Typical metal complexes of these compounds are also studied from a structural point of view. For convenience this chapter is divided into two sections. **Section 1** is on the 6-aryl hexanoids having

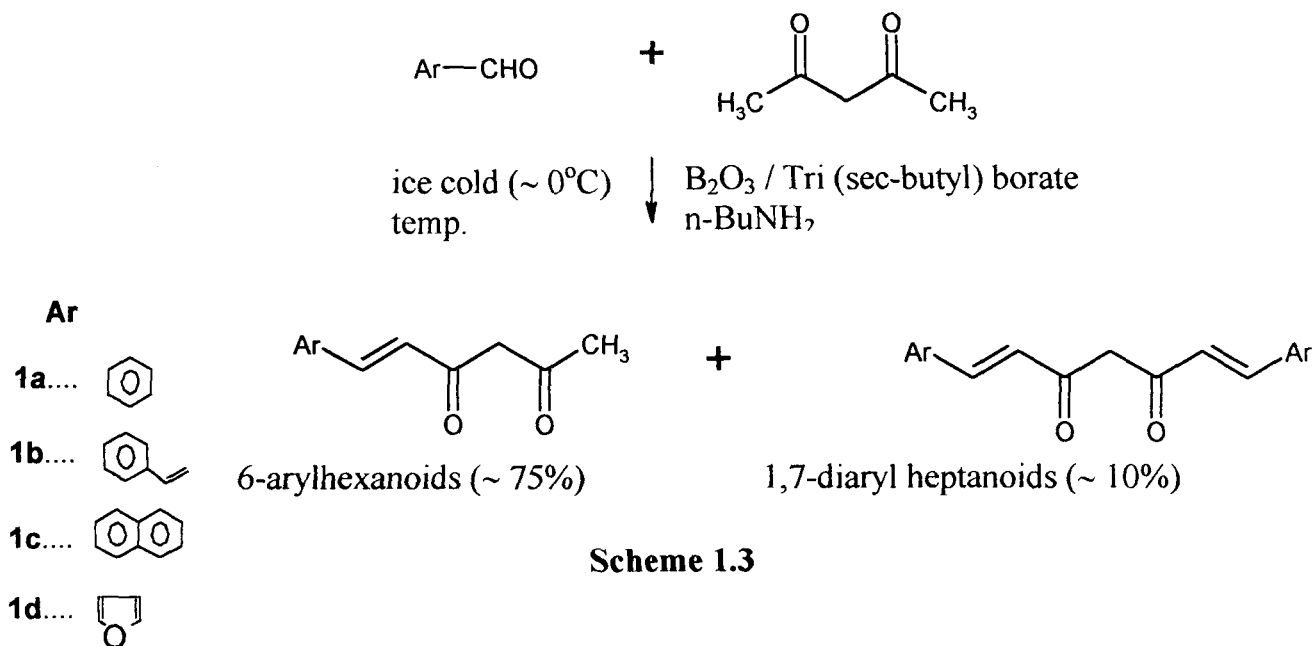
different aryl groups such as phenyl, cinnamoyl, naphthyl and furyl. Details on the synthesis and characterisation of a series of phenyl substituted 6-arylhexanoids and their metal complexes are given in **Section 2**.

Section 1

Synthesis and characterisation of 6-aryl-5-hexenoids-2,4-diones and their metal complexes

Synthesis of the 6-aryl-5-hexene-2,4-diones

The 6-aryl-5-hexene-2,4-diones were prepared by the condensation of aromatic aldehydes (benzaldehyde/cinnamaldehyde/napthaldehyde/furfural) with acetylacetone under specified conditions. The reaction leads to a mixture of products as given in the reaction **scheme 1.3**. The 6-arylhexanoid is the major product under the reaction condition which can be separated by column chromatography. A typical synthetic procedure is given below.



Acetylacetone (0.075 mol, 7.5 g) mixed with boric oxide (0.055 mol, 3.75 g) suspended in dry ethyl acetate containing tri-(*sec*-butyl)borate (0.1 mol, 23 g) was stirred for ~ 1 h. To this mixture kept at 0°C, a solution of the aromatic aldehyde (0.025 mol) in dry ethylacetate (15 ml) together with *n*-butylamine (0.5 ml) were added dropwise during 90 min with constant stirring. The stirring was continued for an additional period of ~ 2 h and the solution was set aside overnight. The reaction mixture was then stirred for ~ 1 h with hot (~ 50°C) hydrochloric acid (0.04 M, 20 ml) and extracted repeatedly with ethyl acetate. The combined extracts were concentrated in vacuum and the 6-aryl-5-hexene-2,4-diones were separated by column chromatography as detailed below.

A silica gel (mesh 60-120) column (2 × 100 cms) was prepared and the concentrated extract was uniformly applied on top of the column and then eluted with a 5:1 v/v mixture of chloroform-acetone at a uniform flow rate of 2 ml per min. As the elution proceeds, two bands were developed in the column, a pale yellow lower band and an yellow to orange red upper band. The lower band is mainly 6-arylhexanoids and the upper band 1,7-diarylheptanoids. When the void volume has been run out, the yellow band comes down and the eluates were collected in aliquots of 10 ml in separate tubes and in each case the homogeneity was established by tlc. The combined eluates on evaporation give 6-aryl-5-hexene-2,4-diones (50-75%). The 1,7-diarylheptanoids (5-10%) can be eluted repeatedly as an orange yellow band retained in the upper portion of the column by using a 2:1

v/v mixture of chloroform and acetone. The isolated 6-aryl-5-hexene-2,4-diones were recrystallised from hot benzene to get chromatographically (tlc) pure material.

Synthesis of metal chelates

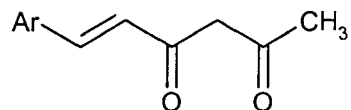
Copper(II), nickel(II), cobalt(II), oxovanadium(IV) and iron(III) complexes of the compounds were prepared by the following general method. To a refluxing solution of the diketone (0.002 mol) in methanol (15ml) an aqueous solution of the metal(II) acetate (0.001 mol, ~ 10ml) was added and the reaction mixture was refluxed for ~ 3 h and cooled to room temperature. In the case of Fe^{+3} and VO^{+2} complexes, ferric chloride and vanadyl sulphate respectively were used. The precipitated product was filtered, washed with water, then with ethanol and dried in vacuum.

Results and discussion

The aldehydes used for the synthesis of the 6-aryl-5-hexene-2,4-diones (**1a-d**) considered in this investigation are brought out in table 1.1. All the compounds are crystalline in nature with sharp melting prints and are freely soluble in common organic solvents. The yield and systematic names of the compounds are also included in table 1.1.

TABLE 1.1

Synthetic details of the 6-aryl-5-hexene-2,4-diones



Compounds	Aldehydes used for synthesis	Ar	Systematic name	Yield (%)
1a	Benzaldehyde		6-phenyl-5-hexene-2,4-dione	45
1b	Cinnamaldehyde		8-phenyl-5,7-octadiene-2,4-dione	70
1c	2-Naphthaldehyde		6-(2-naphthyl)-5-hexene-2,4-dione	60
1d	Furfural		6-(2-furyl)-5-hexene-2,4-dione	60

The elemental analysis data and observed molecular weight (Table 1.2) of the compounds suggests that only one equivalent of the aromatic aldehyde has condensed with one equivalent of acetylacetone.

Characterisation of 6-aryl-5-hexene-2,4-diones

uv spectra

The uv absorption maxima of 1,3-diketones depend on the degree of enolisation. The $n \rightarrow \pi^*$ absorption of the carbonyl chromophore occurs at higher wavelength when the factors predominate the percentage enol form.^{3,108-110} The presence of α,β -unsaturation also increases the wave length of the carbonyl absorption maxima. The 6-aryl-5-hexene-2,4-diones are typical α,β -unsaturated 1,3-diketones and their absorption maxima are significantly greater than those reported for simple saturated 1,3-diketones.^{111,112-115}

The uv spectra of the compounds in 95% ethanol (10^{-3} M) show two bands with $\lambda_{\max} \sim 290$ and ~ 380 nm. From a comparison of the reported spectra of related 1,3-diketones such as acetylacetone the low energy band at ~ 380 nm corresponds to the $n \rightarrow \pi^*$ transition of enolised dicarbonyl functions and the observed bathochromic shift of this band (table 1.2) can be correlated with extended conjugation and also to the nature of the aryl groups present. However the high energy band at ~ 280 nm due to $\pi \rightarrow \pi^*$ transitions of the fully conjugated system is only marginally influenced by different aryl groups .

TABLE 1.2

Physical, analytical and uv spectral data of the 6-aryl-5-hexene-2,4-diones

Compounds Molecular formula (formula weight)	Elemental Analysis (%) found/calculated		Colour	Yield (%)	M.P. °C	λ_{\max} nm	log ϵ
	C	H					
1a C ₁₂ H ₁₂ O ₂ (188)	75.52 (76.60)	6.27 (6.38)	yellowish brown	45	124	256 338	4.02 4.53
1b C ₁₄ H ₁₄ O ₂ (214)	78.5 (78.13)	6.54 (6.51)	yellowish red	70	82	284 388	3.9102 4.2113
1c C ₁₆ H ₁₄ O ₂ (238)	80.67 (80.33)	5.88 (5.85)	reddish brown	60	68	290 382	3.4161 4.2188
1d C ₁₀ H ₁₀ O ₃ (178)	75.59 (75.3)	5.62 (5.58)	Brown	60	140	291 321	3.562 4.4881

Infrared Spectra

1,3-Diketones such as acetylacetone, benzoylacetone, etc. exists as mixtures of tautomeric diketo and enol forms related by a 1,3-hydrogen shift.³ Acetylacetone with a boiling point of 140° exists to an extent of 81.4% in the enolic form.²² The characteristic carbonyl band of the enol form appeared at ~ 1613 cm⁻¹ and that of the diketo form at ~ 1712 and ~1725 cm⁻¹ where considerable interaction between the carbonyl groups exist.¹¹

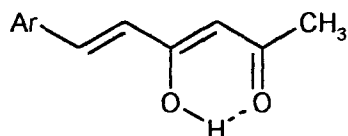
The six membered chelate ring has 3n-5 vibrational modes possible, the $\nu_{\text{O-H}}$, $\nu_{\text{C-O}}$ and $\nu_{\text{C-C}}$ are significant. The enolic OH stretching absorption is usually seen

as a broad band at 2700-3000 cm^{-1} presumably due to its involvement in strong intramolecular hydrogen bonding.

The position and intensity of the carbonyl stretching band depends on the molecular structure in its immediate vicinity and therefore very useful characterising the type of carbonyl function.^{3,48,51} Carbonyl stretching frequency of aroyl group ($\sim 1660 \text{ cm}^{-1}$) is much lower than that of an acyl group ($\sim 1710 \text{ cm}^{-1}$). A further shift to lower values can be observed in compounds where C=O is in conjugation with C=C. The enol tautomer of 1,3-diketones does not show the normal absorption of conjugated ketones. Instead a broad band appears in the region 1580-1640 cm^{-1} many times more intense than normal carbonyl absorption. This intense and displaced absorption results from strong intramolecular hydrogen bonding. The olefinic $\nu_{\text{C}=\text{C}}$ of the enol ring usually appears in the region 1540-1580 cm^{-1} . However, when aryl group(s) are present, it is very difficult to identify to the $\nu_{\text{C}=\text{C}}$ vibration as it is also the region where aromatic and conjugated systems absorb.

The 6-aryl-5-hexene-2,4-diones studied here are unsymmetrical 1,3-diketones similar to aroyl alkanoyl methanes, where the olefinic group(s) is/are interposed between the aryl and carbonyl group. The ir spectra of the compounds show two prominent bands at $\sim 1670 \text{ cm}^{-1}$ and $\sim 1630 \text{ cm}^{-1}$ assignable to the chelated acetyl and cinnamoyl $\nu_{\text{C}=\text{O}}$ vibrations. The observed position and

intensity of these bands indicate that the compounds exist entirely in the enol form and are enolised towards the cinnamonyl function as given below in **structure 1.1**.



1.1

The intense and broad band in the region $2800-3200\text{cm}^{-1}$ is undoubtedly due to the presence of strong intramolecular hydrogen bonding in these compounds which is also evident from the lowering of acetyl carbonyl stretching frequency. At least four prominent bands are observed in the region $1445-1575\text{cm}^{-1}$ mainly due to $\nu_{\text{C}=\text{C}}$ vibration. The medium intensity band at $\sim 980\text{cm}^{-1}$ is possibly arising from trans $\text{CH}=\text{CH}$ -absorption. The important ir bands and their probable assignments are given in table 1.3.

TABLE 1.3
 Characteristic ir data (cm^{-1}) of 6-aryl-5-hexene-2,4-diones 1a-d

1a	1b	1c	1d	Probable assignments
1669	1689	1690	1670	$\nu_{\text{C=O}}$ acetyl
1623	1630	1625	1630	$\nu_{\text{C=O}}$ cinnamonyl naphthyl
1575 1545	1579 1512	1577 1512	1568 1519	$\nu_{\text{C-C}}$ phenyl / alkenyl
1528	1425	1425	1470	ν_{asym} C-C-C chelate ring
1445	1392	1384	1361	ν_{sym} C-C-C chelate ring
1091 1062	1149 1070	1134 1045	1124 1090	$\beta_{\text{C-H}}$ chelate ring
980	985	970	954	$\nu_{\text{CH=CH}}$ trans
738	756	775	796	$\nu_{\text{C-H}}$ chelate ring

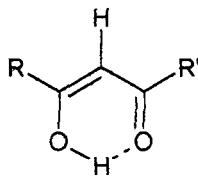
^1H nmr spectra

The ^1H nmr spectroscopy is perhaps the most important tool in studying the keto-enol tautomerism of 1,3-diketones.^{3,116-118} In the case of compounds having strong intramolecular hydrogen bonding the resonance signal of the proton generally is seen at the downfield region of the nmr spectrum with a broad nature. The integrated intensity of these enolic proton signal is an indication of the percentage of enol tautomer. The position of the methine proton signal, which is a characteristic property of the enol form, is influenced by the electronic effects of the groups attached to the carbonyl function.

Reported chemical shift of enolic and methine proton signals of a number of β -diketones are brought out in table 1.4. The data clearly indicate that the position of the enol and methine protons depends on the nature of the alkyl/aryl groups attached to the diketo function. Thus when methyl groups of acetylacetone is replaced by phenyl groups (benzoylacetone and dibenzoylacetone) the positions of both the enolic and methine protons shifted appreciably to low field presumably due to the increase in conjugation of the system.

TABLE 1.4

Characteristic ^1H nmr spectral data of some common β -diketones



R	R'	Chemical shift (δ ppm)	
		Methylene proton	Enolic proton
CH ₃	CH ₃	5.44	15.40
CH ₃	CF ₃	5.90	14.24
CF ₃	CF ₃	6.53	13.00
C ₆ H ₅	C ₆ H ₅	6.80	17.13
CH ₃	C ₆ H ₅	6.08	16.24
CF ₃	C ₆ H ₅	6.56	15.23
2-C ₄ H ₃ S	CF ₃	6.5	16.2

The ^1H nmr spectra of all the 6-aryl-hexanoids give a one proton singlet in the low field at $\sim \delta$ 16 ppm and another singlet at $\sim \delta$ 6.4 ppm due to the strong

intramolecularly hydrogen bonded enolic proton and to the methine hydrogen respectively of structure 1.1. The observed chemical shift of the enolic proton signal can be explained by the electronic and steric effects of the Ar-CH=CH- attached to the enolised carbonyl function. Influence of steric and electronic effects of the groups is also reflected in the positions of the methine proton signal.

The magnitude of coupling constant (J) for vicinal protons on the alkene function is dependent on their spatial geometry. As given by Karplus¹¹⁹ through empirical relations.

$$J_{\text{HH}'} = 10 \cos^2\theta; \quad 0^\circ \leq \theta \leq 90^\circ$$

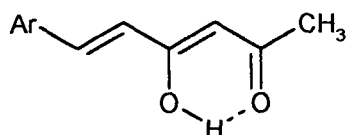
$$J_{\text{HH}'} = 16 \cos^2\theta; \quad 90^\circ \leq \theta \leq 180^\circ,$$

The magnitude of $J_{\text{HH}'}$ is influenced by the dihedral angle θ between their relative orientation planes as the coupling is mediated through the interacting orbitals within the bonding framework. The coupling constant for the *trans* hydrogens, where the dihedral angle of $\sim 180^\circ$, are > 14 Hz. In the *cis* double bonds, where the dihedral angle of $\sim 0^\circ$ coupling constants are usually < 10 Hz.

In the case of 6-aryl-5-hexene-2,4-diones, the alkenyl proton signals with the observed coupling constant of ~ 16 Hz suggest the *trans* nature of the olefinic double bond. The chemical shifts of various proton signals and their details are given in table 1.5. Integrated intensities of all the signals appeared in the spectra

are in agreement with the structure 1.1 of the compounds. Spectra of **1b** and **1c** are reproduced in figure 1.1 and 1.2.

TABLE 1.5
Characteristic ^1H nmr spectral data of 6-aryl-5-hexene-2,4-dione



Compounds of				Probable assignment chemical shift (δ ppm)
1a	1b	1c	1d	
16.19	15.90	15.85	--	enolic
7.91 (1H) 7.88 (1H)	7.51 (1H) 7.50 (1H)	8.66 (1H) 8.46 (1H)	7.48 (1H) 7.47 (1H)	alkenyl
7.49 – 6.86 (5H)	7.49 – 6.88 (5H)	8.41 – 7.11 (7H)	7.36 – 7.26 (3H)	aryl
6.44	6.05 (1H)	6.58 (1H)	6.68 (1H)	methine
2.50	2.41 (3H)	2.50 (3H)	2.41 (3H)	methyl

Mass spectra

Detailed mass spectral analysis of different types of 1,3-dicarbonyls are available.^{120,121} Nature of alkyl/aryl substituents attached to the carbonyl groups decides the fragmentation pattern. For example, CO and ketene ($\text{CH}_2=\text{C}=\text{O}$) elimination from the molecular ion is characteristic of acetylacetone, where as

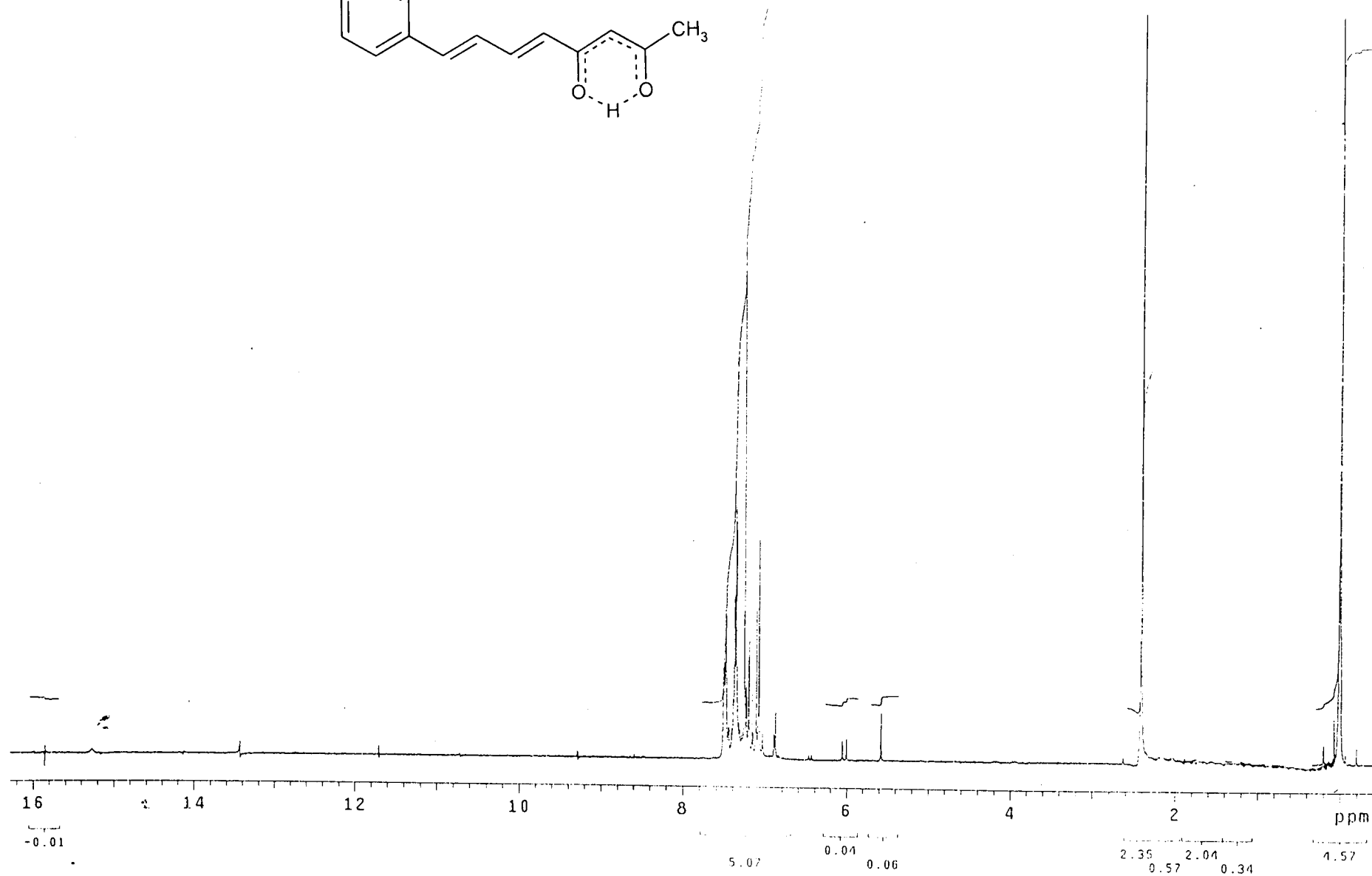
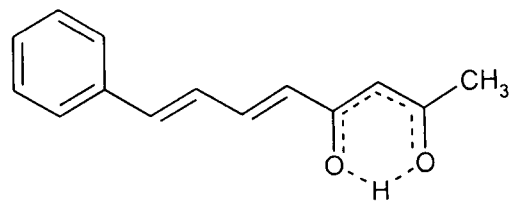
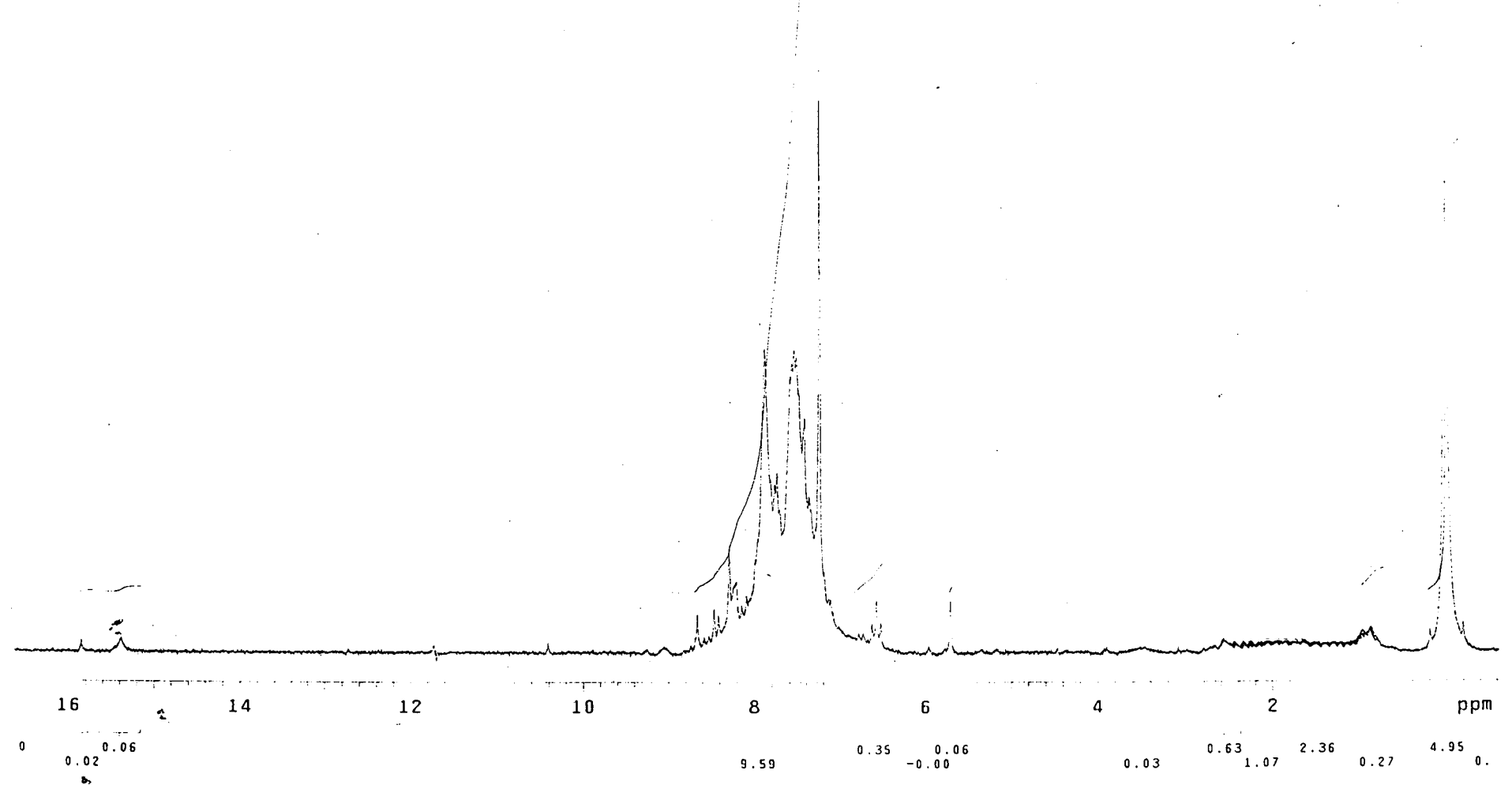
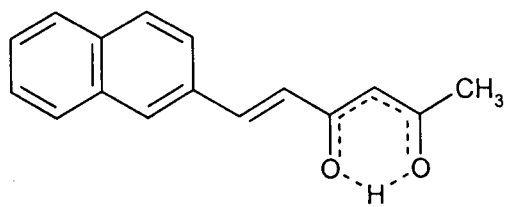


Fig. 1.1. ¹H NMR spectrum of 1b

117



49

Fig. 1.2. ¹H NMR spectrum of 1c

(P-CO)⁺ is absent in the spectra of benzoylacetone and dibenzoylmethane. Intense peaks due to the elimination of O, OH and C₃HO₂⁺ species from the molecular ion is the most characteristic feature of the mass spectra of 1,3-diketones having at least one aryl group.

All the 6-arylhexanoids show intense molecular ion peak and which is the most characteristic feature of the mass spectra of the compounds. The cleavage of the (-CH₂-CO-CH₃) fragment from the molecular ion explains the origin of the (P-57)⁺ peak, a typical feature of all the spectra. Other prominent peaks appeared in the spectra are due to (P-CH₃CO)⁺, (P-CH₃COCH₂CO)⁺, (P-CH₃)⁺, Ar-CH=CH⁺, Ar⁺, etc. The mass spectra for the compounds are given in figures 1.3-1.5. The formation of important peaks can be conveniently explained by the fragmentation pattern given in scheme 1.4.

Characterisation of metal chelates of 6-aryl-5-hexene-2,4-diones

The analytical and physical data of the metal complexes are given in table 1.6-1.11. The observed elemental analysis data of the chelates agree well with their 1:2 metal-ligand stoichiometry except for Fe³⁺ which are of 1:3 stoichiometry. All the metal complexes behaved as non electrolytes in dmf (specific conductance < 10 Ω⁻¹cm⁻¹ ; 10⁻³M solution) and do not contain the anion of the metal salt used for their preparation. Copper(II), cobalt(II), oxovanadium(IV) and iron(III) chelates showed a normal magnetic moment, while nickel(II) complexes are diamagnetic.

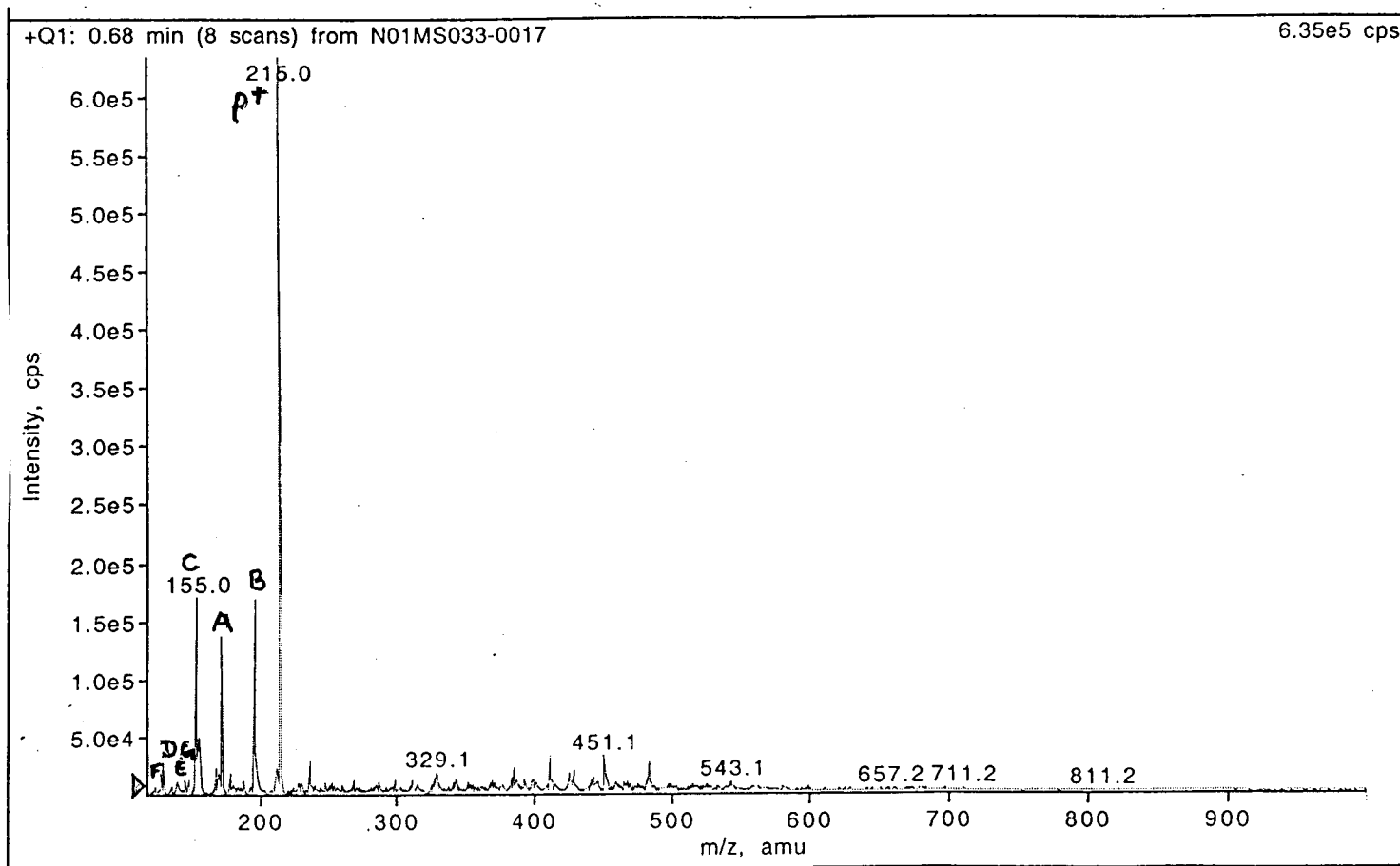
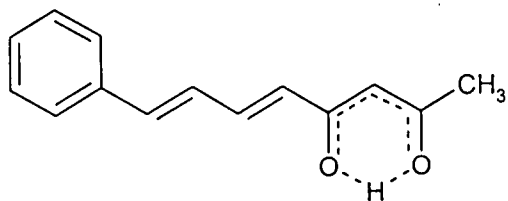


Fig. 1.3. Mass spectrum of 1b

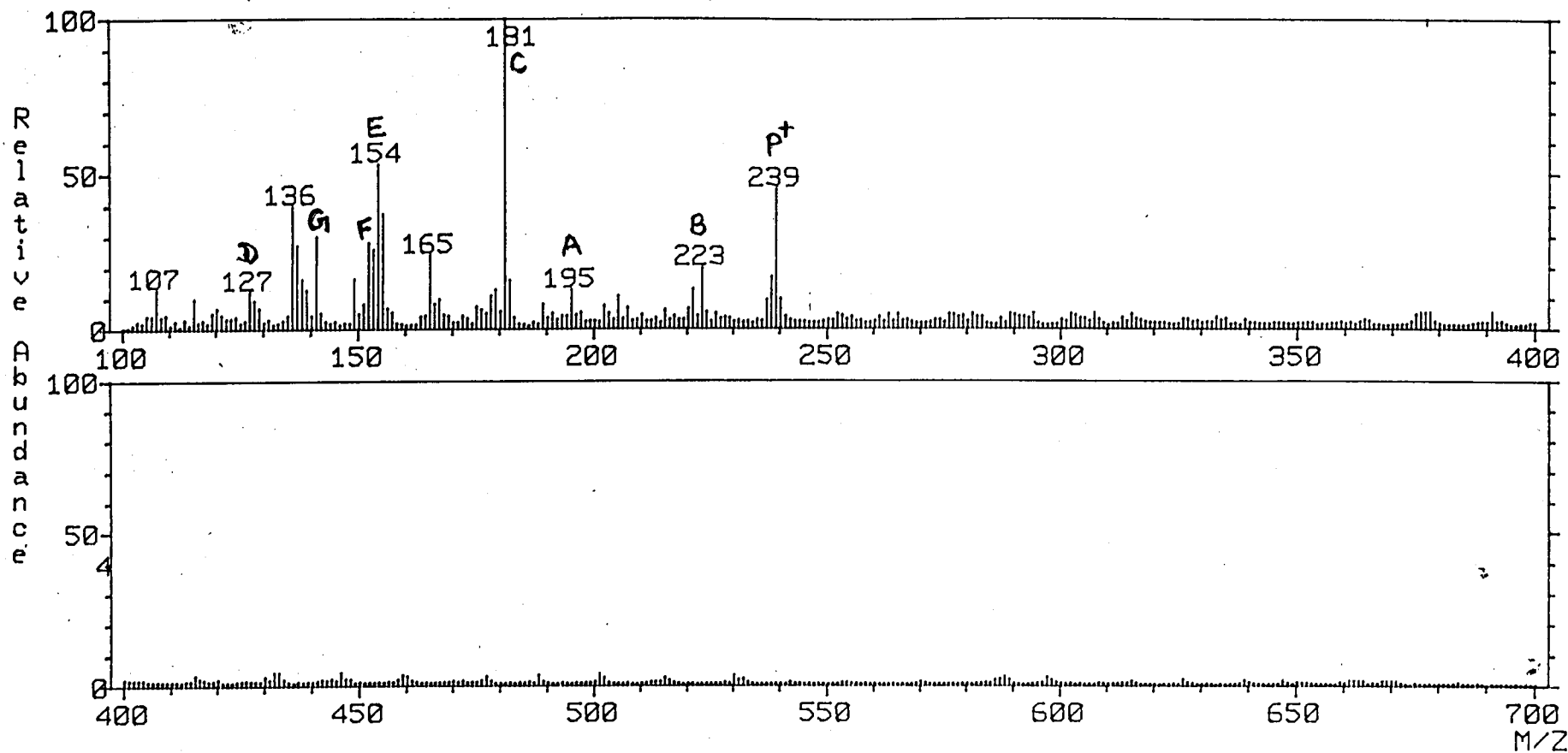
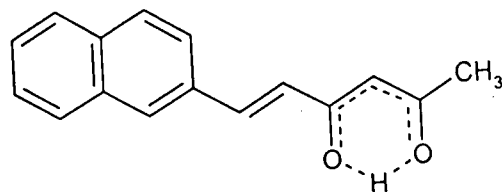


Fig. 1.4. Mass spectrum of 1c

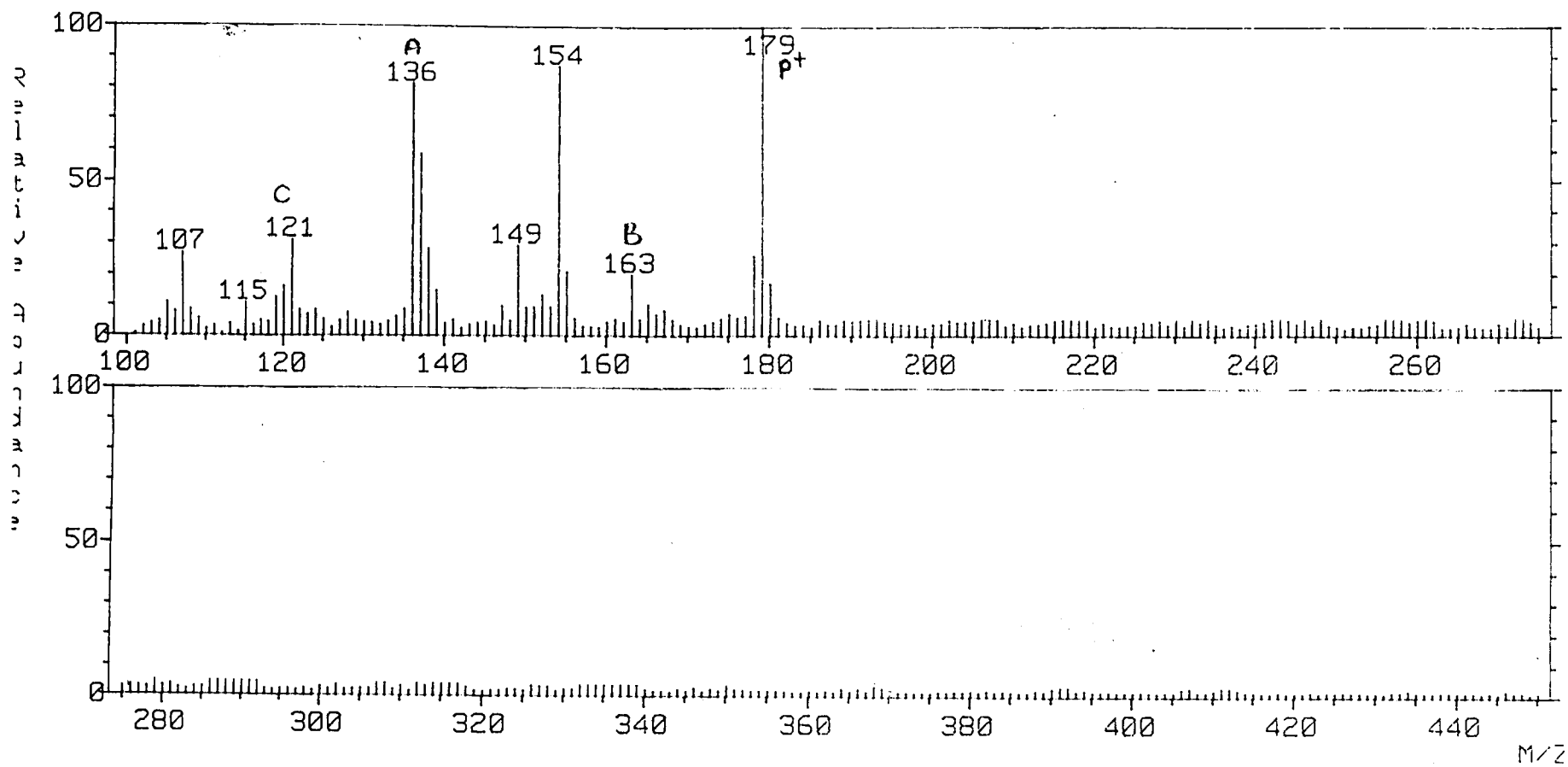
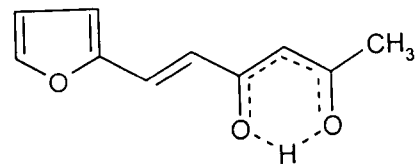
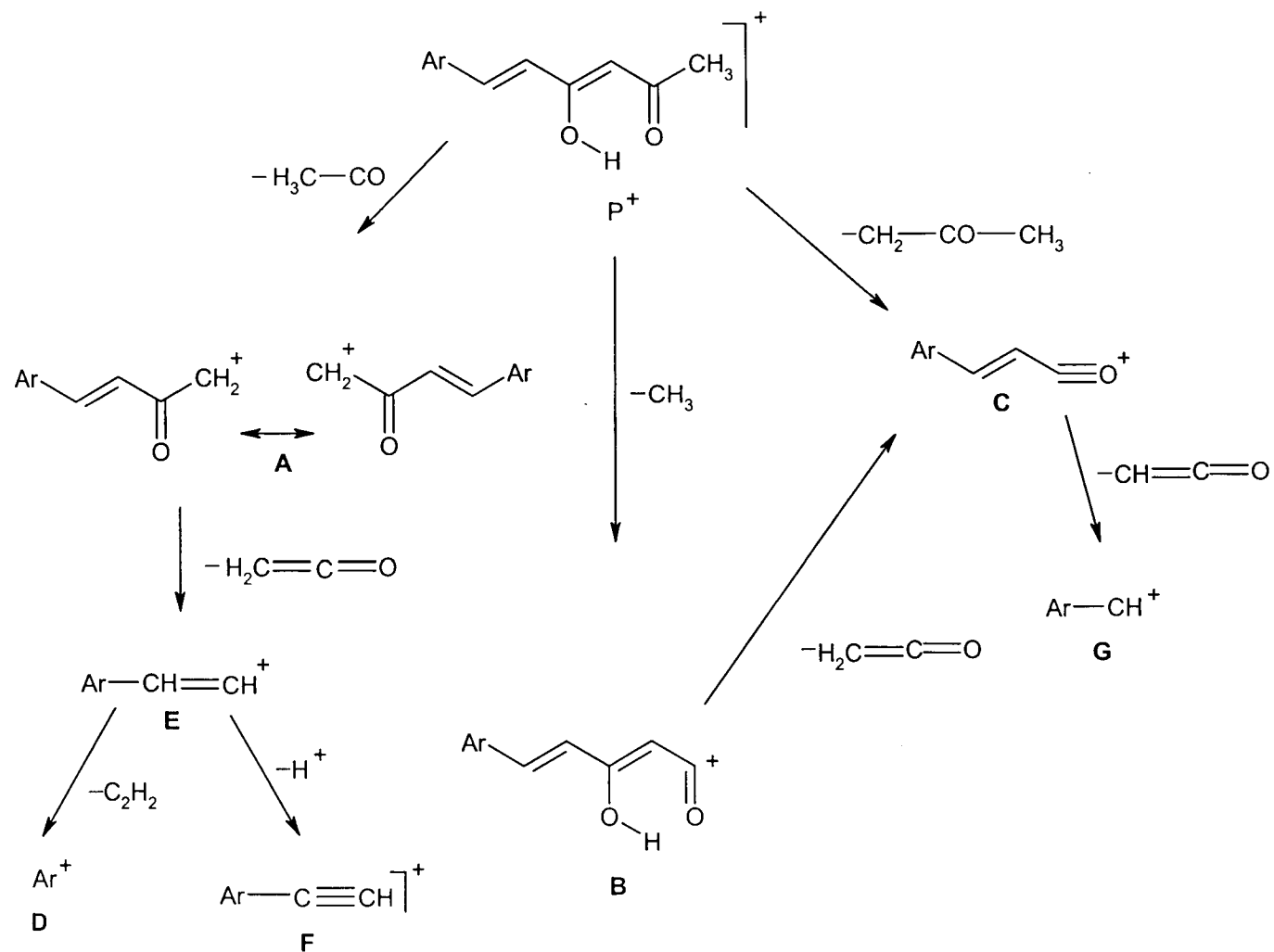
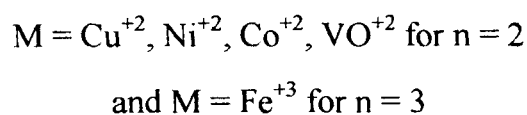
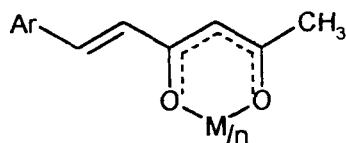


Fig. 1.5. Mass spectrum of 1d



Scheme 1.4 Fragmentation Pattern for 1a - d

The observed uv, ir, nmr and mass spectral data of the complexes are in agreement with structure **1.2**.



1.2

Uv spectra

The UV absorption bands of the ligands remained almost unchanged in the metal complexes which suggest that no structural change has occurred during complex formation. The $n \rightarrow \pi^*$ transition of the carbonyl moiety of the free ligands showed a slight bathochromic shift indicating the involvement of the dicarbonyl moiety in the complex formation. The uv absorption of the complexes are given tables 1.6 to 1.9.

TABLE 1.6
Physical, analytical and uv spectral data of copper(II) complexes of 6-aryl-5-hexene-2,4-diones, 1a-d

Copper(II) chelate of (Molecular formula)*	Yield (%)	M.P. °C	μ_{eff} (B.M.)	Elemental Analysis calculated/ found			λ_{max} (nm)
				C	H	M	
1a (C ₁₂ H ₁₁ O ₂) ₂ Cu	65	245	1.76	65.88 (65.08)	5.03 (4.75)	14.51 (14.25)	256 341
1b (C ₁₄ H ₁₃ O ₂) ₂ Cu	70	> 300	1.74	68.64 (68.57)	5.31 (5.30)	12.98 (12.97)	290 459
1c (C ₁₆ H ₁₃ O ₂) ₂ Cu	60	> 300	1.78	71.44 (71.38)	4.84 (4.83)	11.82 (11.81)	291 382
1d (C ₁₀ H ₉ O ₃) ₂ Cu	70	> 300	1.80	57.48 (57.41)	4.31 (4.30)	15.22 (15.2)	293 353

*The molecular formula given correspond to [CuL₂] stoichiometry, where L stands for the deprotonated ligand moiety.

TABLE 1.7
Physical, analytical and uv spectral data of nickel(II) complexes of 6-aryl-5-hexene-2,4-diones, 1a-d

Nickel(II) chelate of (Molecular formula)*	Yield (%)	M.P. °C	Elemental Analysis calculated/ found			λ_{max} (nm)
			C	H	M	
1a (C ₁₂ H ₁₁ O ₂) ₂ Ni	60	234	66.56 (66.48)	5.08 (5.00)	13.57 (13.25)	256 340
1b (C ₁₄ H ₁₃ O ₂) ₂ Ni	70	> 300	69.32 (69.13)	5.37 (5.54)	12.11 (12.07)	278 366
1c (C ₁₆ H ₁₃ O ₂) ₂ Ni	60	> 300	72.09 (71.9)	4.88 (4.86)	11.82 (10.99)	295 365
1d (C ₁₀ H ₉ O ₃) ₂ Ni	60	> 300	58.15 (57.97)	4.36 (4.34)	14.22 (14.17)	290 361

*The molecular formula given correspond to [NiL₂] stoichiometry, where L stands for the deprotonated ligand moiety.

TABLE 1.8

**Physical, analytical and uv spectral data of cobalt(II) complexes of
6-aryl-5-hexene-2,4-diones, 1a-d**

Co(II) chelate of (Molecular formula)*	Yield (%)	M.P. °C	μ_{eff} (B.M.)	Elemental Analysis calculated/ found			λ_{max} (nm)
				C	H	M	
1a (C ₁₂ H ₁₁ O ₂) ₂ Co(H ₂ O) ₂	60	> 300	4.76	66.12 (66.06)	5.01 (5.00)	13.3 (13.26)	260 340
1b (C ₁₄ H ₁₃ O ₂) ₂ Co(H ₂ O) ₂	60	> 300	4.83	69.29 (69.13)	5.36 (5.34)	12.15 (12.12)	289 366
1c (C ₁₆ H ₁₃ O ₂) ₂ Co(H ₂ O) ₂	50	> 300	4.72	72.06 (71.91)	4.88 (4.86)	11.05 (11.03)	297 398
1d (C ₁₀ H ₉ O ₃) ₂ Co(H ₂ O) ₂	60	> 300	4.83	58.12 (57.97)	4.36 (4.34)	14.27 (14.23)	287 319

*The molecular formula given correspond to [CoL₂(H₂O)₂] stoichiometry, where L stands for the deprotonated ligand moiety.

TABLE 1.9

**Physical, analytical and uv spectral data of iron(III) complexes of
6-aryl-5-hexene-2,4-diones, 1a-d**

Iron(III) chelate of (Molecular formula)	Yield (%)	M.P. °C	μ_{eff} (B.M.)	Elemental Analysis calculated/ found			λ_{max} (nm)
				C	H	M	
1a (C ₁₂ H ₁₁ O ₂) ₂ Fe	60	> 300	5.85	71.1 (70.6)	5.12 (5.06)	7.96 (7.78)	275 350
1b (C ₁₄ H ₁₃ O ₂) ₂ Fe	65	160	5.9	72.54 (72.41)	5.61 (5.60)	8.04 (8.02)	284 366
1c (C ₁₆ H ₁₃ O ₂) ₂ Fe	60	> 300	5.84	75.11 (75.0)	5.09 (5.07)	7.28 (7.27)	297 398
1d (C ₁₀ H ₉ O ₃) ₂ Fe	50	> 300	5.76	61.34 (61.22)	4.60 (4.59)	9.52 (9.50)	289

*The molecular formula given correspond to [FeL₃] stoichiometry, where L stands for the deprotonated ligand moiety.

Infrared spectra

The ir spectral data have been highly useful in establishing the structure and nature of bonding in numerous metal 1,3-diketonates. Infrared spectra of metal 1,3-diketonates have been studied extensively. Theoretical band assignments were carried based on normal coordinate analysis and isotope shift studies for diverse types of β -diketone complexes by various investigators.^{26-30,122} All these studies show that the carbonyl stretching frequencies of the β -diketo/ β -ketoenol decreases appreciably on metal coordination. Further, appearance of new bands in the region 420-500 cm^{-1} due to $\nu_{\text{M-O}}$ are characteristic of the ir spectra of metal 1,3-diketonates.

In the ir spectra of the complexes of the 6-arylhexanoids, no band of appreciable intensity observed in the region 1650-1800 cm^{-1} assignable to free or hydrogen bonded acetyl and cinnamoyl groups. However spectra of all the complexes are characterised by the presence of two new bands of medium intensity in the region 1590-1640 cm^{-1} in addition to the various $\nu_{\text{C=C}}$. These bands can confidently be assigned to metal bonded acetyl carbonyl and cinnamoyl carbonyl functions^{123,124} (Table 1.10). The broad free ligand band in the region 2900-3100 cm^{-1} is cleared up in the spectra of all metal complexes showing that the chelated proton is replaced by metal ion during complexation. The region above 2000 cm^{-1} in the spectra of complexes show several medium and weak intensity

bands due to various aliphatic and aromatic CH stretching vibrations. Presence of weak bands in the spectra of cobalt(II) complexes in the region 3200-3400 cm^{-1} suggest the presence of coordinated water molecule.

The additional evidence for complex formation is from the appearance of two medium intensity bands in the region 400-500 cm^{-1} due to $\nu_{\text{M-O}}$ vibrations. Thus the ir spectral data suggest the **structure 1.2** of the complexes. The position of the trans CH=CH bands ($\sim 980 \text{ cm}^{-1}$) remains unaltered in the case of metal complexes also. Important ir bands observed in the spectra and their probable assignments are given in table 1.10-1.13. All the vanyl complexes showed a medium intensity band at $\sim 960 \text{ cm}^{-1}$ presumably due to the stretching of the V=O group.

TABLE 1.10
**Characteristic ir data (cm⁻¹) of copper chelate of the
 6-aryl-5-hexene-2,4-diones**

Copper(II) chelate of				Probable assignments
1a	1b	1c	1d	
1632	1615	1620	1610	$\nu_{C=O}$ metal chelated acetyl
1598	1585	1590	1568	$\nu_{C=O}$ metal chelated cinnanoyl
1570 1540	1530 1465	1561 1515	1460 1407	ν_{C-C} phenyl / alkenyl
1523	1415	1440	1365	ν_{asym} C-C-C chelate ring
1428	1403	1404	1320	ν_{asym} C-C-C chelate ring
1103 1073	1136 1060	1165 1025	1110 1035	β_{C-H} chelate ring
982	994	970	954	$\nu_{CH=CH-}$ trans
738	755	776	800	ν_{C-H} chelate ring
455 421	485 460	490	478 418	ν_{M-O} chelate ring

TABLE 1.11
**Characteristic of ir data (cm^{-1}) of nickel(II) chelate of the
 6-aryl-5-hexene-2,4-diones**

Nickel(II) chelate of			Probable assignments
1b	1c	1d	
1610	1645	1625	$\nu_{\text{C=O}}$ metal chelated acetyl
1563	1599	1568	$\nu_{\text{C=O}}$ metal chelated cinnanoyl
1512 1430	1560 1423	1519 1407	$\nu_{\text{C-C}}$ phenyl / alkenyl
1410	1395	1363	$\nu_{\text{asym C-C-C}}$ chelate ring
1350	1318	1330	$\nu_{\text{asym C-C-C}}$ chelate ring
1176 1026	1164 1034	1170 1020	$\beta_{\text{C-H}}$ chelate ring
991	974	954	$\nu_{\text{CH=CH-}}$ trans
752	775	798	$\nu_{\text{C-H}}$ chelate ring
505	472	480 418	$\nu_{\text{M-O}}$ chelate ring

TABLE 1.12
 Characteristic of ir data (cm^{-1}) of cobalt(II) chelates of the
 6-aryl-5-hexene-2,4-diones

Cobalt(II) chelate of			Probable assignments
1b	1c	1d	
1640	1610	1610	$\nu_{\text{C=O}}$ metal chelated acetyl
1599	1585	1568	$\nu_{\text{C=O}}$ metal chelated cinnanoyl
1509 1445	1547 1430	1519 1409	$\nu_{\text{C-C}}$ phenyl / alkenyl
1380	1398	1380	ν_{asym} C-C-C chelate ring
1357	1350	1315	ν_{asym} C-C-C chelate ring
1135 1026	1168 1024	1174 1020	$\beta_{\text{C-H}}$ chelate ring
995	971	970	$\nu_{\text{CH=CH}}$ trans
752	774	740	$\nu_{\text{C-H}}$ chelate ring
40	472	418 405	$\nu_{\text{M-O}}$ chelate ring

TABLE 1.13
**Characteristic of ir data (cm^{-1}) of iron(III) and oxovanadium(IV)
 chelates of the 6-aryl-5-hexene-2,4-diones**

Iron (III) chelate of		VO ²⁺ chelate of			Probable assignments
1a	1d	1b	1c	1d	
1641	1605	1646	1620	1613	$\nu_{\text{C=O}}$ metal chelated acetyl
1570	1571	1606	1598	1580	$\nu_{\text{C=O}}$ metal chelated cinnanoyl
1517 1463	1485 1409	1580 1447	1560 1420	1510 1414	$\nu_{\text{C-C}}$ phenyl / alkenyl
1396	1361	1394	1354	1361	ν_{asym} C–C–C chelate ring
1325	1305	1314	1277	1290	ν_{asym} C–C–C chelate ring
1170 1091	1175 1115	1142 1076	1186 1024	1169 1016	$\beta_{\text{C-H}}$ chelate ring
980	954	996	982	956	$\nu_{\text{CH=CH-}}$ trans
760	813	751	778	758	$\nu_{\text{C-H}}$ chelate ring
476 418	485	499 459	472	472 475	$\nu_{\text{M-O}}$ chelate ring

¹H nmr spectra

The ¹H nmr spectrum of the diamagnetic nickel(II) chelate of **1b** is given in figure 1.6. In conformity with the structure 1.2, the enolic proton signal ($\delta \sim 16$ ppm) of the free ligand, disappeared in the spectrum of the nickel(II) chelate indicating that the enolic proton has been replaced by the metal ion during complexation. The methine proton signals are shifted towards the down field of the spectra indicating the decreased electron density around the central carbon atom of the pseudo-aromatic metal chelate ring system. The integrated intensities of the various signals are in agreement with their formulation.

Mass spectra

In the case of metal complexes of 1,3-diketones^{2,125-127} mass spectroscopy has been a powerful tool for the determination of the stoichiometry and structural elucidation. It has been shown from the mass spectral analysis of a series of copper(II) chelates of 1,3-diketones, that stepwise removal of alkyl/aryl group(s) attached to the dicarbonyl function also influence the stability of various fragments formed under mass spectral conditions. Formation of several stable cyclic species involving metal ion have also been detected.

The FAB mass spectra of copper(II) chelates of the 6-aryl-5-hexene-2,4-diones were obtained and reproduced in figures 1.7-1.9. All the spectra show a relatively intense $P^+/(P+1)^+$ peaks in agreement with their (ML_2) formulation. The

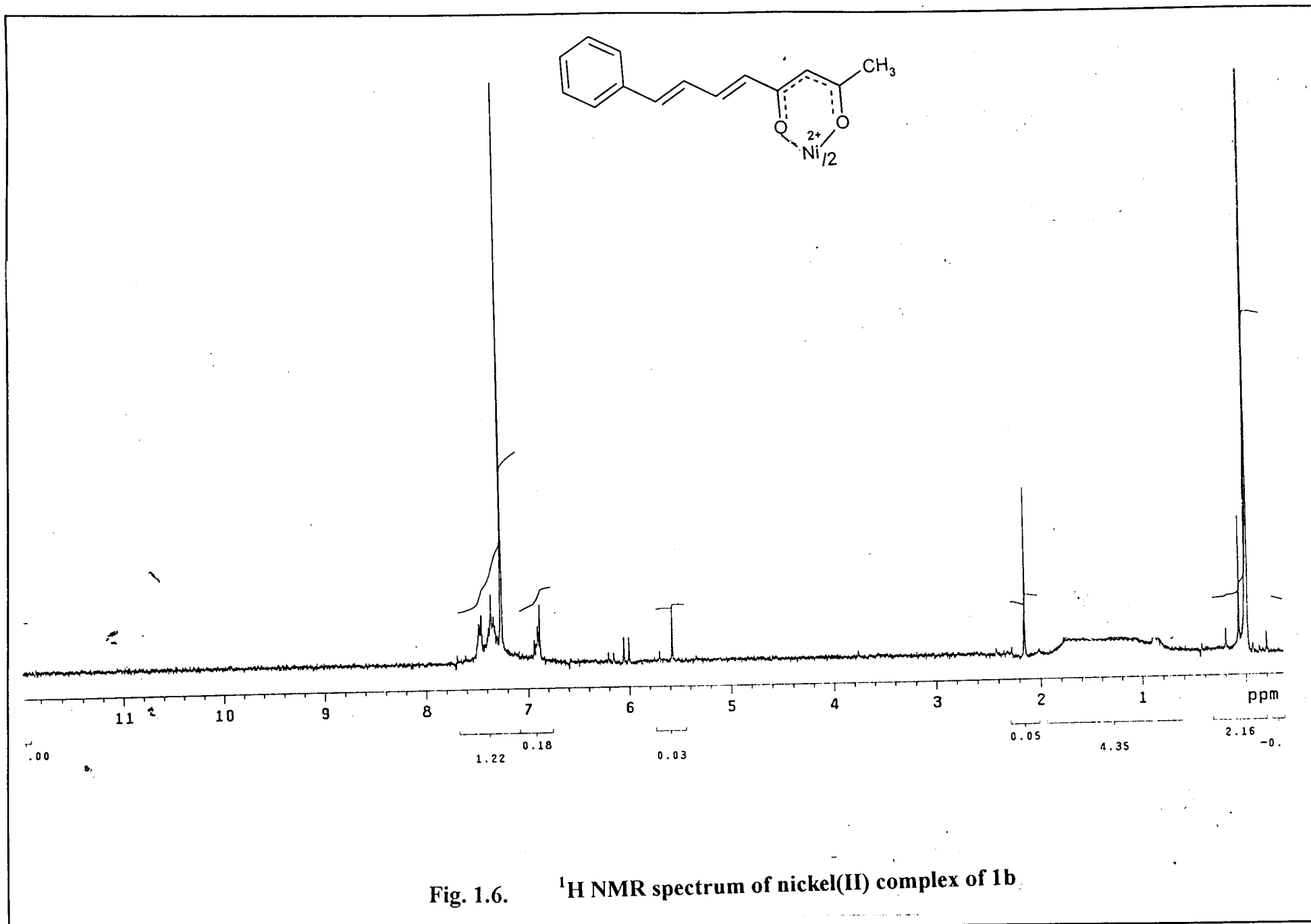


Fig. 1.6. ^1H NMR spectrum of nickel(II) complex of 1b.

base peak in all spectra are due to the ligand moiety and peaks due to $(\text{CuL})^+$, L^+ and fragments of L^+ are sometimes more intense than the molecular ion peak. Intense peaks due to the elimination of CH_3 , CH_3CO , CH_3COCH_2 , groups from the molecular ion are also observed. One striking feature of all the spectra is the appearance of a number of fragments containing copper. They are easily identified because of the 2:1 natural abundance of ^{63}Cu and ^{65}Cu isotopes.

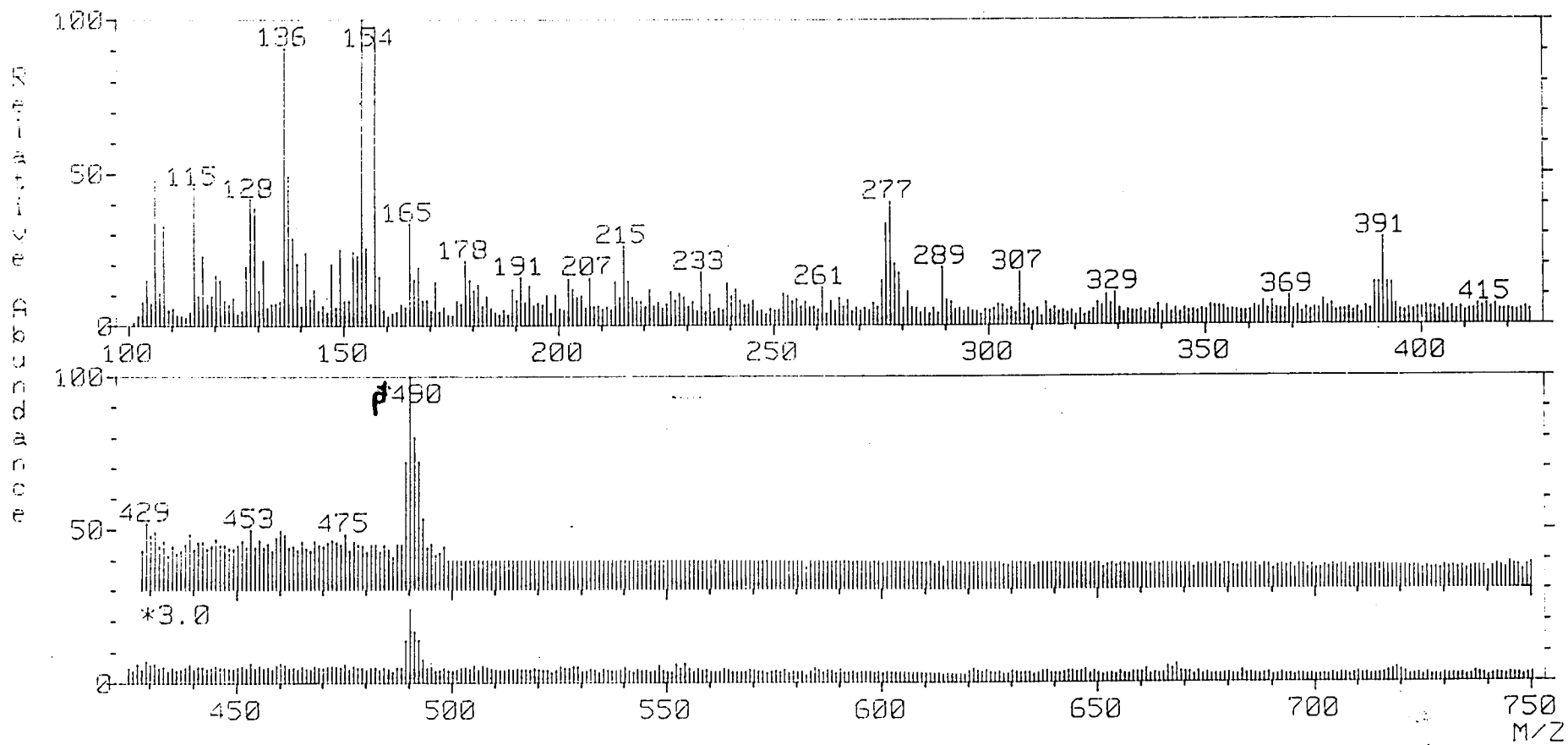
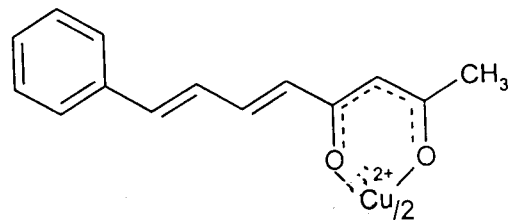


Fig. 1.7. Mass spectrum of copper(II) complex of 1b

67

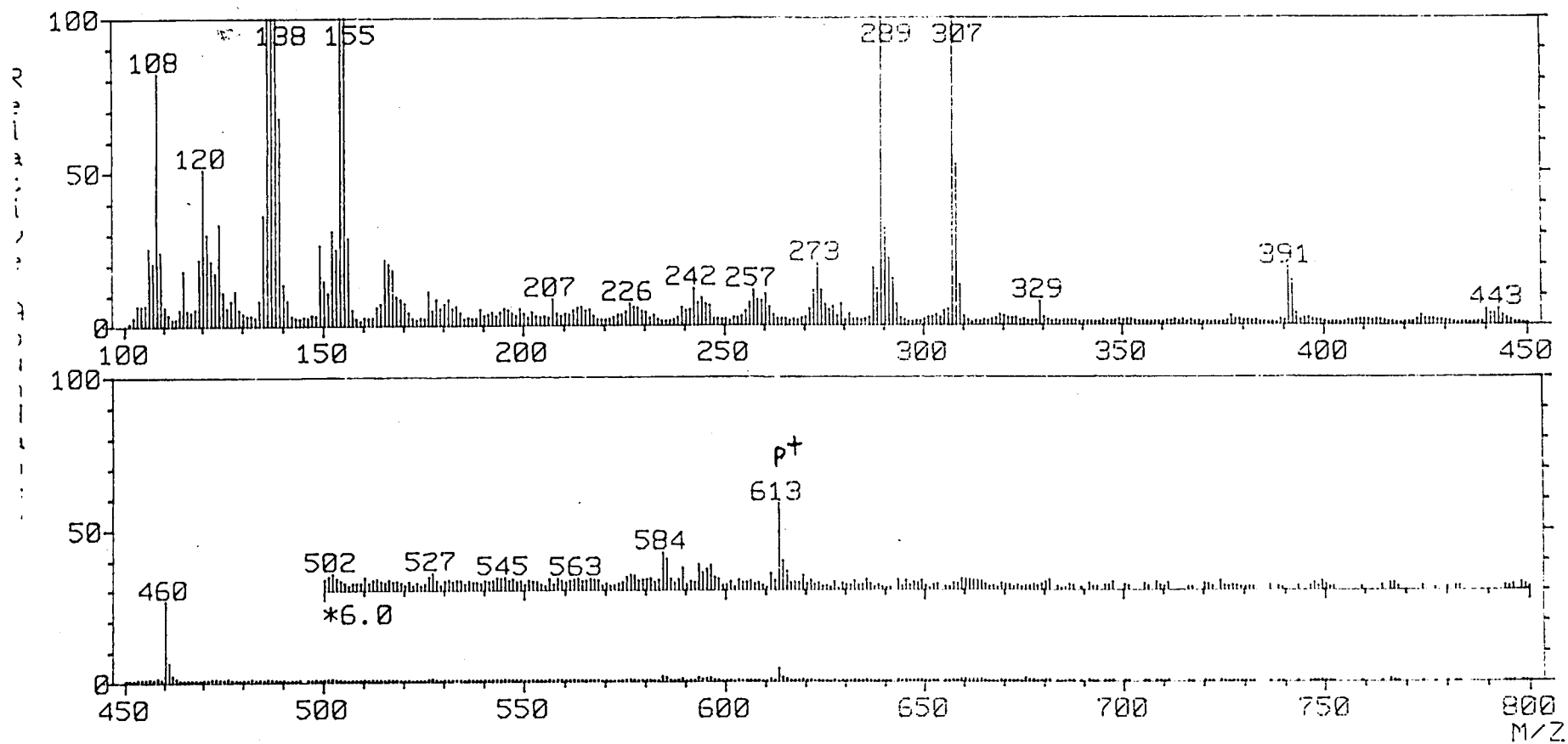
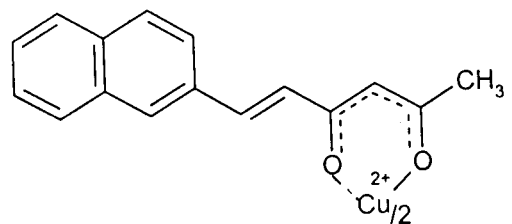


Fig. 1.8. Mass spectrum of copper(II) complex of 1c

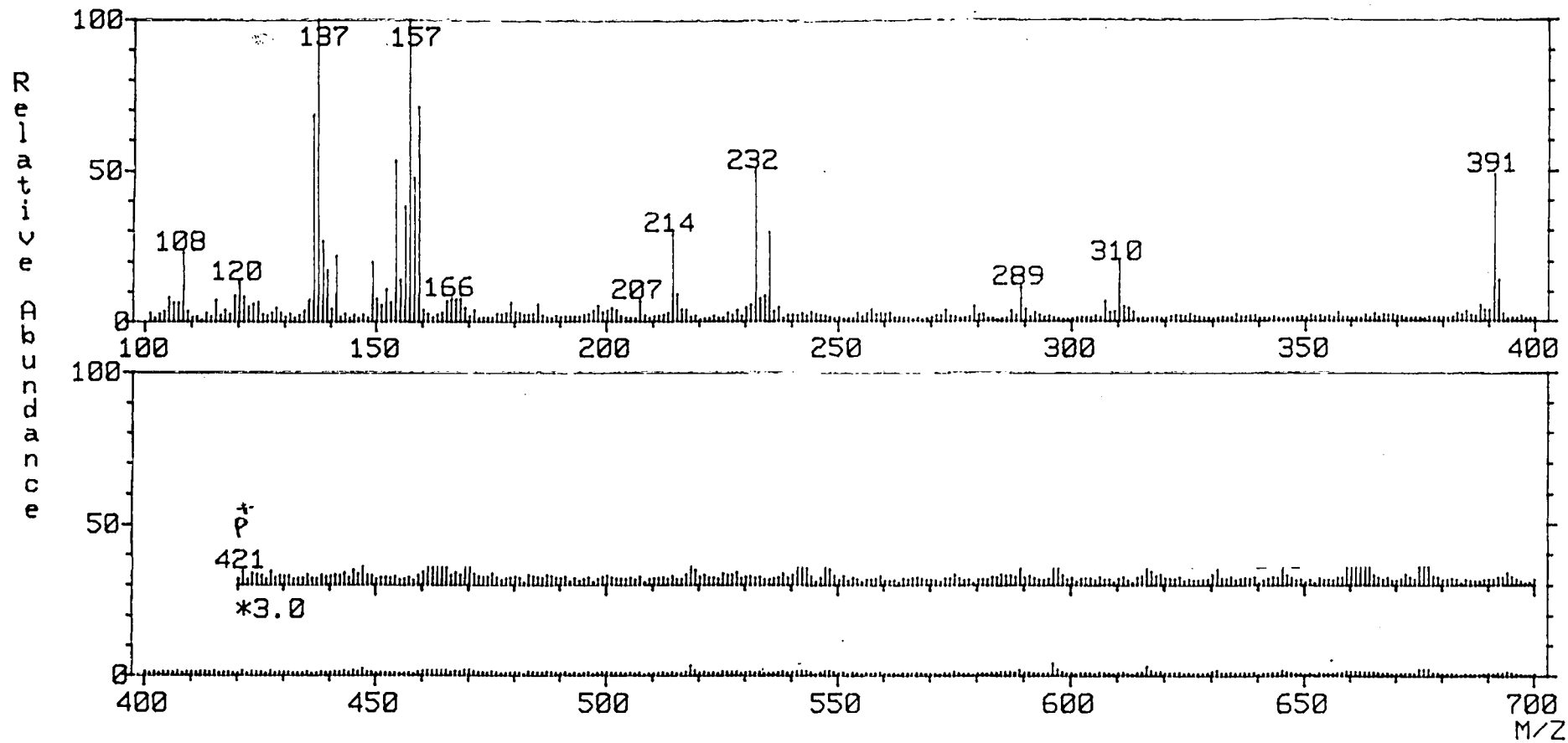
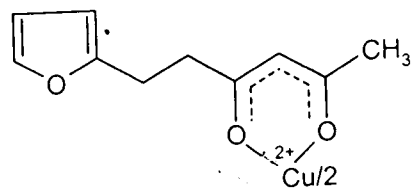


Fig. 1.9. Mass spectrum of copper(II) complex of 1d

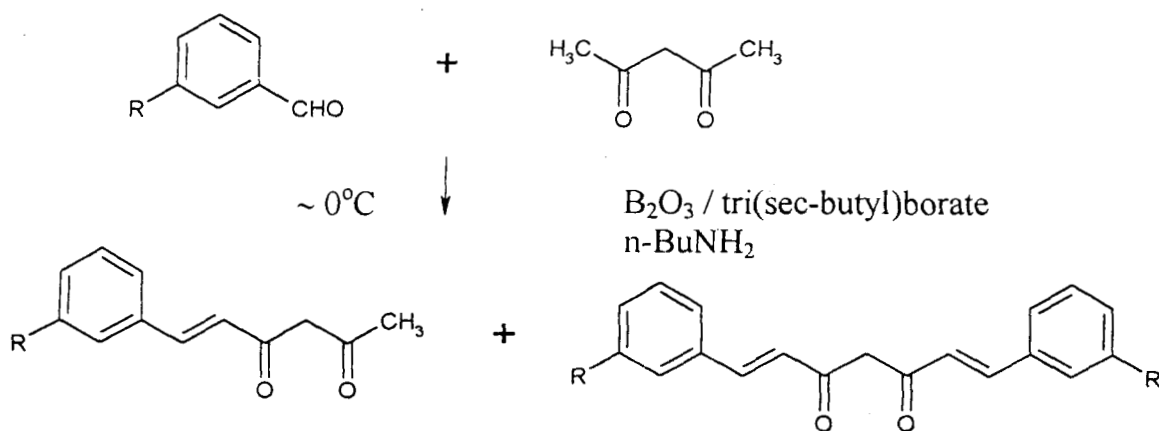
69

Section 2

Synthesis and characterisation of 6-(substituted aryl)-5-hexene-2,4-diones and their metal complexes

Synthesis of the 6-(substituted aryl)-hexanoids

The 6-arylhexanoids considered in this section were synthesized¹²⁸⁻¹³⁰ by the condensation of substituted aromatic aldehydes (2-methylbenzaldehyde, 4-ethoxybenzaldehyde / piperonaldehyde / 4-(dimethylamino)benzaldehyde / 2-hydroxynaphthaldehyde / salicylaldehyde) with acetylacetone in the presence of boric oxide and tri(sec butyl) borate using n-butylamine as the condensing agent as given in the reaction **scheme 2.1** below. The detailed procedure for the synthesis are similar to that given in section 1.



Scheme 2.1

2a



2d



2b



2e



2c



2f



The 6-(substituted aryl) hexanoids were recrystallised from hot benzene to get chromatographically (tlc) pure material.

Synthesis of metal chelates

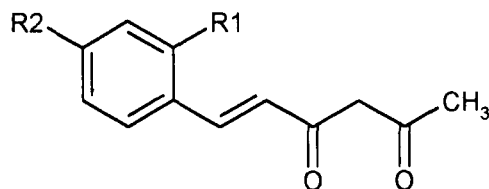
Copper(II), nickel(II), cobalt(II), oxovanadium(IV) and iron(III) chelates of the compounds were prepared by the following general method. To a refluxing solution of the compound (0.002 mol) in methanol (15 ml) an aqueous solution of metal(II) acetate (0.001 mol, 10 ml) was added and the reaction mixture was refluxed for ~ 3 h and cooled to room temperature. The precipitated product was filtered, washed with water, then with ethanol and dried in vacuum. In the case of VO^{2+} and Fe^{3+} complexes vanadyl sulphate and ferric chloride hydrated were employed.

Results and discussion

All the compounds are crystalline in nature with sharp melting points and are soluble in common organic solvents. The yield, systematic name and other synthetic details of the compounds are given in table 2.1. The elemental analytical data and observed molecular weight (Table 2.2) of the compounds suggest that only one equivalent of the substituted aromatic aldehyde has condensed with one equivalent of acetylacetone.

TABLE 2.1

Synthetic details of the substituted 6-aryl-5-hexene-2,4-diones



Compounds	Aldehydes used for synthesis	R ₁	R ₂	Systematic name	Yield (%)
2a	2-methylbenzaldehyde	CH ₃	H	6-(2-methylphenyl)-5-hexene-2,4-dione	40
2b	4-ethoxybenzaldehyde	H	-OCH ₂ -CH ₃	6-(4-ethoxyphenyl)-5-hexene-2,4-dione	60
2c	pipernaldehyde	H		6-(3,4-dioxymethylene)-5-hexene-2,4-dione	50
2d	4(N,N-dimethylamino)benzaldehyde	H	-N(CH ₃) ₂	6-(4-N,N-dimethylamino)-5-hexene-2,4-dione	70
2e	2-hydroxynaphthaldehyde	-OH	3,4-phenyl	6-(2-hydroxynaphthyl)-5-hexene-2,4-dione	65
2f	Salicylaldehyde	-OH	H	6-(2-hydroxyphenyl)-5-hexene-2,4-dione	50

Characterisation of the 6-(substituted aryl)-hexanoids

The compounds were characterised on the basis of their uv, ir, nmr and mass spectral data.

Uv spectra

The uv spectra of the compounds in 95% ethanol (10^{-3}M) show two absorption bands at $\lambda_{\text{max}} \sim 410$ nm (due to the $n \rightarrow \pi^*$ transition of the carbonyl chromophore) and at ~ 308 nm (assignable to the $\pi \rightarrow \pi^*$ transition). The observed shifts of bands (Table 2.2) can be correlated to the electronic effects of the substituents in the aryl ring.

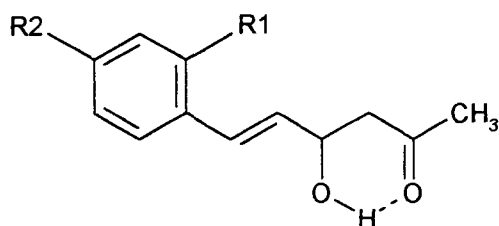
Infrared spectra

The ir spectra of the compounds show two prominent bands at ~ 1670 and at ~ 1630 cm^{-1} assignable respectively to the chelated acetyl and cinnamoyl $\nu_{\text{C=O}}$ vibrations. The observed position and intensity of these bands indicate that the compounds exist entirely in the enol form¹¹ and are enolised towards the cinnamoyl function as in structure 2.1.

TABLE 2.2

Physical, analytical and uv spectral data of the 6-arylpentanoids, 2a-f

Compounds	Molecular formula (formula weight)	Elemental analysis (%) calculated/(found)		Colour	M.P. °C	λ_{\max} nm	log ϵ
		C	H				
2a	C ₁₃ H ₄ O ₂ (202)	77.22 (76.84)	6.9 (6.8)	brown	82	312 409	4.3805 4.5605
2b	C ₁₄ H ₁₆ O ₃ (232)	72.41 (72.10)	6.89 (6.86)	yellowish brown	75	335 415	3.8613 3.8629
2c	C ₁₃ H ₁₂ O ₄ (232)	67.24 (66.95)	5.17 (5.15)	brown	122	310 401	4.2682 4.2062
2d	C ₁₄ H ₁₇ NO ₂ (231)	72.72 (72.39)	7.35 (7.3)	reddish brown	60	328 410	4.2041 4.1093
2e	C ₁₆ H ₁₄ O ₄ (254)	67.42 (67.04)	5.51 (5.49)	grey	89	308 377	4.1249 3.9557
2f	C ₂₁ H ₁₂ O ₃ (204)	70.59 (70.24)	5.88 (5.89)	light brown	92	300 366	3.7679



2.1

Compared to the unsubstituted 6-arylhexanoids considered in section 1 these carbonyl bands show a bathochromic shift. The intense and broad band observed in the region $2700\text{-}3500\text{ cm}^{-1}$ is undoubtedly due to the presence of strong intramolecular hydrogen bonding in these compounds which is also evident from the lowering of acetyl carbonyl stretching frequency. Several prominent bands appeared in the region $1500\text{-}1600\text{ cm}^{-1}$ are assignable to various olefinic and aromatic $\nu_{\text{C}=\text{C}}$ vibrations. A medium intensity band observed at $\sim 972\text{ cm}^{-1}$ is possibly arising from the trans $\text{-CH}=\text{CH-}$ absorption. Important ir absorption bands of the compounds and their possible assignments are given in table 2.3.

TABLE 2.3

Characteristic ir data (cm^{-1}) of the substituted 6-aryl-5-hexene-2,4-diones, 2a-f

2a	2b	2c	2d	2e	2f	Probable assignments
1665	1665	1660	1666	1670	1665	$\nu_{\text{C=O}}$ acetyl
1615	1625	1630	1620	1631	1612	$\nu_{\text{C=O}}$ cinnamonyl / naphthyl
1589 1550 1510	1600 1560 1510	1596 1560 1570	1600 1541 1510	1593 1555 1512	1575 1560 1490	$\nu_{\text{C=C}}$ phenyl / alkenyl
1480	1475	1492	1485	1463	1456	ν_{asym} -C-C-C chelate ring
1100 1039	1170 1114 1043	1161 1103 1035	1163 1062	1170 1082	1125 1033	$\beta_{\text{C-H}}$ chelate ring
930	921	931	939	964	941	$\nu_{\text{CH=CH}}$ - trans
727	725	730	725	746	756	$\nu_{\text{C-H}}$ chelate ring

^1H nmr spectra

The ^1H nmr spectra of the 6-(substituted aryl)hexanoids show a one proton singlet in the low field region at ~ 16 ppm and another singlet at ~ 6.4 ppm. The singlet at ~ 16 ppm is assignable to the intramolecularly hydrogen bonded enol proton of the compounds and the signal at ~ 6.4 ppm due to the methine proton signal. The ^1H nmr spectra of the compounds are reproduced in the figure 2.1-2.5. The characteristic chemical shift of various protons of the compounds are summarised in table 2.4. These signals are assigned through their multiplicity pattern and using earlier results¹²⁴ reported for structurally related compounds. In

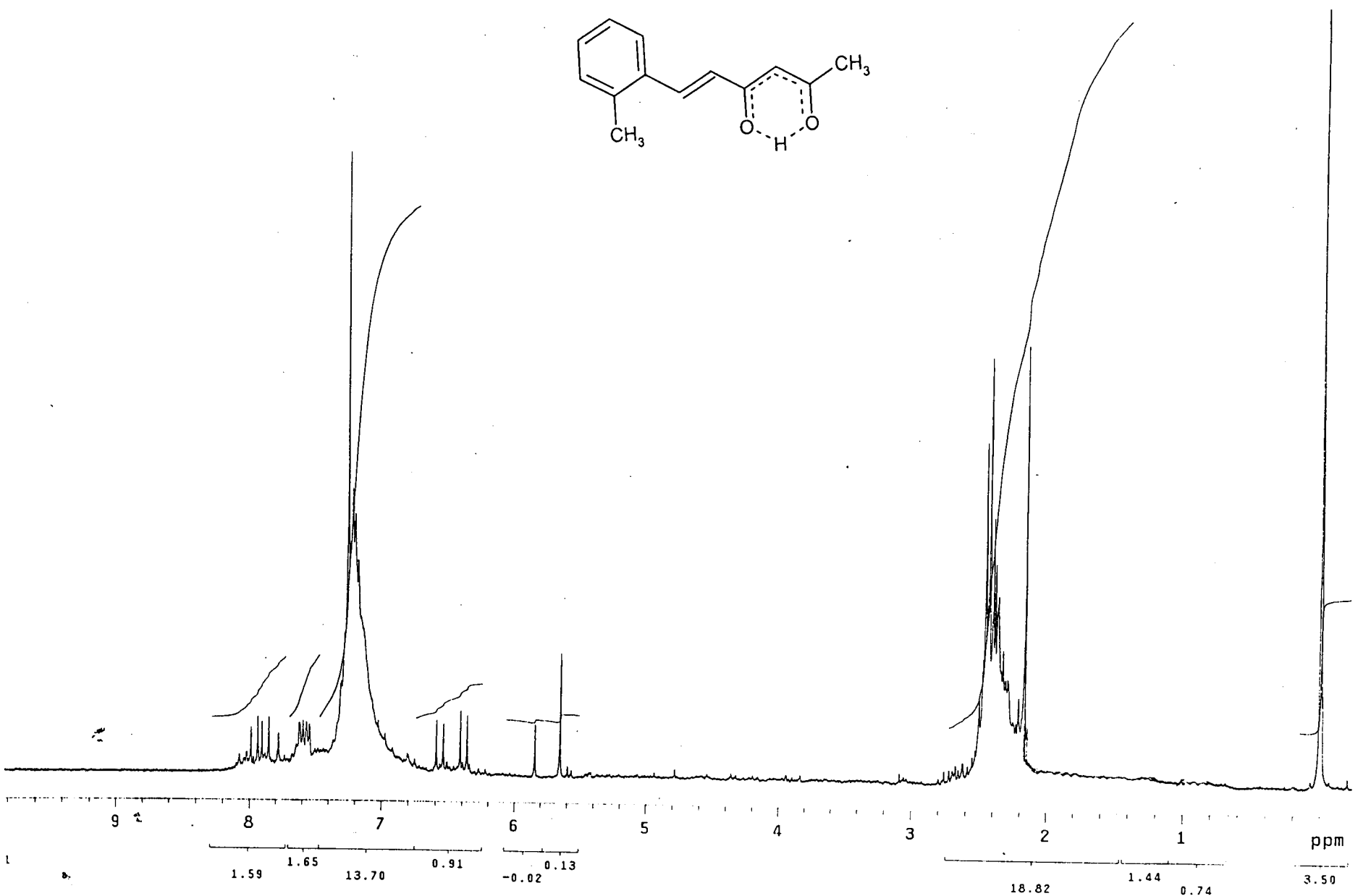
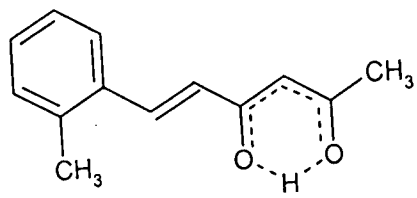


Fig. 2.1. ¹H NMR spectrum of 2a

tt

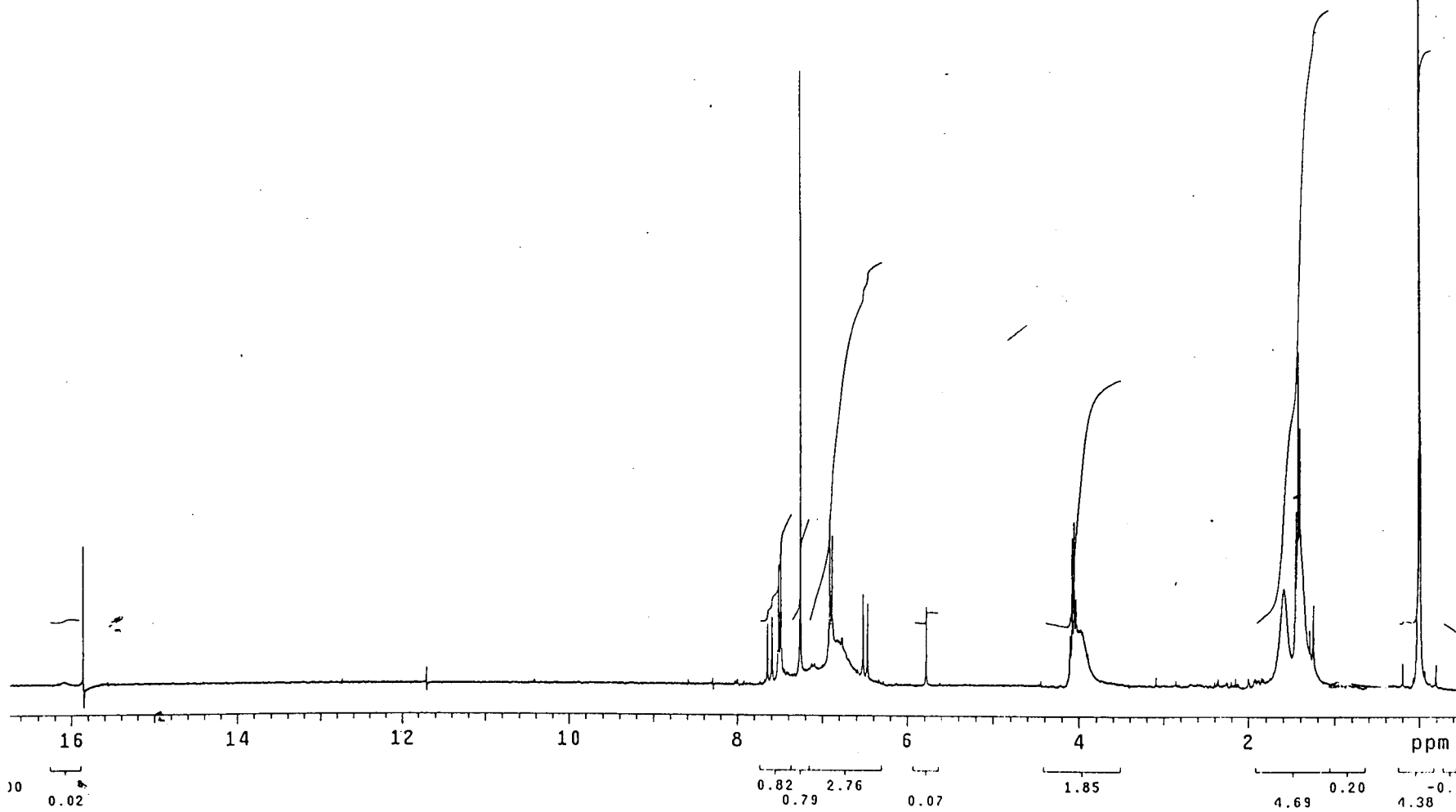
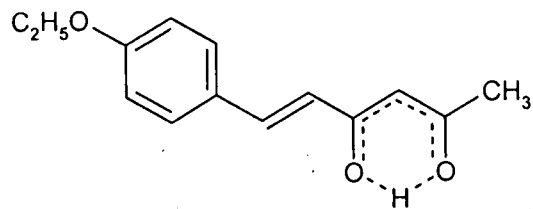
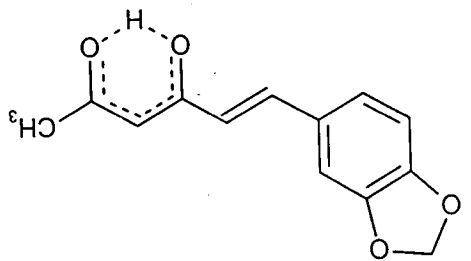
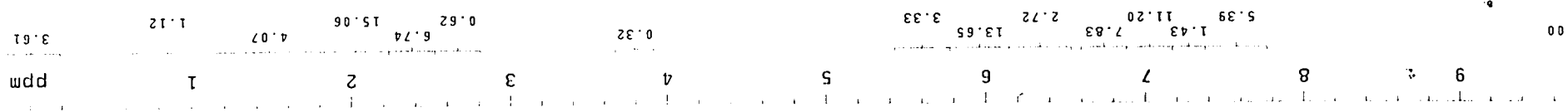


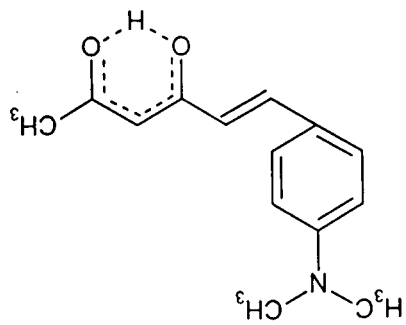
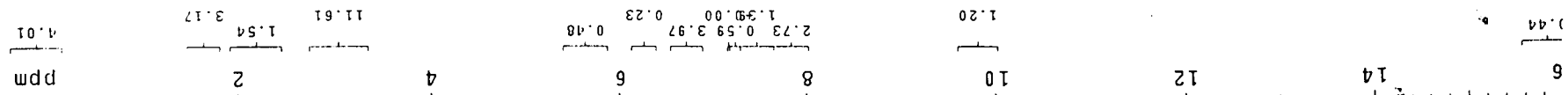
Fig. 2.2. ¹H NMR spectrum of 2b

Fig. 2.3. ¹H NMR spectrum of 2c.



67

Fig. 2.4. ¹H NMR spectrum of 2d



2d

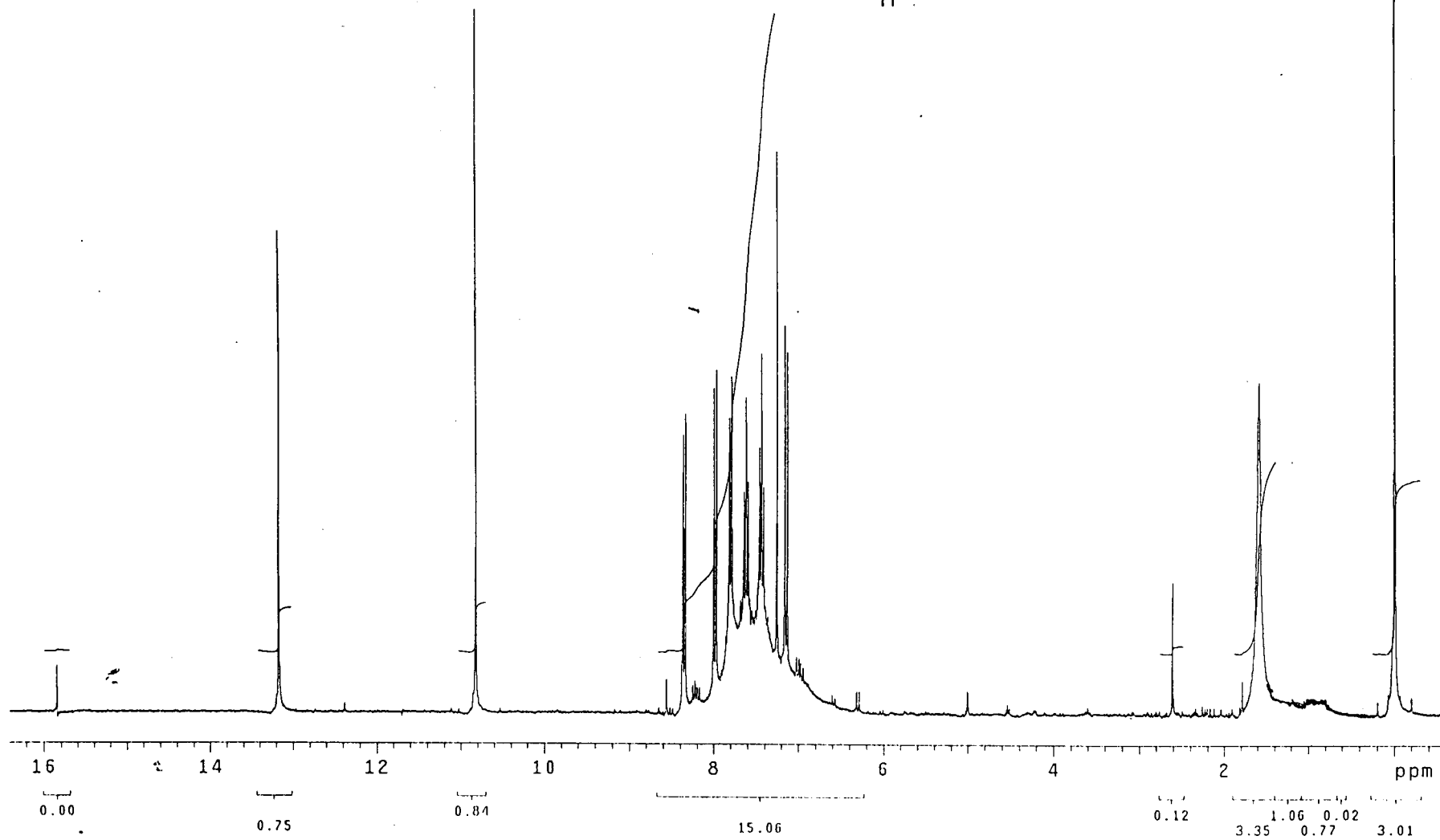
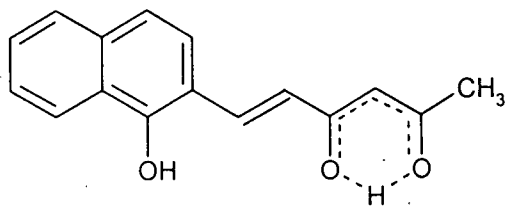


Fig. 2.5. ^1H NMR spectrum of 2e

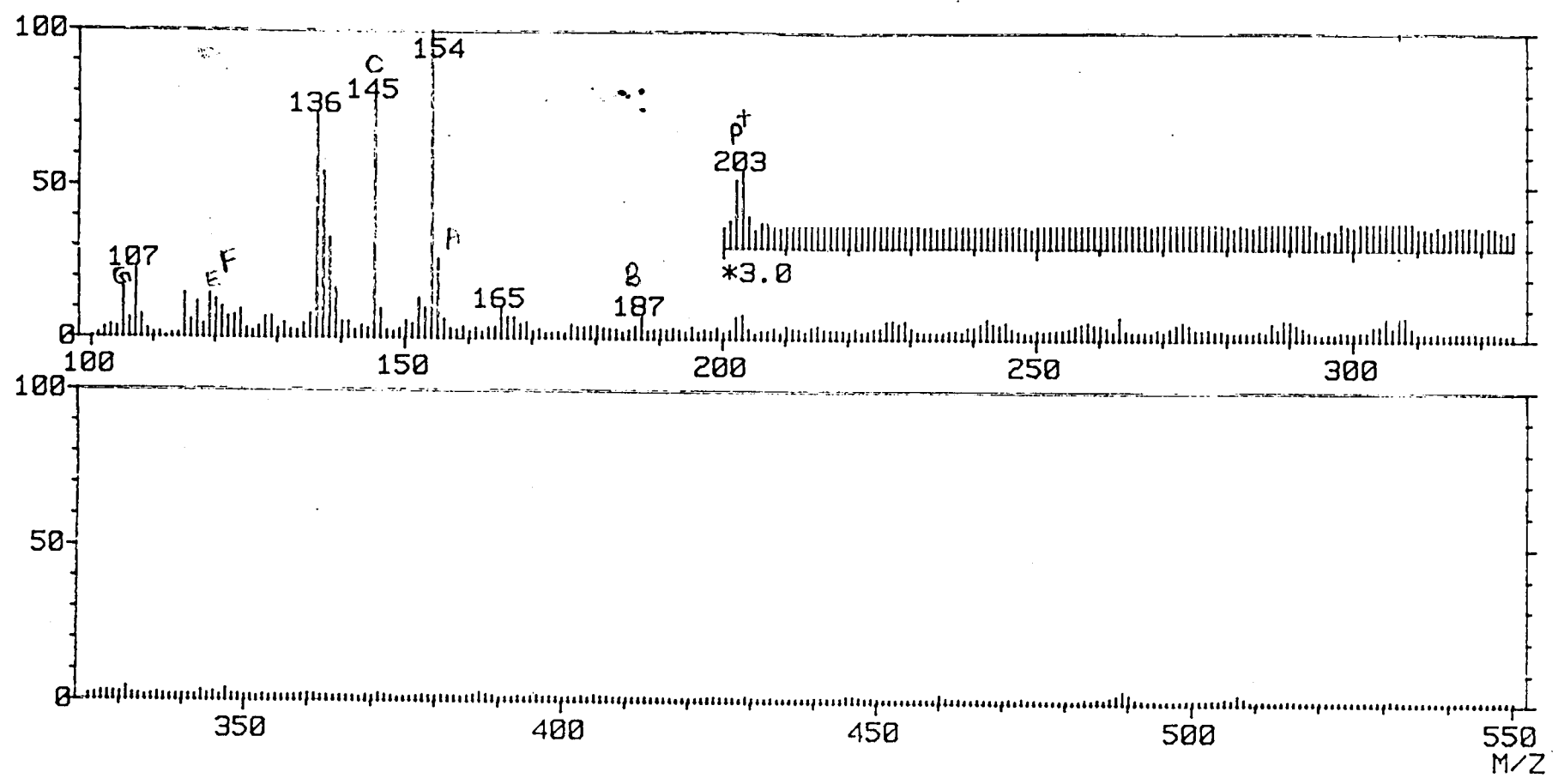
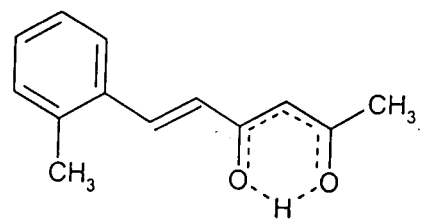
the case of **2e** and **2f** the phenolic proton signals are observed as expected at ~ 11 ppm.

TABLE 2.4
¹H nmr spectral data of the substituted 6-aryl-5-hexanoids, 2a-f

Compounds of						Probable assignments chemical shift (δ ppm)
2a	2b	2c	2d	2e	2f	
15.84	15.86	15.85	16.05	15.85	--	enolic
8.07 (1H)	7.63 (1H)	7.61 (1H)	7.57 (1H)	8.32 (1H)	7.74 (1H)	alkenyl
7.90 (1H)	7.59 (1H)	7.47 (1H)	7.53 (1H)	8.34 (1H)	7.76 (1H)	
7.87 – 6.97 (4H)	7.51 – 7.25 (4H)	7.69 – 7.26 (3H)	7.45 – 6.65 (4H)	7.98 – 7.25 (6H)	7.2 – 6.8 (4H)	aryl
6.414 (1H)	6.477 (1H)	6.002 (1H)	6.288 (1H)	7.128 (1H)	6.07 (1H)	methine
2.474 (3H)	1.29 (3H)	2.32 (3H)	2.12 (3H)	2.608 (3H)	2.502 (3H)	methyl aryl substituted
2.17 (3H)	1.45 (3H)	2.15 (2H)	3.07 (3H)			
	4.04 (2H)		3.003 (3H)			
				10.80	13.95	phenolic

Mass spectra

The FAB mass spectra of the 6-(substitutedaryl) hexanoids reproduced in figures 2.6 to 2.11, show intense molecular ion peaks $P^+/(P+1)^+$. In the case of **2e** and **2f**, the $(P-OH)^+$ is the most prominent peak. The cleavage of the acetyl fragment



825

Fig. 2.6. Mass spectrum of 2a

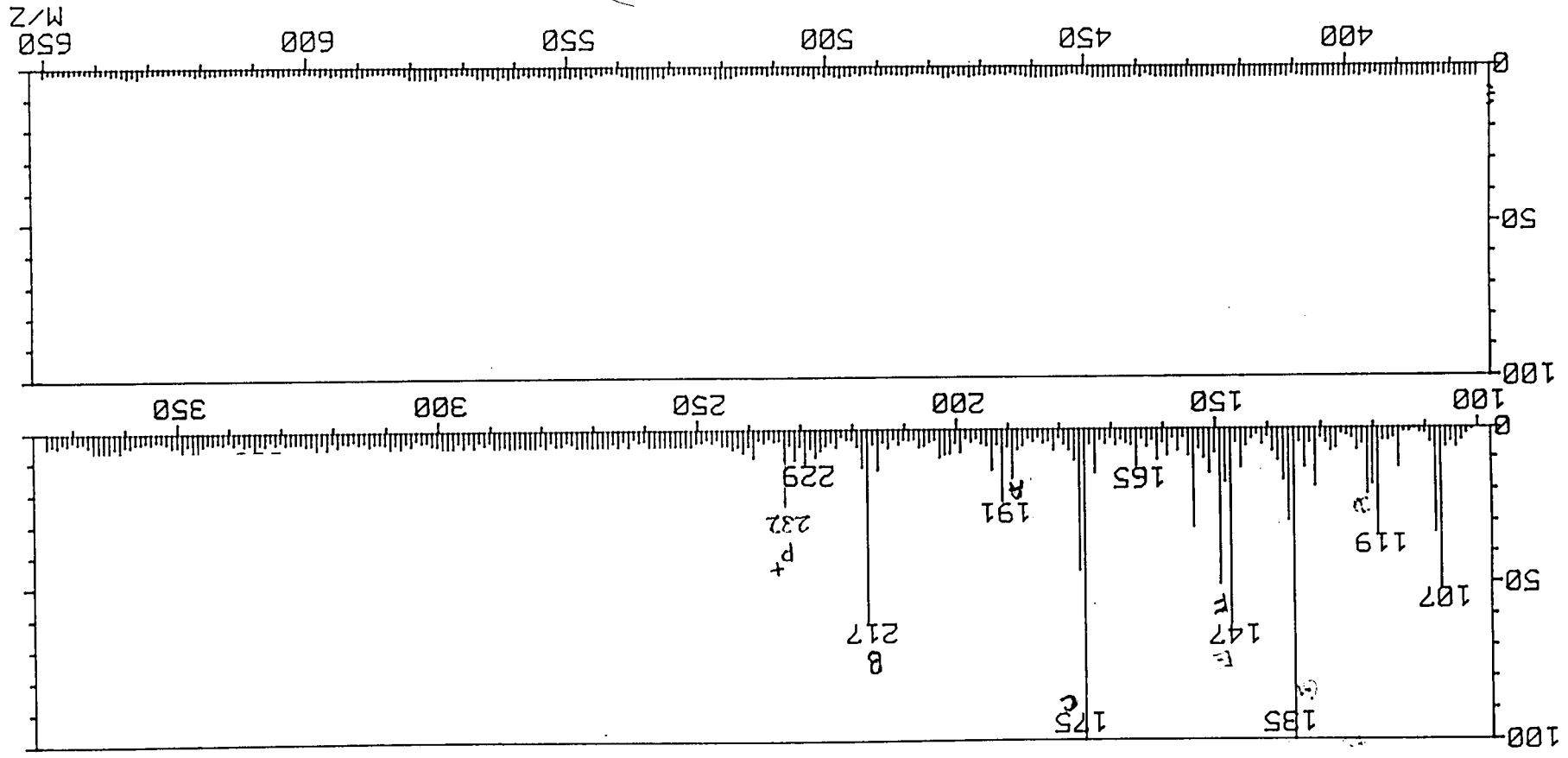
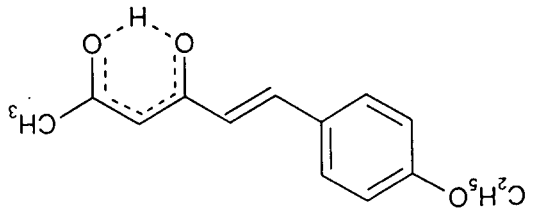


Fig. 2.7. Mass spectrum of 2b

504

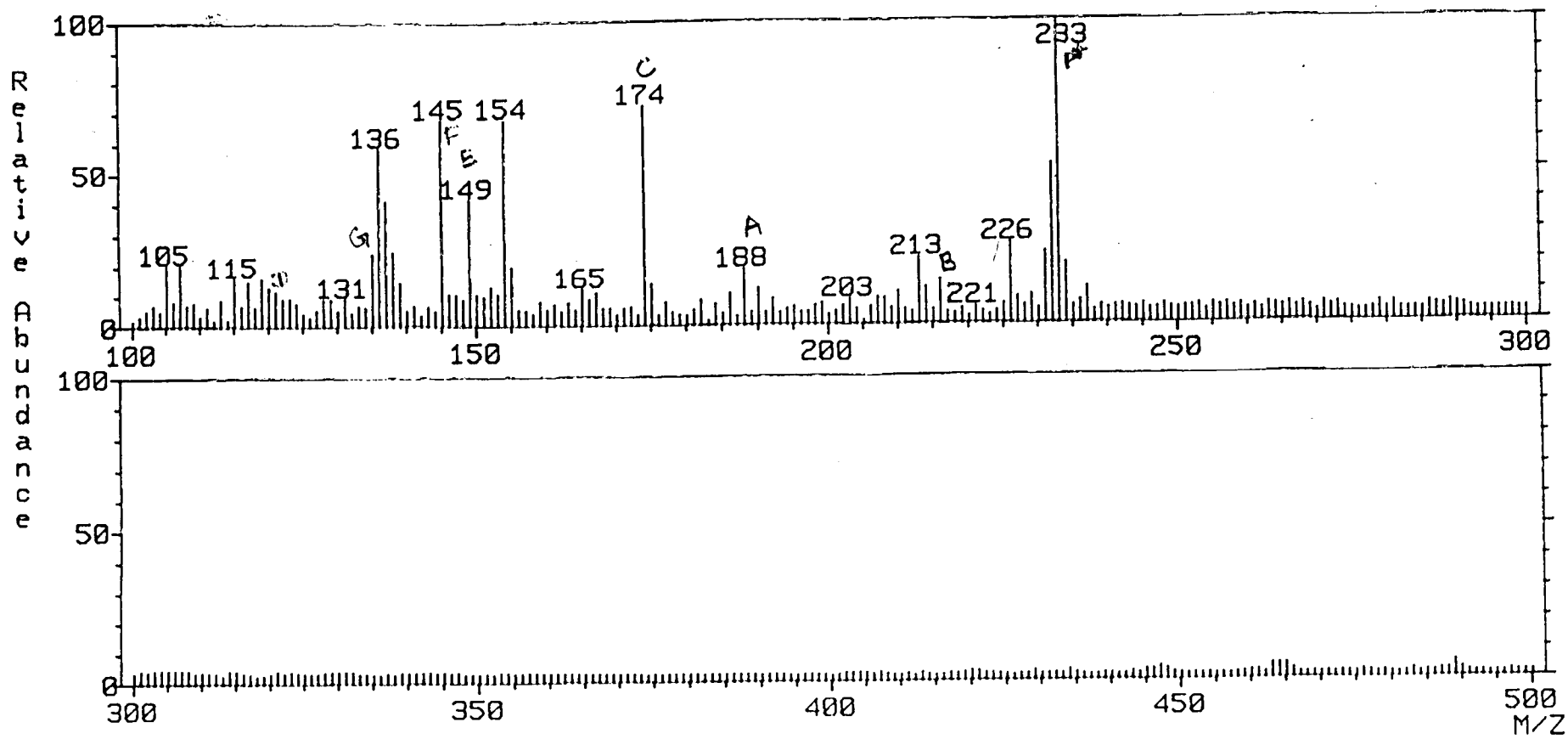
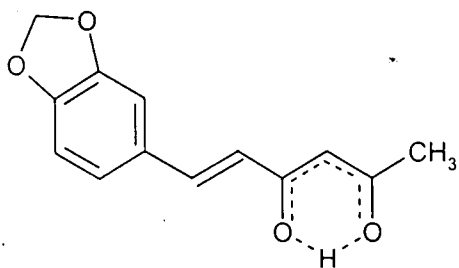


Fig. 2.8. Mass spectrum of 2c

53

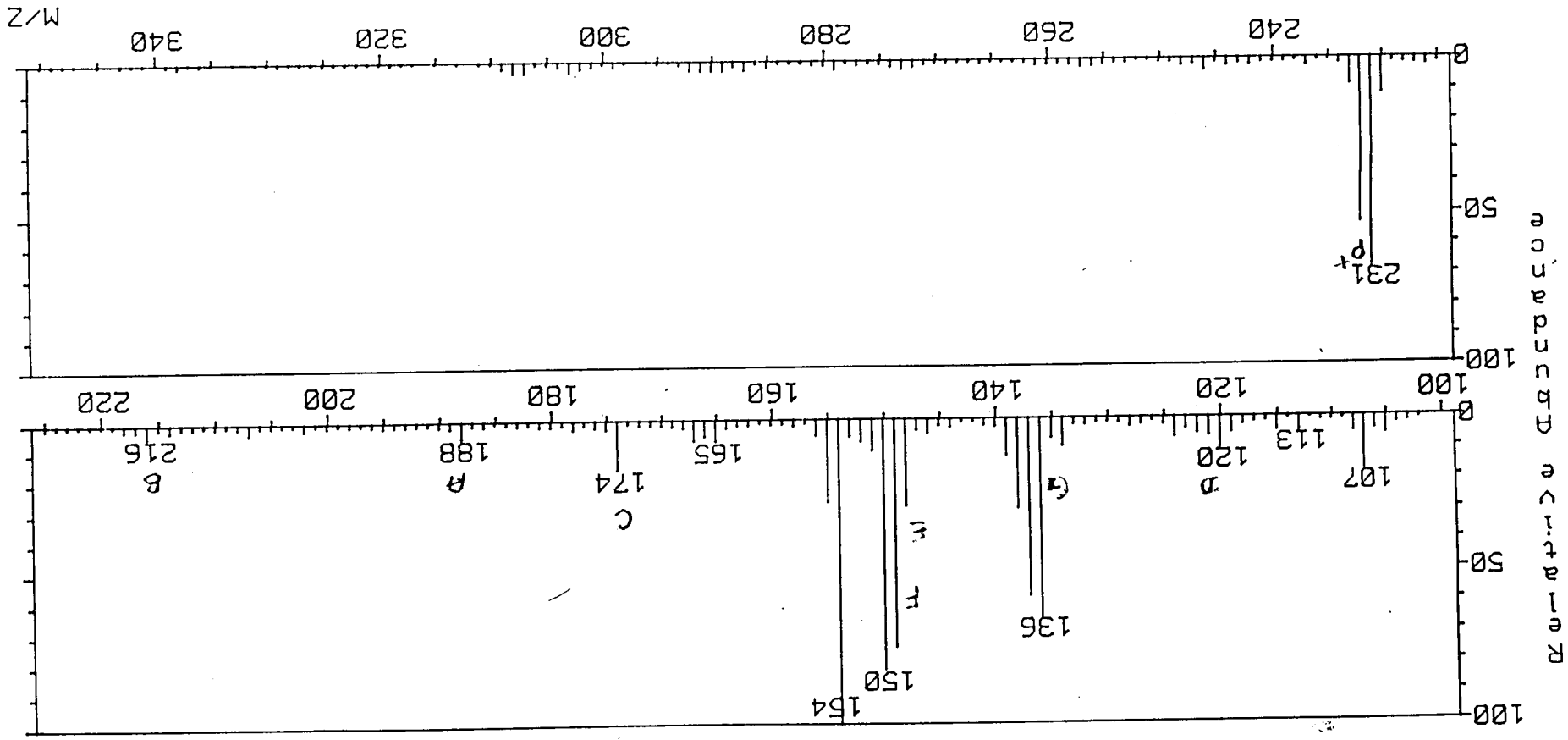
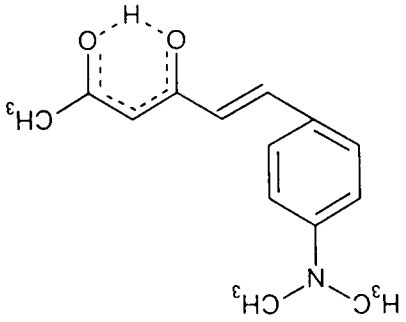
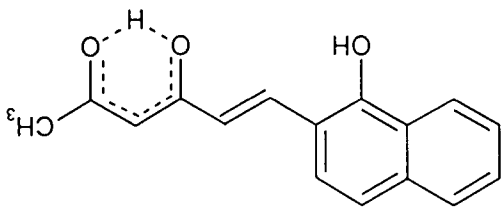
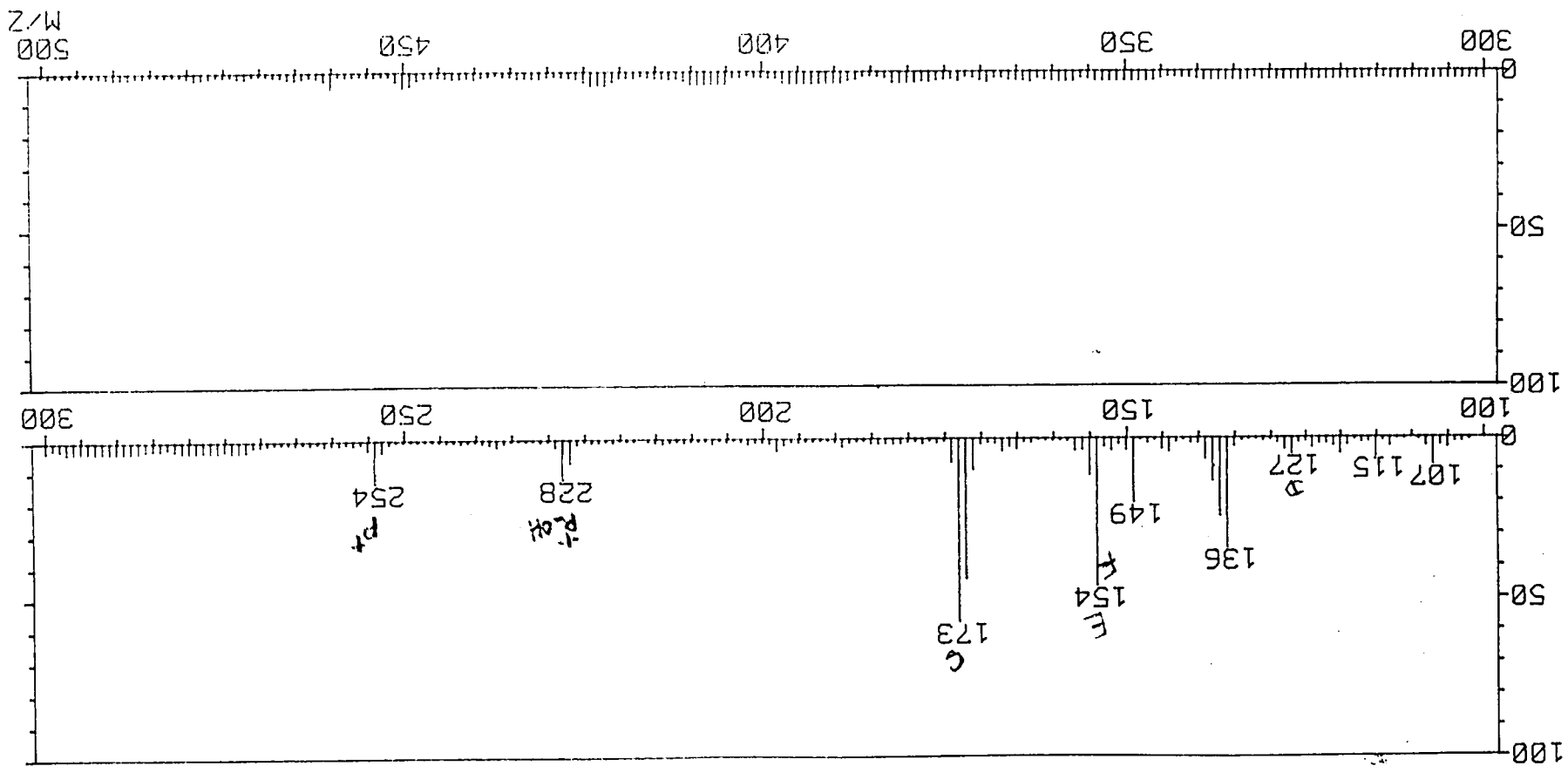


Fig. 2.9. Mass spectrum of 2d

Fig. 2.10. Mass spectrum of 2c



43

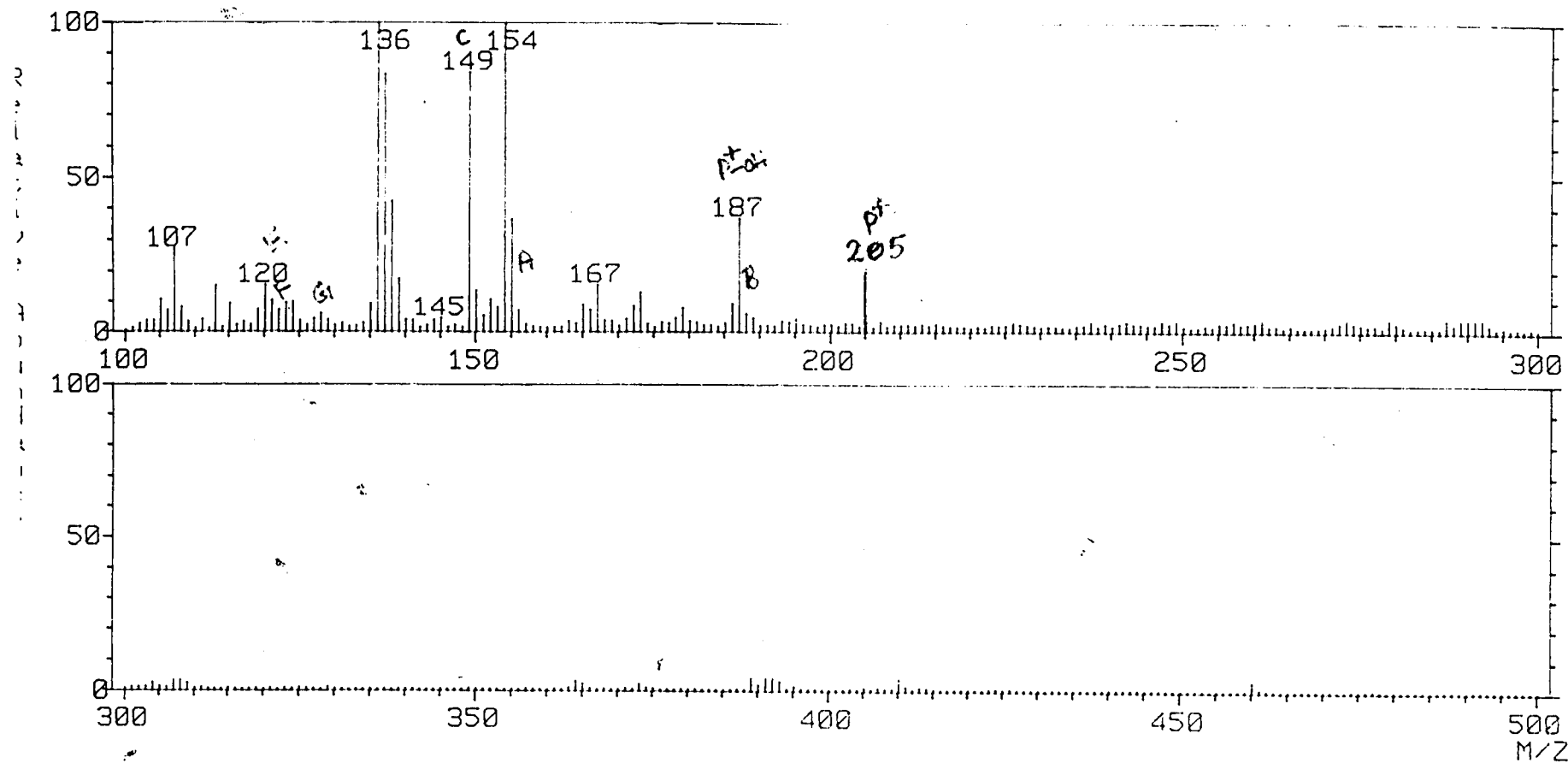
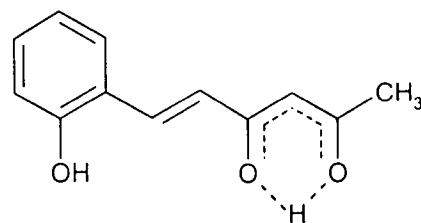
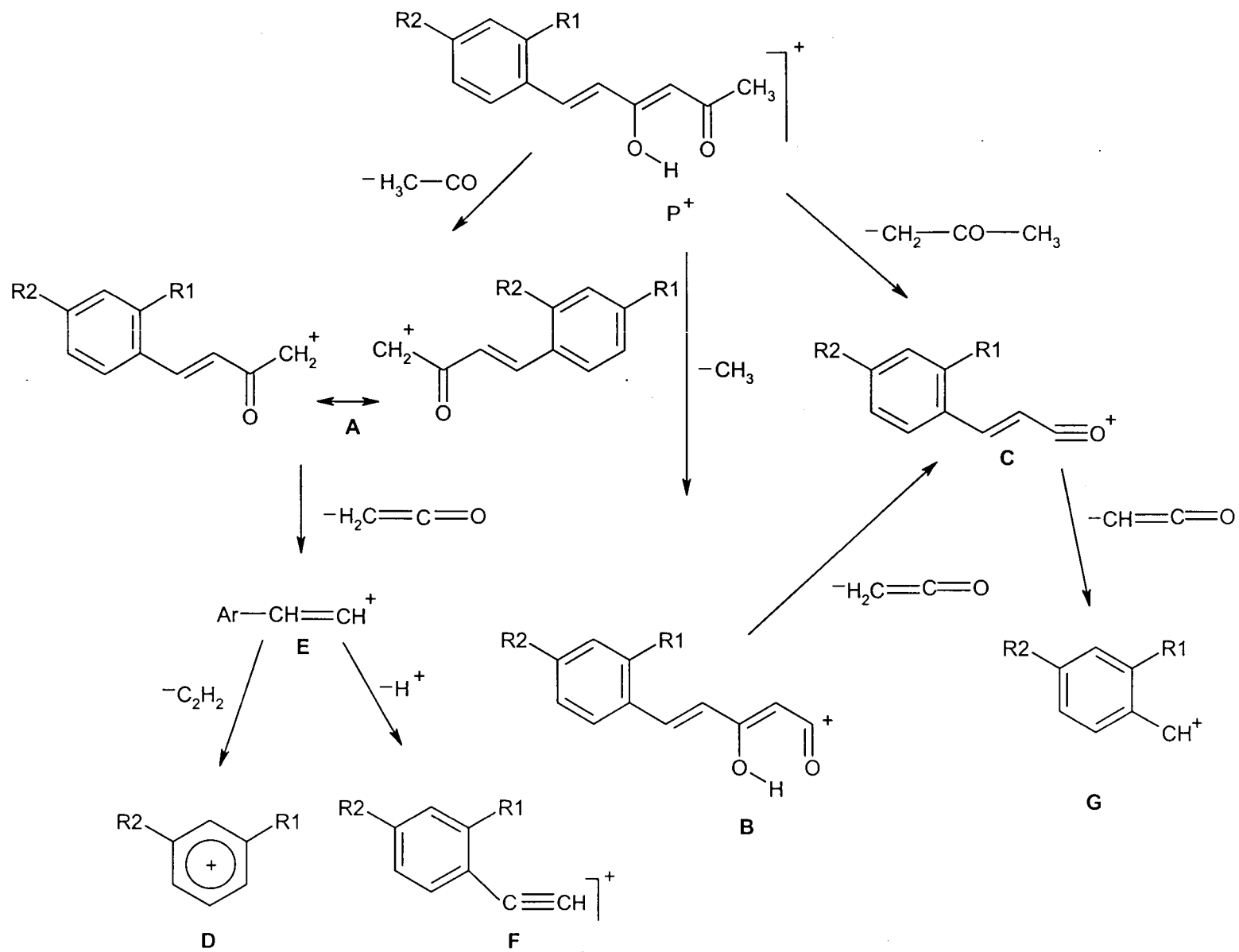


Fig. 2.11. Mass spectrum of 2f

from the molecular ion explains the origin of the intense (P-43)⁺ peak, a characteristic of all the spectra. Other prominent peaks appeared in the spectra are due to (P - CH₃CoCH₂)⁺, (P - CH₃COCH₂CO)⁺, ArCH⁺, Ar⁺, etc. Important peaks appeared in the spectra of all the 6-(substituted aryl)hexanoids can be conveniently explained by the fragmentation pattern given in **scheme 2.2**. Thus all these spectral evidence support the structure 2.1 of the compounds.

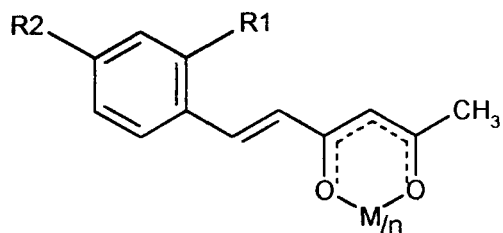
Characterisation of metal chelates of 6-(substituted aryl)hexanoids

The observed analytical and physical data of the metal chelates given in tables 2.5-2.11 agreed well with the [ML₂] stoichiometry for copper(II), nickel(II), cobalt(II) and oxovanadium(IV) complexes and [ML₃] in the case of Fe(III) complexes. The conductivity measurements (10⁻³ M solution in dmf) indicated their non ionic nature (specific conductance < 10 Ω⁻¹ cm⁻¹). Copper(II), cobalt(II), iron(III) and oxovanadium(IV) complexes showed normal magnetic moments while nickel(II) complexes are diamagnetic. The structure and nature of bonding in the metal complexes were established on the basis of their electronic, ir, ¹H nmr and mass spectral data.



Scheme 2.2 Fragmentation Pattern for 2a - f

96



$M = \text{Cu}^{+2}, \text{Ni}^{+2}, \text{Co}^{+2}$ for $n = 2$

and $M = \text{Fe}^{+3}$ for $n = 3$

2.2

Uv spectra

The uv absorption maxima of the complexes bear close resemblance to that of the free ligands indicating that no structural alternation of the ligand has occurred during complexation. The $n \rightarrow \pi^*$ transition of the carbonyl chromophore of the free ligands showed a slight bathochromic shift indicating the involvement of dicarbonyl moiety in the chelate formation. The spectral data are included in tables 2.5-2.8.

TABLE 2.5

Analytical and characteristic uv spectral data of copper(II) complexes of the substituted 6-aryl-5-hexene-2,4-diones, 2a-f

Copper(II) chelate of (Molecular formula)*	Yield %	M.P. °C	μ_{eff} (B.M.)	Elemental Analysis % calculated / (found)			λ_{max} (nm)
				C	H	M	
2a (C ₁₃ H ₁₅ O ₂) ₂ Cu	70	234	1.78	67.01 (66.95)	5.58 (5.57)	13.65 (13.63)	314 409
2b (C ₁₄ H ₁₁ O ₃) ₂ Cu	65	230	1.80	63.94 (63.81)	5.71 (5.70)	12.09 (12.07)	333 443
2c (C ₁₆ H ₁₁ O ₄) ₂ Cu	70	232	1.75	59.37 (59.31)	4.18 (4.17)	12.09 (12.07)	285 391
2d (C ₁₄ H ₁₆ NO ₂) ₂ Cu	70	228	1.76	64.18 (64.12)	6.11 (6.10)	12.13 (11.88)	288 416
2e (C ₁₆ H ₁₃ O ₃) ₂ Cu	65	> 300	1.81	67.31 (67.42)	4.56 (4.55)	11.16 (11.14)	318 370
2f (C ₁₂ H ₁₁ O ₃) ₂ Cu	55	> 300	1.79	61.34 (61.15)	4.69 (4.67)	13.53 (13.49)	308

*The molecular formula given correspond to [CuL₂] stoichiometry, where L stands for the deprotonated ligand moiety.

TABLE 2.6

Analytical and characteristic uv spectral data of nickel(II) complexes of 6-aryl-5-hexene-2,4-diones, 2a-f

Nickel(II) chelate of (Molecular formula)*	Yield %	M.P. °C	Elemental Analysis % calculated / (found)			λ_{\max} (nm)
			C	H	M	
2a (C ₁₃ H ₁₃ O ₂) ₂ Ni	75	> 300	67.73 (67.53)	5.64 (5.62)	12.74 (12.70)	289 409
2b (C ₁₄ H ₁₅ O ₃) ₂ Ni	70	236	64.53 (64.36)	5.76 (5.74)	11.27 (11.24)	530 416
2c (C ₁₃ H ₁₁ O ₄) ₂ Ni	75	> 300	59.92 (59.77)	4.22 (4.21)	11.27 (11.24)	286 397
2d (C ₁₄ H ₁₆ NO ₂) ₂ Ni	75	284	64.78 (64.61)	6.16 (6.15)	11.3 (11.28)	288 409
2e (C ₁₆ H ₁₃ O ₃) ₂ Ni	55	> 300	68.01 (67.84)	4.60 (4.59)	10.39 (10.36)	319 359
2f (C ₁₂ H ₁₁ O ₃) ₂ Ni	50	280	61.97 (61.8)	4.73 (4.72)	12.63 (12.59)	297

*The molecular formula given correspond to [NiL₂] stoichiometry, where L stands for the deprotonated ligand moiety.

TABLE 2.7

**Analytical and characteristic uv spectral data of cobalt(II) complexes of
6-aryl-5-hexene-2,4-diones, 2a-f**

Cobalt(II) chelate of (Molecular formula)*	Yield %	M.P. °C	μ_{eff} (B.M.)	Elemental Analysis % calculated / (found)			λ_{max} (nm)
				C	H	M	
2a (C ₁₃ H ₁₃ O ₂) ₂ Co(H ₂ O) ₂	75	260	4.90	67.69 (67.56)	5.6 (5.4)	12.78 (12.72)	299 400
2b (C ₁₄ H ₁₅ O ₃) ₂ Co(H ₂ O) ₂	60	210	4.79	64.5 (64.36)	5.76 (5.74)	11.31 (11.28)	315 416
2c (C ₁₃ H ₁₁ O ₄) ₂ Co(H ₂ O) ₂	70	230	4.89	59.99 (55.37)	4.22 (4.45)	11.31 (11.29)	277 402
2d (C ₁₄ H ₁₆ NO ₂) ₂ Co(H ₂ O) ₂	75	250	4.77	64.75 (64.03)	6.17 (6.05)	11.36 (11.35)	289 415
2e (C ₁₆ H ₁₃ O ₃) ₂ Co(H ₂ O) ₂	60	285	4.82	67.98 (67.84)	4.60 (4.59)	10.43 (10.41)	318 359
2f (C ₁₂ H ₁₁ O ₃) ₂ Co(H ₂ O) ₂	50	230	4.84	61.95 (61.8)	4.73 (4.72)	12.68 (12.64)	308

*The molecular formula given correspond to [CoL₂(H₂O)₂] stoichiometry, where L stands for the deprotonated ligand moiety.

TABLE 2.8

**Analytical and characteristic uv spectral data of iron(III) complexes of
6-aryl-5-hexene-2,4-dione, 2a-f**

Iron(III) chelate of (Molecular formula)*	Yield %	M.P. °C	μ_{eff} (B.M.)	Elemental Analysis % calculated / (found)			λ_{max} (nm)
				C	H	M	
2a (C ₁₃ H ₁₃ O ₂) ₃ Fe	70	> 300	5.92	71.03 (70.90)	5.92 (5.90)	8.48 (8.46)	330
2b (C ₁₄ H ₁₅ O ₃) ₃ Fe	60	240	5.89	67.3 (67.2)	6.007 (6.00)	8.75 (7.44)	416
2c (C ₁₃ H ₁₃ O ₄) ₃ Fe	70	> 300	5.90	62.5 (62.4)	4.409 (4.4)	7.5 (7.44)	361 408
2d (C ₁₄ H ₁₄ NO ₂) ₃ Fe	50	> 300	5.87	67.58 (67.46)	6.44 (6.42)	7.49 (7.46)	346 416
2e (C ₁₆ H ₁₃ O ₃) ₃ Fe	55	250	5.83	70.69 (70.58)	4.79 (4.78)	6.85 (6.84)	317 352
2f (C ₁₂ H ₁₃ O ₃) ₃ Fe	50	> 300	5.92	64.98 (64.86)	4.96 (4.95)	8.40 (8.38)	312

*The molecular formula given correspond to [FeL₃] stoichiometry, where L stands for the deprotonated ligand moiety.

Infrared spectra

Both the carbonyl bands of the free ligands shifted to lower frequency in the ir spectra of all the complexes and these band appeared in the region 1550-1600 cm^{-1} assignable to metal bonded carbonyl vibrations. In addition to this various $\nu_{\text{C}=\text{C}}$ vibrations also appeared in the ir region of the spectra of complexes. Further evidence for the involvement of the carbonyl groups in metal chelate formation is evident from the appearance of two medium intensity bands in the region 400-500 cm^{-1} due to $\nu_{\text{M}-\text{O}}$ vibrations. All these factors supports the structure 2.2 for these complexes. The position of the trans CH=CH bands ($\sim 960 \text{ cm}^{-1}$) remains unaltered in the case of metal complexes. The replacement of the enol proton by metal ion is evident from the disappearance of the broad absorption band of the free ligands in the region 2500-3500 cm^{-1} . However in the spectra of **2e** and **2f** show a relatively broad medium intensity band at $\sim 3200 \text{ cm}^{-1}$ assignable to $\nu_{\text{O}-\text{H}}$ vibration. This suggests that the phenolic OH group of **2e** and **2f** remains free and not involved in bonding with the metal ion. The ir spectral data of the various metal complexes are given in table 2.9-2.13.

TABLE 2.9

**Characteristic ir data (cm⁻¹) of the copper(II) chelate of the
6-aryl-5-hexene-2,4-diones**

Copper(II) chelate of						Probable assignment
2a	2b	2c	2d	2e	2f	
1624	1640	1631	1628	1624	--	$\nu_{C=O}$ (metal coordinated acetyl)
1590	1614	1602	1607	1537	1595	$\nu_{C=O}$ (metal coordinated cinnamonyl)
1575 1518	1580 1512	1585 1523	1590 1507	1457 1427	1485 1459	$\nu_{C=C}$ phenyl / alkenyl
1480	1470	1470	1480	1401	1384	$\nu_{asym} C-C-C$ (chelate ring)
1460	1450	14435	1450	1368	1350	$\nu_{sym} C-C-C$ (chelate ring)
1103 1040	1170 1120 1043	1180 1103 1029	1157 1026	1140 1025	1130 1038	β_{C-H} (chelate ring)
971	960	968	951	978	987	$\nu_{CH=CH}$ trans
732	720	720	737	742	762	ν_{C-H} chelating
490	493	476	476	467	460	ν_{M-O} chelate ring

TABLE 2.10
**Characteristic ir data (cm⁻¹) of nickel(II) chelate of the
 6-aryl-5-hexene-2,4-diones**

Nickel(II) chelate of						Probable assignment
2a	2b	2c	2d	2e	2f	
1627	1640	1635	1631	1605	1603	$\nu_{C=O}$ (metal coordinated acetyl)
1585	1606	1605	1607	1541	1550	$\nu_{C=O}$ (metal coordinated cinnamonyl)
1562 1515	1580 1512	1580 1512	1585 1510	1460 1395	1486 1381	$\nu_{C=C}$ phenyl / alkenyl
1480	1475	1485	1485	1367	1365	$\nu_{asym} C-C-C$ (chelate ring)
1450	1450	1450	1440	1310	1320	$\nu_{sym} C-C-C$ (chelate ring)
1171 1102 1030	1166 1105 1047	1172 1099 1033	1163 1161 1060 1025	1186 1040	1184 1041	β_{C-H} (chelate ring)
975	981	975	968	978	935	$\nu_{CH=CH}$ trans
730	725	740	763	744	753	ν_{C-H} chelating
495	486	488	469	490	485	ν_{M-O} chelate ring

TABLE 2.11

**Characteristic ir data (cm^{-1}) of cobalt(II) chelate of the
6-aryl-5-hexene-2,4-diones**

Cobalt(II) chelate of						Probable assignment
2a	2b	2c	2d	2e	2f	
1626	1625	1640	1640	1639	1641	$\nu_{\text{C=O}}$ (metal coordinated acetyl)
1585	1600	1605	1606	1540	1558	$\nu_{\text{C=O}}$ (metal coordinated cinnamonyl)
1555 1513	1585 1513	1580 1512	1585 1515	1507 1420	1521 1410	$\nu_{\text{C=C}}$ phenyl / alkenyl
1480	1474	1485	1394	1394	1384	$\nu_{\text{asym C-C-C}}$ (chelate ring)
1450	1427	1440	1430	1361 1301	1320	$\nu_{\text{sym C-C-C}}$ (chelate ring)
1170 1103 1027	1169 1109 1043	1174 1099 1033	1166 1126 1040	1162 1043	1150 1026	$\beta_{\text{C-H}}$ (chelate ring)
972	976	970	948	976	925	$\nu_{\text{CH=CH}}$ trans
731	730	730	725	744	763	$\nu_{\text{C-H}}$ chelating
515 471	519 418	478 418	484 418	459 426	466 418	$\nu_{\text{M-O}}$ chelate ring

TABLE 2.12

**Characteristic ir data (cm⁻¹) of oxovanadium(IV) chelate of
6-aryl-5-hexene-2,4-diones**

Oxovanadium(II) chelate of					Probable assignment
2b	2c	2d	2e	2f	
1620	1633	1659	1637	1593	$\nu_{C=O}$ (metal coordinated acetyl)
1601	1593	1610	1542	1553	$\nu_{C=O}$ (metal coordinated cinnamonyl)
1570 1511	1580 1500	1593 1513	1461 1394	1513 1447	$\nu_{C=C}$ phenyl / alkenyl
1477	1485	1455	1360	1374	$\nu_{asym} C-C-C$ (chelate ring)
1455	1447	1434	1315	1308	$\nu_{sym} C-C-C$ (chelate ring)
1173 1088 1044	1175 1102 1023	1162 1062 1029	1156 1020	7175 1069	β_{C-H} (chelate ring)
982	975	976	950	956	$\nu_{CH=CH}$ trans
728	751	725	760	777	ν_{C-H} chelating
475	498	479	491	489	ν_{M-O} chelate ring

NB 2997
 541.2242 TH
 MAT/M

TABLE 2.13

Characteristic ir data (cm^{-1}) of iron(III) chelate of
 6-aryl-5-hexene-2,4-diones

Iron(III) chelate of					Probable Assignments
2a	2b	2c	2e	2f	
1635	1635	1623	1629	1602	$\nu_{\text{C=O}}$ (metal coordinated acetyl)
1618	1604	1599	1570	1565	$\nu_{\text{C=O}}$ (metal coordinated cinnamonyl)
1575 1515	1590 1512	1580 1500	1514 1460 1388	1514 1454 1385	$\nu_{\text{C=C}}$ phenyl / alkenyl
1485	1485	1485	1365	1356	$\nu_{\text{asym C-C-C}}$ (chelate ring)
1459	1455	1448	1309		$\nu_{\text{sym C-C-C}}$ (chelate ring)
1164 1104 1032	1166 1112 1041	1126 1103 1033	1199 1085	1150 1034	$\beta_{\text{C-H}}$ (chelate ring)
976	989	972	977	955	$\nu_{\text{CH=CH}}$ trans
735	722	730	746	754	$\nu_{\text{C-H}}$ chelating
490	484 418	485 475	468 418	485 425	$\nu_{\text{M-O}}$ chelate ring

^1H nmr spectra

The proton nmr spectra of the diamagnetic nickel(II) complexes of the 6-(substituted aryl)-hexanoids are reproduced in figure 2.12 to 2.13. The enolic proton signal ($\sim \delta$ 16 ppm) of the free ligand disappeared in the spectra of the complexes. This indicates the replacement of the enolic proton by metal ion during

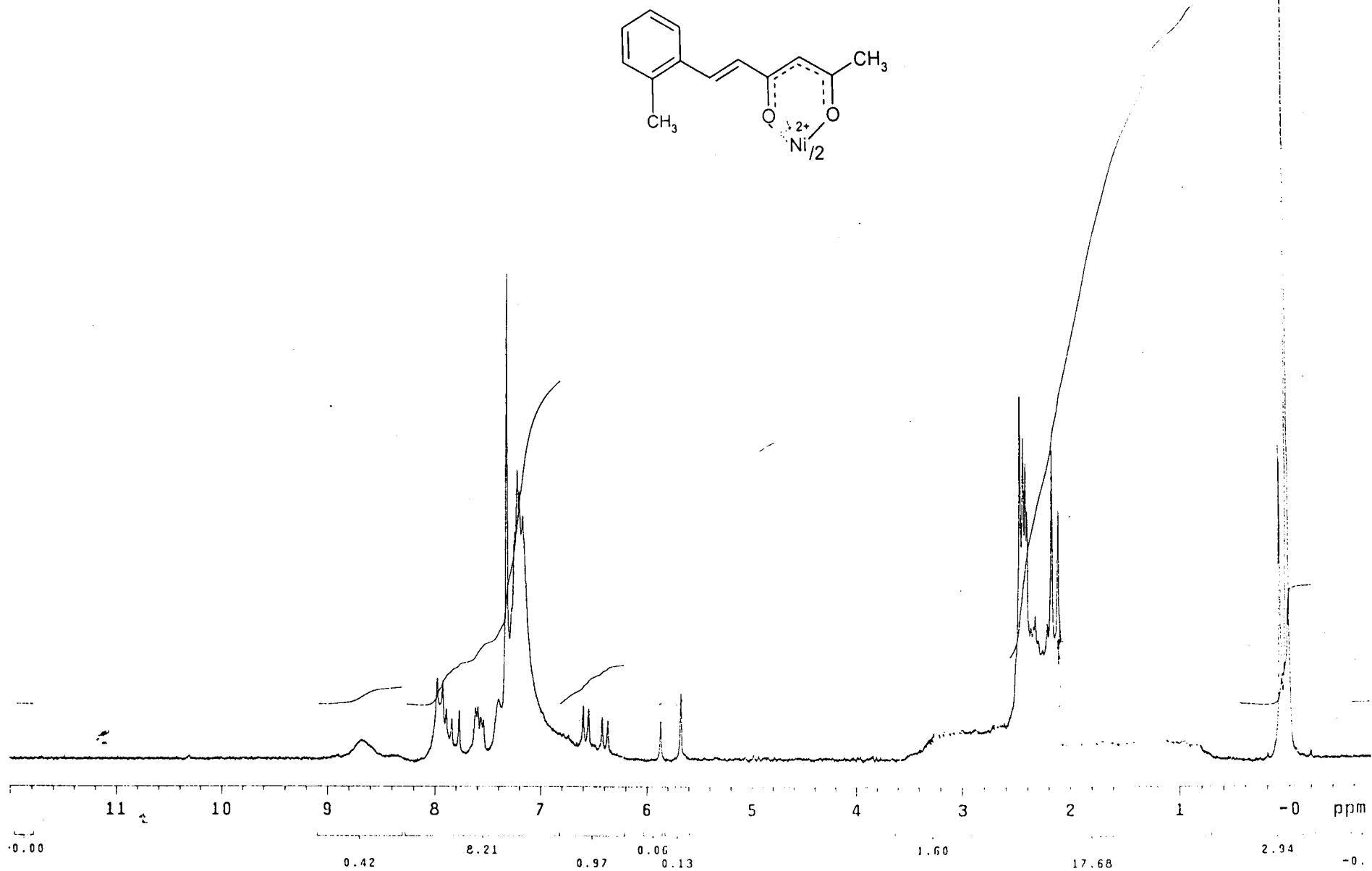
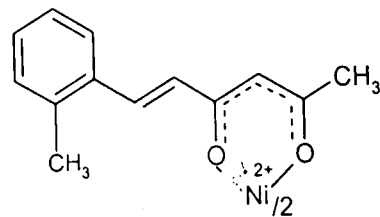


Fig. 2.12. ¹H NMR spectrum of nickel(II) complex of 2a

107

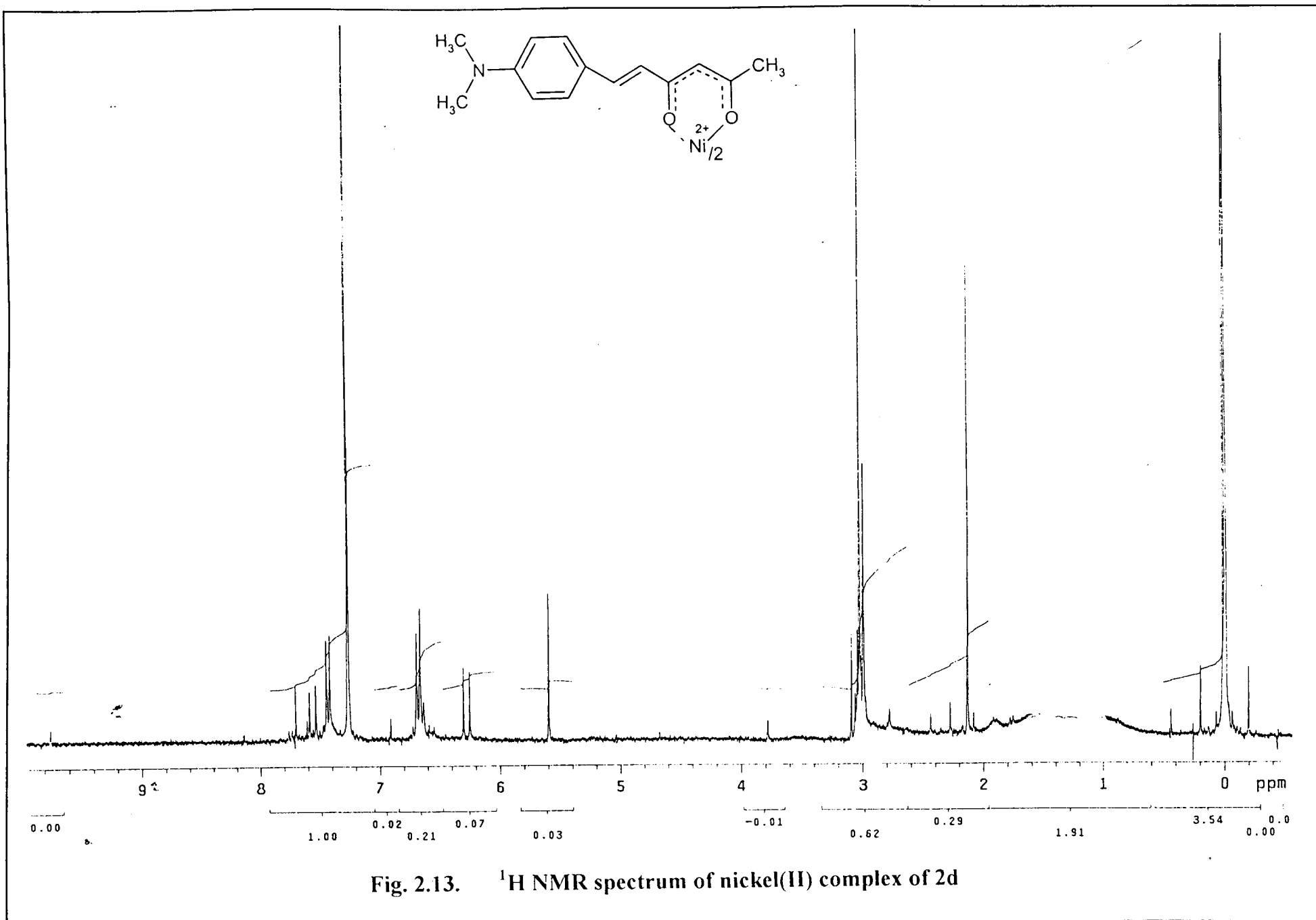


Fig. 2.13. ¹H NMR spectrum of nickel(II) complex of 2d

103

complexation. The methine proton signals are shifted towards the downfield region of the spectra indicating the decreased electron density around the central carbon atom of the pseudo aromatic metal chelate ring system. The integrated intensities of the methyl, aryl, aryl substituents and alkenyl signals are in agreement with their formulation. The phenolic proton signal of the complexes of **2e** and **2f** remains unaltered and this strongly support the fact that the phenolic proton is not involved in bonding with metal ion.

Mass spectra

The FAB mass spectra of copper(II) complexes of the 6-(substitutedaryl) hexanoids (**2a-2f**) are reproduced in figures 2.14 to 2.19. All the complexes show a relatively intense $P^+/(P+1)^+$ peaks in agreement with their $[ML_2]$ stoichiometry. The base peak in all the spectra are due to the ligand moiety and peaks due to $[CuL]^+$, L^+ and fragments of L^+ are sometimes more intense than the molecular ion peak. Intense peaks due to the elimination of CH_3 , CH_3CO , CH_3COCH_2 groups from the molecular ion are also observed. The suggested formulation and structure of the complexes clearly in agreement with the observed spectra of the copper complexes.

Esr spectra of copper complexes of 6-arylhaxanoids

Complexes of copper(II), a d^9 metal ion have been very popular for ESR studies. This is mainly because Cu(II) with a nuclear spin of $3/2$ give rise to a clearly resolvable nuclear hyperfine structure and the structures are usually close to

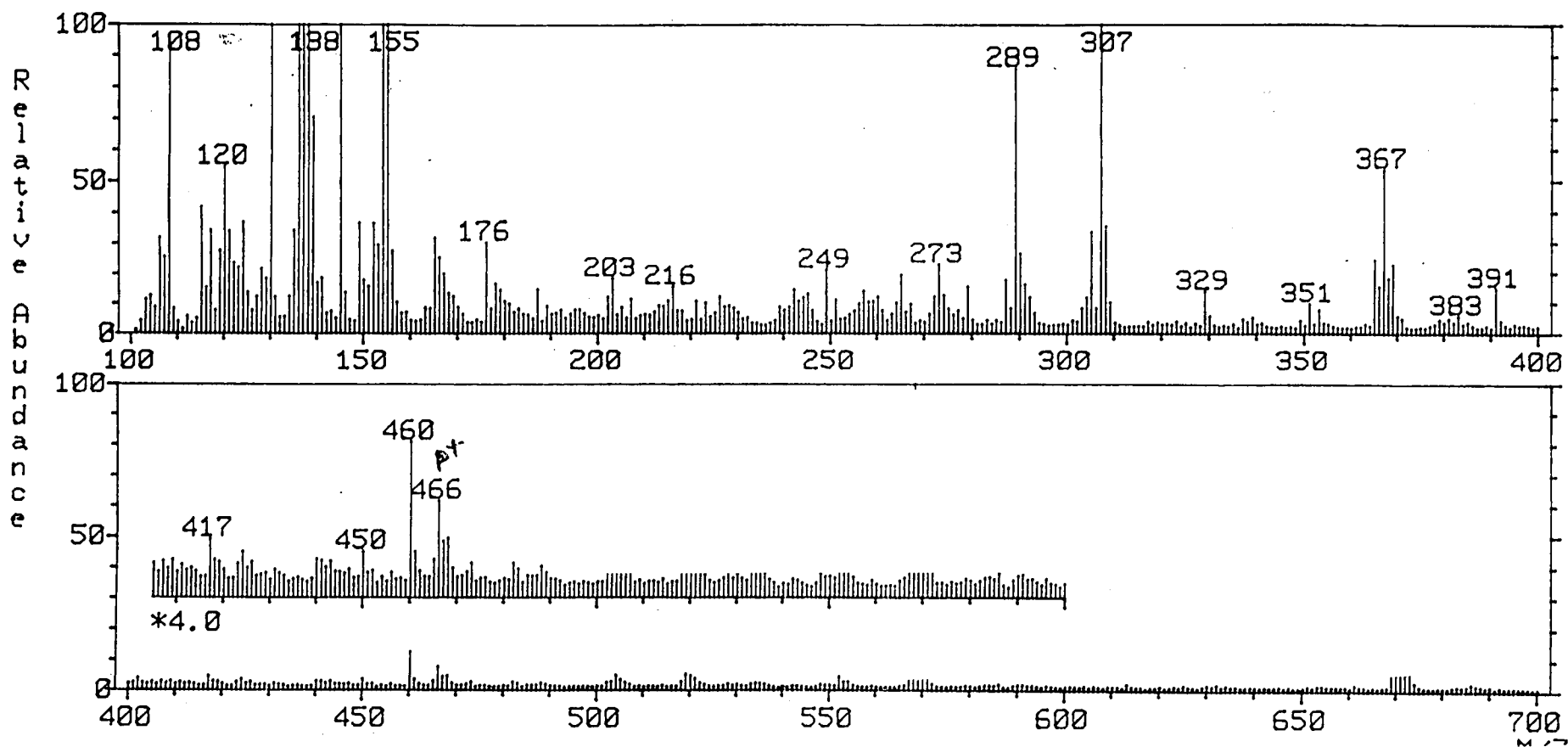
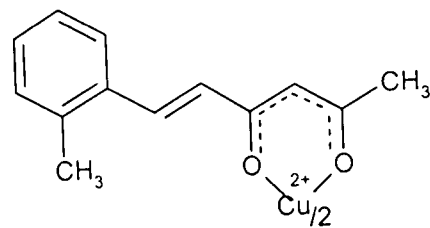


Fig. 2.14. Mass spectrum of copper(II) complex of 2a

105

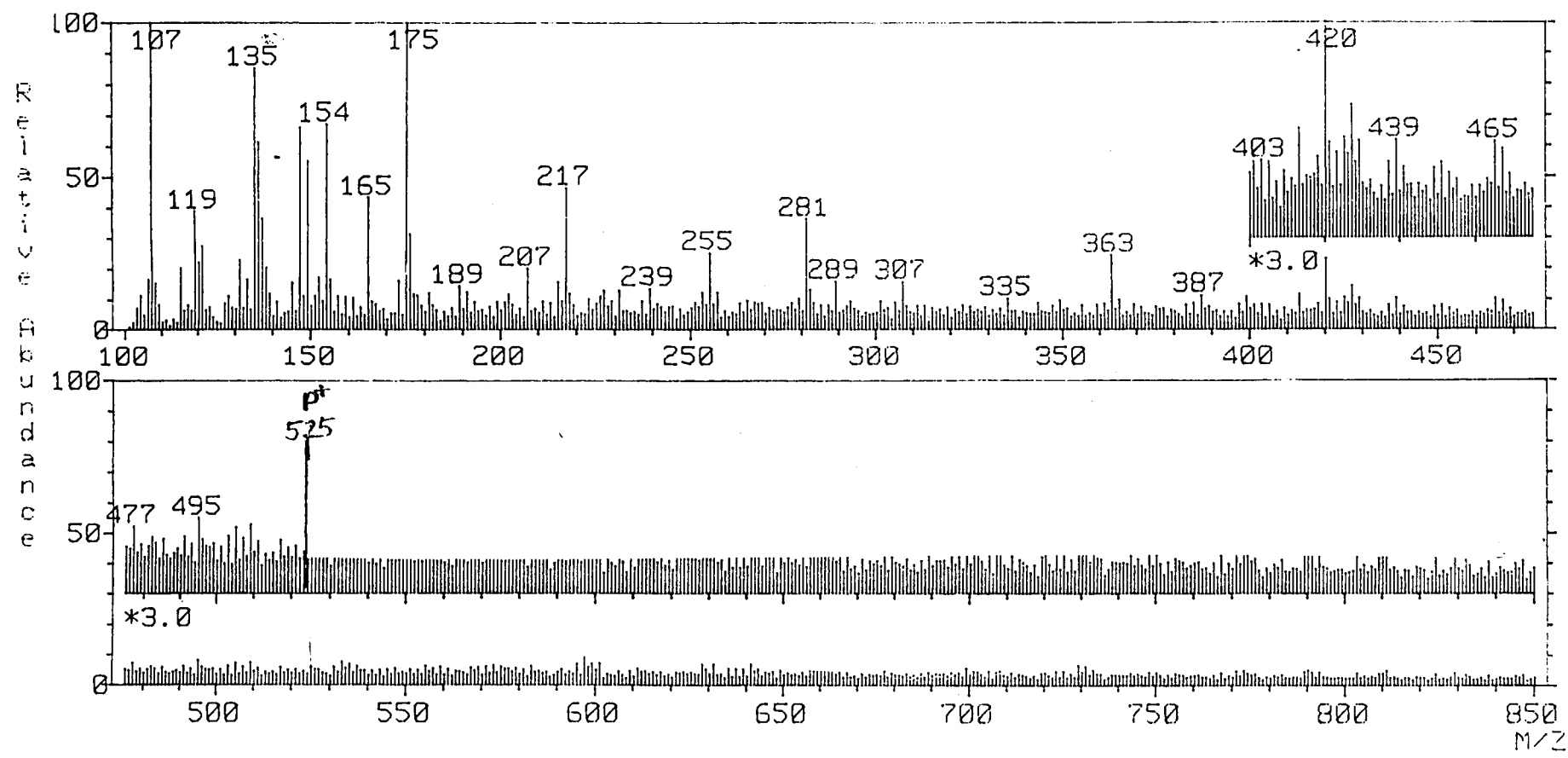
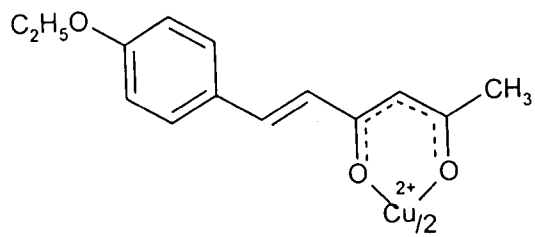


Fig. 2.15. Mass spectrum of copper(II) complex of 2b

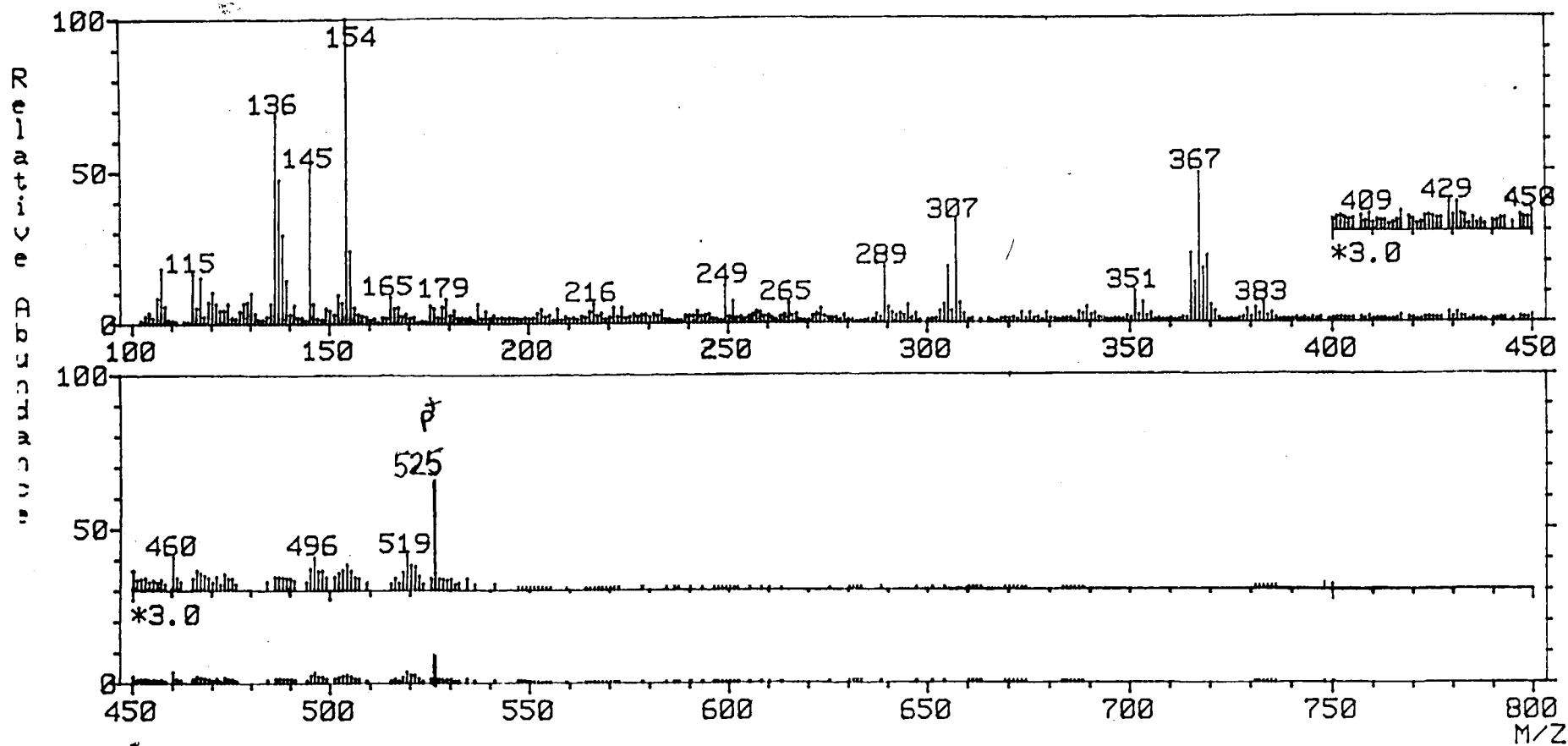
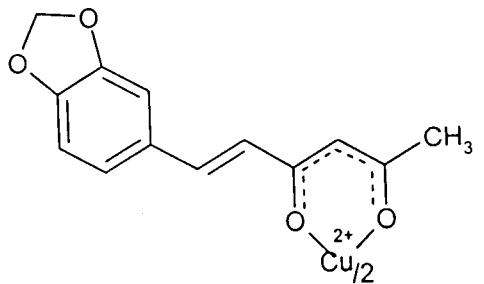


Fig. 2.16. Mass spectrum of copper(II) complex of 2c

101

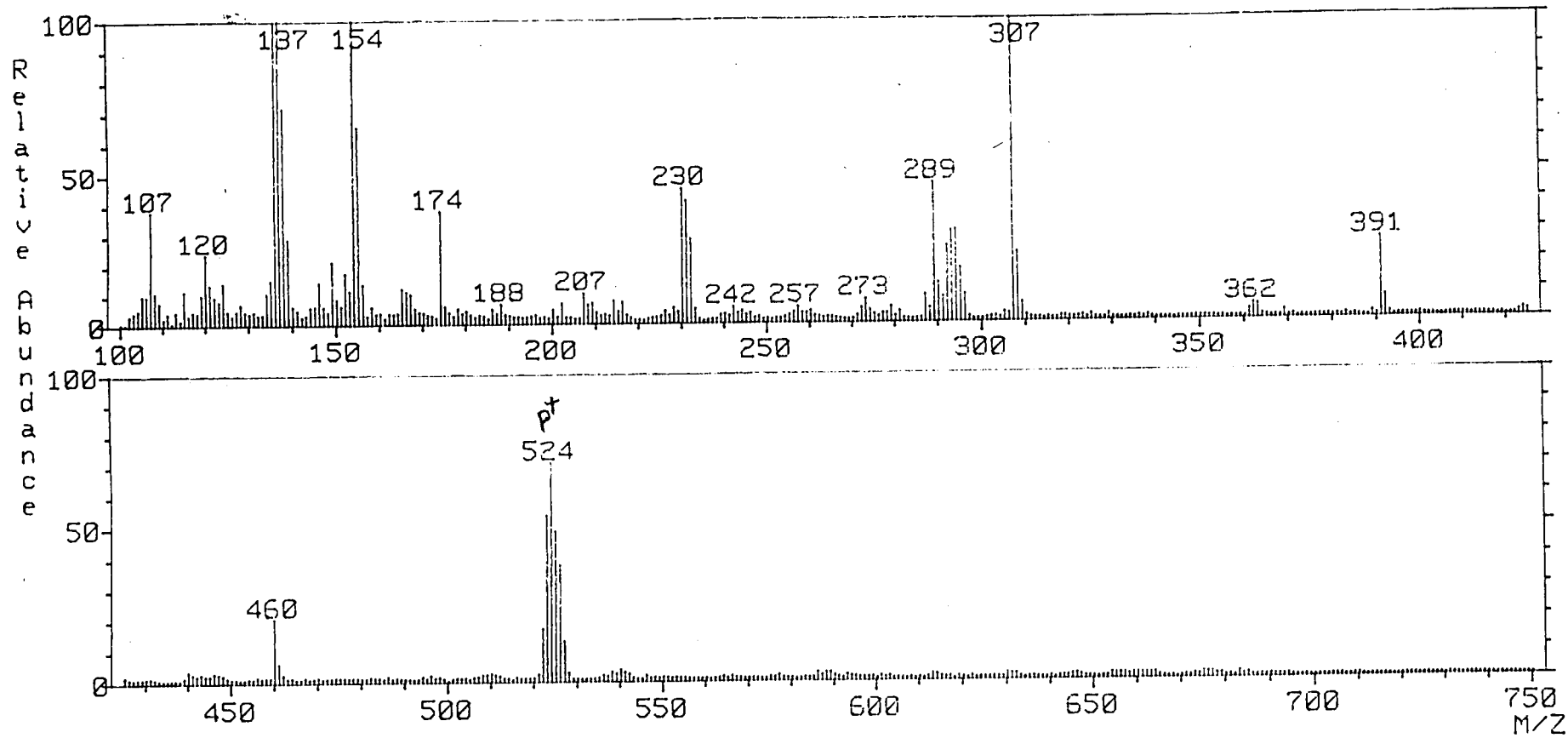
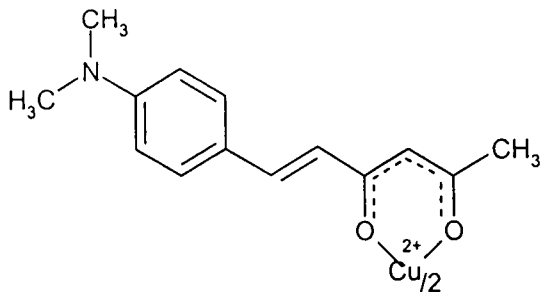


Fig. 2.17. Mass spectrum of copper(II) complex of 2d

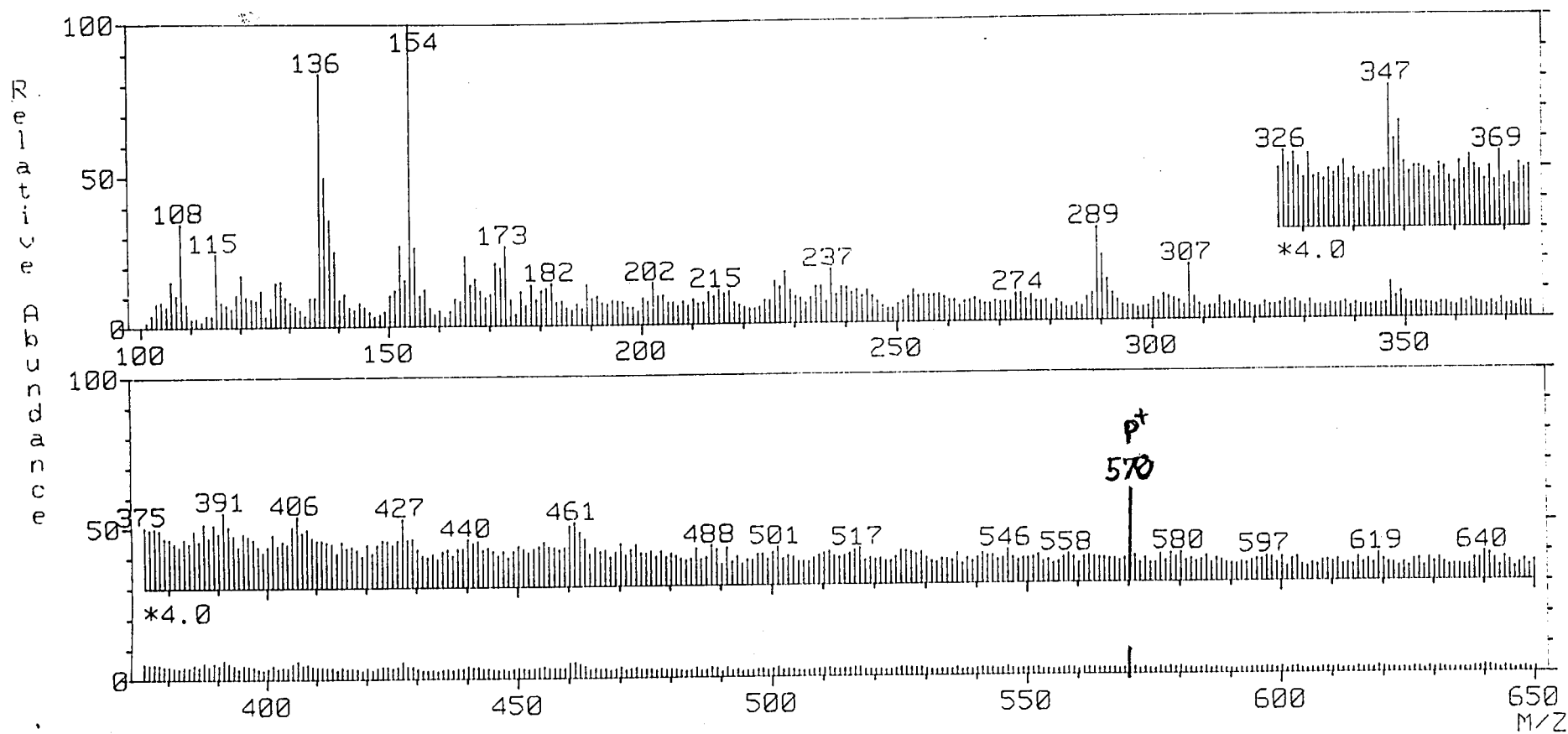
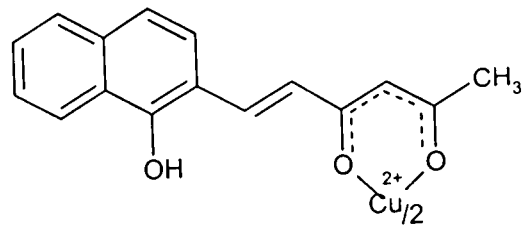


Fig. 2.18. Mass spectrum of copper(II) complex of 2e

109

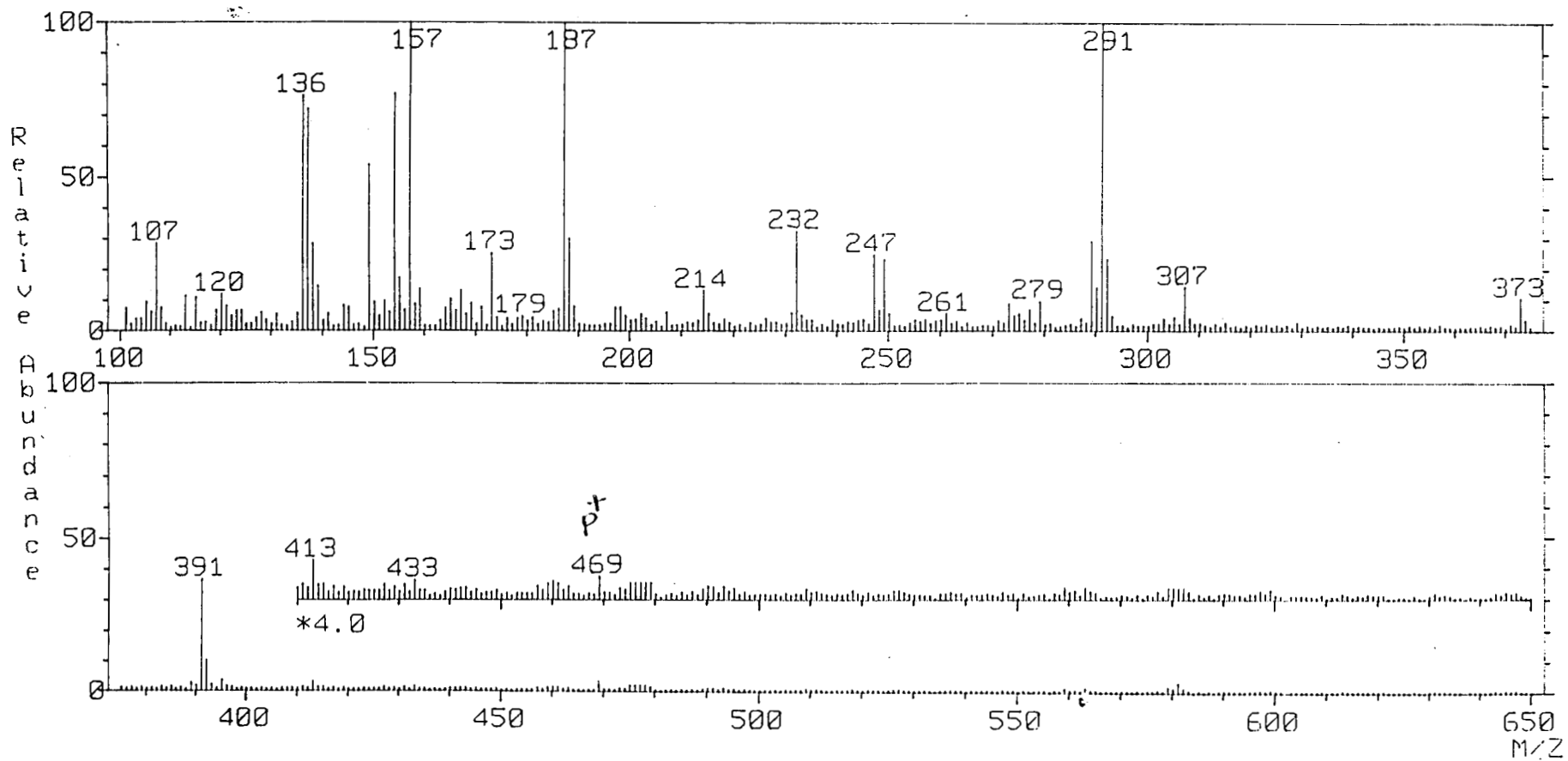
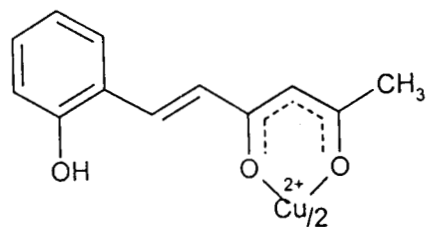
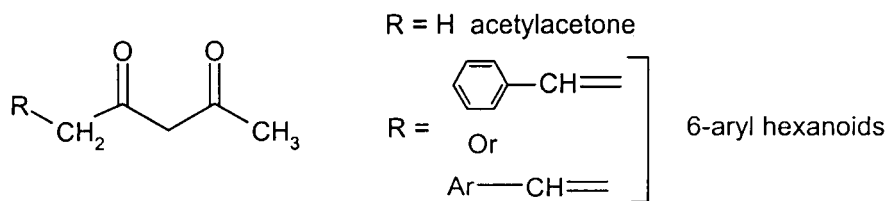


Fig. 2.19. Mass spectrum of copper(II) complex of 2f

square planar thus simplifying the theoretical analysis. In square planar configuration the unpaired electron will be in the d orbital of suitable symmetry to form bonds with the ligands. This feature makes Cu(II) complexes a highly useful system for studying the influence of ligands on the nature of metal-ligand bond, especially the electronic effects of substituents on the ligand species. This aspect has been clearly demonstrated in the case of copper(II) complex of acetylacetonone and related ligand systems.¹³¹⁻¹³⁶

The 6-arylhexanoids considered in the present investigation are related to acetylacetonone in the sense that both the carbonyl groups are linked to methyl groups. However there exist an important structural differences that in one of the CH₃ group, two H atoms are substituted by a Ar-CH= group. This substitution of Ar-CH= group on acetylacetonone will have definite influence on the coordination ability of the compound. With this intention esr spectra of some Cu(II) chelates of 6-arylhexanoids were obtained and the results are discussed below.



The spectrum of the Cu(II) chelate of 6-arylhexanoids **1b**, **2a** and **2d** were recorded at liquid nitrogen temperature (LNT) in dmf solution and are reproduced in

figure 2.20-2.22. The esr data of copper complex of **1b**, **2a** and **2d** are given in table 2.14. Also included in the table the literature data of $\text{Cu}(\text{acac})_2$ (in dmf) and $\text{Cu}(\text{ba})_2$ (in dmf) for comparison purposes. It has been well demonstrated that the electronegativity of the groups attached to the diketo function can influence the g and A values significantly. Thus the g_{\parallel} and g_{\perp} values are greater for $\text{Cu}(\text{hfa})_2$ ($\text{hfa} = \text{CH}_3\text{COCHO}\cdot\text{CF}_3$) and lower for $\text{Cu}(\text{ba})_2$ ($\text{ba} = \text{C}_6\text{H}_5\text{COCHOCH}_3$). The reverse order has been observed for A_{\parallel} and A_{\perp} . In general A values will increase with greater covalency of metal ligand bond, and a g value above 2.30 qualitatively indicates a greater ionic character (for instance g_{\parallel} value reported for CuCl_2 is 2.340, table 2.14).

The solvent (dmf) used for measuring the esr spectra was a strongly coordinating solvent and therefore the geometry of the complex may change and the esr parameter will also change. So the observed values cannot be interpreted as due to a square planar copper complex. It is likely that the complexes will be hexagonally distorted octahedral environment. Similar structural changes have been reported in the case of copper acetylacetonates in dmf, pyridine, etc. solvents¹³¹⁻¹³⁶. The dependence of solvent on g and A values have been well established.

From a comparison of the g values of $\text{Cu}(\text{acac})_2$ in dmf with the values of the copper complexes considered here (Table 2.14) reveal that g_{\parallel} and A_{\parallel} values are

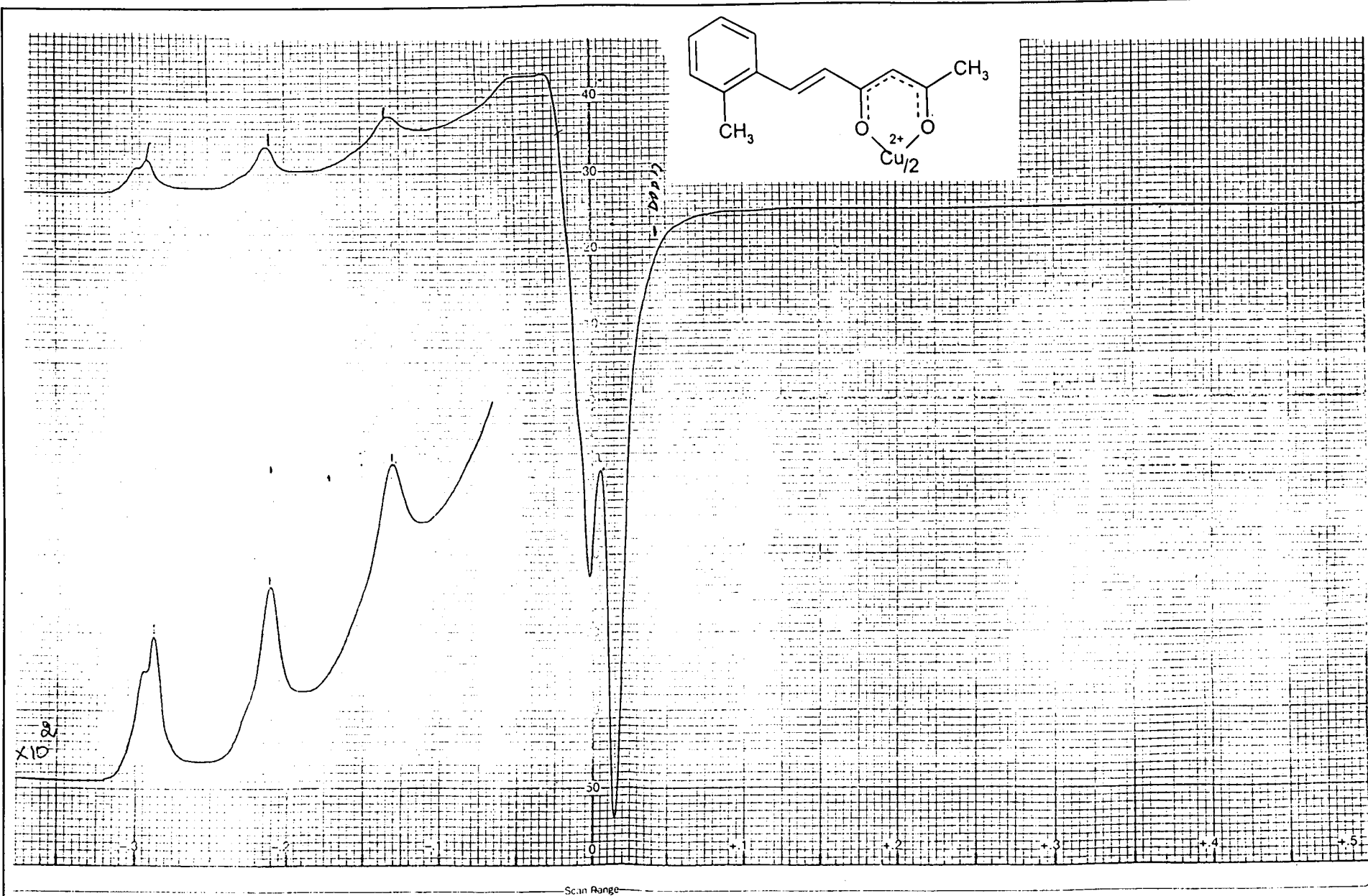


Fig. 2.20. ESR spectra of copper(II) complex of 2a

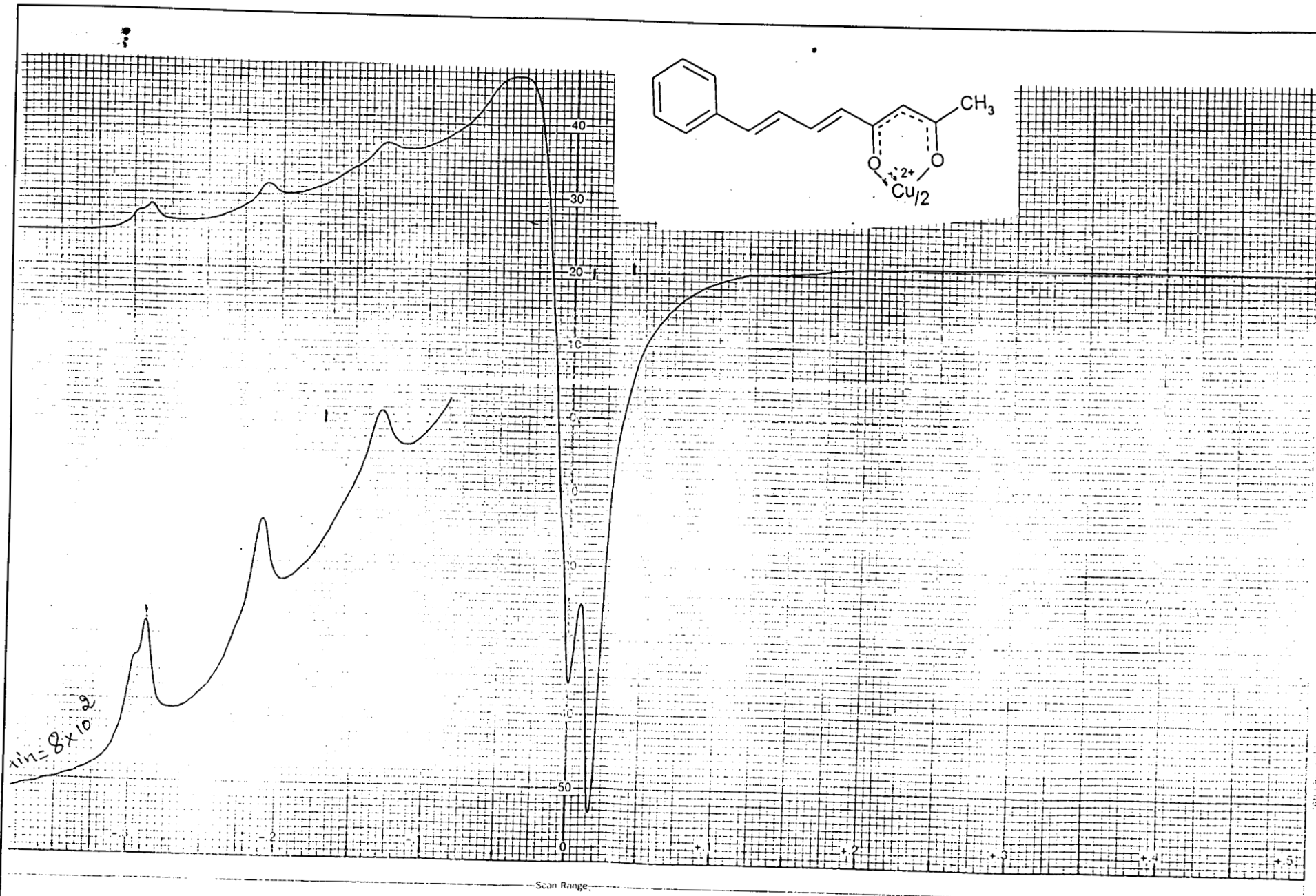


Fig. 2.21 ESR spectra of copper(II) complex of 1b

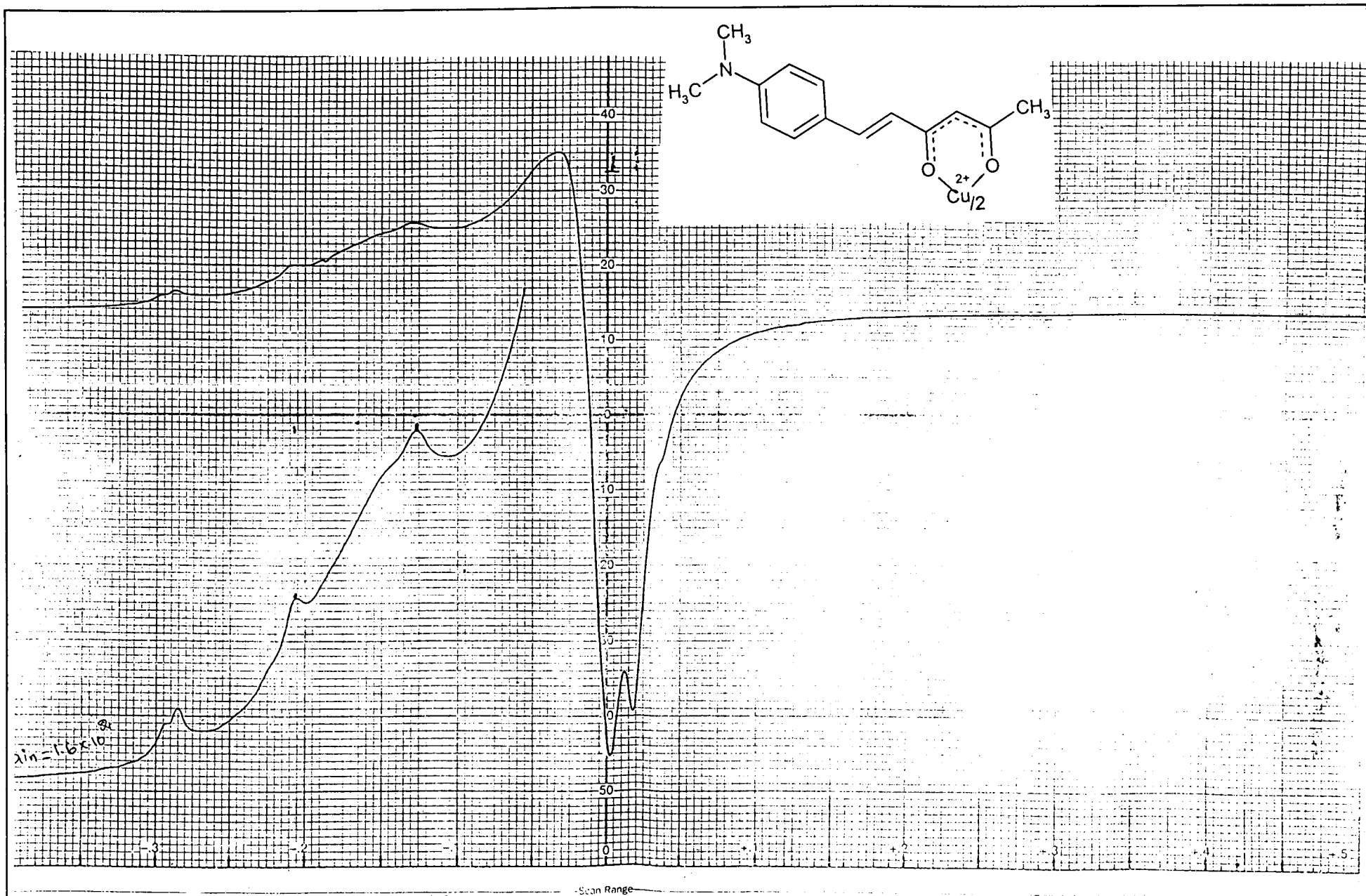
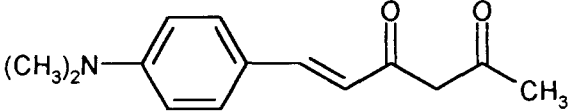
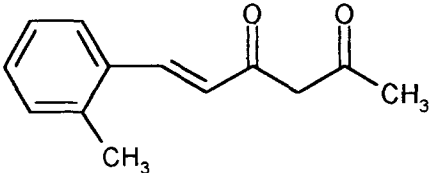
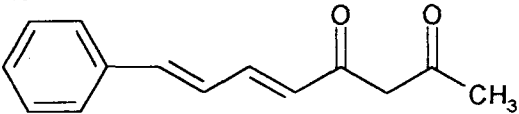
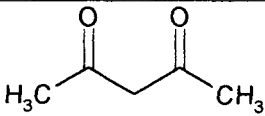
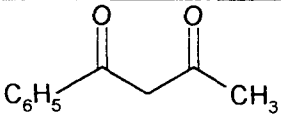


Fig. 2.22 ESR spectra of copper(II) complex of 2d

115

Table 2.14

The esr data of Cu(II) complexes of 6-aryl hexanoids (1b, 2a, 2d)
and related compounds

Cu(II) chelates of		g_{\parallel}	g_{\perp}	A_{\parallel}	A_{\perp}	
1b,		2.298	2.0418	160	26	
2a,		2.206	2.045	~160	32	
2d,		2.2146	2.0386	162	28	
acac,		Py	3.302	2.091	164	35
		d m f	2.293	2.061	172	13.1
		CHCl ₃	2.285	2.042	175	28.2
ba		d m f	2.281	2.046	176	26.6
	CuCl ₂		2.340	2.05	112	-

much lower in these conjugated β -diketones. This indicates greater π bonding in the six membered C_3O_2Cu ring systems compared to that of $Cu(acac)_2$. This may probably due to the increase in conjugation and the possible extended delocalisation of the complexes.

Thermogravimetric Studies

When subjected to heat majority of the metal complexes suffer physical as well as chemical changes and these changes are charactersitic of the substance. The data obtained from such thermal studies can be used for qualitative and quantitative anlaysis and often give information impossible to obtain by other analytical methods.

Among the thermal methods, thermogravimetry (TG), is the most popular. Though TG curves appear to be simple several interesting features of a compound can be established from it.¹³⁷⁻¹³⁹ Some of the important informations that can be gathered from TG curves are: (a) The temperature below the compound has a constant weight and the temperature at which it begins to decompose, (b) How far the decomposition reaction can proceed and from the decrease in weight loss an idea about the stoichiometry of the compound, (c) formation of intermediate products during decomposition, the temperature range of formation of the intermediate and its stability (d) temperature of the final decomposition and the nature of the end product if any.

The TG techniques can be used to study the kinetics of the decomposition reaction and to determine basic kinetic factors such as rate constant, activation energy, order of the reaction, frequency factor, etc. Now it has been developed as a main source of information concerning heterogeneous kinetics.¹⁴⁰⁻¹⁴³ The use and limitations of thermogravimetry in reaction kinetics of solid and liquid state thermal decomposition reactions through both isothermal and non isothermal methods have been summarized by Lukaszewski and Redfern.^{141,144}

For the determination of various kinetic parameters for non isothermal reaction, the three non mechanistic equations developed by Coats-Redfern,¹⁴¹ Horowitz-Metzger¹⁴² and Maccallum-Tanner¹⁴³ are usually employed. The order of each stage of decomposition can also be determined from these equations. These methods are briefly mentioned below.

(a) Integral method using the Coats-Redfern equation:¹⁴¹ Coats and Redfern derived the following equations for the determination of various kinetic factors.

$$\log \frac{1 - (1 - \alpha)^{1-n}}{T^2 (1 - n)} = \log \frac{AR}{\phi E} (1 - 2RT/E) - \frac{E}{2.303 RT} \quad \text{for } n \neq 1 \quad (1)$$

$$\text{and } \log - \log \frac{(1 - \alpha)}{T^2} = \frac{-\log AR}{QE (1-2RT/E)} - \frac{E}{2.303 RT} \quad \text{for } n = 1 \quad (2)$$

where $\alpha = (w/w_\alpha)$, w is the mass loss at time t , and w_α is the maximum mass loss, n is the order of reaction and k , the rate constant given by $K = A \exp(-E/RT)$ where A is the frequency factor (statistical or preexponential factor; min^{-1}), E is the activation energy of the reaction, R is the gas constant and T , the absolute temperature of the reaction and ϕ is the heating rate ($^\circ\text{C min}^{-1}$). Usually E is of the order of 10^5 Joules, $R = 8.3 \text{ JK}^{-1} \text{ mol}^{-1}$ and $T < 1000 \text{ K}$. Hence $(2RT/E) \approx 0$ and $1 - (2RT/E) \approx 1$. This reduces the first term on the left hand of eqn. (1) to a constant. A plot of the left hand side of equation (1) against $1/T$ should therefore be a straight line. From the slope of the linear plot, E can be calculated and knowing the value of E , A can be calculated from the intercepts. The entropy of activation, ΔS , is given by the relation

$$A = \frac{kT_s e^{\Delta S/R}}{h}$$

T_s = Temperature at which dc/dT is a maximum

C = Weight fraction present at temperature T and is defined as $C = (w_\alpha - w)/w_\alpha$

where w_α is the total mass loss at T . The expression derived for the determination of the order of the reaction, n , is $C_s = n^{(1-1/n)}$, where C_s is the value of C at the temperature T_s . From theoretical curve of n versus C_s using various values of C_s corresponding to $n = 1, 1/2, 1/3, 2/3$, the value of n can be evaluated.

b) Approximation method using the Horowitz-Metzger equation:¹⁴² For a first order reaction H-M derived the equation

$$\ln \ln \frac{W_0 - W_t}{W - W_t} = \frac{E\theta}{RT_s^2}$$

where w is the weight remaining at a given temperature and W_0 and W_t are the initial and final weights, $\theta = T - T_s$. When the reaction is not 1st order the expression will be of

$$1 - C^{1-n} = (1 - n) e^{E\theta/RT_s} \text{ where } C = \frac{W - W_t}{W_0 - W_t}$$

$$\log \frac{1 - c^{(1-n)}}{1 - n} = \frac{E\theta}{RT_s^2}$$

Once n has been estimated, a plot of left hand side Vs θ should give a straight line where slope is (E/RT_s^2) .

c) MacCallum-Tanner equation:¹⁴³ According to M-T, for the n^{th} order the equation is

$$\log \frac{1 - (1 - \alpha)^{1-n}}{1 - n} = \log \frac{AE}{\phi R} - 0.483 E^{0.435} - \frac{0.449 + 0.21 \pi E \times 10^3}{T}$$

where ϕ = heating rate dT/dt

The left hand of the equation is plotted against $1/T$, values of E , Δ and ΔS can be calculated.

Mechanism of reaction from non isothermal TG traces

Thermal decomposition of solids can be explained in terms of a general hypothesis that the reaction consists of the formation and growth of nuclei for which several theories are formulated.¹⁴⁹⁻¹⁵¹ Thus any particular solid decomposition may be according to the model assumed in the derivation of the equation. But it would be kept in mind that, in searching for an analytical description of the reaction kinetics in solids and the functions obtained are only a mathematical expression of a hypothetical model chosen. If the model actually characterises the situation, the derived kinetic parameters will have real meaning. Otherwise, even the most elegant method of kinetic calculation will only be a mathematical exercise.¹⁵¹

The type of mechanism most frequently encountered in solid state reactions¹⁴⁹⁻¹⁵¹ are shown in Table 2.15. The expressions in Table 2.15 are grouped according to the shape of α -temperature curves as acceleratory, sigmoid or deceleratory. The deceleratory group is subdivided according to the controlling factor assumed in the derivation as geometric, diffusion or reaction order.

TABLE 2.15

Broad classification of solid state kinetic expressions¹⁴⁵

Function	Rate controlling process	Kinetic expression
1.	Deceleratory equations	
a)	Based on diffusion mechanisms	
D1	One dimensional diffusion	$\alpha^2 = kt$
D ₂	Two dimensional diffusion	$(1 - \alpha) \ln (1 - \alpha) + \alpha = kt$
D3	Three dimensional diffusion Jander equation	$[1 - (1 - \alpha)^{1/3}]^2 = kt$
b)	Based on geometrical models	
R ₂	Contracting area	$[1 - (1 - \alpha)]^{1/2} = kt$
R ₃	Contracting area	$[1 - (1 - \alpha)]^{1/3} = kt$
c)	Based on the order of reaction	
F1	First order random nucleation Mampel equation	$-\ln (1 - \alpha) = kt$
2.	Sigmoid- α -temperature curves	
A ₂	Avrami-Erofeev I	$[-\ln (1 - \alpha)]^{1/2} = kt$
A ₃	Avrami-Erofeev II	$[-\ln (1 - \alpha)]^{1/3} = kt$

Numerous reports are available on thermogravimetric studies on diverse types of metal 1,3-diketonates.^{146,147} Effect of different groups (such as allyl, aryl, heteroaryl etc.) attached to the dicarbonyl function on the thermal stability and relative volatilities have been studied in detail. Thus it has been observed that groups increase the volatility and thermal stability. Similarly the nature of metal

ion, oxidation state, etc. also have pronounced influence on the thermal properties of metal 1,3-diketonates.

It can be seen that most of these studies are on metal- β -diketones in which the dicarbonyl function is attached to alkyl/and or substituted alkyl/aryl group. Therefore, TG studies of β -diketones of the type considered in the present study, where the diketo function attached to olefinic groups has considerable importance. With this intention thermograms of typical 6-arylhexanoid metal chelates have been studied and evaluated the possible kinetic and other parameters.

Thermal decomposition studies of 6-aryl-5-hexene-2,4-diones and their metal complexes

Thermogravimetric analysis of **2c** and its Cu(II), Ni(II), Co(II) and iron(III) complexes were studied and the analytical data are presented here. Kinetic parameters such as apparent activation energy (E), pre-exponential factor (A) and entropy of activation (ΔS) of each stage were evaluated based on the three non-mechanistic equations, Coats-Redfern, Horowitz-Metzger and MacCallum-Tanner and the results were tabulated. The order of each stage of the decomposition reaction was determined.¹³⁸ The correlation coefficient (r) were computed by the weighted Least Square Method (LSM) for the three equations.

Experimental details: Thermal analysis was carried out using a **TGA Vs. IA Dupond 2100** system, in an atmosphere of N₂ throughout the experiment. A sample

size of ~ 5 mg were employed in each study at a heating rate of 10°C per minute. Computational works were carried out with a computer using kprograms in Fortran language.

Thermogravimetric Analysis: The thermograms of **2c** shows a two stage decomposition pattern (figure 2.23). The compound is stable upto 395° K and then decomposition begins slowly with a sharp drop in the mass upto about 553 K. The peak temperature in DTG is at 503° K. Immediately after the 1st stage further decomposition starts with a peak temperature of 773° K. The mass loss obtained from the thermal analysis and from theoretical calculations are in good agreement (Table 2.16). The order of the reactions was found to be unity for both the stages. The kinetic parameters, activation energy (E), pre-exponential factor (A), entropy change ΔS and the correlation coefficient (r) were calculated using the three non-mechanistic expressions and are given in Table 2.17.

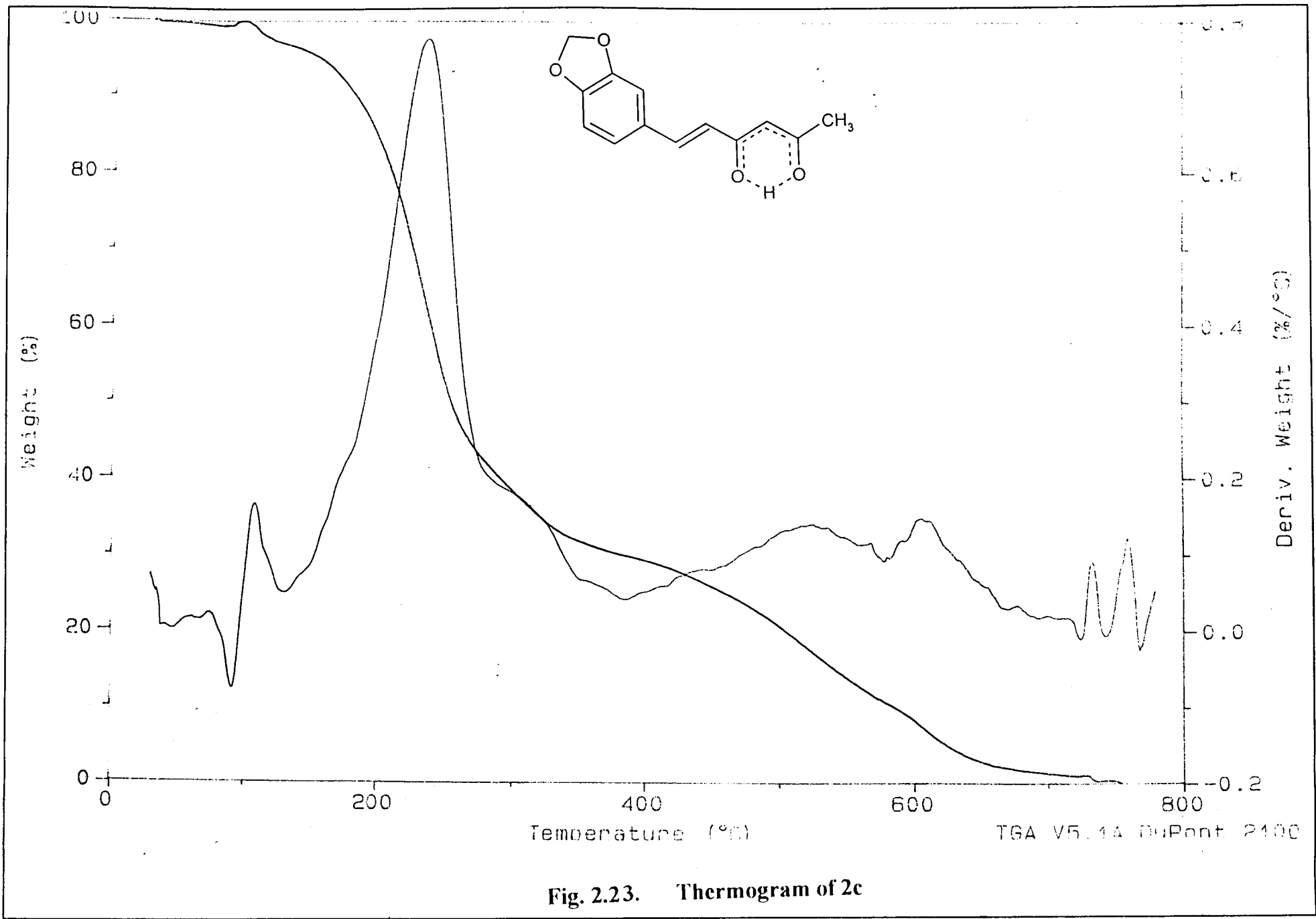


TABLE 2.16

**Thermal Decomposition of the 2c (HL) and its Cu(II), Ni(II),
Co(II) and Fe(III) chelates**

Compound/ complexes (Molecular mass)	Temp. ranges in TG (K)	Peak temp. (K)	Mass loss %		Pyrolysis %	Final product
			TG	Theore- tical		
1c = HL, C ₁₃ H ₁₂ O ₄ (232)	395-553	503	51	52.59	100	--
	563-1013	773	49	47.41		
CuL ₂ (525.54)	505-623	583	46.4	45.5	87.91	CuO
	633-913	733	32	42.41		
NiL ₂ (520.69)	573-543	693	88.16	85.66	85.6	NiO
CoL ₂ (H ₂ O) ₂ (520.93)	403-553	493	16.01	16.12	84.6	Co ₃ O ₄
	554-740	663	64.89	68.48		
FeL ₃ (748.85)	420-553	493	13.95	13.01	89.33	Fe ₂ O ₃
	563-753	663	71.22	76.32		

Thermogravimetric analysis of metal complexes

(a) Cu(II) complexes of 2c (CuL₂)

The Cu(II) complex showed a two stage decomposition pattern. The first stage of decomposition is between 505-623 (°K) with a peak temperature at 583° K. The TG-DTG curves of the complex are given in figure 2.24.

The 2nd stage of decomposition begins at 633° K and continues upto 913° K with a peak temperature of 733° K. The end product appears to be CuO since the

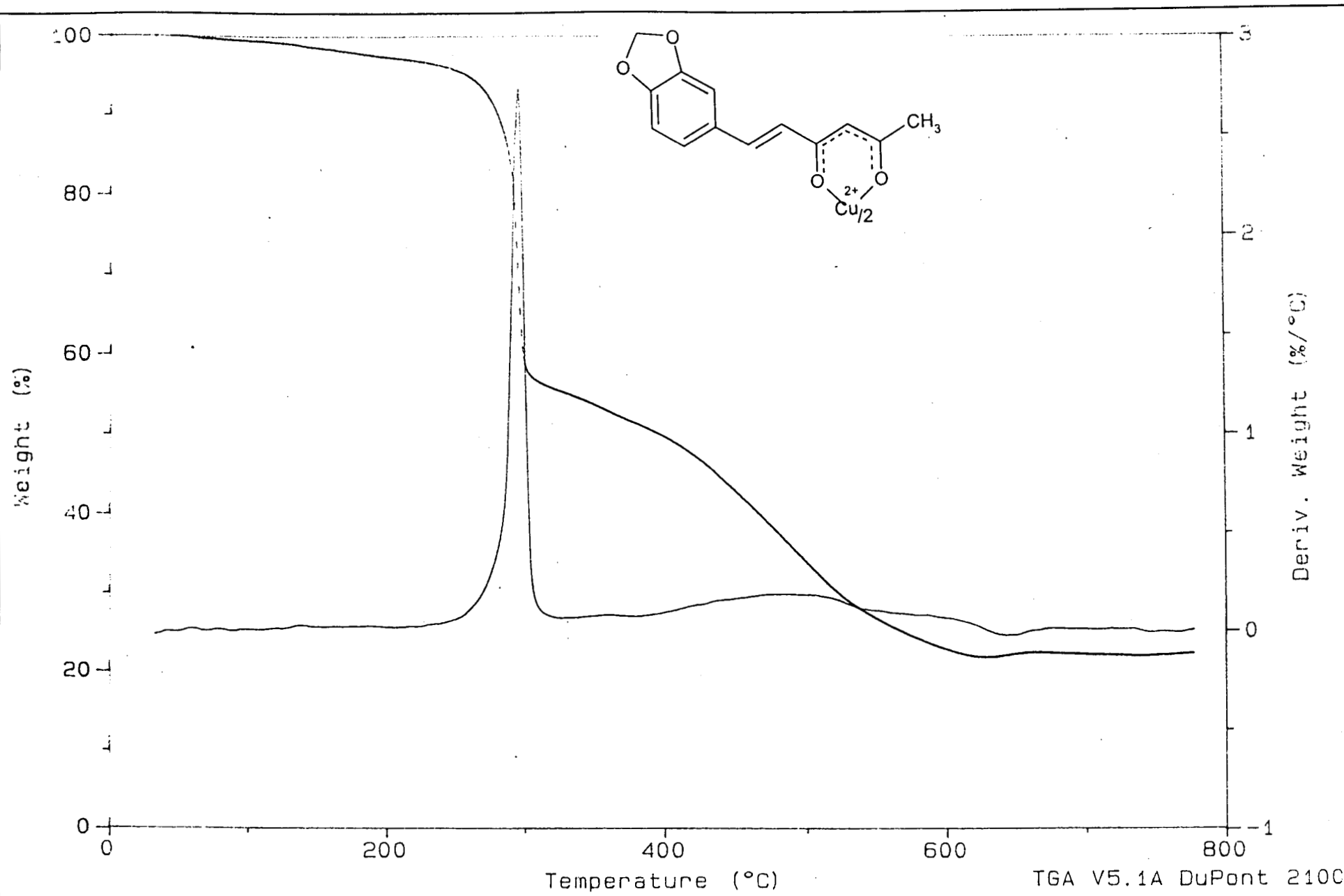


Fig. 2.24. Thermogram of Cu(II) complex of 2c

TGA V5.1A DuPont 2100

127

mass loss from the TG curve agrees well with the theoretical value (Table 2.16). The order of the reaction was found to be unity in both cases. The kinetic parameters, calculated on the basis of the three non mechanistic equations for both the stages are given in table 2.17.

(b) Ni(II) complexes of 1c (NiL_2)

In the case of the nickel(II) complex the thermal decomposition goes through a single stage starting at 573°K and goes upto 943°K with a peak temperature of 693°K . The TG-DTG curves are presented in figure 2.25. The end product seems to be NiO since the mass loss from TG curve agrees well with the theoretical value (Table 2.16). The order of the reaction was found to be unity. The kinetic parameters E , ΔS and A were calculated using the three non-mechanistic equations are given in Table 2.17.

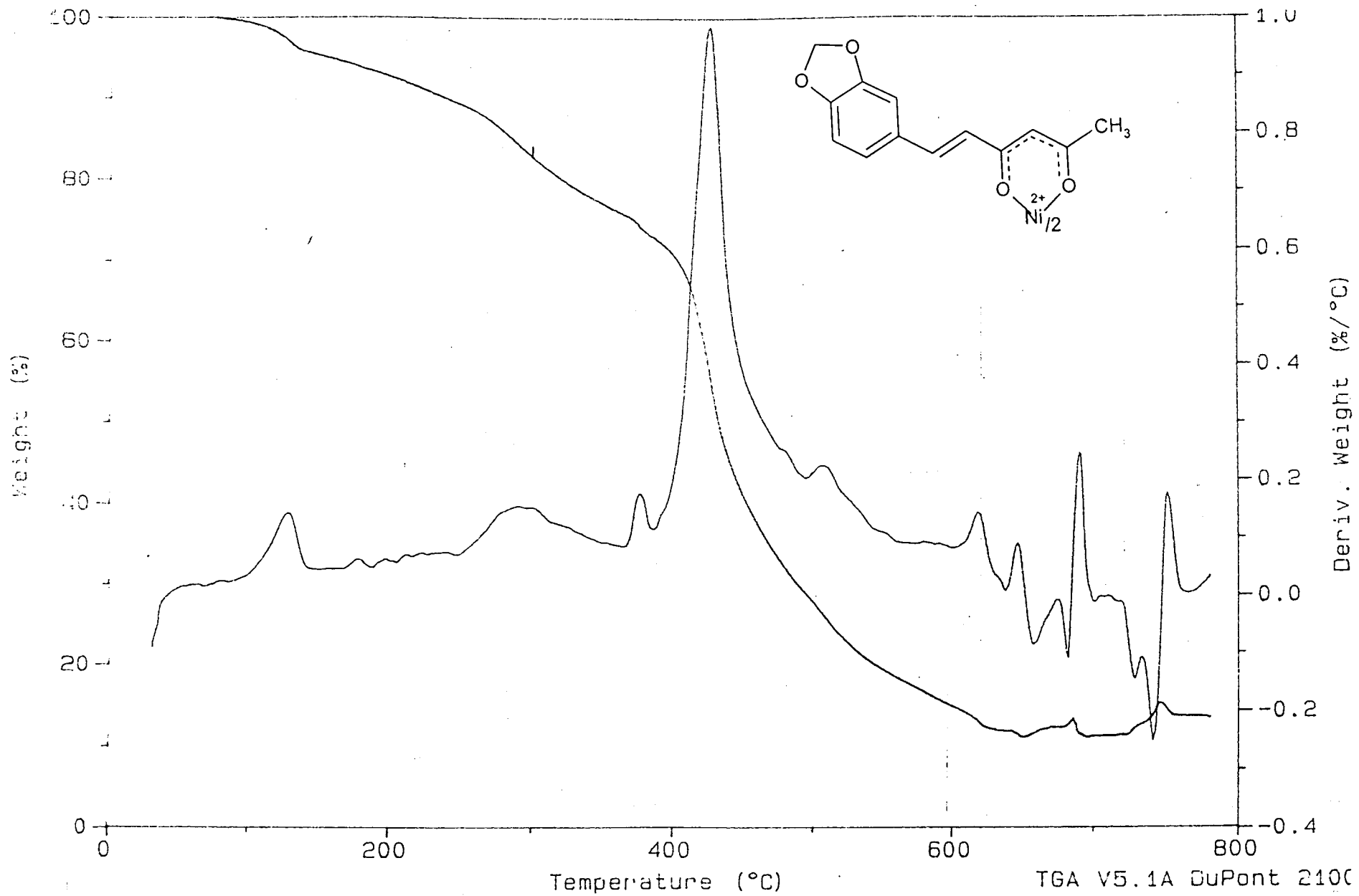


Fig. 2.25. Thermogram of Ni(II) complex of 2c

129

TABLE 2.17

Kinetic Parameters for the decomposition of 1c and its metal complexes

Compound/ Complexes	Equation	E kCal mol ⁻¹	log A s ⁻¹	ΔS kcal deg ⁻¹ mol ⁻¹	Correlation coefficient (r)
2c = C ₁₃ H ₁₂ O ₄ 1 st Stage	CR	11.32	2.38	-48.68	0.996
	MT	9.13	4.46	-39.14	0.994
	HM	11.13	2.20	-49.49	0.990
2 nd stage	CR	17.04	1.68	-52.74	0.988
	MT	18.41	4.84	-38.27	0.992
	HM	17.56	1.85	-51.95	0.988
(C ₁₃ H ₁₁ O ₄) ₂ Cu 1 st stage	CR	27.81	8.38	-21.47	0.97
	MT	32.64	13.38	1.42	0.96
	HM	36.57	11.93	-5.24	0.97
2 nd stage	CR	21.98	3.68	-43.48	0.987
	MT	23.08322.	6.71	-29.61	0.991
	HM	27	3.72	-43.26	0.981
(C ₁₃ H ₁₁ O ₄) ₂ Ni Single stage	CR	15.30	2.04	-50.85	0.968
	MT	16.19	5.08	-36.95	0.977
	HM	17.07	2.64	-48.09	0.971
(C ₁₃ H ₁₁ O ₄) ₂ CO(H ₂ O) ₂ 1 st stage	CR	3.00	0.260	-67.51	0.984
	MT	4.23	2.56	-47.78	0.990
	HM	6.30	0.12	-58.97	0.994
2 nd stage	CR	51.26	14.55	6.47	0.994
	MT	52.18	17.56	20.26	0.995
	HM	54.90	16.75	11.96	0.995
(C ₁₃ H ₁₁ O ₄) ₃ Fe 1 st stage	CR	9.82	1.96	-50.56	0.996
	MT	9.79	4.76	-37.72	0.997
	HM	11.84	2.92	-46.16	0.997
2 nd stage	CR	44.77	12.36	-3.53	0.981
	MT	45.69	15.35	10.15	0.983
	HM	46.59	12.97	-0.74	0.979

CR = Coats-Redfern; MT = MacCallum-Tanner; HM = Horowitz-Metzger

(c) Co(II) Complexes of 2c [CoL₂(H₂O)₂]

The thermogram of the [CoL₂(H₂O)₂] is presented in fig. 2.26. The curves displayed a well defined double stage decomposition pattern. The 1st stage decomposition is in the range of 403-553° K with a peak temperature of 493° K. Mass loss corresponding to the elimination of the coordinated water molecule is evident from the observed mass loss (Table 2.16).

The 2nd stage of decomposition begins at 554° K and continues upto 740° K with a peak temperature of 663° K. The end product appears to be Co₃O₄ since the mass loss from the TG curve agrees well with the theoretical value (Table 2.16). The kinetic parameters E, ΔS and A for both stages were calculated using the three non mechanistic expressions with the order as unity. The correlation coefficient was also calculated and compared as in table 2.17.

(d) Fe(III) complexes of 2c (FeL₃)

The TG analysis of FeL₃ are given figure 2.27. The compound shows a double stage decomposition curve. It is stable upto 420 K from which 1st stage decomposition starts and continues upto 553 K with a peak temperature of 493 K. The 2nd stage decomposition range is from 563 K to 753 K with a peak temperature of 663 K. The end product seems to be Fe₂O₃ since the mass loss from the TG curve agrees well with the theoretical value (Table 2.16). The kinetic parameters E,

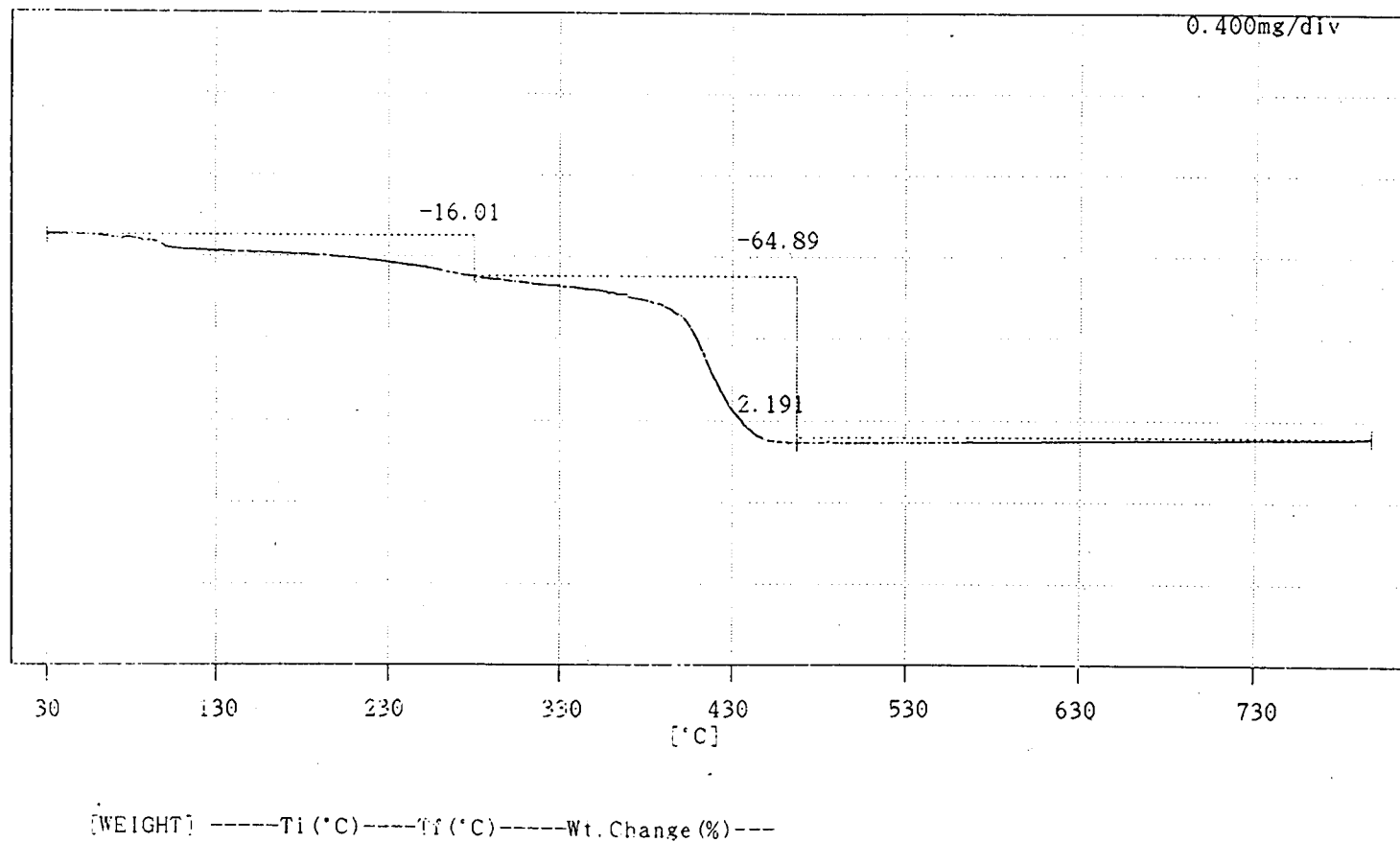
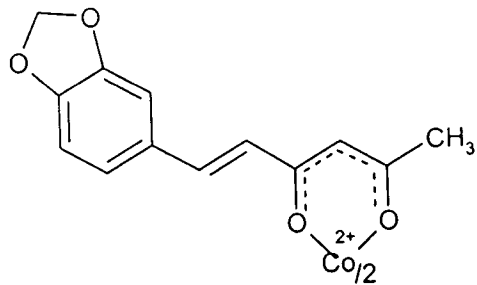


Fig. 2.26. Thermogram of Co(II) complex of 2c

1992

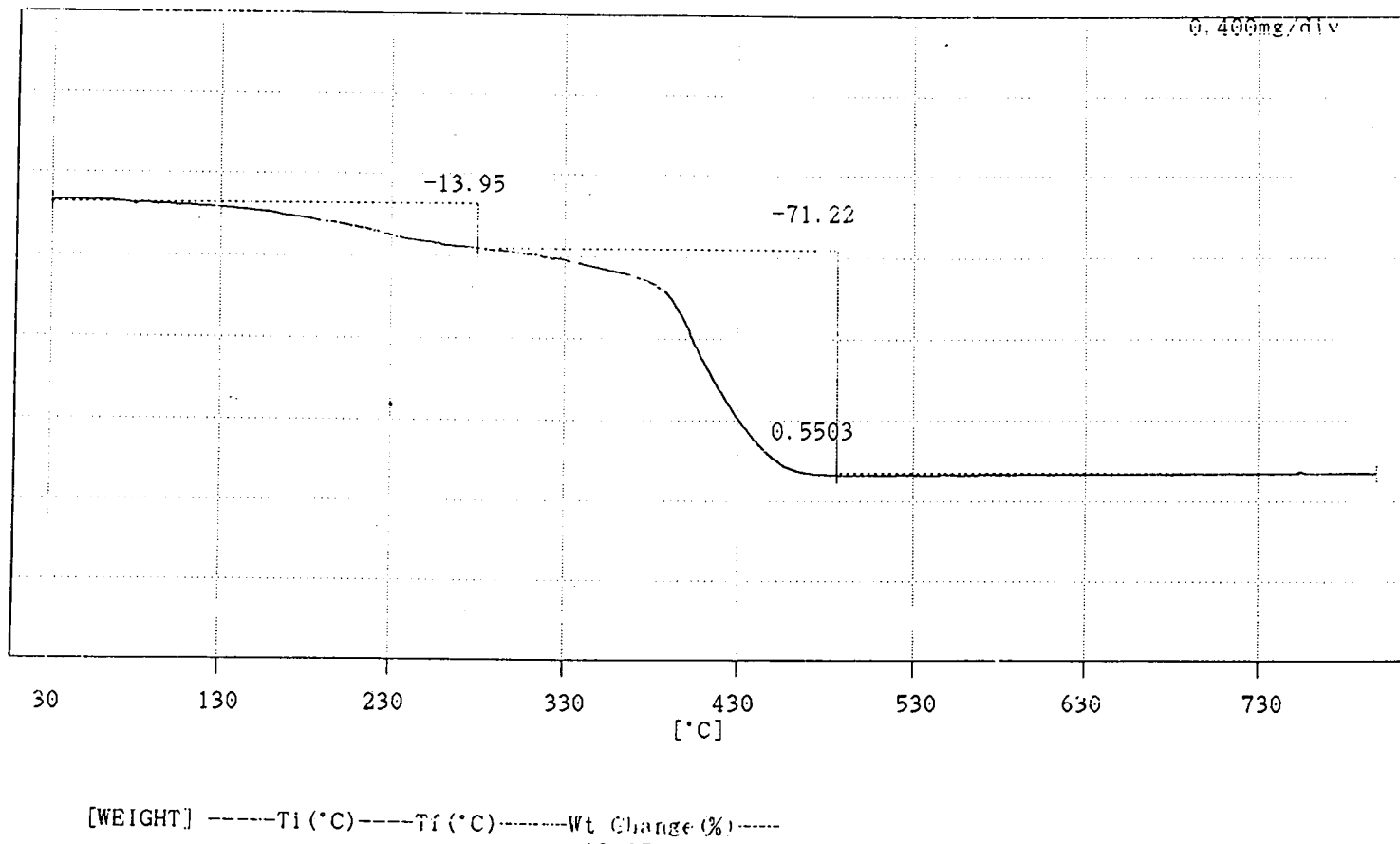
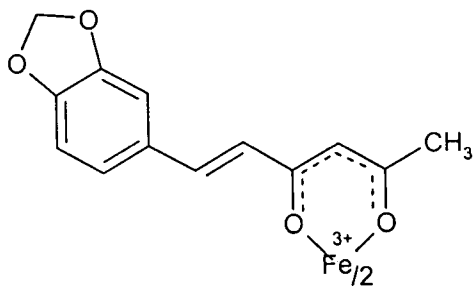


Fig. 2.27. Thermogram of Fe(III) complex of 2c

1.8.13

A, ΔS for both the stages were calculated using the non mechanistic equations and given in table 2.17 along with the correlation coefficient values for the order $n = 1$.

Data comparison of kinetic parameters of compound/complexes with other β -diketone complexes

The thermal decomposition of bis(acetylacetonate)copper(II), $[\text{Cu}(\text{acac})_2]$, has been studied by dynamic thermogravimetry.¹⁴⁰ The compound reported to be stable and ionisable upto 191° (m.p.) decomposes at high temperature, in static air it forms residue as CuO. The kinetic parameters were calculated. The moderately negative entropy of activation indicates formation of an ordered transition state. It is also reported that the complex decomposes by random nucleation.

In comparison metal complexes of 2c are stable upto the melting points and decomposes at high temperature and forms stable metal oxides as residue (in N_2 atom). Like in β -diketone complexes the kinetic parameters are comparable and their similarity indicates a common reaction mode. The activation energy are low for 1st stage transition compared with 2nd stage decomposition. For decomposition kinetics¹⁴⁹ it can be concluded that higher the activation energy for decomposition greater the thermal stability of the complex. The lowest value of activation energy are for cobalt complexes wherein the 1st stage decomposition coordinated water molecule are removed which involves only very low energy (3.00 – 6.31 kcal/mol). It can be concluded that a negative ΔS value indicates a more ordered activated

structure as in β -diketone complexes. Initial decomposition temperatures and inflection temperature can be used to determine the stability of the complex. The thermal behaviour of copper(II) chelates of 38 aryl β -diketones have been examined by combined thermogravimetry and differential thermal analysis and volatility was found to be depended on the nature of the alkyl moiety of the β -diketones.¹⁵²⁻¹⁵⁹

BIOLOGICAL STUDIES

Curcuminoids, the active chemical constituent of turmeric, have a broad spectrum of beneficial physiological activities. The antiinflammatory, antitumour, antioxidant, antifungal, antibacterial activities of curcuminoids are well established.¹⁶⁵⁻¹⁷⁸ Since the compounds considered in the present investigation are structurally related to curcuminoids, some of the biological activities of these compounds were also studied. The results of fungicidal and bactericidal activities of the 6-arylhexanoids and their typical metal complexes are discussed below.

The organisms used for studying the antifungal activity are *Aspergillus niger*, *Aspergillus parasiticus*, *Candida albicans* and *Rhizopus oryzae*.

The term *Aspergillosis* is used to define the infections caused by *Aspergillus* species in which *Aspergillus niger* and *Aspergillus paracitus* belong. The most common human disease caused by *Aspergillus niger* is otomycosis, a fungal infection of external ear. *Aspergillus* asthma occurs in atopic individuals. In bromopulmonary aspergillosis, the fungus grow within the lumen of bronchioles. Colonising aspergillosis develops usually in preexisting pulmonary cavities such as tuberculosis or cystic diseases. Aspergilloma causes massive haemoptysis. In invasive aspergillosis,¹⁶¹ the fungus invades the lung tissue. Disseminated aspergillosis¹⁶⁶ involving the brain, kidney and other organs are fatal.

Candida albicans is a yeast like fungus,¹⁶² isolated in patients with all forms of candidiasis. Internal candidiasis is a frequent sequel to oral antibiotic therapy and may present as diarrhea not responding to treatment. Systemic infection such as septicemia, endocarditis and meningitis may occur as terminal complications in severe generalised diseases such as leukemia and in persons on prolonged immunosuppression. Oral candidiasis is considered as a defining illness for AIDS.

Rhizopus oryzae is the most prevalent agent of mucormycosis ~ 60% of human mucormycosis and nearly 90% of rhinocerebral cases are caused by *Rhizopus oryzae*. The fungus is affected at paranasal, rhinoorbital, rhinocerebral, cerebral, pulmonary and gastro intestinal regions and in the soft tissues of extremities.

The organism selected for antibacterial study was *Staphylococcus aureus*.¹¹⁵ It constitutes a group of microorganism that may be detected in air, dust and natural water. They are mainly found living on the skin, skin glands and mucous membranes of mammals and birds. Sometimes found in the mouth, blood, mammary glands and intestinal, genital, urinary and upper respiratory tracts of their hosts. The victims suffer from vomiting and sometimes diarrhoea accompanied by sweating, fever, hypothermia, headache and muscular cramps.

Experimental

The cup-plate technique was employed for antifungal activity and 'disk diffusion technique'^{163,164} for antibacterial activity. The principle behind both the technique is fairly simple. When an antibiotic impregnated disc is placed on agar previously inoculated with the test organism and on moistening, the antibiotic diffuses rapidly outwards through the agar producing an antibiotic concentration gradient. A clear zone or ring will present if the agent inhibits microbial growth. The wider the zone surrounding the disc the more active is the substance.¹⁶³

Media used and their composition

Nutrient agar media was used for maintaining pure fungal/bacterial culture and to lawn the fungus/bacteria for detecting the antimicrobial activity. It was prepared by dissolving peptone (1g), meat extract (0.5g) NaCl (0.5g) and agar (2.5g) in distilled water (100ml) and adjusting the pH of the medium to 7.2-7.4 using 10% NaOH.

Subaraud's agar media was used for maintaining pure culture of all four fungus. It was prepared by dissolving peptone (1g), D-glucose (4g) and agar (2.5g) in distilled water (100ml) and adjusting the pH of the medium about 5.6-6.0 using 10% HCl.

Nutrient broth was used for preparing broth culture of the test fungus/bacteria and its composition was the same as that of nutrient agar, excluding agar. *Normal saline* was used a suspension of fungal/bacterial spores for lawning. It was prepared by dissolving NaCl (0.95g) in distilled water (100ml). Solutions of the test compounds were prepared in DMSO and for sterilising, all the media used were autoclaved at 121°C for 20min.

Detection of antimicrobial activity

The fungus *Aspergillus niger*, *Aspergillus paraciticus* and *Rhizopus oryzae* species, suspension of spores were prepared in normal saline. For this each fungi were grown on subaraud's glucose agar slauts till they get sporulated. These spores were scrapped off and suspended in about 3.5ml of normal saline. In the case of *Candida albicans* the suspension was made by using the cells collected from the slope of the subourand's agar.

To prepare the mat growth of fungi on petriplates, this spore suspension was poured on the surface of the plates. Plates were allowed to dry in an incubator at 37°C for 1h. Using an agar punch, wells (10 mm) were made on these plates. In each well 75µls (2000 ppm) of the compounds in DMSO were added. Each plate was having a well for the control, that is the solvent DMSO and also one for the reference antibiotic, Nistatin. This wells were properly labelled and the plates were prepared in triplicate and incubated at room temperature for 24-48 hours. The anti

fungal activity was detected by measuring the diameter of the inhibitory zone around each well. The greater diameters shown by the compounds than the control indicates their antifungal activity.

In the case of antibacterial activity a uniform lawn of bacteria *Staphylococcus* (gm +ve) was spreaded evenly in petriplates as in the case for fungi. Discs impregnated with the compound in DMSO was placed and the antibacterial activity measured from the diameter of the zone of inhibition (mm).

Results and Discussion

The results of antifungal activities of the 6-aryl hexanoids are given in table 2.18 and their typical metal complexes in table 2.19. The data revealed that some of the compounds possess antifungal activity comparable to that of the drug "Nistatine". Among the compounds **2e** and **2f** were found to be highly active against all the four fungal strains studied. In both these compounds an OH group is present in the ortho position of the aryl ring. In the curcuminoids also, it has been reported that their antifungal and other biological activities depend to a large extent on the presence of groups such as OH in the aryl ring. Thus it can be stated that presence of OH group in the aryl ring of these types of unsaturated 1,3-diketones is a structural requirement for their biological activities.

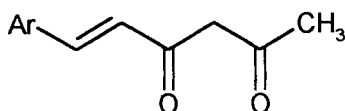
In many cases metal complexation increased the activity of the 6-aryl hexanoids (Table 2.19). Copper(II) complexes are found to be highly active. This is particularly true in the case of copper complexes of **2e** and **2f**. It is to be pointed

out that in these complexes also the OH group of **2e** and **2f** remains free. Thus OH group on aryl ring facilitates the antifungal activity of the compounds.

In the case of antibacterial activity preliminary studies on some of the diketones and their complexes revealed that none of them showed significant activity against *Styphylococcus aureus*.

TABLE 2.18

Antifungal activity of 6-aryl-5-hexene-2,4-diones

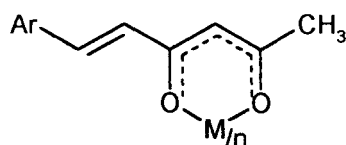


Compound		Diameter of the zone of inhibition (mm)			
No.*	Ar	<i>Aspergillus niger</i>	<i>Aspergillus parasiticus</i>	<i>Rhizopus oryzae</i>	<i>Candida albicans</i>
1b	Cinnamyl	14	14	16	12
1c	naphthyl	14	14	12	11
1d	furyl	12	12	10	10
2a	2-methyl phenyl	10	10	10	10
2b	4-ethoxy phenyl	10	10	10	10
2c	(3,4-dioxymethylene) phenyl	10	10	10	10
2d	(4-dimethylamino) phenyl	10	10	10	10
2e	2-hydroxy naphthyl	26	36	45	30
2f	2-hydroxy phenyl	15	14	14	15

*The numbers are according to name of compounds in respective chapters given before.

TABLE 2.19

Antifungal activity of the metal complexes of 6-aryl-5-hexene-2,4-diones



$n = 2$ for $M = \text{Cu}^{+2}$,
 Ni^{+2} , Co^{+2} and $n = 3$
 for $M = \text{Fe}^{+2}$

Compound			Diameter of the zone of inhibition (mm)			
No.*	Ar	M	<i>Aspergillus niger</i>	<i>Aspergillus parasiticus</i>	<i>Rhizopus oryzae</i>	<i>Candida albicans</i>
1c	naphthyl	Cu	26	10	10	10
1c	naphthyl	Ni	14	10	12	10
1c	naphthyl	Fe	12	10	10	10
1d	furyl	Cu	26	10	10	10
1d	furyl	Ni	10	10	10	10
1d	furyl	Co	18	10	10	10
1d	furyl	Fe	10	10	10	10
2e	2-hydroxy naphthyl	Cu	29	12	15	20
2e	2-hydroxy naphthyl	Ni	16	21	12	20
2e	2-hydroxy naphthyl	Co	18	24	13	17
2e	2-hydroxy naphthyl	Fe	22	22	20	22
2f	2-hydroxy phenyl	Cu	26	12	12	14
2f	2-hydroxy phenyl	Ni	14	12	12	12
2f	2-hydroxy phenyl	Co	14	12	12	14
2f	2-hydroxy phenyl	Fe	14	11	12	11

DMSO	10	10	10	10
Nistatine	12	12	11	12

*The numbers are according to name of compounds in respective chapters given before.

SYNTHESIS AND CHARACTERISATION OF 5-ARYL-1-PHENYL-4-PENTENE-1,3-DIONES

Mathew Paul Ukken “Metal complexes of 5-aryl-1-phenyl-4-pentene-1,3-diones and 6-aryl-5-hexene-2,4-diones ” Thesis. Department of Chemistry , University of Calicut, 2002

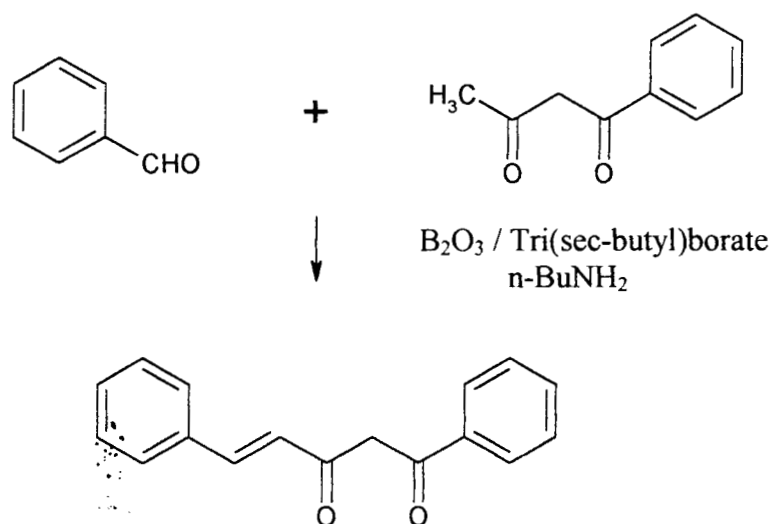
12/17

CHAPTER II

**SYNTHESIS AND CHARACTERISATION OF
5-ARYL-1-PHENYL-4-PENTENE-1,3-DIONES**

Synthesis and Characterisation of 5-Aryl-1-phenyl-4-pentene-1,3-diones and their metal complexes

Condensation of two equivalents of aromatic aldehyde at the methyl groups of acetylacetone leads to the formation of 1,7-diarylheptanoids. While condensation involving only one methyl group the product is 6-arylhexanoids, whereas in the case of benzoylacetone which contains only one methyl group, mono condensation alone will take place as in the reaction below (scheme 3.1).



Scheme 3.1

In the present investigation a series of such β -diketones in which one of the carbonyl group is directly linked to olefinic groups are synthesised and

characterised.^{129,130} These compounds can be systematically named as 5-aryl-1-phenyl-4-pentene-1,3-diones. Typical metal complexes of these unsaturated 1,3-diketones were also synthesised and characterised. For convenience this chapter is divided into two sections. In **Section 1** details of the synthesis and characterisation of 1-phenyl-5-aryl pentanoids and their metal complexes in which no substituents are present on the aryl ring are given. In **Section 2** all aryl substituted 1-phenyl-5-aryl pentanoids and their metal complexes are included.

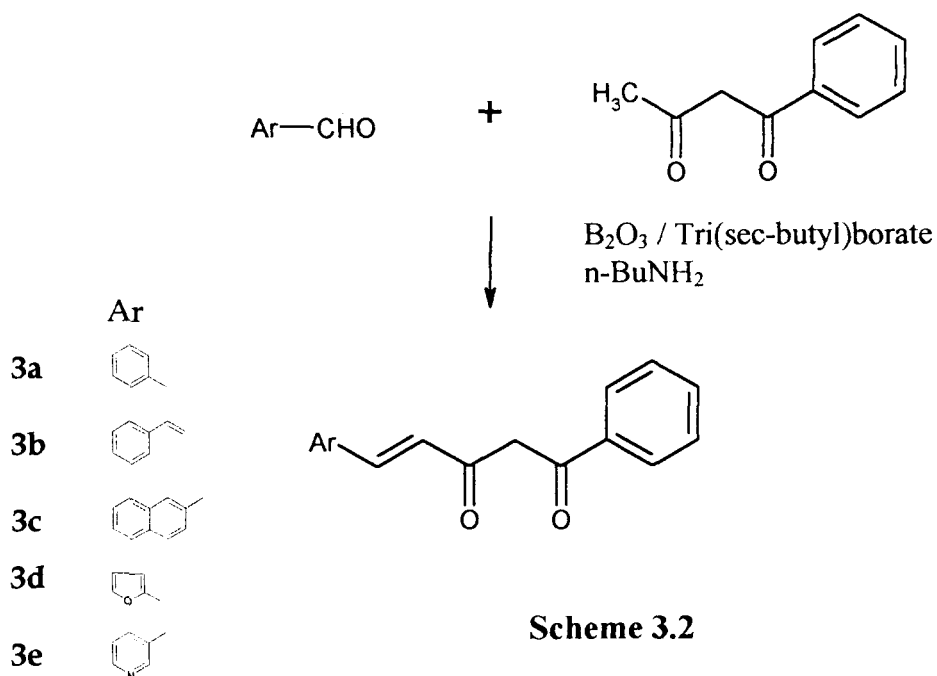
Section 1

Synthesis and Characterisation of 5-Aryl-1-phenyl-4-pentanoids and their metal complexes

In this section synthesis and characterisation of a new series of 5-aryl-1-phenyl-4-pentene-1,3-diones and their metal complexes are considered. The aryl groups include phenyl, naphthyl, cinnamyl and heteroaryl groups such as furyl and pyridyl groups.

Synthesis of 5-aryl-1-phenyl-4-pentene-1,3-diones

The compounds were synthesised^{129,130} by the condensation of aromatic aldehydes (benzaldehyde/cinnamaldehyde/naphthaldehyde/ furfural/pyridine-3-aldehyde) with benzoylacetone at room temperature in presence of tri(sec-butyl)borate, B₂O₃ and n-butylamine as given below.



In a typical procedure, benzoylacetone (0.005 mol) was mixed with boric oxide (0.005 mol) and 5 ml dry ethylacetate was stirred well for ~ 1 h. The stirring was further continued for ~ 1 h with the slow addition of a solution of aromatic aldehyde (0.005 mol) in 5 ml dry ethylacetate, followed by tri(sec-butyl)borate (0.01 mol) and n-butylamine (0.05 mol). After stirring for an additional period of ~ 3 h, the solution was set aside overnight. Then 7.5 ml of 0.4 M hot (~ 60°C) hydrochloric acid was added to this mixture and again stirred for ~ 1 h and extracted with ethyl acetate. The washed extracts were combined, concentrated and the residual paste obtained was stirred with hydrochloric acid (2 M, 10 ml). The separated solid product was collected, washed with water then with ethanol and dried under reduced pressure. The compounds were recrystallised from hot benzene to get chromatographically (tlc) pure material.

Synthesis of metal complexes

Copper(II), nickel(II), cobalt(II), oxovanadium(IV) and iron(III) complexes of the compounds were prepared by the following general method. To a refluxing ethanolic solution of the compound (0.02 mol, 20 ml) an aqueous solution of the metal salt (0.001 mol, 15 ml) was added, refluxed for ~ 2 h and the volume was reduced to half. The precipitated complex was filtered after cooling to room temperature, washed with water and dried in vacuum. The complexes were

recrystallised from hot methanol. The metal salts used were acetates of Cu^{2+} , Ni^{2+} and Co^{2+} , VO_2SO_4 and hydrated FeCl_3 .

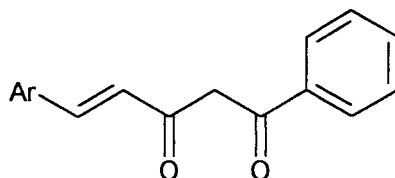
Results and discussion

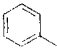
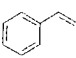
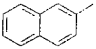
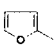
The aromatic aldehydes used for the preparation of 5-aryl-1-phenyl-4-pentene-1,3-diones considered here are given in table 1.1. All the compounds are crystalline in nature with sharp melting points and are soluble in common organic solvents. The carbon, hydrogen percentages are in agreement with their formulation. The yield and systematic names are also included in table 3.1.

However the elemental analysis and mass spectral data of the condensation product of pyridine-3-carbaldehyde with benzoylacetone shows that it is quite different from the compounds obtained from the other aldehydes. The product obtained has been established as a triketone. Therefore the analytical and spectral details of the condensation products of pyridine-3-aldehyde and its metal complexes are discussed separately.

TABLE 3.1

Synthetic details of 5-aryl-1-phenyl-4-pentene-1,3-diones



Compounds	Aldehyde used for Synthesis	Ar	Systematic name	Yield %
1a	Benzaldehyde		1,5-diphenyl-4-pentene-1,3-dione	55
1b	Cinnamaldehyde		1-phenyl-5-(cinnamyl)-4-pentene-1,3-dione	60
1c	Naphthaldehyde		1-phenyl-5-(naphthyl)-4-pentene-1,3-dione	70
1d	Furfural		1-phenyl-5-furyl-4-pentene-1,3-dione	65

Characterisation of the 1-phenyl-5-arylpentanoids

The structure and the nature of the tautomeric forms of the compounds were characterised on the basis of their uv, ir, ^1H nmr and mass spectral data.

Uv spectra

The uv spectra of the compounds (10^{-3} M, 95% ethnol) show two absorption maxima at ~ 400 nm and ~ 290 nm (Table 3.2). These absorption maxima are significantly at longer wave length compared to those reported for simple saturated 1,3-diketones.^{50,111} The low energy band (~ 400 nm) corresponds to the $n \rightarrow \pi^*$ transition of the dicarbonyl function. The observed absorption maxima of this band (Table 3.2) can be correlated with electronic effects of different aryl groups. The band at ~ 290 nm due to the $\pi \rightarrow \pi^*$ transition is only marginally influenced by the configuration of the aryl group.

Infrared spectra

The infrared spectra of the 5-aryl-1-phenyl-4-pentene-1,3-diones show two prominent bands at ~ 1630 cm^{-1} and ~ 1615 cm^{-1} and several medium intensity bands in the region 1450 - 1600 cm^{-1} . The position and intensity of the bands at ~ 1630 cm^{-1} and ~ 1615 cm^{-1} indicates that the compound exists predominantly in the enol form and enolised towards the cinnamoyl functions.^{52,123} This is inferred from the fact tht no free benzoyl carbonyl band (~ 1660 cm^{-1}) or cinnamoyl carbonyl band (~ 1645 cm^{-1}) are observed in the double bond region of the spectra. The observed bands in these region suggests the enolisation of the active methylene proton and its involvement in strong intramolecular hydrogen bonding as in structure 3.1. Considering the variation electronic effects of the different aryl

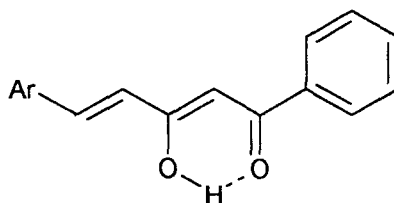
TABLE 3.2

Physical, analytical and uv spectral data of the 5-aryl-1-phenyl-4-pentene-1,3-diones, 3a-d

Compounds	Molecular formula (formula weight)	Elemental Analysis (%) found/(calculated)		Yield (%)	M.P. °C	λ_{\max} (nm)	log ϵ
		C	H				
3a	C ₁₇ H ₁₄ O ₂ (250)	80.53 (81.63)	5.20 (5.60)	55	158	269 365	4.06 4.13
3b	C ₁₉ H ₁₆ O ₂ (276)	82.31 (82.61)	5.77 (5.80)	70	78	289 413	4.1134 3.4719
3c	C ₂₁ H ₁₆ O ₂ (300)	84 (83.71)	5.33 (5.31)	60	70	231 411	3.4213 3.8828
3d	C ₁₅ H ₁₂ O ₃ (240)	74.69 (75)	4.98 (5)	54	103	290 398	3.8246 4.1951

150

groups on the carbonyl stretching frequencies, it is to be expected that **3d** (Ar = furyl) should exhibit high stretching frequency for its carbonyl groups compared to other compounds. This is fully justified in the recorded spectrum of the compound (Table 3.3).



3.1

The intense broad band in the region $2500\text{-}3500\text{ cm}^{-1}$ is undoubtedly due to the presence of strong intramolecular hydrogen bonding that exists in these compounds. A medium intensity band at $\sim 972\text{ cm}^{-1}$ is due to the trans -CH=CH- absorption as the *cis* ethylene double bonds usually show weak intensity bands at a much lower region. The characterisation ir bands of the compounds are brought out in table 3.3.

TABLE 3.3

Characteristic ir data (cm^{-1}) of 5-aryl-1-phenyl-4-pentene-1,3-diones, 3a-d

Compounds of				Probable assignments
3a	3b	3c	3d	
1635	1628	1629	1640	$\nu_{\text{C=O}}$ chelated benzoyl
1615	1619	1610	1622	$\nu_{\text{C=O}}$ chelated cinnamoyl
1576 1570	1589 1589	1590 1581	1585 1575	$\nu_{\text{C-C}}$ phenyl / alkenyl
1528	1440	1440	1434	ν_{asy} C-C-C chelate ring
1440	1380	1388	1377	ν_{sym} -C-C-C chelate ring
1098 1063	1141 1072 1030	1168 1080 1024	1185 1080 1024	$\beta_{\text{C-H}}$ chelate ring
967	991	972	970	$\gamma_{\text{CH=CH-}}$ trans
738	752	773	769	$\gamma_{\text{C-H}}$ chelate ring

nmr spectra

The chemical shift of the enolic proton in the nmr spectra as a measure of the strength of the hydrogen bond has been clearly demonstrated for several 1,3-diketones by Nonhebel.⁶³ The ^1H nmr spectra of 5-aryl-1-phenyl-4-pentene-1,3-diones shows a downfield singlet at $\sim \delta$ 16 ppm which can be assigned to the intramolecularly hydrogen bonded enolic proton of the compound. The methine proton signal appeared in the range δ 6.1-6.9 ppm. The ^1H nmr spectra of the compounds are reproduced in figures 3.1-3.3. The alkenyl signals with their

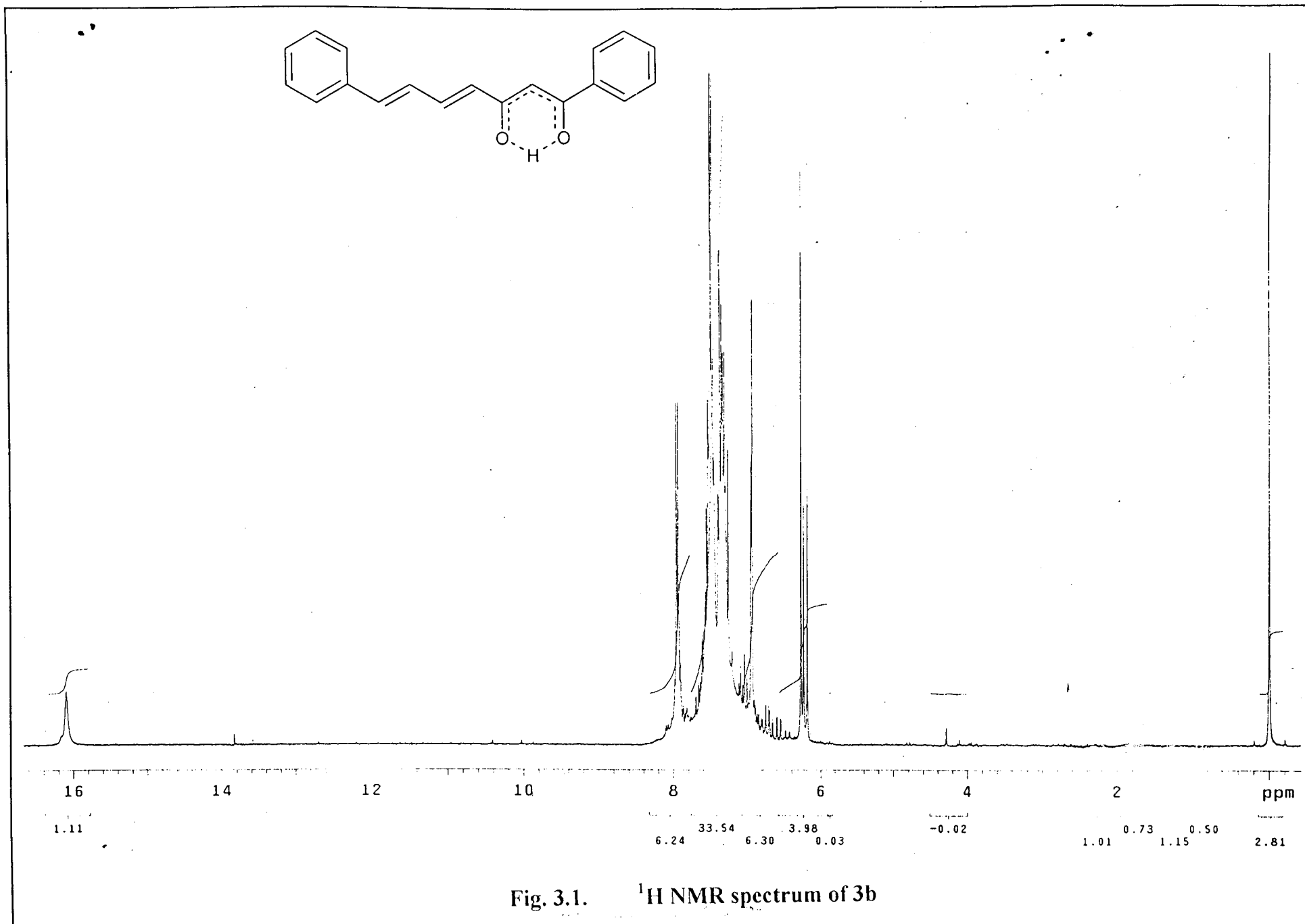


Fig. 3.1. ¹H NMR spectrum of 3b

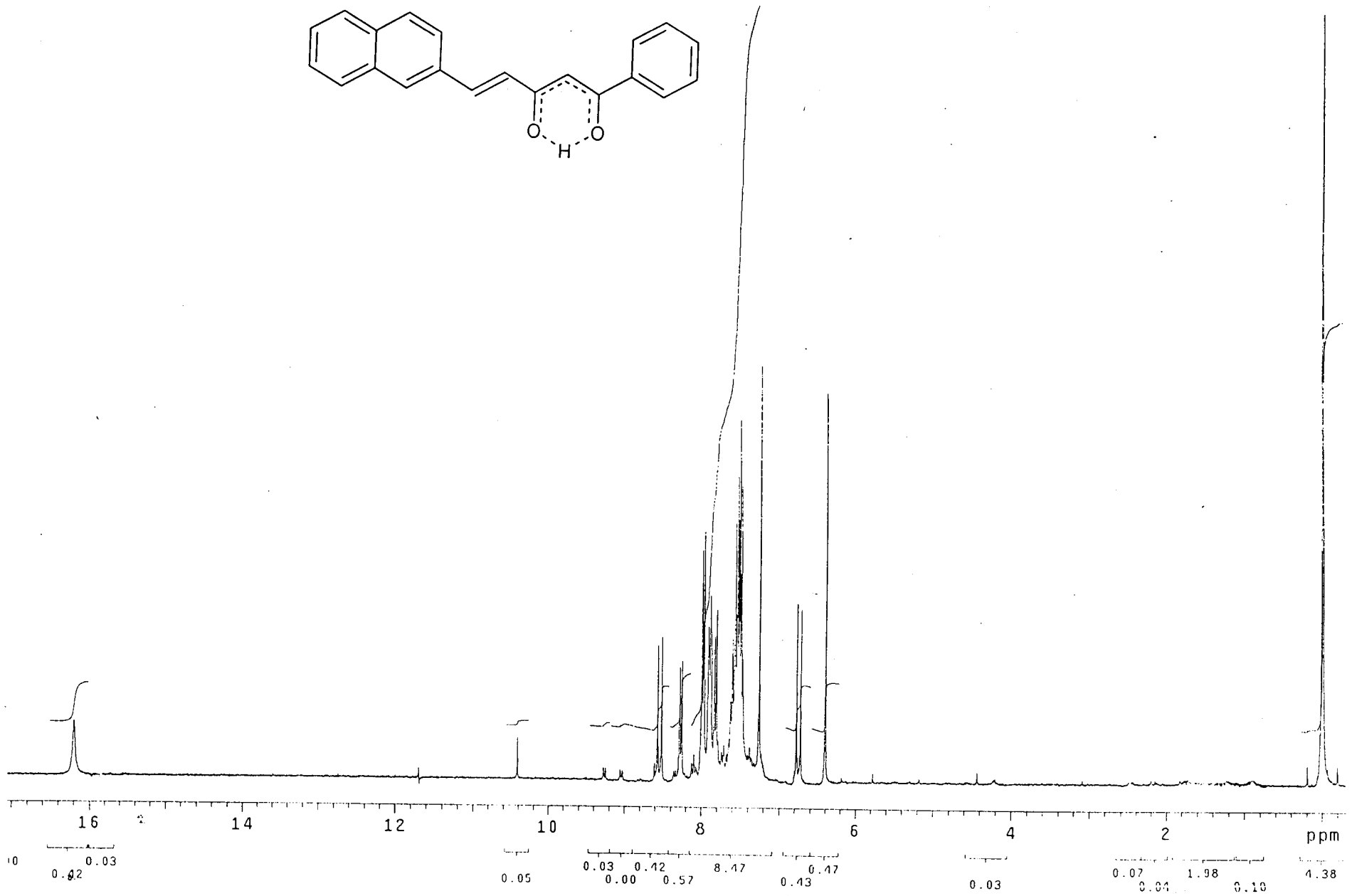
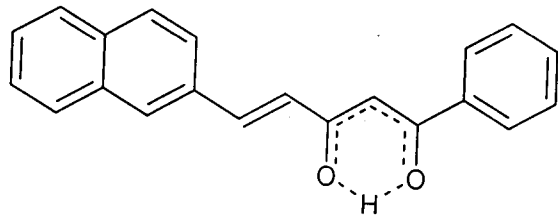


Fig. 3.2. ¹H NMR spectrum of 3c

154

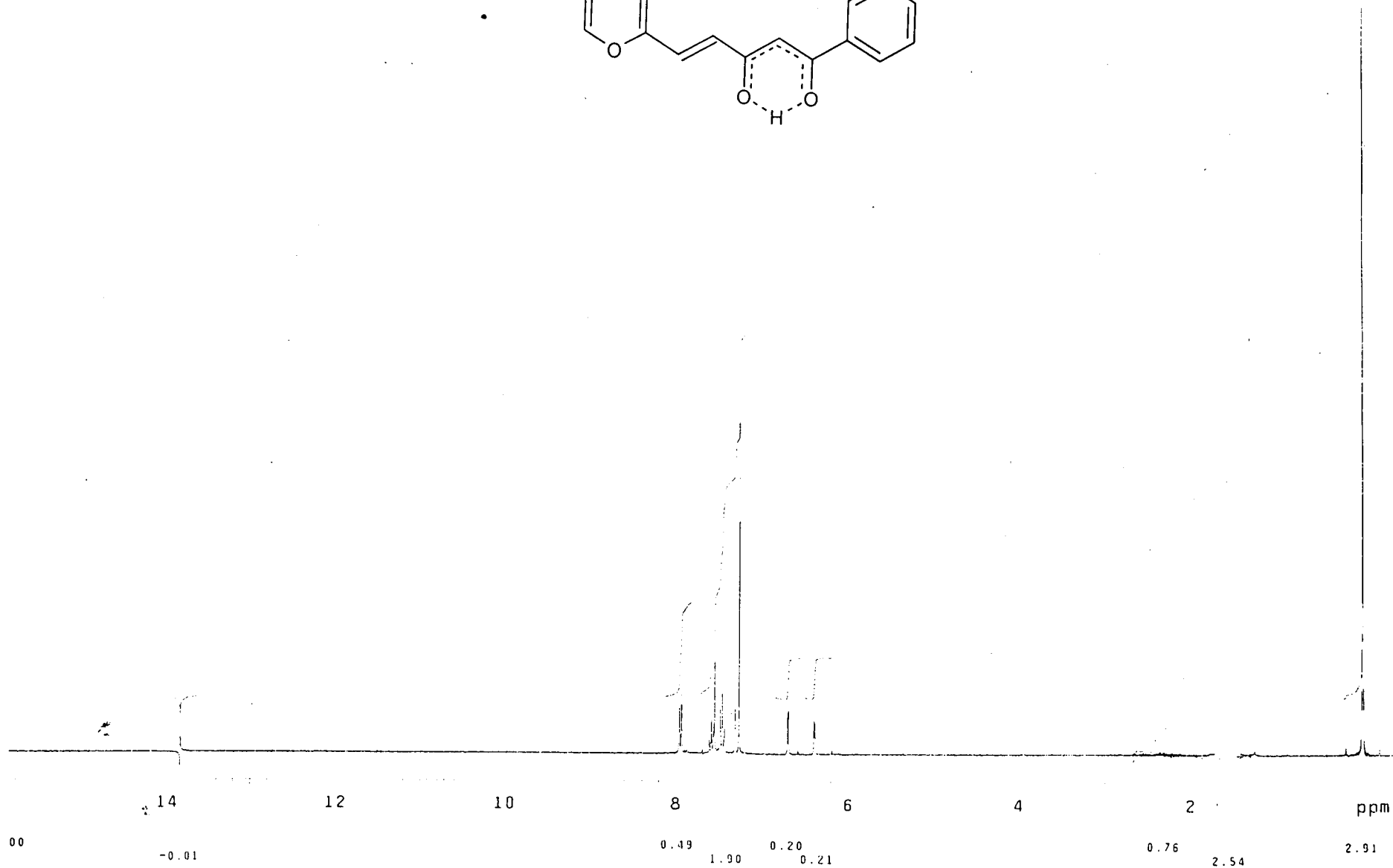
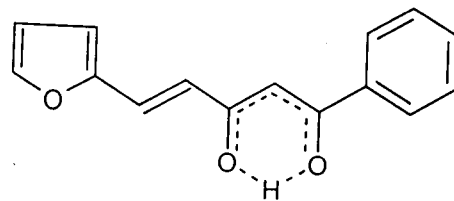


Fig. 3.3. ¹H NMR spectrum of 3d

155

observed J values suggest a trans configuration about the olefinic function in the compounds. The characteristic chemical shift of various protons are summarised in table 3.4. The integrated intensities of all the signals appeared in the spectra agree well with **structure 3.1** of the compounds.

TABLE 3.4

Characteristic ^1H nmr spectral data of 5-aryl-1-phenyl-4-pentene-1,3-diones, 3a-3d

Compounds of				Probable assignments Chemical shift (ppm)
3a	3b	3c	3d	
16.85	16.08	16.20	--	enolic
7.9926 (1H) 7.9792 (1H)	8.0960 (1H) 7.980 (1H)	8.5708 (1H) 8.2840 (1H)	7.9586 (1H) 7.9348 (1H)	alkenyl
7.50-7.79 (10H)	6.927-7.954 (10H)	7.259-7.999 (12H)	7.259-7.891 (8H)	aryl
6.85 (1H)	6.2734 (1H)	6.4064 (1H)	6.184 (1H)	methine

Mass spectra

The mass spectra^{120,121} of all the compounds showed intense molecular ion $\text{P}^+/\text{(P+1)}^+$ peaks in conformity with their formulation. Peaks due to $(\text{P-Ph})^+$, $(\text{P-Ph-CO})^+$, PhCO^+ , Ph^+ , $(\text{P-PH COCH}_2)^+$, are characteristic of all the spectra. The appearance of major peaks in the spectra of all the compounds can be accounted by considering the fragmentation pattern given in **scheme 3.2**. The mass spectra of the compounds are reproduced in figures 3.4-3.6.

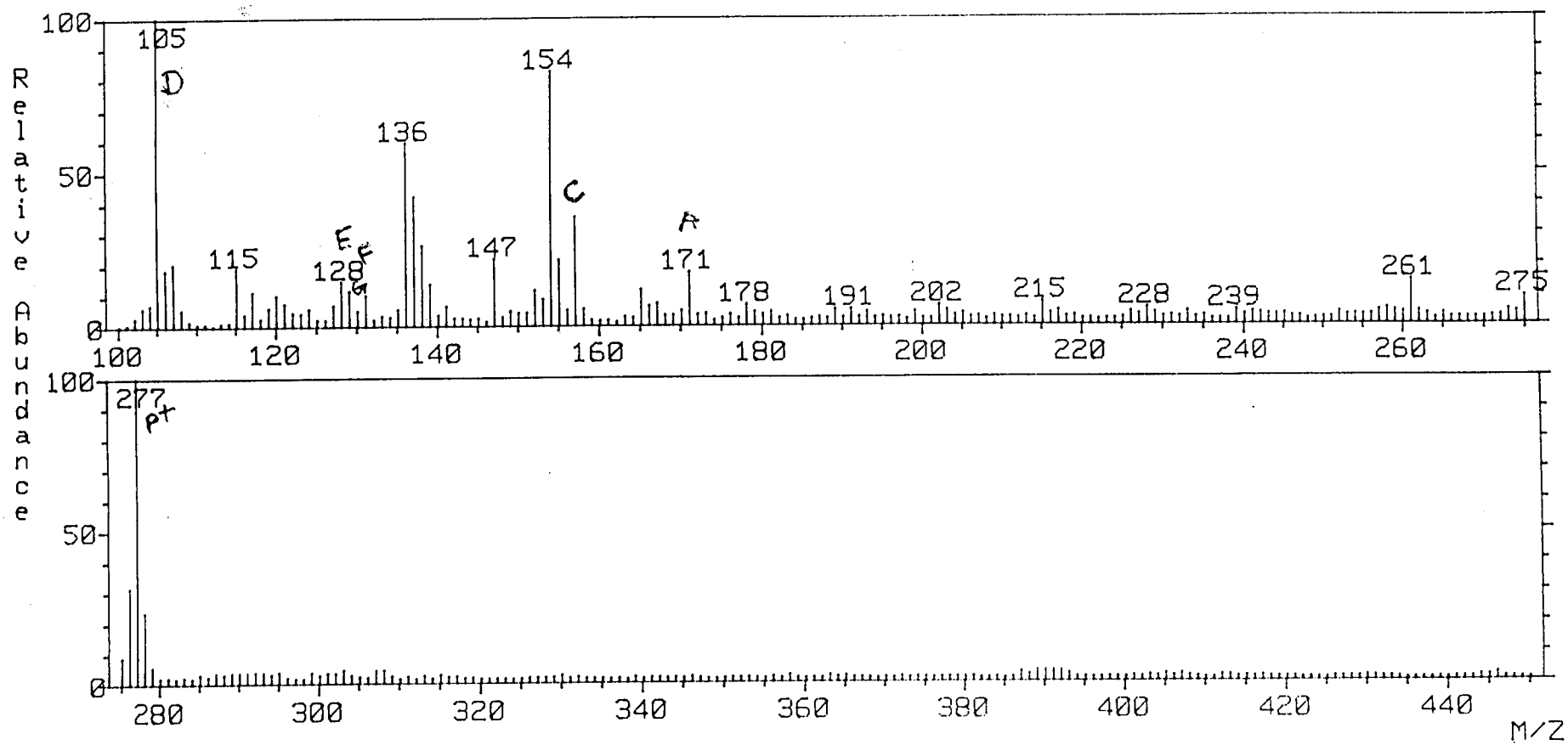
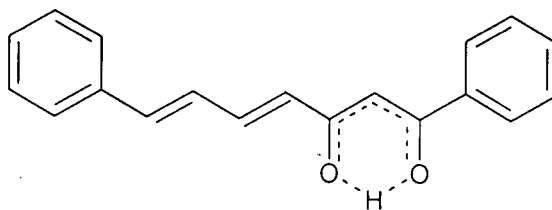


Fig. 3.4. Mass spectrum of 3b

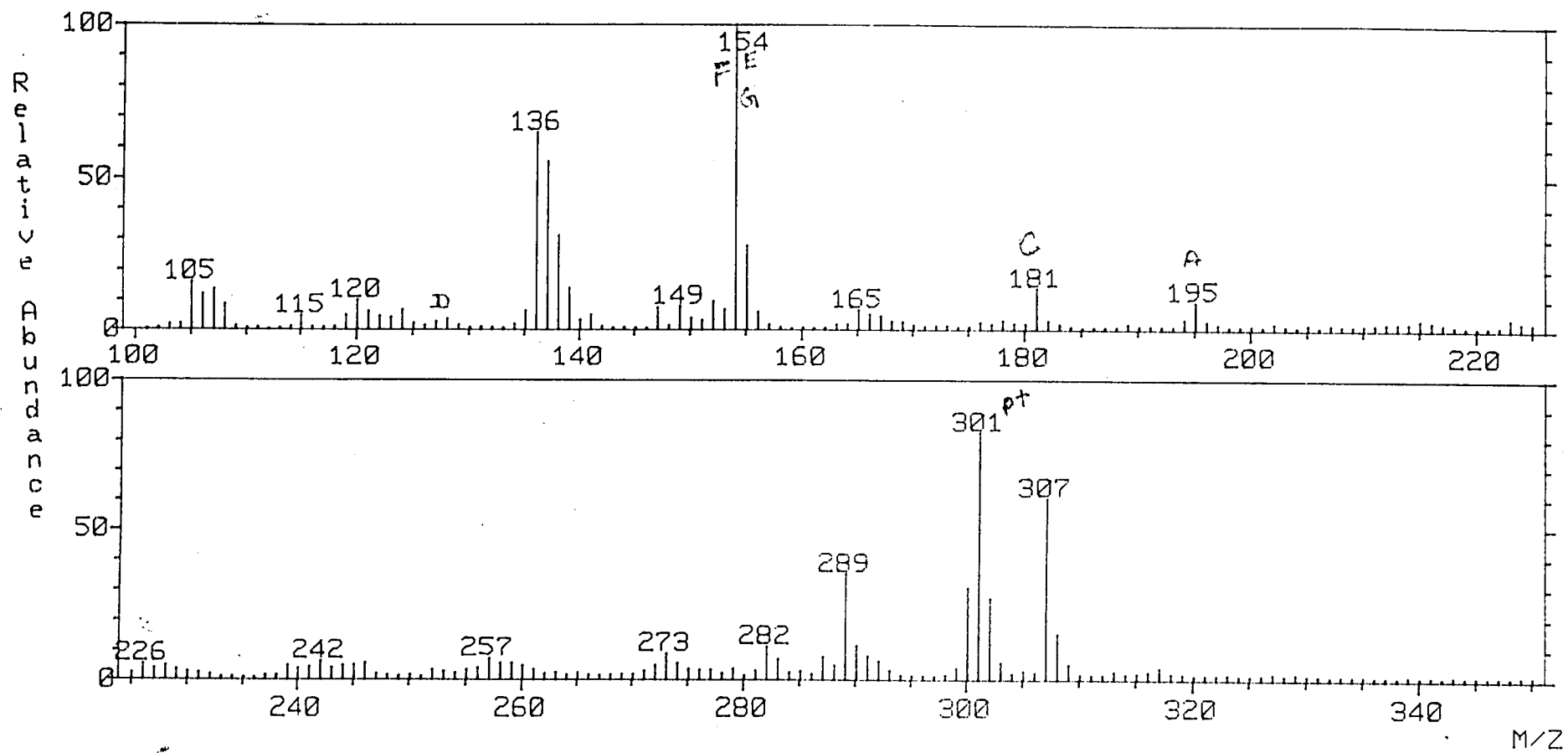
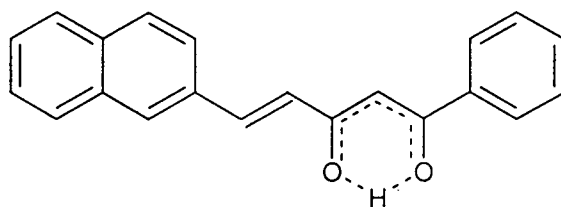


Fig. 3.5. Mass spectrum of 3c

158

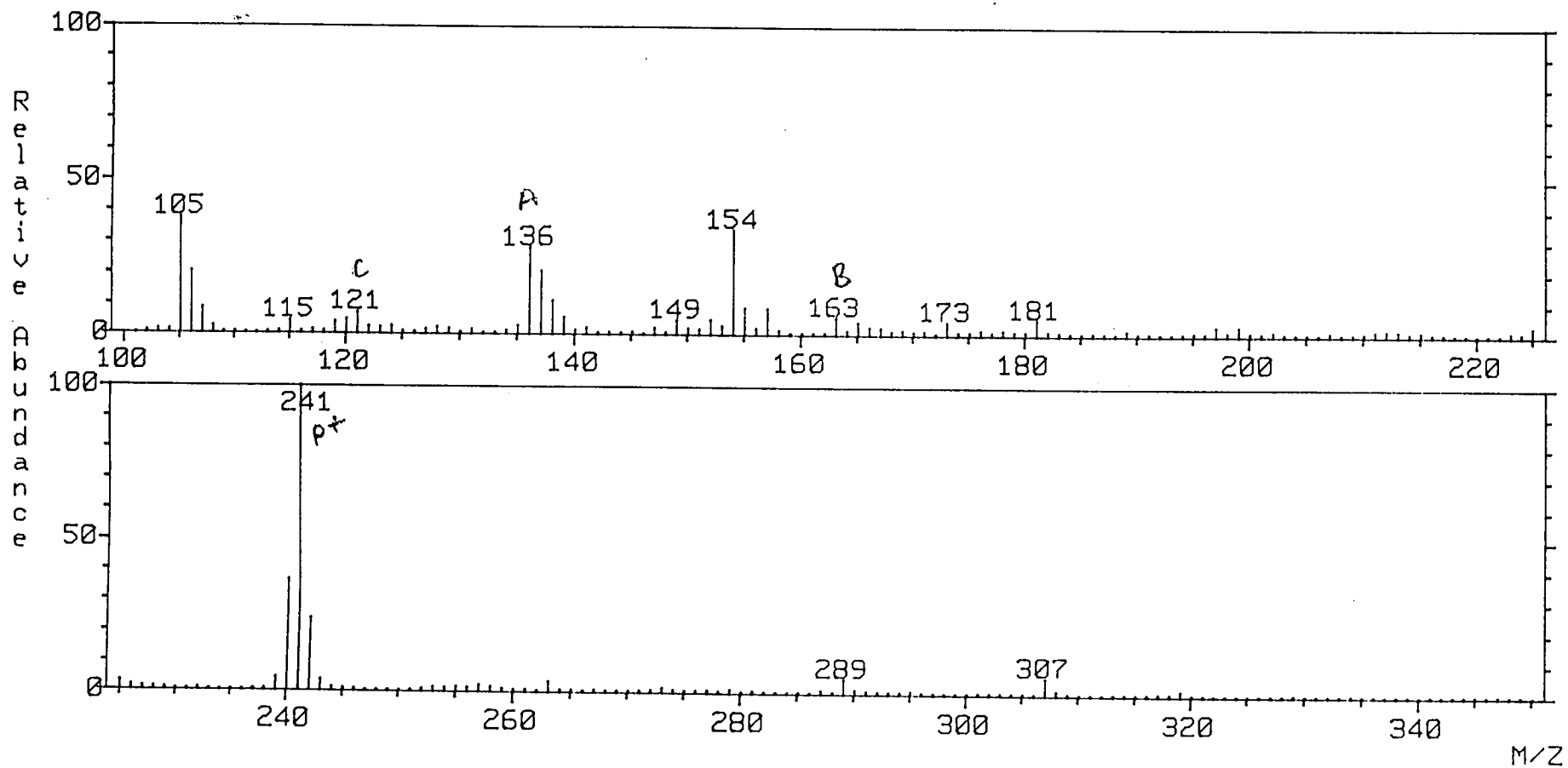
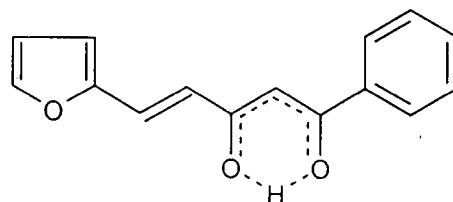
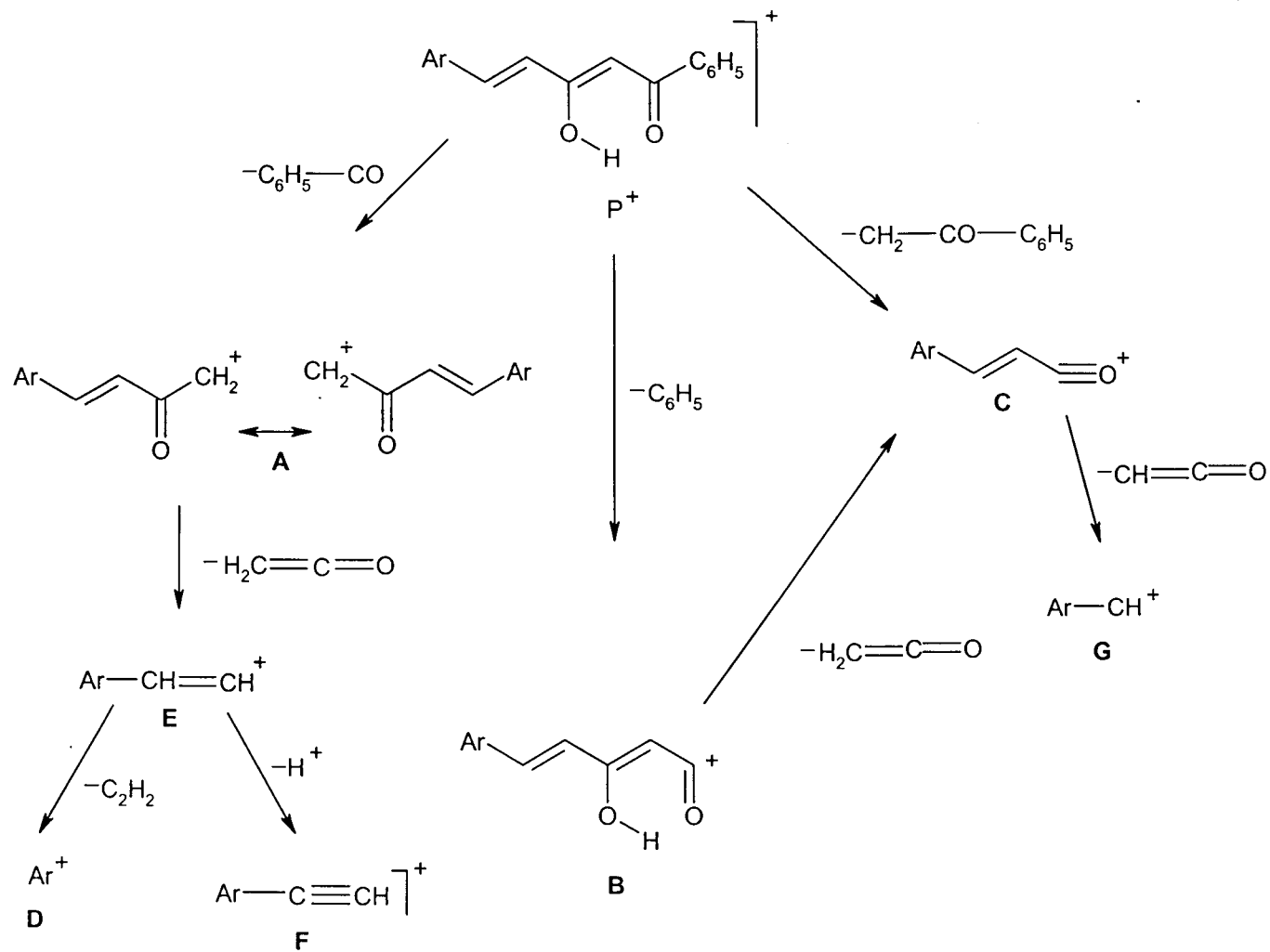


Fig. 3.6. Mass spectrum of 3d

159

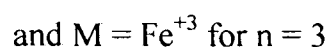
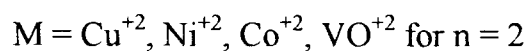
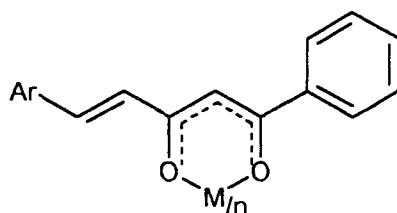


Scheme 3.3 Fragmentation Pattern for 3a - d

160

Characterisation of metal chelates of 5-aryl-1-phenyl-4-pentene-1,3-diones

The analytical and physical data of the metal complexes are given in table 3.4-3.6. The observed elemental analysis data of the complexes suggests that they are of $[ML_2]$ stoichiometry, for iron(III) it is of $[ML_3]$ stoichiometry. All the complexes behave as non electrolytes (specific conductance $< 15 \Omega^{-1}cm^{-1}$ in dmf) and do not contain the anion of the metal salt used for their preparation. Copper(II), cobalt(II), oxovanadium(IV) and iron(III) complexes show normal magnetic moment where as nickel(II) are diamagnetic. The electronic, ir, nmr and mass spectral data of the complexes are in agreement with the structure that would result when the chelated enol proton of the ligand is replaced by metal ion as in **structure 3.2**.



3.2

Uv spectra

The observed uv absorption maxima of the complexes are given in tables 3.5-3.8. They bear close resemblance to that of the free ligands indicating that no structural alternation of the ligand has occurred during complexation. However, the slight bathochromic shift of the two major bands of the complexes compared to the free ligands suggest that both the carbonyl oxygens are involved in bonding with the metal ion.

TABLE 3.5

Analytical and characteristic uv spectral data of copper(II) complexes of 5-aryl-1-phenyl-4-pentene-1,3-diones, 3a-d

Copper(II) chelates of, (Molecular formula)*	Yield %	M.P. °C	μ_{eff} (B.M.)	Elemental Analysis Calculated / (found)			λ_{max} (nm)
				C	H	M	
3a (C ₁₇ H ₁₃ O ₂) ₂ Cu	70	227	1.81	72.67 (71.87)	4.63 (4.32)	11.31 (11.08)	261 390
3b (C ₁₉ H ₁₅ O ₂) ₂ Cu	70	198	1.80	74.32 (74.14)	4.89 (4.87)	10.36 (10.33)	289 409
3c (C ₂₁ H ₁₅ O ₂) ₂ Cu	65	242	1.79	76.19 (76.02)	4.54 (4.52)	9.59 (9.52)	281 389
3d (C ₁₅ H ₁₁ O ₃) ₂ Cu	60	150	1.76	66.48 (66.42)	4.26 (4.05)	11.73 (11.72)	291 392

*The molecular formula given correspond to [CuL₂] stoichiometry, where L stands for the deprotonated ligand moiety.

TABLE 3.6

Analytical and characteristic uv spectral data of nickel(II) complexes of 5-aryl-1-phenyl-4-pentene-1,3-diones, 3a-d

Nickel(II) chelates of, (Molecular formula)*	Yield %	M.P. °C	Elemental Analysis Calculated / (found)			λ_{\max} (nm)
			C	H	M	
3a (C ₁₇ H ₁₃ O ₂) ₂ Ni	70	243	73.29 (72.47)	4.67 (4.51)	10.54 (10.23)	259 390
3b (C ₁₉ H ₁₅ O ₂) ₂ Ni	70	> 300	74.92 (74.75)	4.93 (4.91)	9.64 (9.62)	284 408
3c (C ₂₁ H ₁₅ O ₂) ₂ Ni	65	120	76.75 (76.59)	4.57 (4.55)	8.94 (8.92)	280 385
3d (C ₁₅ H ₁₁ O ₃) ₂ Ni	60	160	67.08 (67.03)	4.09 (4.08)	11.84 (11.83)	285 322

*The molecular formula given correspond to [NiL₂] stoichiometry, where L stands for the deprotonated ligand moiety.

1649

TABLE 3.7

Analytical and characteristic uv spectral data of cobalt(II) 2H₂O complexes of 5-aryl-1-phenyl-4-pentene-1,3-diones, 3a-d

Cobalt(II)2H ₂ O chelates of, (Molecular formula)*	Yield %	M.P. °C	μ_{eff} (B.M.)	Elemental Analysis Calculated / (found)			λ_{max} (nm)
				C	H	M	
3a (C ₁₇ H ₁₃ O ₂) ₂ Co(H ₂ O) ₂	65	250	4.90	72.69 (72.56)	4.05 (4.0)	10.51 (10.20)	260 395
3b (C ₁₉ H ₁₅ O ₂) ₃ Co(H ₂ O) ₂	60	110	4.77	74.89 (74.75)	4.93 (4.91)	9.68 (9.16)	284 416
3c (C ₂₁ H ₁₅ O ₂) ₂ Co(H ₂ O) ₂	50	130	4.82	76.72 (76.59)	4.57 (4.55)	8.97 (8.95)	280 385
3d (C ₁₅ H ₁₁ O ₃) ₂ Co(H ₂ O) ₂	60	> 300	4.84	67.55 (67.71)	4.13 (4.0)	10.3 (10.01)	290 329

*The molecular formula given correspond to [CoL₂(H₂O)₂] stoichiometry, where L stands for the deprotonated ligand moiety.

TABLE 3.8

Analytical and characteristic uv spectral data of iron(III) complexes of 5-aryl-1-phenyl-4-pentene-1,3-diones, 3a-d

Iron(III)2H ₂ O chelates of, (Molecular formula)*	Yield %	M.P. °C	μ_{eff} (B.M.)	Elemental Analysis Calculated / (found)			λ_{max} (nm)
				C	H	M	
3a (C ₁₇ H ₁₃ O ₂) ₃ Fe	60	178	5.92	72.89 (72.64)	4.72 (4.69)	6.9 (6.8)	270 395
3b (C ₁₉ H ₁₅ O ₂) ₃ Fe	60	138	5.89	77.65 (77.55)	5.11 (5.10)	6.34 (6.33)	289 409
3c (C ₂₁ H ₁₅ O ₂) ₃ Fe	55	120	5.83	79.34 (79.24)	4.72 (4.70)	5.86 (5.85)	292 388
3d (C ₁₅ H ₁₁ O ₃) ₃ Fe	70	> 300	5.87	69.87 (69.85)	4.27 (4.26)	7.2 (7.1)	285 327

*The molecular formula given correspond to [FeL₃] stoichiometry, where L stands for the deprotonated ligand moiety.

166

Infrared spectra

The most characteristic feature of the ir spectra of the metal complexes of 5-aryl-1-phenyl-4-pentene-1,3-diones is the absence of any strong bands in the region 1700-1600 cm^{-1} due to free or hydrogen bonded carbonyl function. It has been reported that the carbonyl stretching frequency of 1,3-diketones shift (10-40 cm^{-1}) to lower values during metal complexation. However two new bands appeared in the spectra of metal(II) chelates at $\sim 1625 \text{ cm}^{-1}$ and $\sim 1590 \text{ cm}^{-1}$ of appreciable intensity, apart from the various medium intensity bands arising from aromatic and alkenyl C=C vibrations. These bands can safely be assigned to the metal chelated carbonyl groups. This is further supported by the appearance of medium intensity bands at $\sim 480 \text{ cm}^{-1}$ and $\sim 420 \text{ cm}^{-1}$ arising from $\nu_{\text{M-O}}$ vibrations.

The replacement of enolic proton by metal ion is also evident from the absence of the broad free ligand band in the region 3400-2800 cm^{-1} in the spectra of complexes. The characteristic ir data of various metal complexes and their probable assignments are given in table 3.9 to 3.13.

TABLE 3.9

Characteristic ir data (cm^{-1}) of copper(II) chelates of
5-aryl-1-phenyl-pentanoids, 3a-d

Copper(II) chelate of				Probable assignments
3a	3b	3c	3d	
1607	1630	1629	1595	$\nu_{\text{C=O}}$ metal chelated benzoyl
1582	1586	1587	1565	$\nu_{\text{C=O}}$ metal chelated cinnamoyl
1570 1540	1520 1448	1523 1459	1519 1456	$\nu_{\text{C-C}}$ phenyl / alkenyl
1525	1395	1406	1404	$\nu_{\text{asym.}}$ C-C-C-chelating
1435	1370	1346	1385	ν_{sym} -C-C-C-chelating
1096 1060	1180 1139 1072	1187 1167 1025	1178 1085 1020	$\beta_{\text{C-H}}$ chelate ring
967	994	966	960	$\nu_{\text{CH=CH-}}$ (trans)
732	750	767	777	ν_{CH} chelate ring
450 418	503	481	457 418	$\nu_{\text{M-O}}$ chelate ring

TABLE 3.10
 Characteristic ir data (cm^{-1}) of nickel(II) chelates of
 5-aryl-1-phenyl-pentanoids, 3a-d

Nickel(II) chelate of			Probable assignments
3b	3c	3d	
1630	1631	1598	$\nu_{\text{C=O}}$ metal chelated benzoyl
1595	1589	1560	$\nu_{\text{C=O}}$ metal chelated cinnamoyl
1520 1450	1547 1451	1519 1452	$\nu_{\text{C-C-C}}$ phenyl / alkyl
1395	1409	1415	ν_{asym} C-C-C chelate ring
1353	1346	1386	ν_{sym} C-C-C chelate ring
1159 1125 1058	1167 1102 1027	1180 1068 1016	$\beta_{\text{C-H}}$ chelate ring
951	970	960	$\gamma_{\text{CH=CH}}$ trans
755	771	761	$\gamma_{\text{C-H}}$ chelate ring
487	474	469 428	$\gamma_{\text{M-O}}$ chelate ring

TABLE 3.11
 Characteristic ir data (cm^{-1}) of cobalt(II) chelate of
 5-aryl-1-phenyl-pentanoids

Cobalt(II) chelate of		Probable assignments
3b	3c	
1630	1627	$\nu_{\text{C=O}}$ metal chelated benzoyl
1585	1590	$\nu_{\text{C=O}}$ metal chelated cinnamoyl
1518 1450	1483 1450	$\nu_{\text{C-C}}$ phenyl / alkyl
1389	1398	ν_{asym} C-C-C chelate ring
1350	1346	ν_{sym} C-C-C chelate ring
1178 1072	1167 1055 1028	$\beta_{\text{C-H}}$ chelate ring
996	967	$\gamma_{\text{CH=CH}}$ trans
751	772	$\gamma_{\text{C-H}}$ chelate ring
500	472	$\gamma_{\text{M-O}}$ chelate ring

TABLE 3.12

Characteristic ir data (cm^{-1}) of oxovanadium(IV) of 5-aryl-1-phenyl-pentanoids

Oxovanadium(IV) chelate of			Probable assignments
3b	3c	3d	
1613	1626	1600	$\nu_{\text{C=O}}$ metal chelated benzoyl
1586	1586	1560	$\nu_{\text{C=O}}$ metal chelated cinnamoyl
1520 1447	1546 1447	1522 1466	$\nu_{\text{C-C-C}}$ phenyl / alkyl
1374	1420	1401	ν_{asym} C-C-C chelate ring
1314	1341	1375	ν_{sym} C-C-C chelate ring
1182 1135 1069	1162 1102 1020	1174 1074 1015	$\beta_{\text{C-H}}$ chelate ring
990	970	970	$\gamma_{\text{CH=CH}}$ trans
751	771	752	$\gamma_{\text{C-H}}$ chelate ring
499 453	550 495	472 419	$\gamma_{\text{M-O}}$ chelate ring

TABLE 3.13

Characteristic ir data (cm^{-1}) iron(III) chelate of 5-aryl-1-phenyl-pentanoids

Iron(III) chelate of			Probable assignments
3b	3c	3d	
1620	1625	1616	$\nu_{\text{C=O}}$ metal chelated benzoyl
1585	1586	1585	$\nu_{\text{C=O}}$ metal chelated cinnamoyl
1519 1450	1517 1447	1550 1471	$\nu_{\text{C-C-C}}$ phenyl / alkyl
1377	1387	1420	ν_{asym} C-C-C chelate ring
1360	1346	1377	ν_{sym} C-C-C chelate ring
1145 1099	1165 1102 1025	1180 1125 1016	$\beta_{\text{C-H}}$ chelate ring
995	966	974	$\gamma_{\text{CH=CH}}$ trans
782	769	750	$\gamma_{\text{C-H}}$ chelate ring
432 410	470	472 418	$\gamma_{\text{M-O}}$ chelate ring

 ^1H nmr spectra

The most characteristic feature of the ^1H nmr spectra of the diamagnetic nickel(II) chelates is the absence of proton signals at $\delta \sim 16$ ppm. This strongly suggests the replacement of the enolic proton by the metal ions in the complexes as in **structure 3.2**. The methine signals are shifted towards the low field of the spectra indicating the decreased electron density around the central carbon atom of

the aromatic metal chelate ring system. The integrated intensities of the aryl and alkenyl signals are in agreement with the 1:2 metal-ligand stoichiometry of the chelates.

Mass spectra

The FAB mass spectra of the copper(II) chelates of the compounds (figures 3.7-3.9) show prominent peaks due to $[\text{CuL}_2]^+$ which justifies the formation of the chelates. The base peak in all the case is due to the ligand and peaks due to $[\text{CuL}]^+$, L^+ and fragment of L^+ are sometimes more intense than the molecular ion peak. Another striking feature of all the spectra is the presence of a large number of fragments containing copper. Thus the available spectral evidence fully support the monobasic bidentate chelation of the complex as in structure 3.2.

Characterisation of the condensation product of pyridine-3-aldehyde with benzoylacetone and its metal complexes

It is well known that under suitable conditions one molecule of aldehyde or ketone add to a second molecule in such a way that the α -carbon of the first becomes attached to the carbonyl carbon of the second. This reaction is known as aldol condensation. If the aldehyde or ketone does not contain an α -hydrogen, a simple aldol condensation cannot take place. Thus benzoyl acetone in which the carbon groups possess α -hydrogens can very well undergo aldol condensation.

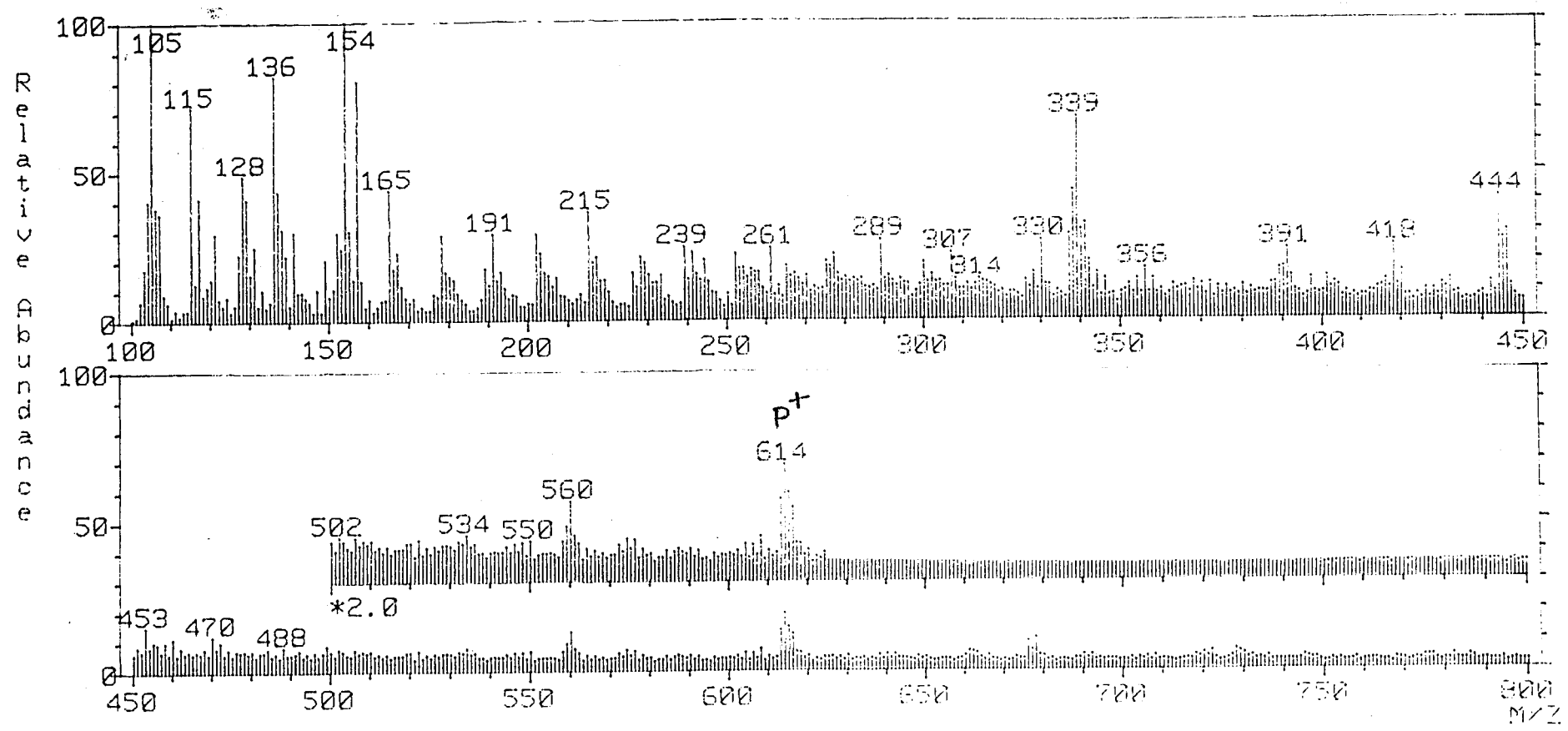
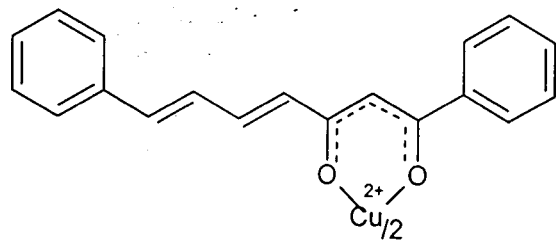


Fig. 3.7. Mass spectrum of copper(II) complex of 3b

174

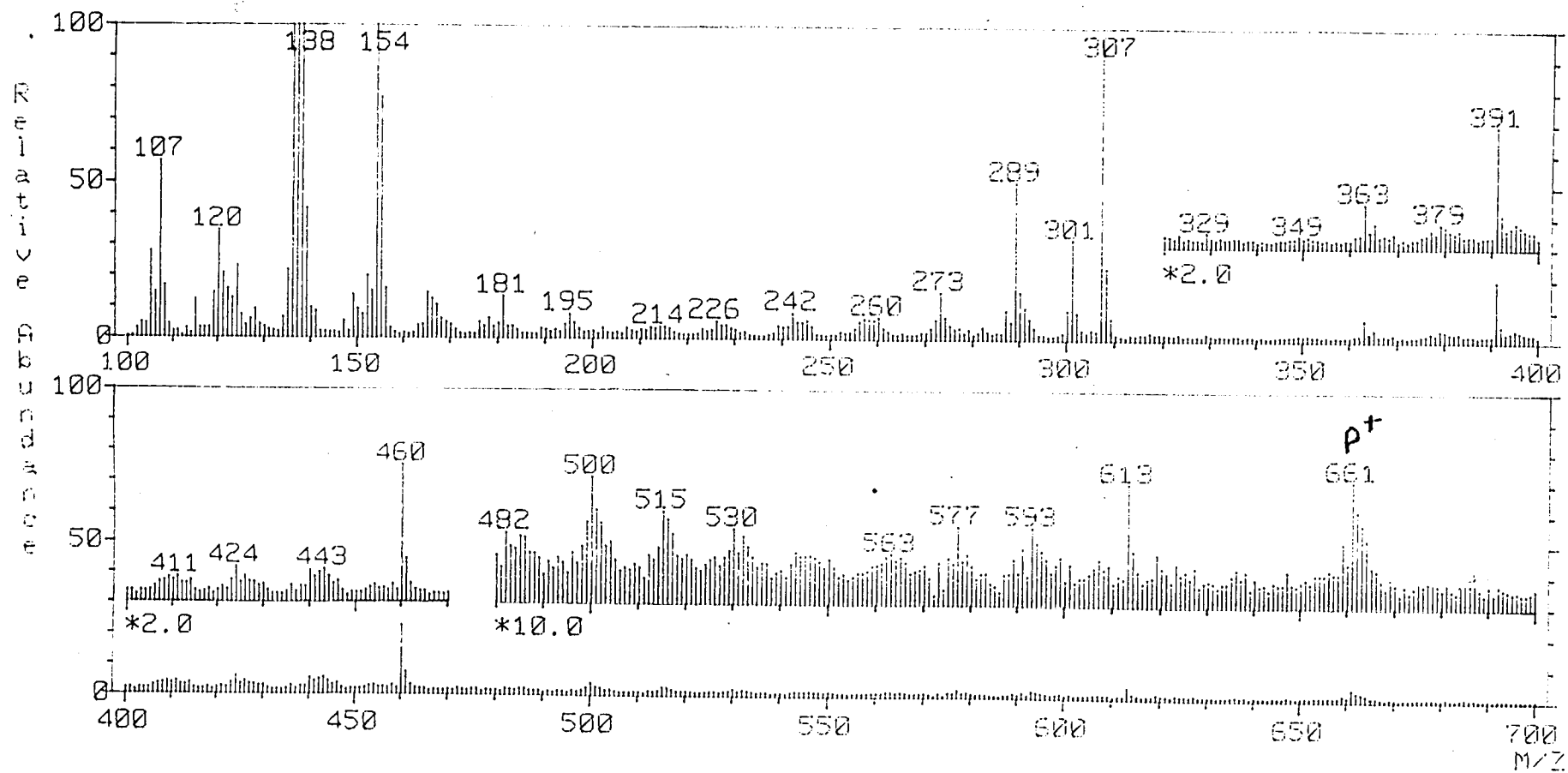
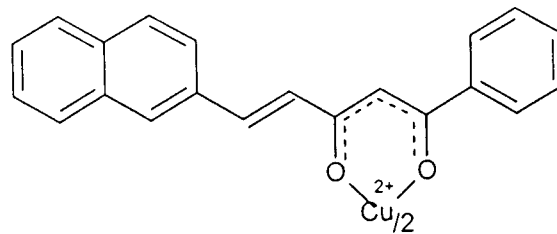


Fig. 3.8. Mass spectrum of copper(II) complex of 3c

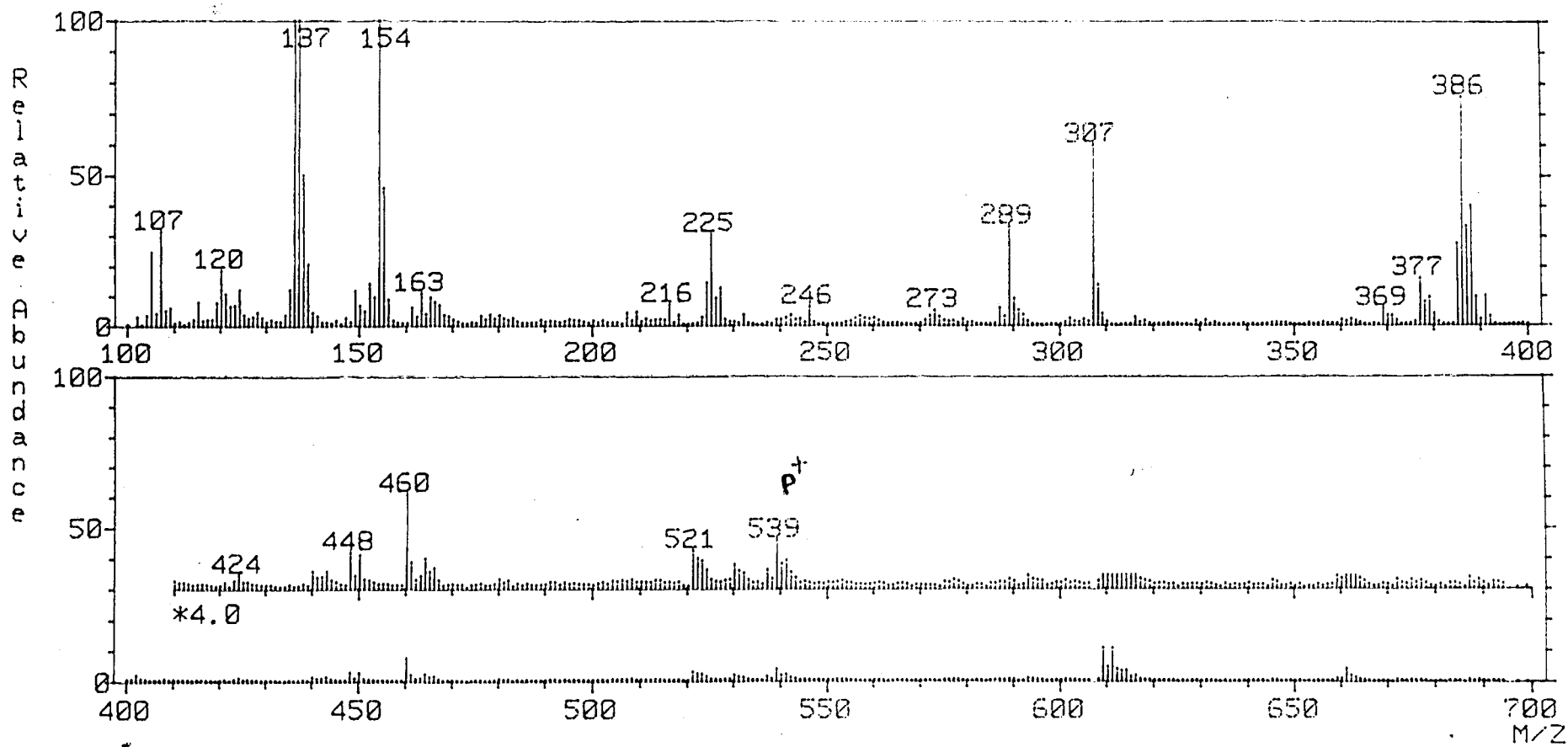
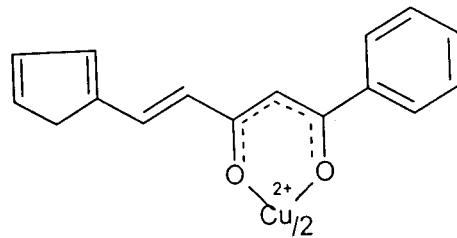
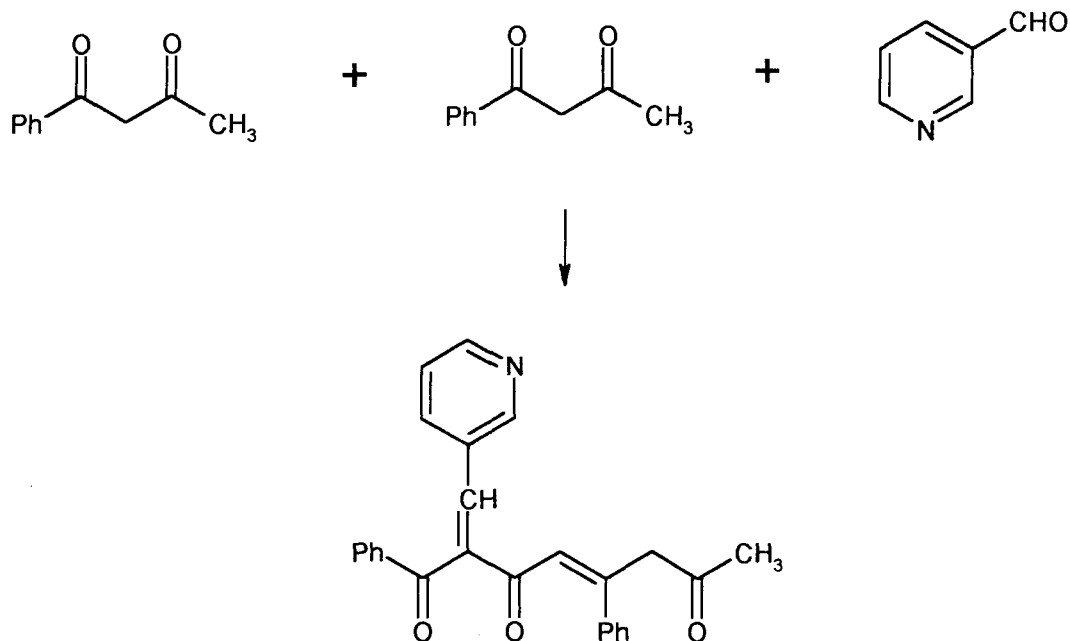


Fig. 3.9. Mass spectrum of copper(II) complex of 3d

176

Similarly heteroaryl aldehydes such as pyridine-3-carbaldehyde is more prone to Knoevenagel type condensation than to aldol condensation compared to benzaldehyde or substituted aldehydes. Thus, the formation of a different product in the case of the condensation reaction between pyridine-3-carbaldehyde and benzoyl acetone is not surprising. The spectral data discussed below are in full agreement with these facts. The compound obtained from the condensation of the pyridine-3-aldehyde with the benzoyl acetone was thoroughly examined using various analytical and spectral techniques. These results are discussed below.

In the mass spectrum of the compound an intense peak observed at m/z 394, which is the highest mass peak in the spectrum (Fig. 3.11). Appearance of this peak can only be explained by considering that both aldol and Knoevenagel type condensations occurred under the reaction conditions as given in **scheme 3.3**. The C, H, N percentage determined also support the formulation of the coordination product (Table 3.15).



4,8-diphenyl-7-(pyridin-3-ylmethylene)-4-octene-2,6,8-trione

Scheme 3.3

Similarly the compound contain an acetyl group is clearly indicated from its mass spectrum (figure 3.11) with the appearance of an intense (P-43)⁺ peak.

The ¹H nmr spectrum of the compound given in figure 3.10 shows a signal at 2.2052 assignable to methyl protons of acetyl group. The signal at 6.182 in the spectrum can safely be assigned to the methylene protons. That the compound contains two phenyl groups is clearly indicated from the splitting pattern of the phenyl proton signals in the range δ 7.430 – 7.554 ppm. The pyridyl ring protons are observed at δ 7.869-7.904 ppm. The peaks in the range δ 7.260-7.424 are due to

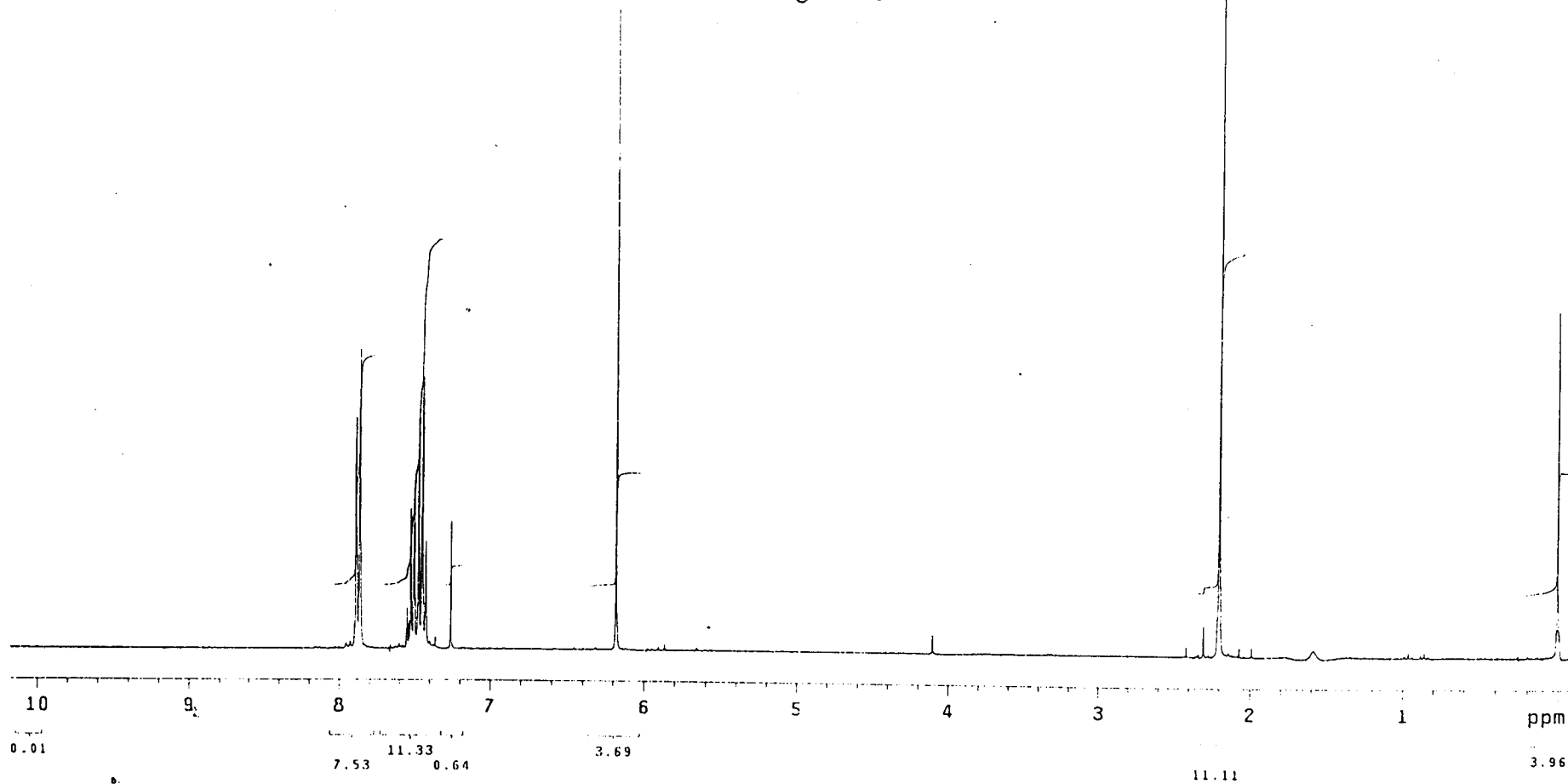
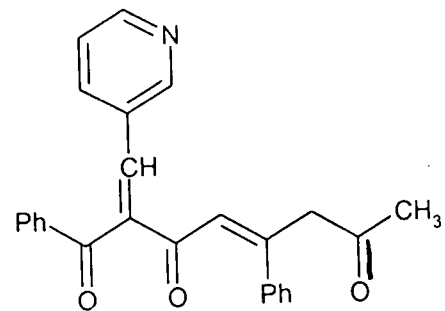


Fig. 3.10. ¹H NMR spectrum of 3e

10/10

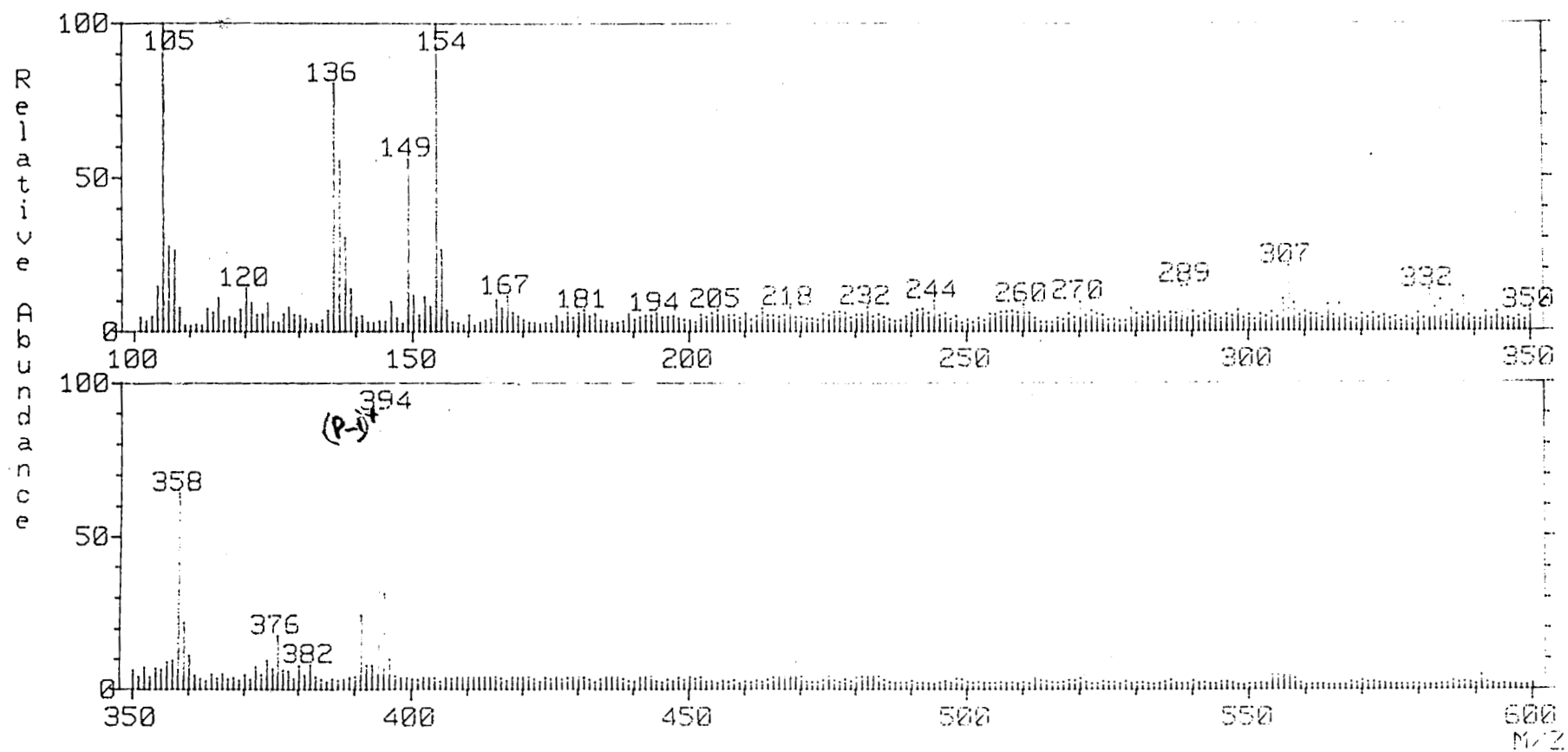
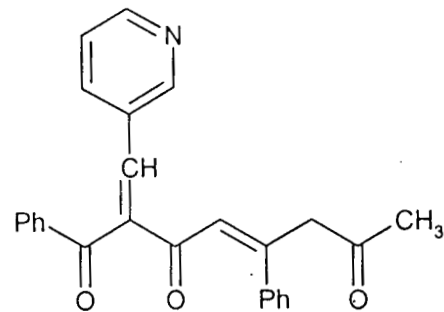


Fig. 3.11. Mass spectrum of 3e

100

The copper(II) and nickel(II) complexes of the compound have been prepared and characterised. The observed analytical data (Table 3.15) suggests $[ML(OAc)_2]$ stoichiometry of the complexes. The mass spectrum of the copper(II) complexes also shows a peak at m/z 578 (figure 3.12) corresponds to composition $[CuL(OAc)_2]$. Other major fragments appeared in the spectrum are due to the removal of OAc, CH_3CO , Ph, PhCO, Py, etc. groups from the molecular ion.

The ir spectra of the complexes are characterised by the presence of four medium intensity bands at $\sim 1700\text{ cm}^{-1}$, 1625 cm^{-1} , 1610 cm^{-1} and 1605 cm^{-1} . The appearance of a band at $\sim 1700\text{ cm}^{-1}$ strongly suggest that the acetyl carbonyl is not involved in bonding with the metal ion. The band at ~ 1625 may probably due to coordinated acetate group and the other two band can be assigned to metal bonded carbonyl groups. Thus the spectrum of the complex support the structure 3.4.

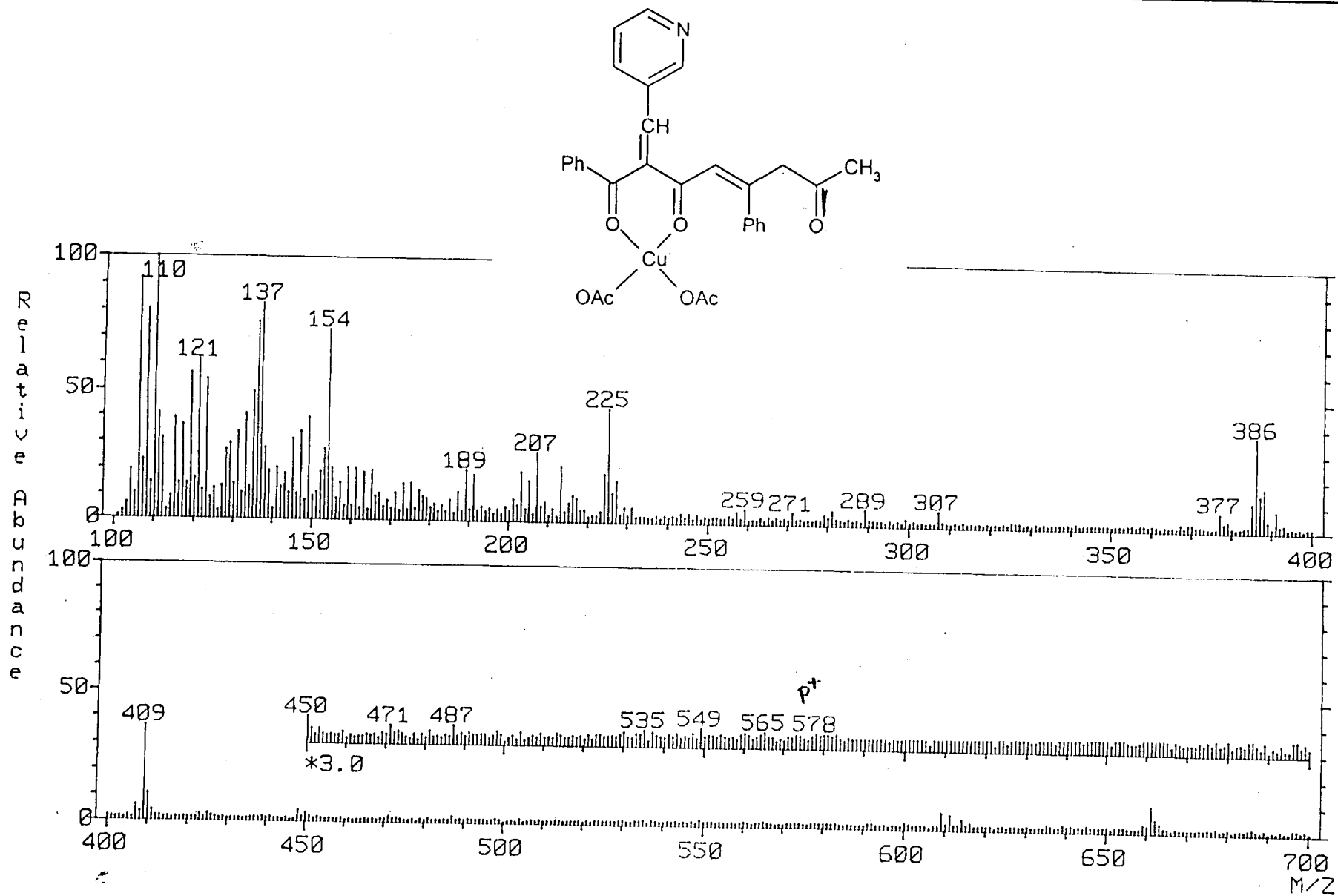


Fig. 3.12. Mass spectrum of copper(II) complex of 3e

the olefinic protons. Thus the ^1H nmr and mass spectral data unequivocally support the formation of 4,8-diphenyl-7-(pyridin-3-ylmethylene)-4-octene-2,6,8-trione (**3e**).

The ir spectrum of the compound also support the presence of an acetyl carbonyl and a benzoyl carbonyl because of the presence of two strong bands at 1710 cm^{-1} and 1650 cm^{-1} assignable respectively to the benzoyl and acetoxy centre of structure. Important ir bands observed in the spectrum of the compound and their probable assignments are given in the table 3.14.

TABLE 3.14
Characteristic ir data (cm^{-1}) of 4,8-diphenyl-7-(pyridin-3-ylmethylene)-4-octene-2,6,8-triones (3e**)**

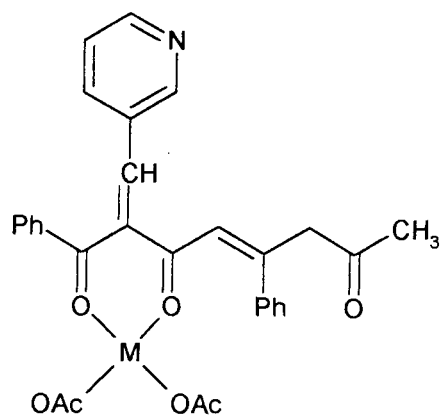
Compound of 3e	Probable assignments
1710	$\nu_{\text{C=O}}$ chelated acetyl
1650	$\nu_{\text{C=O}}$ chelated benzyl
1630 1602	$\nu_{\text{C-C}}$ phenyl / alkenyl
1565	ν_{asy} C-C-C chelate ring
1485	ν_{sym} -C-C-C chelate ring
1197 1078 1020	$\beta_{\text{C-H}}$ chelate ring
962	$\gamma_{\text{CH=CH}}$ trans
763	$\gamma_{\text{C-H}}$ chelate ring

TABLE 3.15

Analytical and characteristic uv spectral data of metal complexes of 4,8-diphenyl-7-(pyridin-3-ylmethylene)-4-octene-2,6,8-trione

Metal(II) chelates of, (Molecular formula)*	Yield (%)	M.P. (°C)	Elemental Analysis			λ_{\max} (nm)
			C	H	M	
3e (C ₂₆ H ₂₁ O ₃ N)Cu(OAc) ₂	60	160	68.14 (68.08)	4.26 (4.25)	11.28 (11.26)	354
3e (C ₂₆ H ₂₁ O ₃ N)Ni(OAc) ₂	65	130	68.73 (68.69)	4.29 (4.28)	11.37 (11.36)	332

*The molecular formula given correspond to [ML(OAc)₂] stoichiometry, where L stands for the deprotonated ligand moiety.



3.4

The unidentate coordination of the acetate group is evident from the presence of a band at $\sim 1300\text{ cm}^{-1}$ due to $\nu_s(\text{CH}_3\text{COO}^-)$ vibration. Important ir bands and their assignments are given in the table 3.16. Thus all available data support the neutral unidentate O,O-coordination of the triketone in which the acetyl carbonyl is in fine coordination with the metal ion.

TABLE 3.16

Characteristic ir data (cm^{-1}) of copper(II) chelates of
4,8-diphenyl-7-(pyridin-3-ylmethylene)-4-octene-2,6,8-trione (3e)

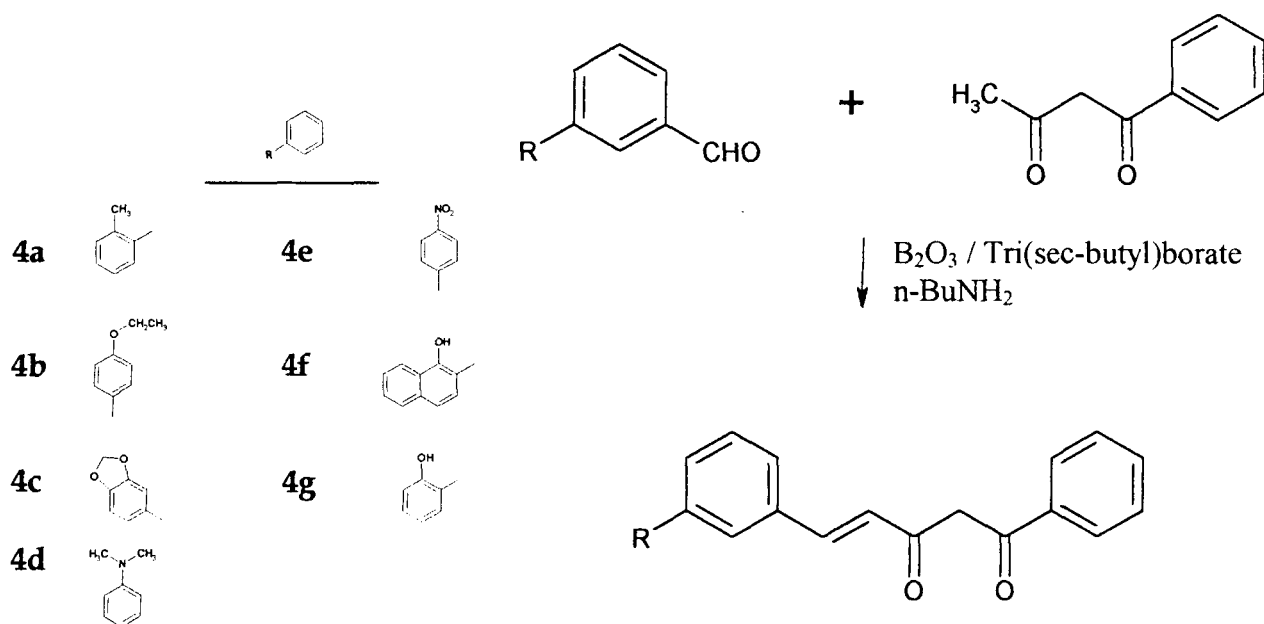
Metal chelates of 3e		Probable assignments
Copper(II)	Nickel(II)	
1700	1710	$\nu_{\text{C=O}}$ acetyl
1650	1652	$\nu_{\text{C=O}}$ chelated benzoyl
1625	1628	Metal chelated acetyl
1602 1585	1598 1590	$\nu_{\text{C-C}}$ phenyl / alkenyl
1565	1562	ν_{asy} C-C-C chelate ring
1458	1452	ν_{sym} -C-C-C chelate ring
1180 1107 1022	1155 1070 1002	$\beta_{\text{C-H}}$ chelate ring
760	758	$\gamma_{\text{C-H}}$ chelate ring
480 418	480 418	$\gamma_{\text{M-O}}$ chelate ring

Section 2

Synthesis and characterisation of 5-(substituted aryl)-1-phenyl-4-pentene-1,3-diones and their metal complexes

Preparation of 5-(substituted aryl)-1-phenyl pentanoids

The compounds were prepared by the condensation of substituted aromatic aldehydes (2-methylbenzaldehyde/4-ethoxybenzaldehyde/piperonaldehyde/4-(N,N-dimethylamino)benzaldehyde/4-nitrobenzaldehyde/2-hydroxynaphthaldehyde and salicylaldehyde) with benzoylacetone in the presence of boric oxide and tri(sec-butyl)borate using *n*-butylamine as the condensing agent at room temperature as outlined below. The detailed procedure for the synthesis is same as reported in section 1.



Scheme 4.1

The compounds were recrystallised from hot benzene to get chromatographically (tlc) pure material.

Preparation of metal complexes

Copper(II), nickel(II), cobalt(II), oxovanadium(IV) and iron(III) chelates of the diketones were prepared by the following general method. To a refluxing ethanolic solution of the compound (0.002 mol, 20 ml) an aqueous solution of metal(II) acetate (0.001 mol, 15 ml) was added and the reaction mixture was refluxed for ~ 2 h. In the case of iron(III) and oxovanadium(IV) chelates ferric chloride and vanadyl sulphate respectively were used. The volume was reduced to half. The precipitated complex on cooling to room temperature was filtered, washed with water and recrystallised from hot methanol.

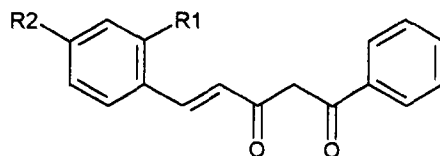
Results and discussion

Synthetic details of the compounds are given in table 4.1. All the compounds are crystalline in nature with sharp melting points and are soluble in common organic solvents. The carbon, hydrogen percentages are in agreement with their formulation. The yield and systematic names are also included in table 4.1.

The uv, ir, nmr and mass spectral data of the compounds are discussed below with a view to establish their structure and tautomeric nature.

TABLE 4.1

Synthetic details of the substituted 5-aryl-1-phenyl-4-pentanoids, 4a-g



Compounds	Aldehydes used for synthesis	R ₁	R ₂	Systematic name	Yield (%)
4a	2-methyl benzaldehyde	CH ₃	H	1-phenyl-5-(2-methylphenyl)-4-pentene-1,3-dione	50
4b	4-ethoxybenzaldehyde	H	O-CH ₂ CH ₃	1-phenyl-5-(4-ethoxyphenyl)-4-pentene-1,3-dione	60
4c	Pipernaldehyde	H		1-phenyl-5-(3,4-dioxymethylene)-4-pentene-1,3-dione	40
4d	4-(dimethylamino) benzaldehyde	H		1-phenyl-5-(4-N,N-dimethylamino)-4-pentene-1,3-dione	70
4e	p-nitro benzaldehyde	H	-NO ₂	1-phenyl-5-(4-nitrophenyl)-4-pentene-1,3-dione	50
4f	2-hydroxynaphthaldehyde	-OH	3,4-phenyl	1-phenyl-5-(2-hydroxynaphthyl)-4-pentene-1,3-dione	65
4g	salicylaldehyde	-OH	H	1-phenyl-5-(2-hydroxyphenyl)-4-pentene-1,3-dione	55

uv spectra

The tautomeric character of certain substituted benzoylacetones have been studied by ultraviolet spectroscopy.⁵⁰ The uv spectra of the compounds in 95% ethanol (10^{-3} M) show two bands with λ_{\max} at ~ 406 nm and ~ 285 nm. From a comparison of the reported spectra of simple 1,3-diketones⁵ such as benzoyl acetone the band at ~ 450 nm can be assigned to the $n \rightarrow \pi^*$ transition of the carbonyl chromophore and the band at ~ 285 nm to the conjugated $-C=C-$ $\pi \rightarrow \pi^*$ transition. The λ_{\max} of low energy $n \rightarrow \pi^*$ transition shows a bathochromic shift when the aryl substituents exerts an electron releasing effect.

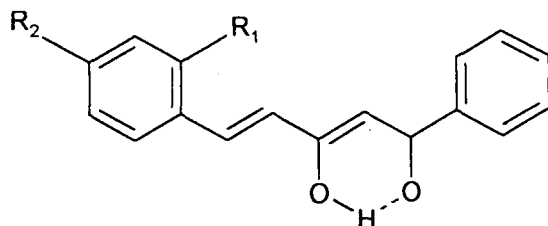
Infrared spectra

The ir spectra of compounds are characterised by the presence of two strong bands at ~ 1635 and ~ 1605 cm^{-1} and several medium intensity bands in the region $1500-1600$ cm^{-1} . It is to be pointed out that no free benzoyl carbonyl (~ 1660 cm^{-1}) or cinnamoyl carbonyl bands (~ 1645 cm^{-1}) are observed in the double bond region of the spectra. The observed bands in this region suggest the enolisation of the active methylene proton and its involvement in strong intramolecular hydrogen bonding as in structure 4.1.

TABLE 4.2

Physical, analytical and uv spectral data of the 5-aryl-1-phenyl-4-pentanoids, 4a-g

Compounds	Molecular formula (formula weight)	Elemental analysis (%) calculated/(found)		Colour	M.P. °C	λ_{\max} nm	log ϵ
		C	H				
4a	C ₁₈ H ₁₆ O ₂ (264)	81.8 (91.5)	6.06 (6.03)	yellow	120	230 406	4.3979 4.2920
4b	C ₁₉ H ₁₆ O ₃ (294)	77.55 (77.28)	5.44 (5.42)	brown	106	328 410	4.1176 4.0355
4c	C ₁₈ H ₁₄ O ₄ (294)	73.77 (73.46)	4.76 (4.71)	brown	142	310 383	4.4833 4.2890
4d	C ₁₉ H ₁₉ NO ₂ (293)	77.8 (76.6)	4.8 (4.8)	reddish brown	108	333 451	3.5691 4.0278
4e	C ₁₇ H ₁₃ O ₄ N (295)	69.15 (68.91)	4.4 (4.39)	yellowish brown	90	474	4.0371
4f	C ₂₁ H ₁₆ O ₃ (316)	79.75 (79.50)	5.06 (5.05)	light grey	140	285 370	3.9189 4.0122
4g	C ₁₇ H ₁₄ O ₃ (266)	76.69 (76.40)	5.26 (5.24)	reddish brown	112	309 370	4.0515 4.2575



4.1

The presence of strong intramolecular hydrogen bonding that exists in these compounds is evident from the occurrence of the intense broad band in the region 2500-3500 cm^{-1} . A medium intensity band appeared at $\sim 970 \text{ cm}^{-1}$ in the spectra of the compounds can be assigned to the trans $-\text{CH}=\text{CH}-$ absorption. Characteristic ir data and their probable assignments are given in table 4.3.

TABLE 4.3

Characteristic ir data (cm^{-1}) of 5-aryl-1-phenyl-4-pentene-1,3-diones, 4a-g

Compounds of							Probable assignments
4a	4b	4c	4d	4e	4f	4g	
1639	1635	1635	1630	1640	1635	1640	$\nu_{\text{C}=\text{O}}$ chelated benzoyl
1610	1600	1608	1595	1596	1606	1604	$\nu_{\text{C}=\text{O}}$ chelate cinnamonyl
1575 1535	1512 1393	1502 1434 1359	1535 1367	1515 1341	1585 1490	1585 1485	$\nu_{\text{C}-\text{C}}$ phenyl / alkenyl
1445	1302	1303	1321	1283	1450	1452	ν_{asym} $-\text{C}-\text{C}-\text{C}$ chelate ring
1390	1255	1242	1238	1237	1375	1361	ν_{sym} $-\text{C}-\text{C}-\text{C}$ chelate ring
1022	1172 1114 1043	1174 1093 1033	1155 1068	1168 1104	1172 1079 1024	1181 1112 1029	$\beta_{\text{C}-\text{H}}$ chelate ring
970	972	977	972	963	974	945	$\nu_{\text{CH}=\text{CH}}$ trans
763	756	767	777	776	754	756	$\nu_{\text{C}-\text{H}}$ chelate ring

¹H nmr spectra

The ¹H nmr spectra of all the substituted 5-aryl-1-phenylpentanoids displayed a one proton singlet at ~ δ 16 ppm. This signal can be assigned to the intramolecularly hydrogen bonded enolic proton of the compounds. Other signals appeared are in the range of 6.02-6.41 (methine protons), 7.94-8.59 (alkenyl proton), and 7.26-8.13 (aryl protons). The spectra of **4g** and **4f** show a singlet at ~ 13 ppm assignable to the phenolic proton of the compounds. The integrated intensities of all the signals appeared in the spectra (Fig. 4.1-4.7) agree well with **structure 4.1** of the compounds. The characteristic chemical shift of various protons are summarised in table 4.4.

TABLE 4.4

**Characteristic ¹H nmr spectral data of substituted
5-aryl-1-phenyl-4-pentanoids, 4a-g**

Compounds of							Probable assignments Chemical Shift (δ ppm)
4a	4b	4c	4d	4e	4f	4g	
16.17 (1H)	16.15 (1H)		16.47 (1H)	15.89 (1H)	16.08 (1H)	16.3 (1H)	enolic
6.0 (1H)	6.31 (1H)	6.02 (1H)	6.28 (1H)	6.41 (1H)	6.19 (1H)	6.19 (1H)	methine
8.00 (1H)	7.96 (1H)	7.96 (1H)	7.96 (1H)	8.27 (1H)	7.95 (1H)	7.89 (1H)	alkenyl
7.97 (1H)	7.94 (1H)	7.95 (1H)	7.94 (1H)	8.25 (1H)	7.93 (1H)	7.87 (1H)	
7.21- 7.62 (9H)	7.45 – 7.68 (9H)	7.44 – 7.94 (8H)	7.44 – 7.69 (9H)	7.26 – 8.13 (9H)	7.26 – 7.56 (11H)	7.26 – 7.52 (9H)	aryl
--	--	--	--	--	13.83	13.83	phenolic

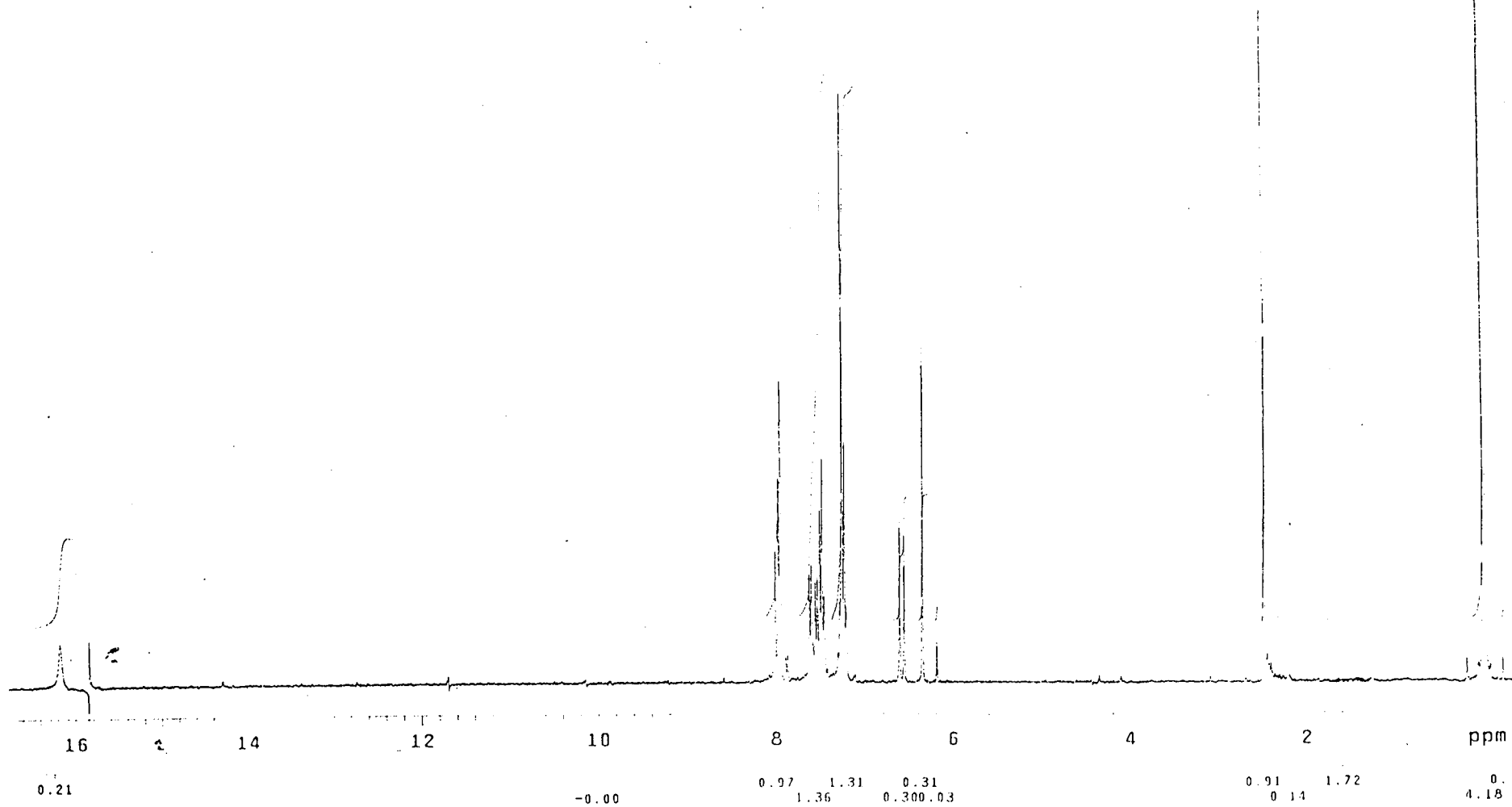
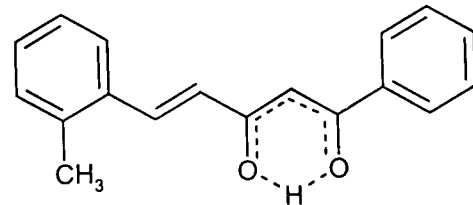


Fig. 4.1. ¹H NMR spectrum of 4a

194

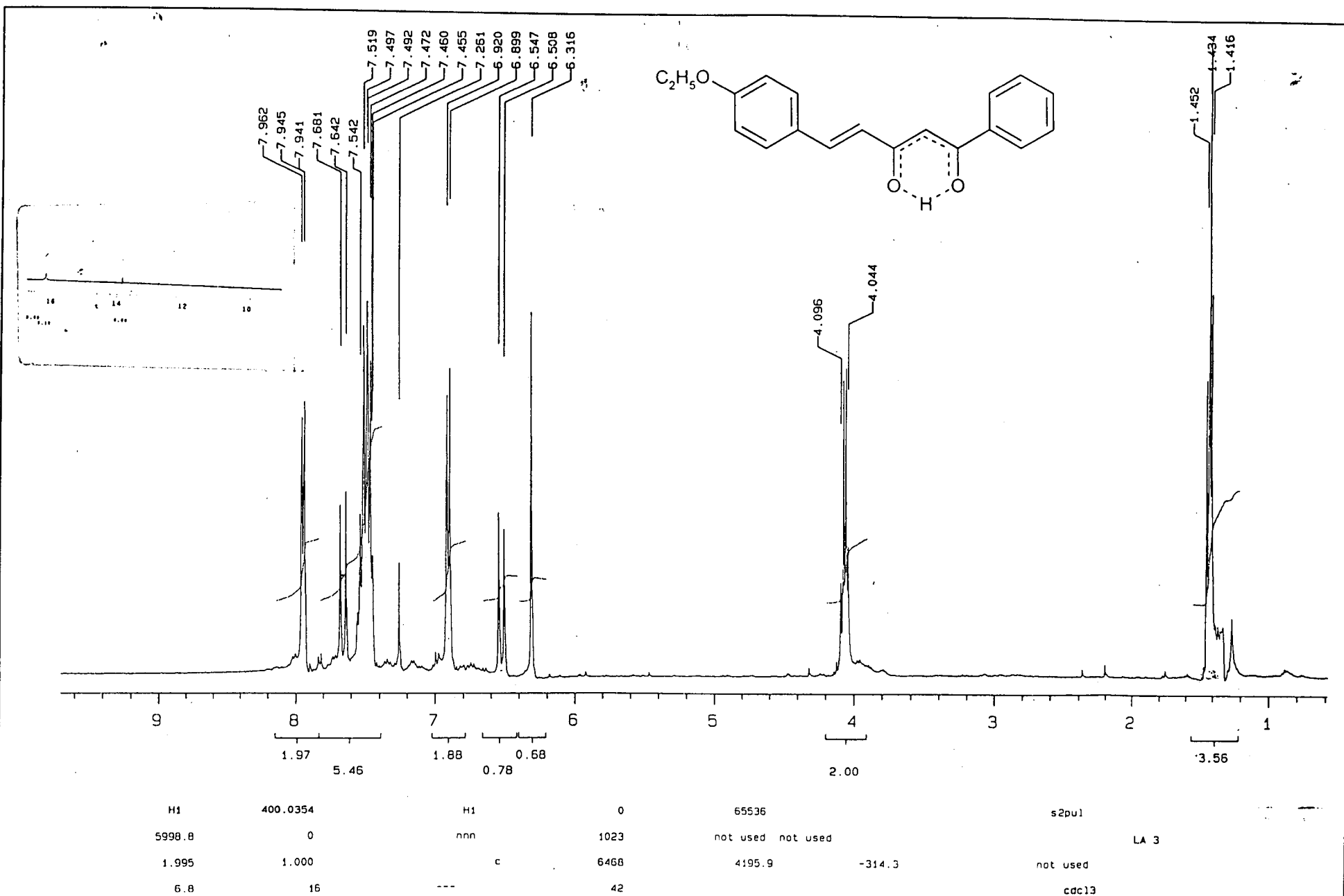


Fig. 4.2. ¹H-NMR spectrum of 4b

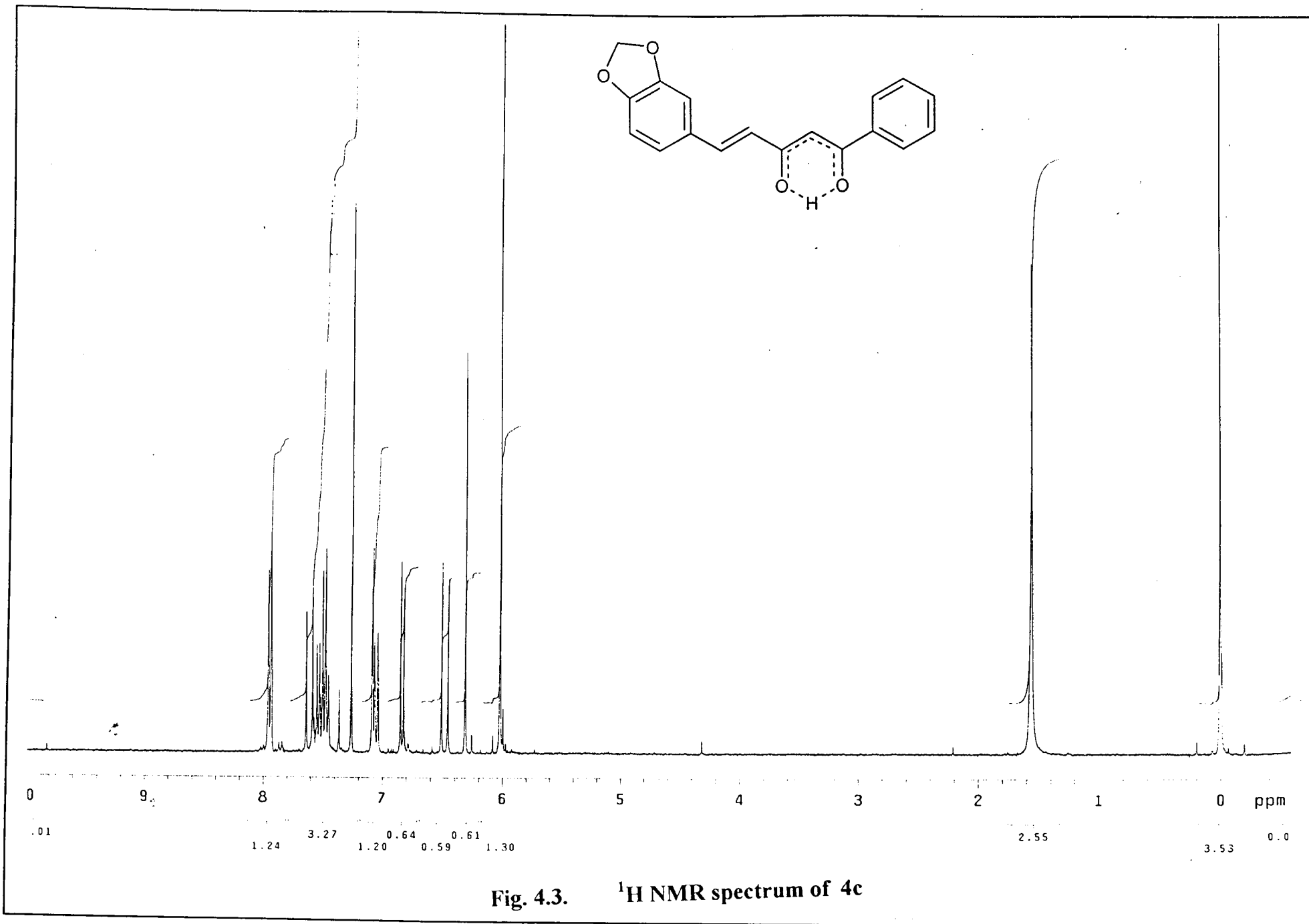


Fig. 4.3. ^1H NMR spectrum of 4c

196

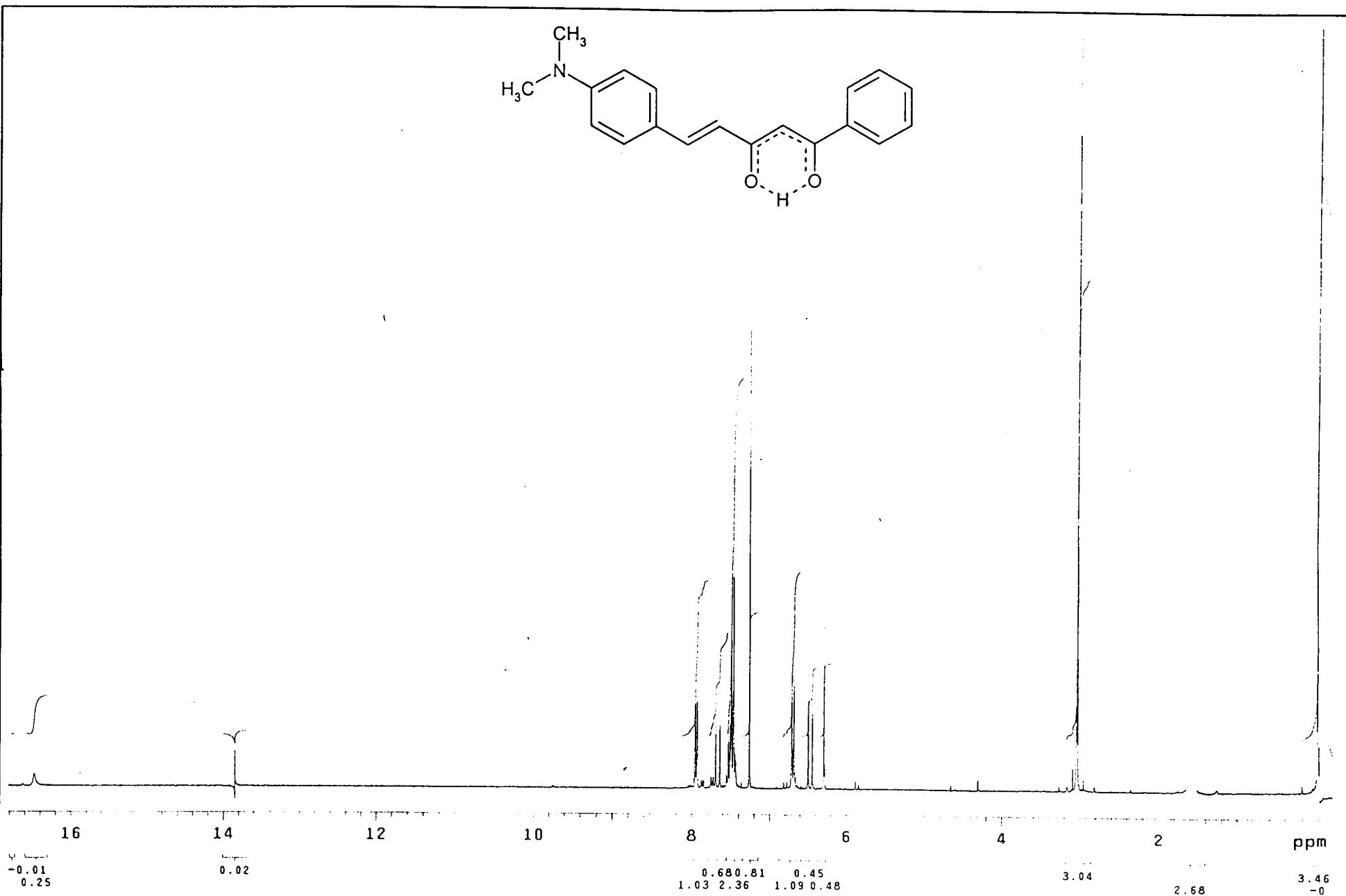
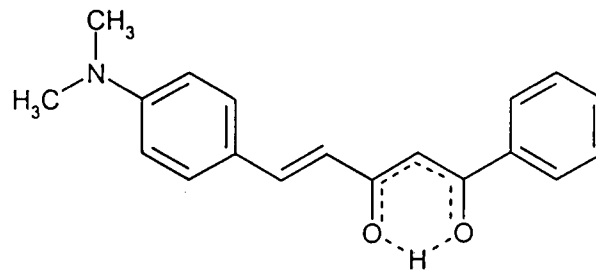
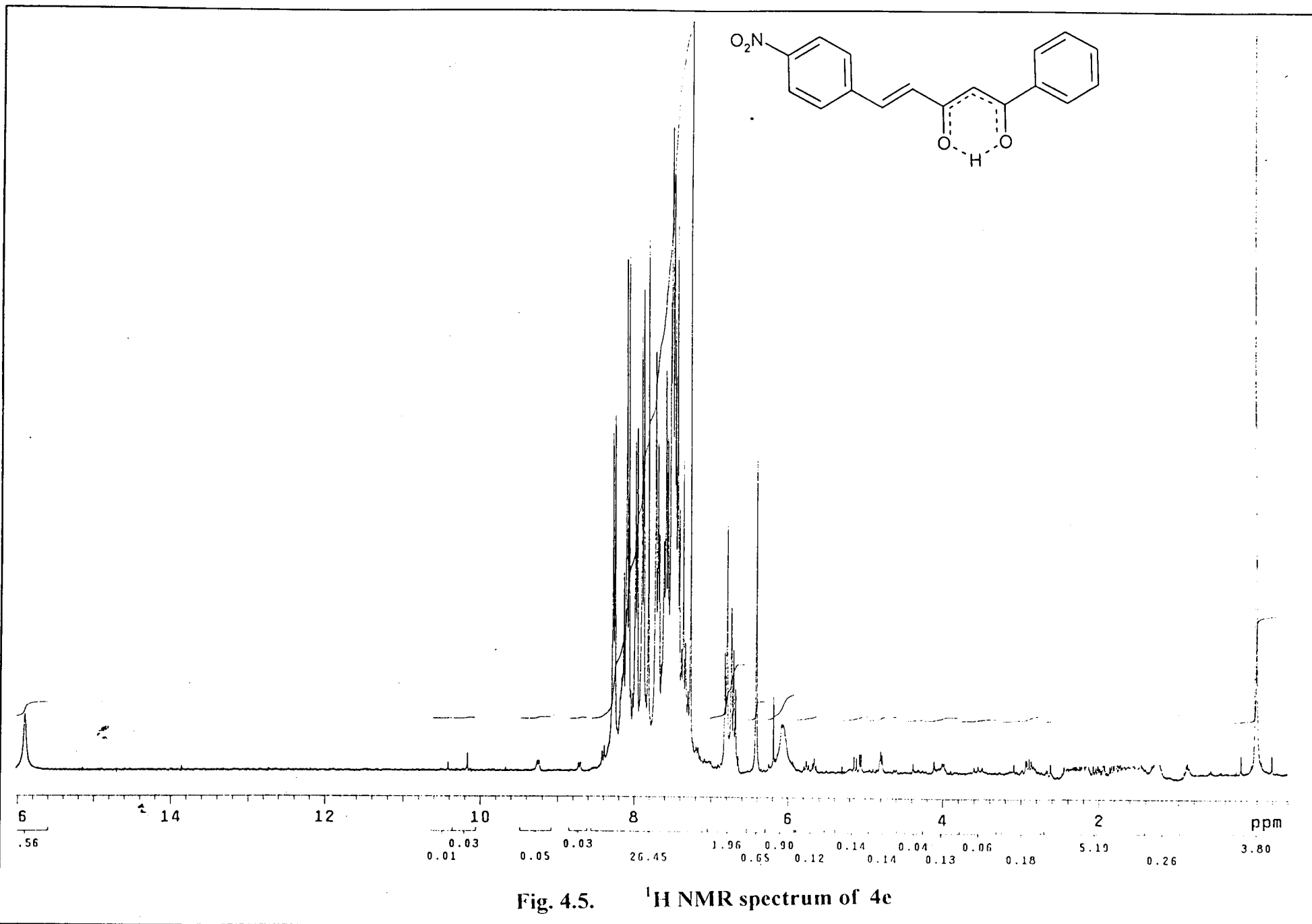


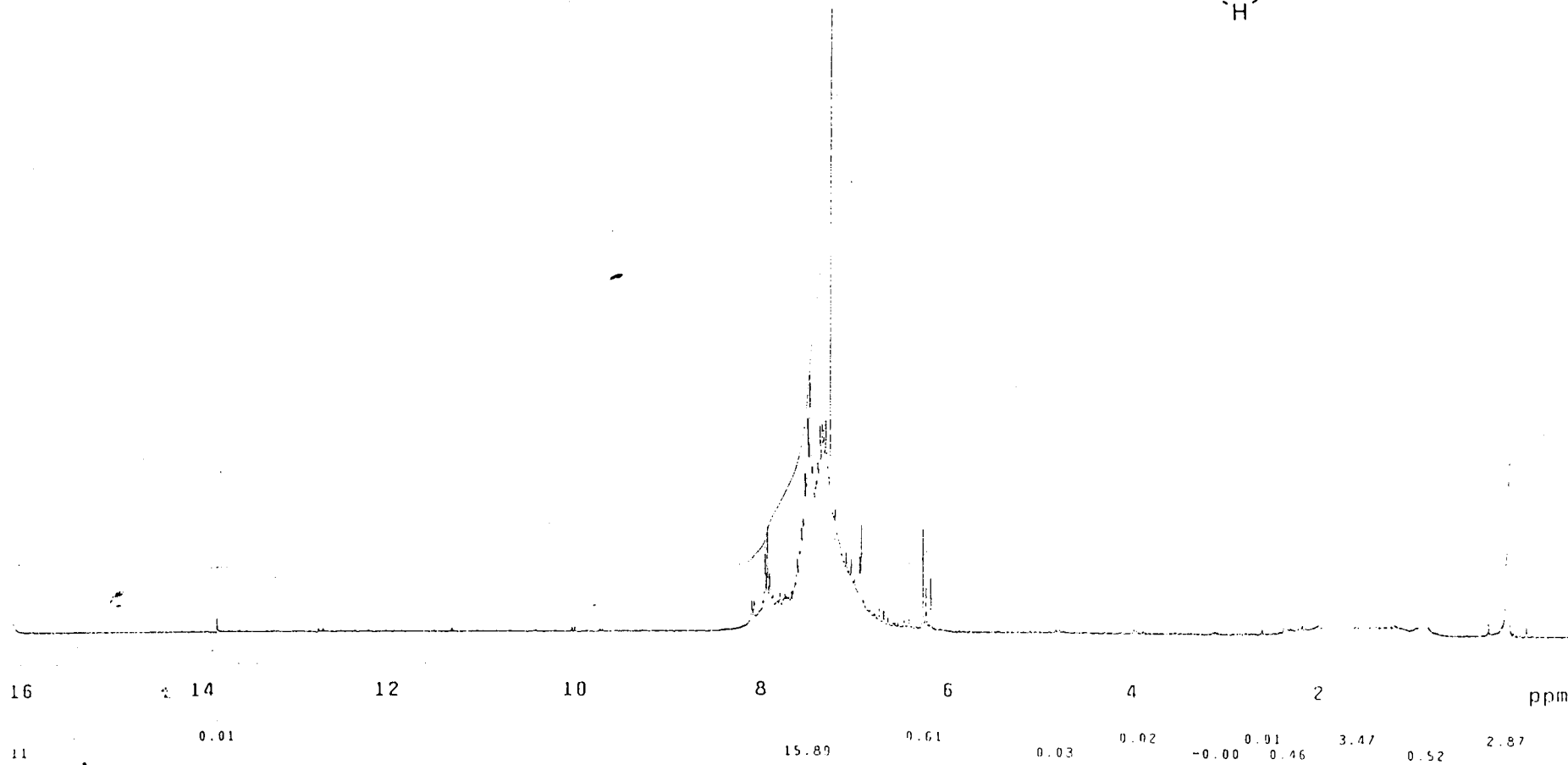
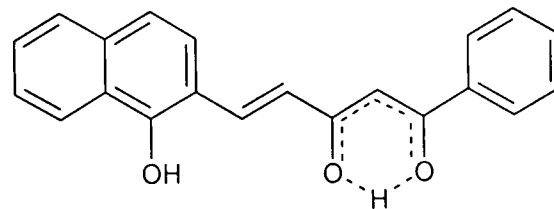
Fig. 4.4. ^1H NMR spectrum of 4d

107



199

Fig. 4.5. ¹H NMR spectrum of 4e



199

Fig. 4.6. ¹H NMR spectrum of 4f

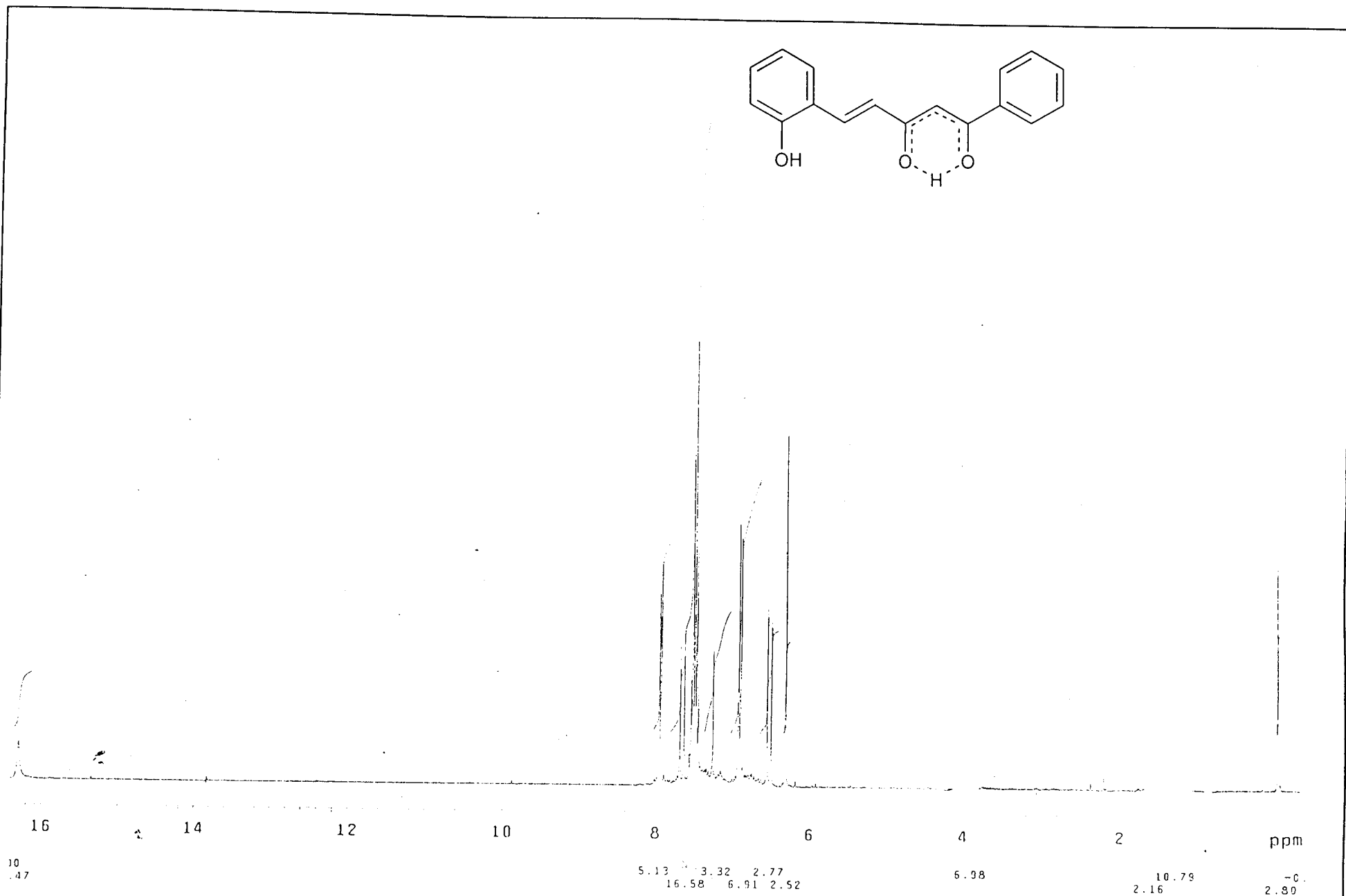
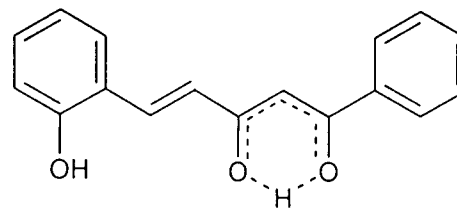


Fig. 4.7. ¹H NMR spectrum of 4g

Mass spectra

The mass spectra of all the compounds show molecular ion $P^+/(P+1)^+$ peaks in conformity with their formulation. In the case of **4f** and **4g** $(P-18)^+$ peak is most intense and is formed by the elimination of H_2O by the ortho effect. Peaks due to $(P-Ph)^+$, $(P-PhCO)^+$, $(P-CH_2COPh)^+$ and elimination of $CH_2=C=O$ from $(P-PhCO)^+$ are characteristic of all spectra. The appearance of major peaks in the spectra of all the compounds can be accounted by considering the fragmentation pattern given in scheme 4.2. The mass spectra of the compounds are reproduced in figures 4.8 to 4.13.

Characterisation of metal chelates

All the diketones formed well defined crystalline metal complexes with sharp melting points. Analytical and physical data of the complexes are given in tables 4.5 to 4.8. The observed elemental analysis data of complexes suggests that they are of $[ML_2]$ stoichiometry except for iron(III) which is $[FeL_3]$. All the complexes behave as non electrolytes (specific conductance $< 15 \Omega^{-1} \text{ cm}^{-1}$ in dmf) and do not contain the anion of the metal salt used for their preparation. The nickel(II) complexes are diamagnetic and all others are paramagnetic. The electronic, ir, nmr and mass spectral data of the complexes are compatible with the structure that would result when the chelated enol proton of the ligand is replaced by metal ion as in structure 4.2.

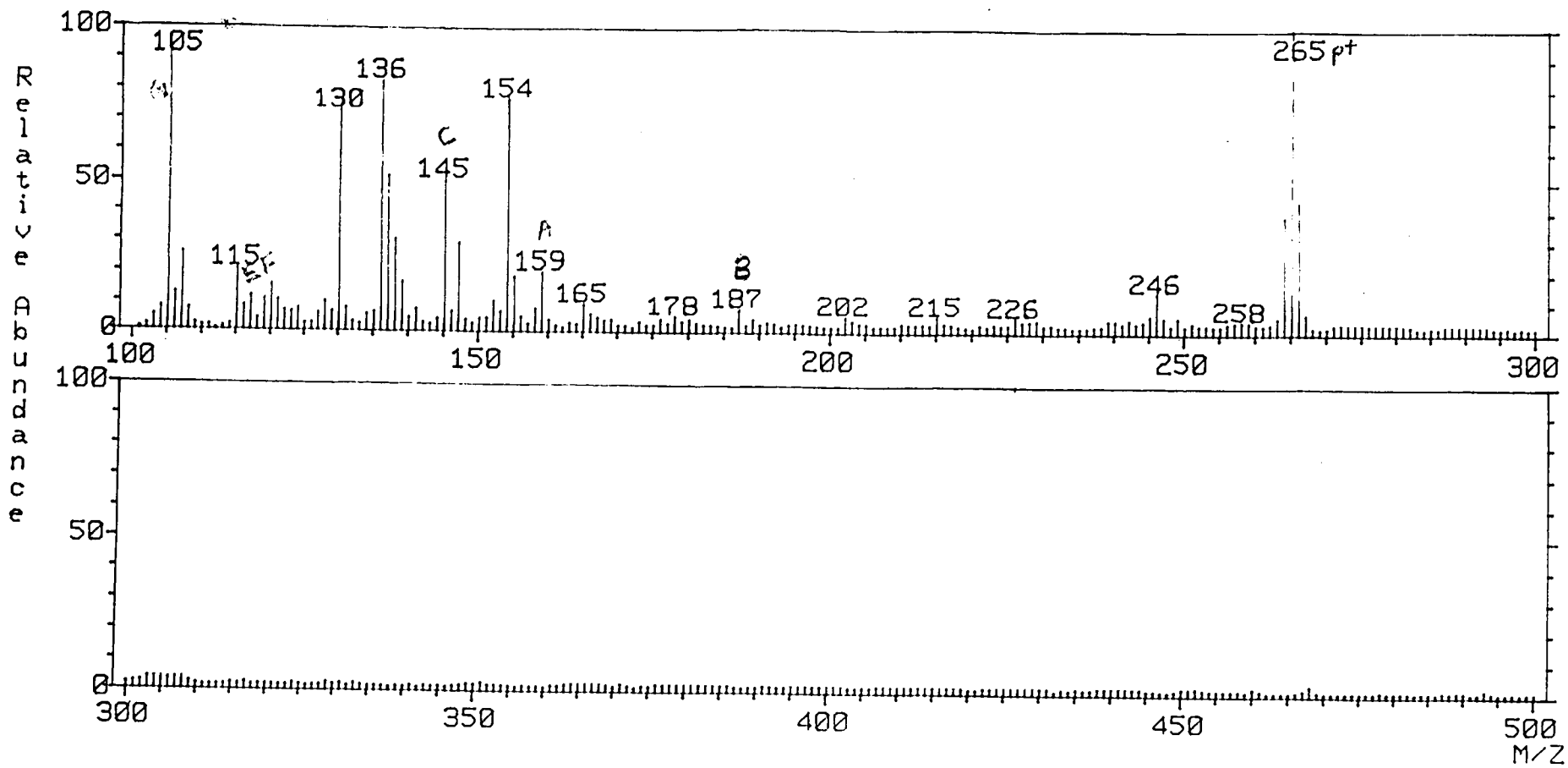
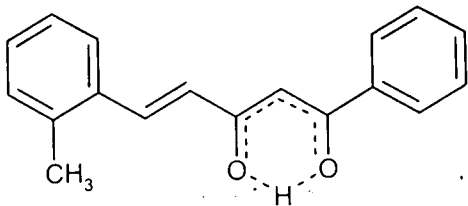


Fig. 4.8. Mass spectrum of 4a

202

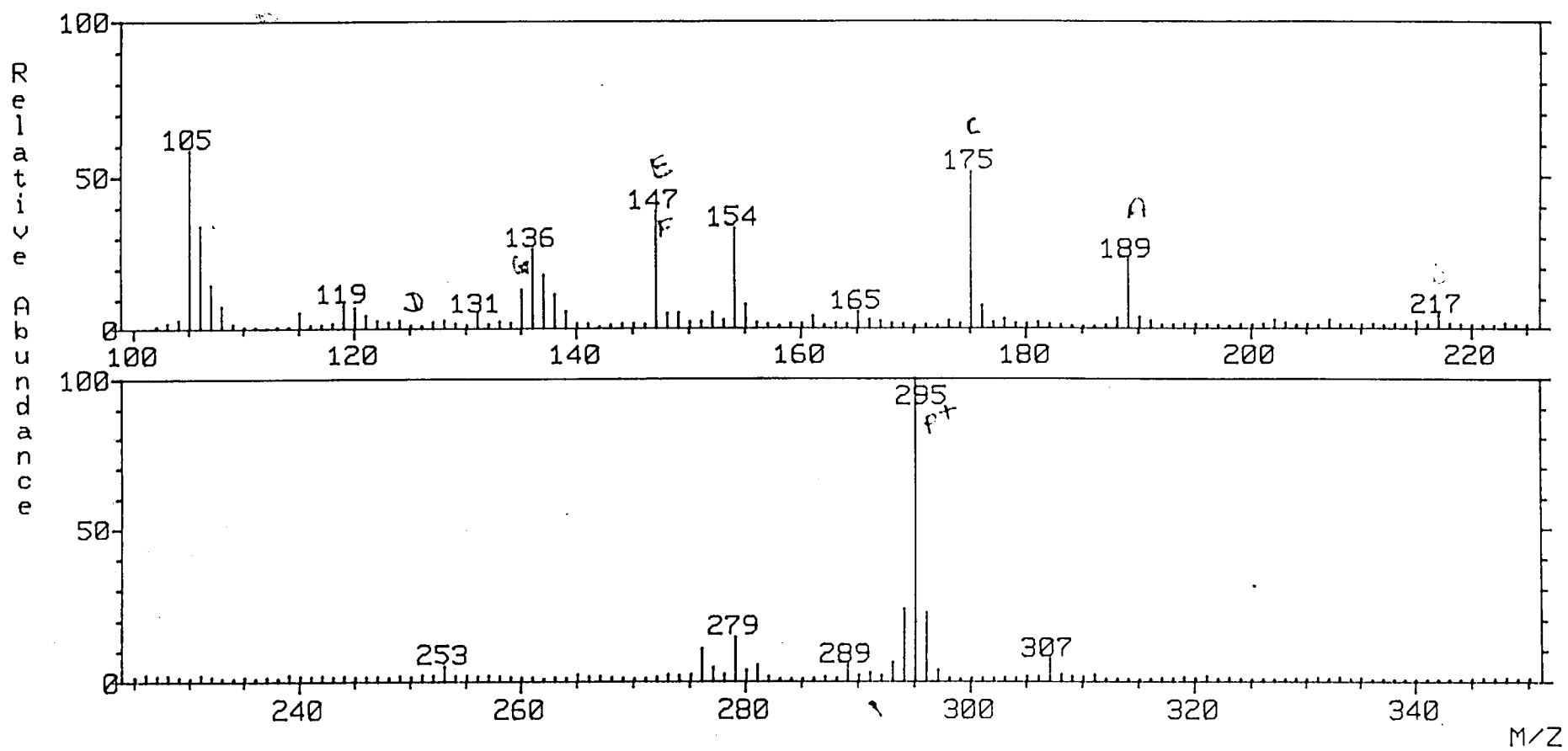
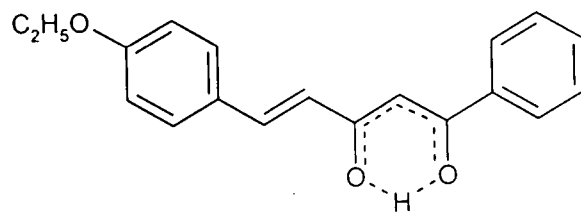


Fig. 4.9. Mass spectrum of 4b

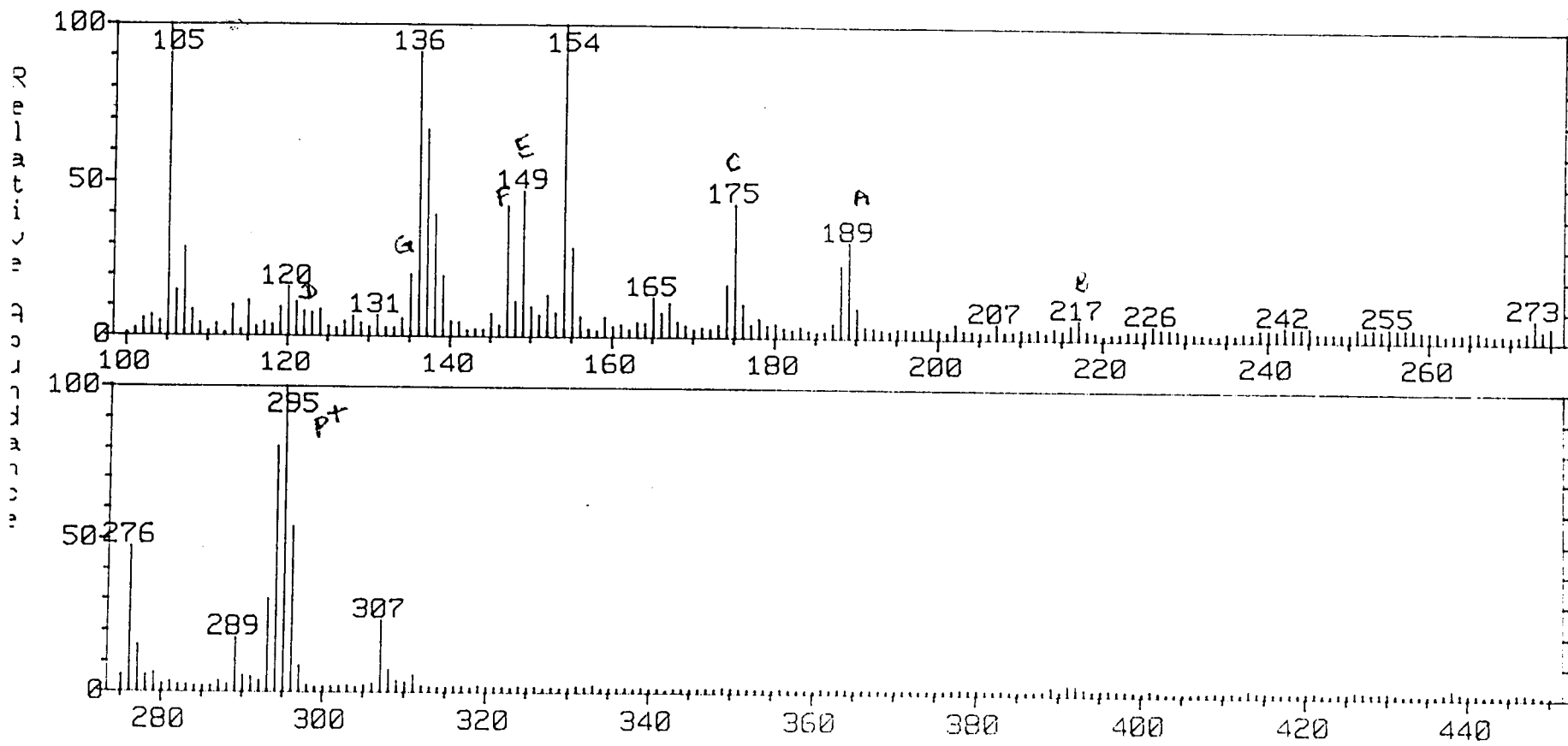
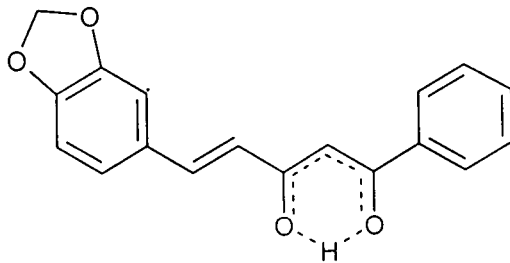


Fig. 4.10. Mass spectrum of 4c

1704

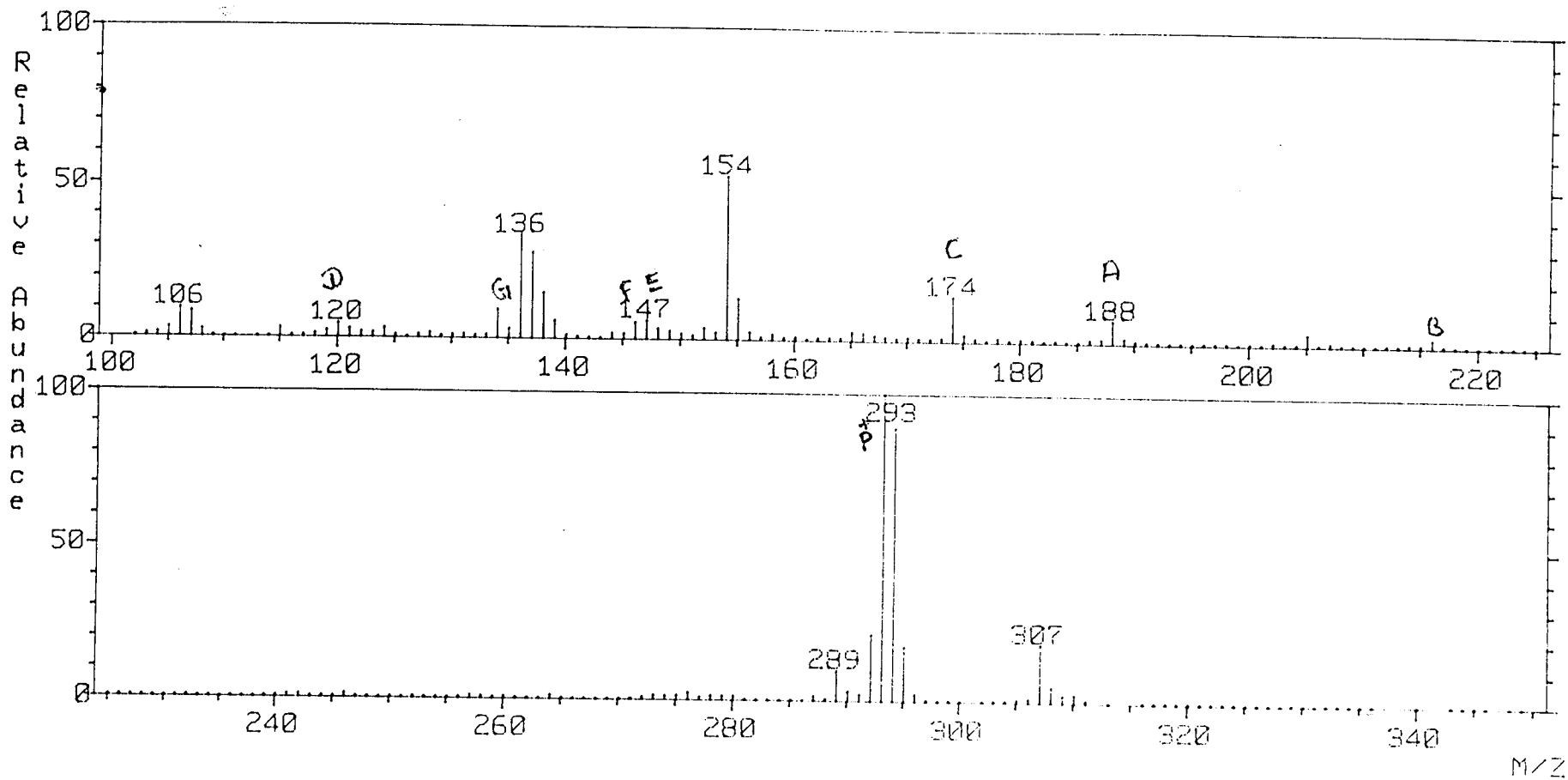
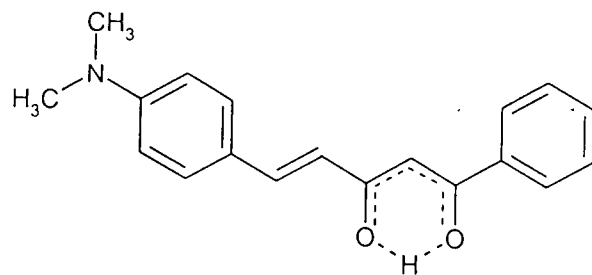


Fig. 4.11. Mass spectrum of 4d

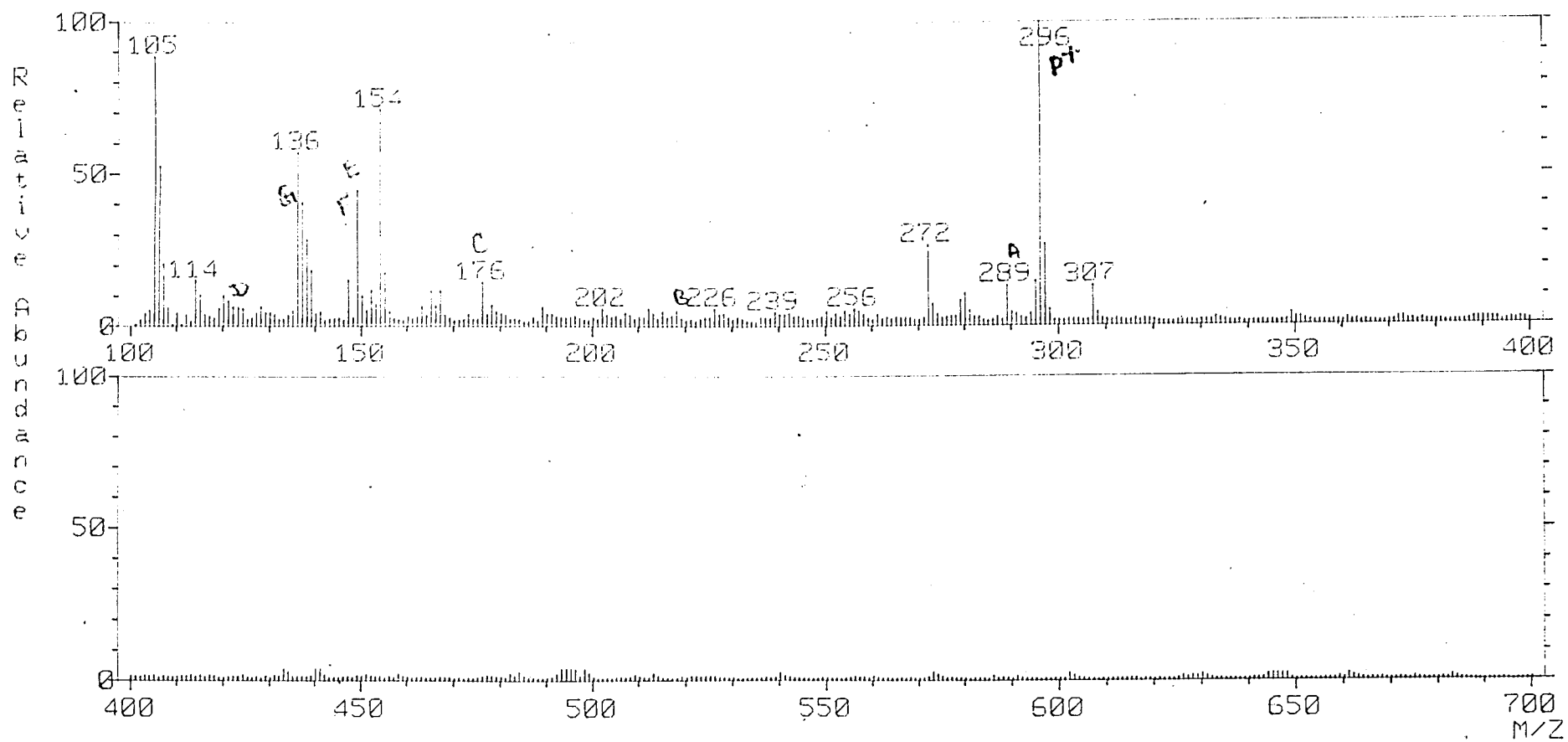
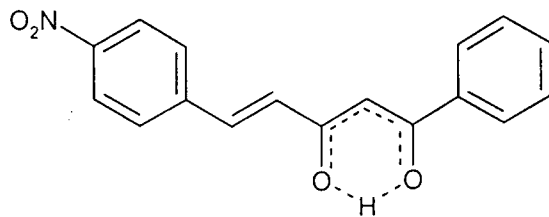


Fig. 4.12. Mass spectrum of 4e

900

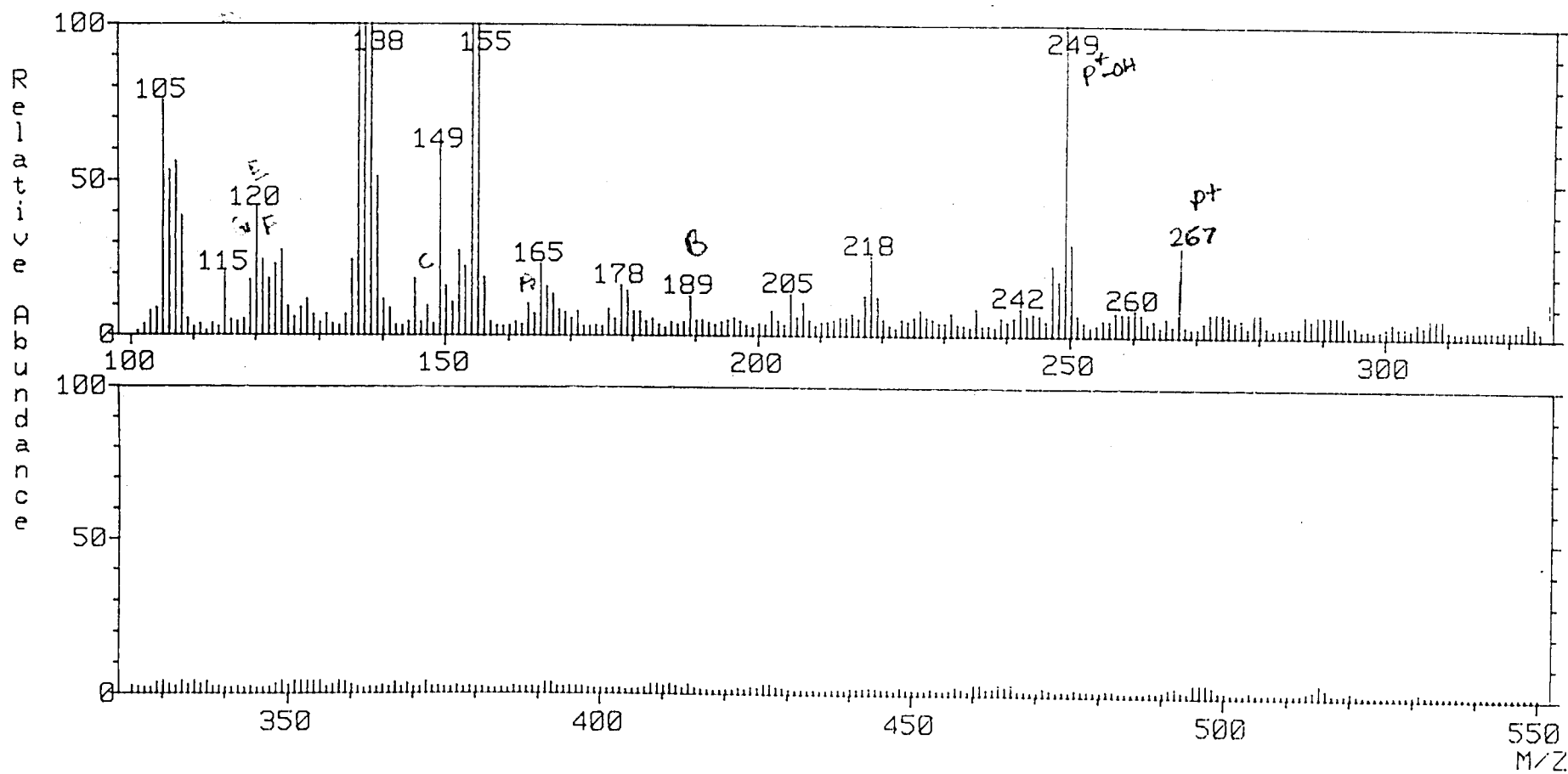
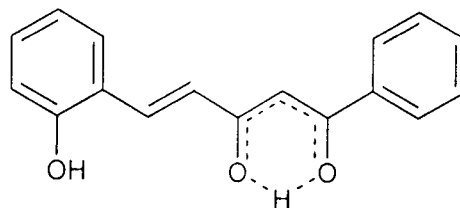
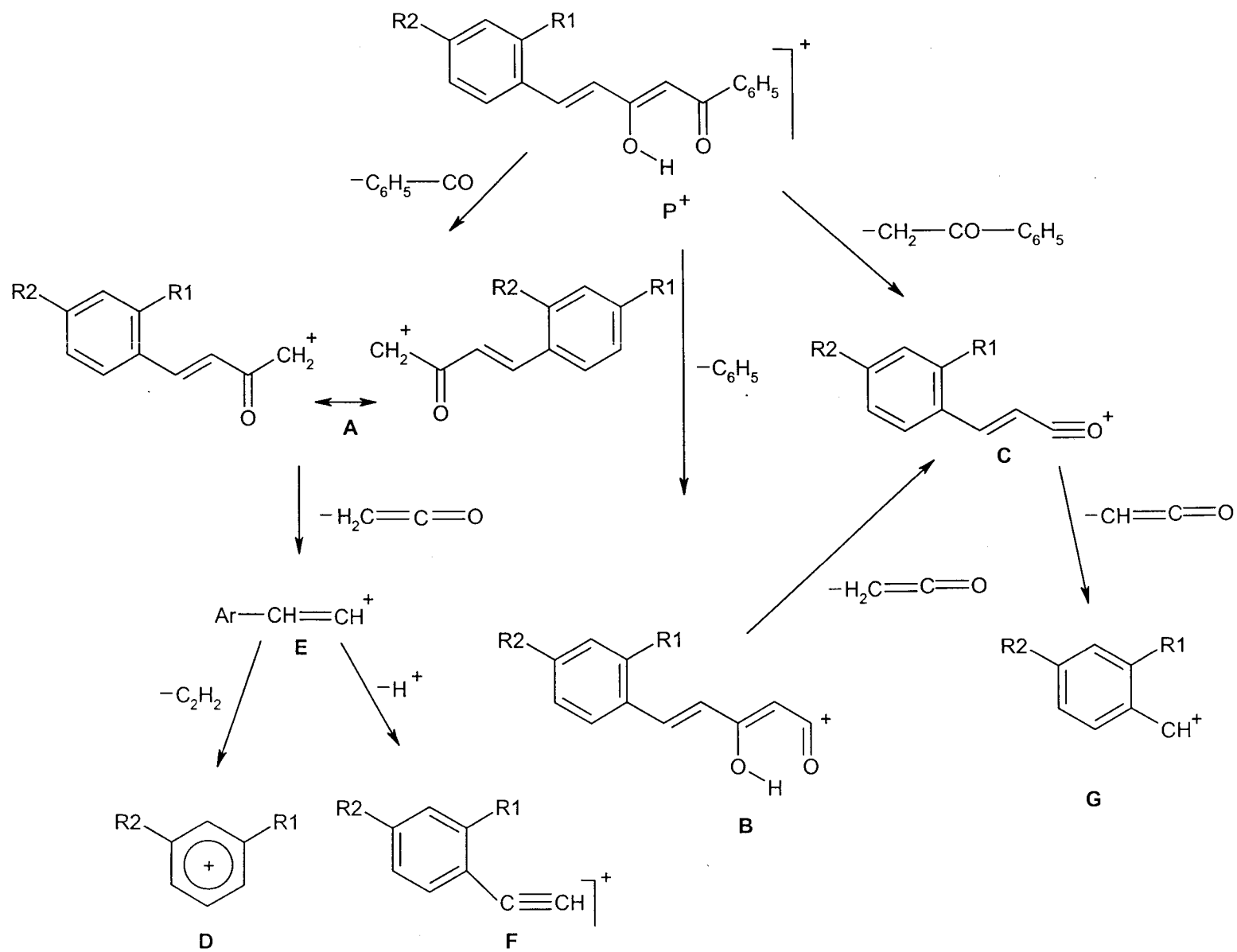
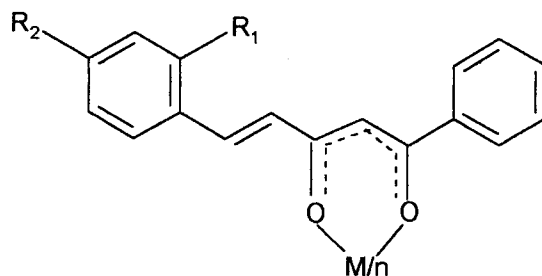


Fig. 4.13. Mass spectrum of 4g



Scheme 4.2 Fragmentation Pattern for 4a - g



$M = \text{Cu}^{+2}, \text{Ni}^{+2}, \text{Co}^{+2}, \text{VO}^{+2}$ for $n = 2$

and $M = \text{Fe}^{+3}$ for $n = 3$

4.2

uv spectra

The uv absorption maxima of the complexes bear close resemblance to that of the free ligands indicating that no structural alternation of the ligand has occurred during complexation. The two major absorption maxima of ligands showed bathochromic shift (5-10 nm) in complexes which suggests the involvement of the carbonyl function in metal complexation. The observed uv absorption maxima of the complexes are given in tables 4.5-4.8.

TABLE 4.5

Analytical and characteristic uv spectral data of copper(II) complexes of 5-aryl-1-phenyl-4-pentanoids, 4a-g

Copper(II) chelate of (Molecular formula)*	Yield %	M.P. °C	μ_{eff} (B.M.)	Elemental Analysis % calculated / (found)			λ_{max} (nm)
				C	H	M	
4a (C ₁₈ H ₁₅ O ₂) ₂ Cu	70	210	1.81	73.28 (73.1)	5.09 (5.07)	10.83 (10.25)	290 392
4b (C ₁₉ H ₁₅ O ₃) ₂ Cu	70	220	1.80	70.20 (70.04)	4.62 (4.61)	9.8 (9.7)	291 415
4c (C ₁₈ H ₁₃ O ₄) ₂ Cu	70	> 300	1.79	66.5 (66.3)	4.0 (3.99)	9.83 (9.76)	308 395
4d (C ₁₉ H ₁₄ NO ₂) ₂ Cu	60	> 300	1.82	70.42 (70.26)	5.56 (5.54)	9.86 (9.77)	292 447
4e (C ₁₇ H ₁₂ NO ₄) ₂ Cu	60	154	1.79	62.62 (62.48)	3.68 (3.67)	9.79 (9.73)	272 387
4f (C ₂₁ H ₁₅ O ₃) ₂ Cu	70	> 300	1.76	72.67 (72.63)	4.33 (4.32)	9.162 (9.06)	268 384
4g (C ₁₇ H ₁₃ O ₃) ₂ Cu	55	145	1.80	68.74 (68.68)	4.38 (4.3)	10.71 (10.69)	285 324

*The molecular formula given correspond to [CuL₂] stoichiometry, where L stands for the deprotonated ligand moiety.

TABLE 4.6

Analytical and characteristic uv spectral data of nickel(II) complexes of 5-aryl-1-phenyl-4-pentanoids, 4a-g

Nickel(II) chelate of (Molecular formula)*	Yield %	M.P. °C	Elemental Analysis % calculated / (found)			λ_{\max} (nm)
			C	H	M	
4a (C ₁₈ H ₁₅ O ₂) ₂ Ni	90	140	73.88 (73.72)	5.13 (5.11)	10.03 (10)	285 409
4b (C ₁₉ H ₁₅ O ₃) ₂ Ni	70	122	71.17 (71.02)	4.68 (4.67)	9.16 (9.07)	333 415
4c (C ₁₈ H ₁₃ O ₄) ₂ Ni	70	> 300	67 (66.87)	4.03 (4.02)	9.1 (9.08)	289 402
4d (C ₁₉ H ₁₄ NO ₂) ₂ Ni	70	124	70.95 (70.80)	5.6 (5.59)	9.13 (9.1)	282 439
4e (C ₁₇ H ₁₂ NO ₄) ₂ Ni	70	> 300	63.09 (62.96)	3.71 (3.7)	9.07 (9.05)	261 385
4f (C ₂₁ H ₁₅ O ₃) ₂ Ni	60	120	73.18 (73.14)	4.36 (4.35)	9.23 (9.21)	319 359
4g (C ₁₇ H ₁₃ O ₃) ₂ Ni	65	130	69.31 (69.3)	4.42 (4.41)	10.79 (10.18)	285 349

*The molecular formula given correspond to [NiL₂] stoichiometry, where L stands for the deprotonated ligand moiety.

TABLE 4.7

**Analytical and characteristic uv spectral data of cobalt(II) complexes of
5-aryl-1-phenyl-4-pentanoids, 4a-g**

Cobalt(II) chelate of (Molecular formula)*	Yield %	M.P. °C	μ_{eff} (B.M.)	Elemental Analysis % calculated / (found)			λ_{max} (nm)
				C	H	M	
4a (C ₁₈ H ₁₅ O ₂) ₂ Co(H ₂ O) ₂	70	142	4.84	73.8 (73.7)	5.2 (5.1)	10.07 (10.05)	289 406
4b (C ₁₉ H ₁₅ O ₃) ₂ Co(H ₂ O) ₂	65	128	4.82	71.12 (71.02)	4.68 (4.67)	9.2 (9.17)	290 411
4c (C ₁₈ H ₁₃ O ₄) ₂ Co(H ₂ O) ₂	70	> 300	4.76	66.98 (66.8)	4.03 (4.02)	9.13 (9.12)	265 419
4d (C ₁₉ H ₁₄ NO ₂) ₂ Co(H ₂ O) ₂	65	130	4.77	70.93 (70.80)	5.60 (5.59)	9.17 (9.15)	293 416
4e (C ₁₇ H ₁₂ NO ₄) ₂ Co(H ₂ O) ₂	50	> 300	4.87	63.06 (62.96)	3.71 (3.69)	9.5 (9.12)	291 400
4f (C ₂₁ H ₁₅ O ₃) ₂ Co(H ₂ O) ₂	65	276	4.86	73.16 (73.1)	4.35 (4.3)	8.55 (8.5)	310 402
4g (C ₁₇ H ₁₃ O ₃) ₂ Co(H ₂ O) ₂	60	180	4.78	69.28 (69.0)	4.4 (4.3)	10.01 (10.0)	214 308

*The molecular formula given correspond to [CoL₂(H₂O)₂] stoichiometry, where L stands for the deprotonated ligand moiety.

TABLE 4.8

**Analytical and characteristic uv spectral data of iron(III) complexes of 5-aryl--
phenyl-4-pentanoids, 4a-g**

Iron(III) chelate of (Molecular formula)*	Yield %	M.P. °C	μ_{eff} (B.M.)	Elemental Analysis % calculated / (found)			λ_{max} (nm)
				C	H	M	
4a (C ₁₈ H ₁₅ O ₂) ₃ Fe	70	220	5.92	76.7 (76.5)	5.32 (5.31)	6.61 (6.60)	297 439
4b (C ₁₉ H ₁₅ O ₃) ₃ Fe	60	230	5.87	73.64 (73.54)	4.84 (4.83)	6.01 (6.005)	297 392
4c (C ₁₈ H ₁₃ O ₄) ₃ Fe	70	> 300	5.83	69.32 (69.23)	4.17 (4.16)	5.97 (5.9)	297 392
4d (C ₁₉ H ₁₄ NO ₂) ₃ Fe	50	> 300	5.89	73.4 (73.3)	5.79 (5.78)	5.99 (5.98)	293 426
4e (C ₁₇ H ₁₂ NO ₄) ₃ Fe	50	168	5.92	65.25 (65.17)	3.84 (3.83)	5.95 (5.94)	309 372
4f (C ₂₁ H ₁₅ O ₃) ₃ Fe	70	220	5.88	75.54 (75.5)	4.49 (4.47)	5.58 (5.56)	317 382
4g (C ₁₇ H ₁₃ O ₃) ₃ Fe	65	> 300	5.84	71.93 (71.90)	4.58 (4.56)	6.56 (6.54)	214 315

*The molecular formula given correspond to [FeL₃] stoichiometry, where L stands for the deprotonated ligand moiety.

Infrared spectra

The broad free ligand band in the region 2700-3200 cm^{-1} is cleared up in the spectra of all metal complexes showing that the chelated proton is replaced by the metal ion during complexation. However, in the spectra of complexes of **4f** and **4g** weak bands assignable to ν_{OH} are observed in addition to various $\nu_{\text{C-H}}$ vibration. The most characteristic feature of the ir spectra of the complexes is the absence of any strong bands in the region 1700-1630 cm^{-1} due to free or hydrogen bonded carbonyl function. However two new bands appeared in the spectra of metal complexes at $\sim 1600 \text{ cm}^{-1}$ and $\sim 1580 \text{ cm}^{-1}$ of appreciable intensity apart from the various medium intensity bands arising from aromatic and alkenyl $\nu_{\text{C=C}}$ vibrations in the region 1400-1600 cm^{-1} . This is further supported by the appearance of medium intensity bands at ~ 470 and $\sim 428 \text{ cm}^{-1}$ arising from $\nu_{\text{M-O}}$ vibrations. The position of the trans $-\text{CH}=\text{CH}$ bands ($\sim 927 \text{ cm}^{-1}$) remains unaltered in the case of metal complexes. All these suggests the **structure 4.2** for the complexes. The ir spectral data of the metal complexes are given in tables 4.8-4.13. Spectra of all the cobalt(II) complex showed bands assignable to coordinated water molecule. The $\nu_{\text{C=O}}$ stretching of the VO^{2+} complexes appeared at $\sim 1627 \text{ cm}^{-1}$.

TABLE 4.9

**Characteristic ir data (cm⁻¹) of copper(II) chelates of
5-aryl-1-phenyl-4-pentanoids, 4a-g**

Copper(II) chelate of							Probable assignments
4a	4b	4c	4d	4e	4f	4g	
1610	1610	1615	1610	1610	1641	1570	$\nu_{C=O}$ metal chelated benzoyl
1585	1598	1590	1598	1594	1580	1570	$\nu_{C=O}$ metal chelated cinnamoyl
1529 1409	1521 1402	1521 1398	1515 1396	1520 1390	1530 1461	1821 1454	ν_{C-C} phenyl / alkenyl
1290 1250	1298 1249	1307 1049	1299 1261	1290 1240	1410	1410	ν_{asym} C-C-C chelate ring
1184 1108	1160 1041	1180 1035	1159 1066	1172 1108	1396	1388	ν_{sym} C-C-C chelate ring
974	977	968	974	970	1150 1002	1180 1030	β_{C-H} chelate ring
763	773	758	763	764	960	960	$\nu_{CH=CH}$ trans
453	472	441	468	496	765	756	ν_{C-H} chelate ring
418 408	415	403	418	416	468 418 416	474 418 407	ν_{M-O} chelate ring

TABLE 4.10

**Characteristic ir data (cm^{-1}) of nickel(II) chelates of
5-aryl-1-phenyl-4-pentanoids, 4a-g**

Nickel(II) chelate of							Probable assignments
4a	4b	4c	4d	4e	4f	4g	
1633	1615	1633	1615	1610	1647	1645	$\nu_{\text{C=O}}$ metal chelated benzoyl
1598	1596	1593	1595	1594	1585	1612	$\nu_{\text{C=O}}$ metal chelated cinnamoyl
1519 1409	1517 1404	1517 1406	1517 1405	1518 1415	1530 1480	1585 1485	$\nu_{\text{C-C}}$ phenyl / alkenyl
1315	1301	1303	1299	1342	1409	1452	ν_{asym} C-C-C chelate ring
1250	1249	1247	1250	1284	1380	1380	ν_{sym} C-C-C chelate ring
1187 1072	1170 1043	1182 1033	1159 1107	1177 1109	1180 1020	1180 1040	$\beta_{\text{C-H}}$ chelate ring
972	974	977	970	985	993	950	$\nu_{\text{CH=CH}}$ trans
763	759	760	759	761	750	756	$\nu_{\text{C-H}}$ chelate ring
520 480	516 470 407	470 407	515 470 412	531 485	454 418	476 418 407	$\nu_{\text{M-O}}$ chelate ring

TABLE 4.11

**Characteristic ir data (cm⁻¹) of cobalt(II) chelates of
5-aryl-1-phenyl-4-pentanoids, 4a-g**

Cobalt(II) chelate of				Probable assignments
4a	4c	4d	4e	
1633	1610	1615	1610	$\nu_{C=O}$ metal chelated benzoyl
1587	1590	1596	1596	$\nu_{C=O}$ metal chelated cinnamoyl
1521 1410	1519 1404	1517 1402	1518 1408	ν_{C-C} phenyl / alkenyl
1319	1315	1367	1346	ν_{asym} C-C-C chelate ring
1281	1301	1299	1260	ν_{sym} C-C-C chelate ring
1188 1028	1182 1033	1161 1099	1173 1108	β_{C-H} chelate ring
973	975	974	982	$\nu_{CH=CH}$ trans
764	763	759	771	ν_{C-H} chelate ring
518 480	470 407	511	515 415	ν_{M-O} chelate ring

TABLE 4.12

**Characteristic ir data (cm⁻¹) of iron(III) chelates of
5-aryl-1-phenyl-4-pentanoids, 4a-g**

Iron(III) chelate of						Probable assignments
4a	4b	4c	4d	4f	4g	
1628	1615	1629	1602	1630	1625	$\nu_{C=O}$ metal chelated benzoyl
1586	1590	1585	1580	1598	1595	$\nu_{C=O}$ metal chelated cinnamoyl
1519 1389	1517 1386	1516 1389	1519 1371	1518 1448	1517 1485	ν_{C-C} phenyl / alkenyl
1320	1299	1302	1294	1410	1450	ν_{asym} C-C-C chelate ring
1286 1220	1249	1253	1255	1380	1380	ν_{sym} C-C-C chelate ring
1167 1027	1166 1041	1169 1094	1170 1114	1181 1020	1182 1020	β_{C-H} chelate ring
971	991	972	970	996	962	$\nu_{CH=CH}$ trans
765	765	764	765	754	758	ν_{C-H} chelate ring
511 470	530 469	489 465	470 408	505 480 465	445 407	ν_{M-O} chelate ring

TABLE 4.13

Characteristic ir data (cm^{-1}) of oxovanadium(IV) chelates of
5-aryl-1-phenyl-4-pentanoids, 4a-g

Oxovanadium(IV) chelate of					Probable assignments
4a	4b	4c	4d	4g	
1639	1627	1633	1620	1620	$\nu_{\text{C=O}}$ metal chelated benzoyl
1586	1601	1593	1593	1600	$\nu_{\text{C=O}}$ metal chelated cinnamoyl
1820 1407	1557 1379	1527 1407	1520 1374	1580 1454	$\nu_{\text{C-C}}$ phenyl / alkenyl
1314	1300	1301	1295	1415	ν_{asym} C–C–C chelate ring
1268 1248	1250	1248	1261	1374	ν_{sym} C–C–C chelate ring
1182 1029	1168 1104	1182 1102	1162 1102	1154 1029	$\beta_{\text{C-H}}$ chelate ring
970	997	963	983	943	$\nu_{\text{CH=CH}}$ trans
788	770	764	771	758	$\nu_{\text{C-H}}$ chelate ring
446 430	455	466 433	506 470	471 410	$\nu_{\text{M-O}}$ chelate ring

^1H nmr spectra

The ^1H nmr spectra of the diamagnetic nickel(II) chelates of the substituted 5-arylpentanoids confirm the replacement of the enolic proton by the metal ion as in **structure 2.2**. This is evident from the absence of the low field proton signal at $\sim \delta$ 16 ppm in the ^1H nmr of nickel(II) complexes. For instance the spectrum of the

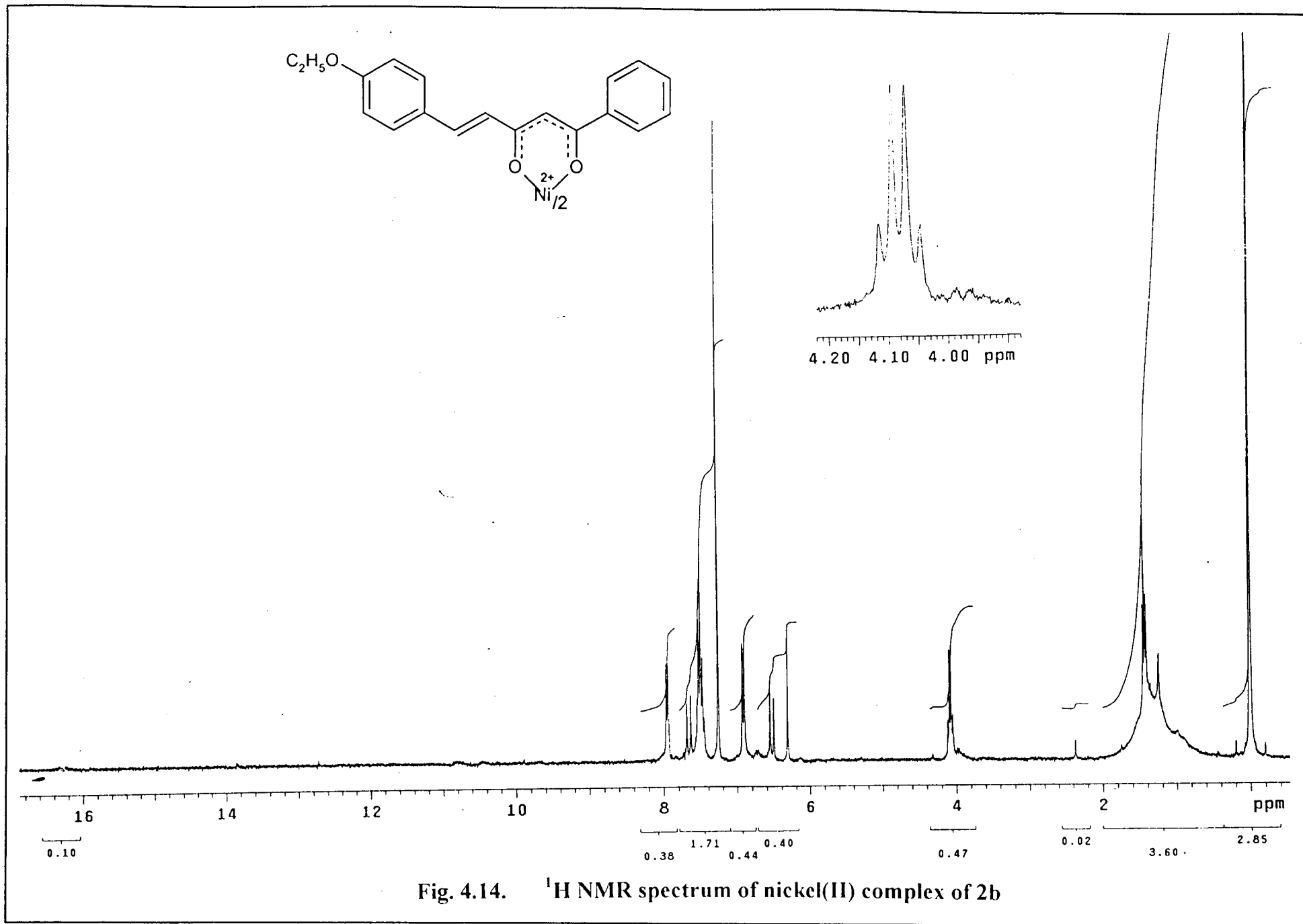
Ni^{2+} complexes of **2b** is given in figure 4.14. However, the phenolic OH signal of the **4f** and **4g** remained almost unaltered in the spectra of their metal chelates indicating that the chelate formation has occurred only through the 1,3-dicarbonyl moiety of the compounds. The integrated intensities of the various signals are as expected of their formulation. The methine signals are shifted towards the downfield of the spectra indicating the decreased electron density around the central carbon atom of the pseudo aromatic metal chelate ring system.

Mass spectra

The FAB mass spectra of the copper(II) chelates are reproduced in figures 4.15-4.20. All the complexes show prominent peaks due to $[\text{CuL}_2]^+$ which justifies the formulation of the chelates as in structure 4.2. The base peak in all the case is due to ligand and peaks due to $[\text{CuL}]^+$, L^+ and fragments of L^+ are sometimes more intense than the molecular ion peak.

Esr spectra of copper(II) complexes of 5-aryl-1-phenyl-4-pentanoids

The unsaturated 5-aryl-1-phenyl-pentanoids considered in this investigation are structurally related to substituted benzoylacetone in the sense that the methyl group of benzoylacetone is substituted with a $\text{Ar}-\text{CH}=\text{C}$ group thereby increasing the degree of conjugation. That is a styryl group and a phenyl group are attached to the diketo function. Compared to 6-arylhexanoids extended conjugation exist in these types of compounds. Therefore it is valuable to study the nature of the $\text{Cu}-\text{O}$ bond



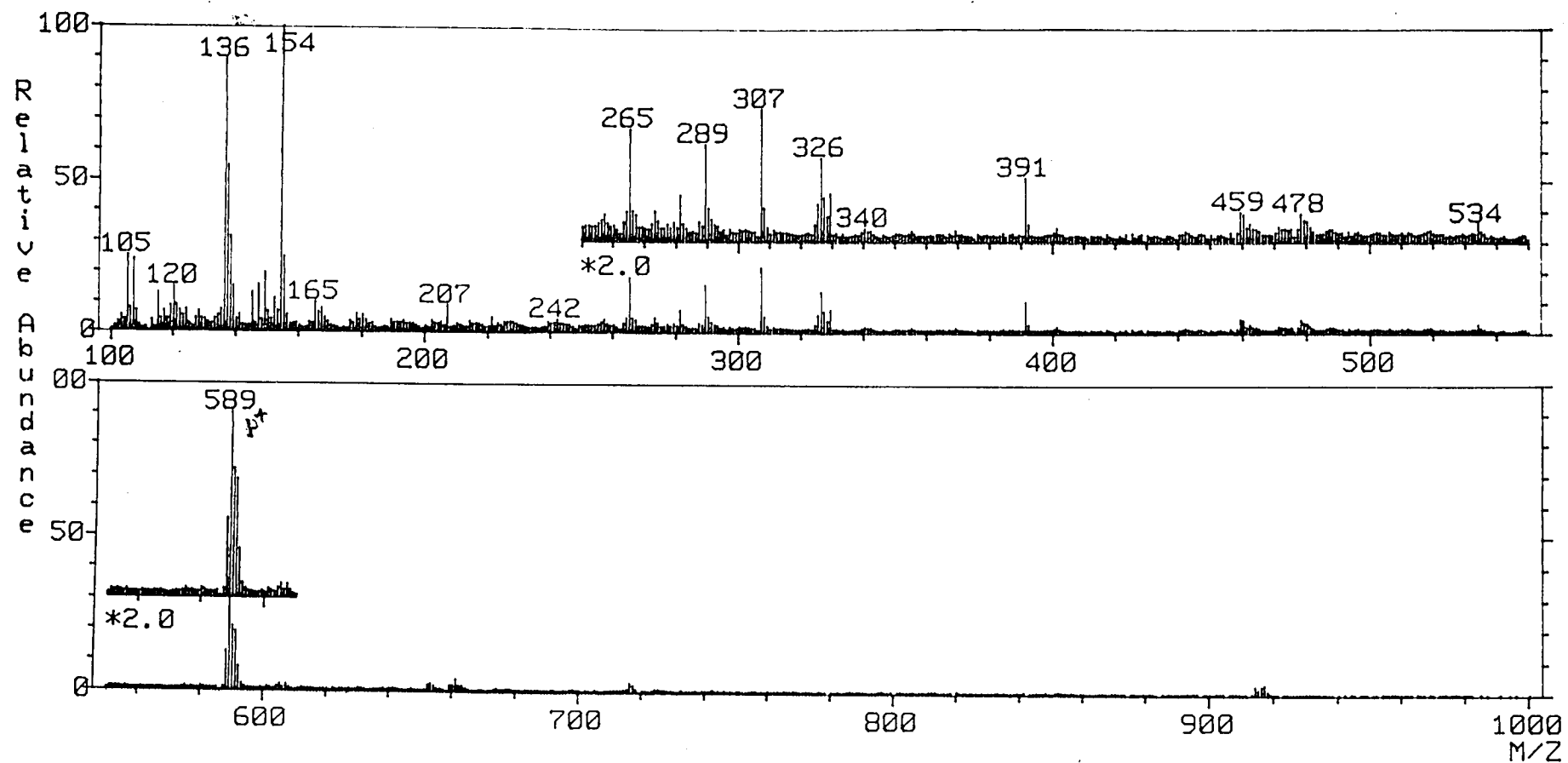
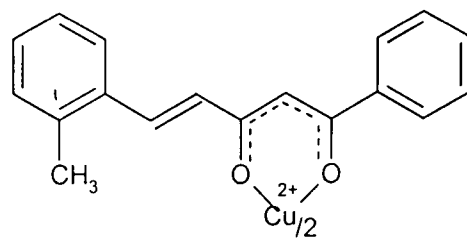


Fig. 4.15. Mass spectrum of copper(II) complex of 4a

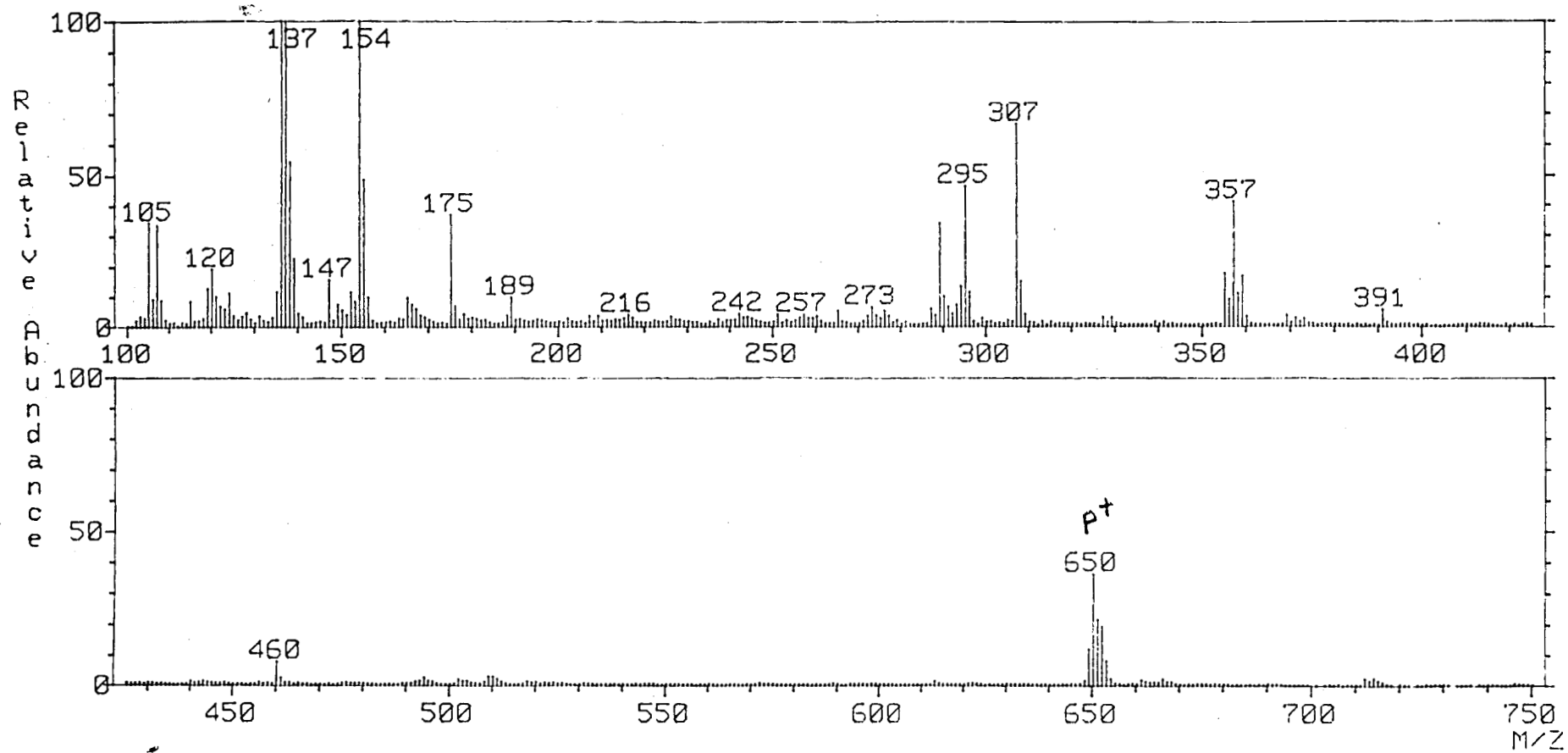
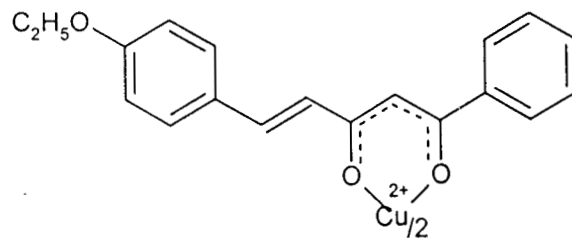


Fig. 4.16. Mass spectrum of copper(II) complex of 4b

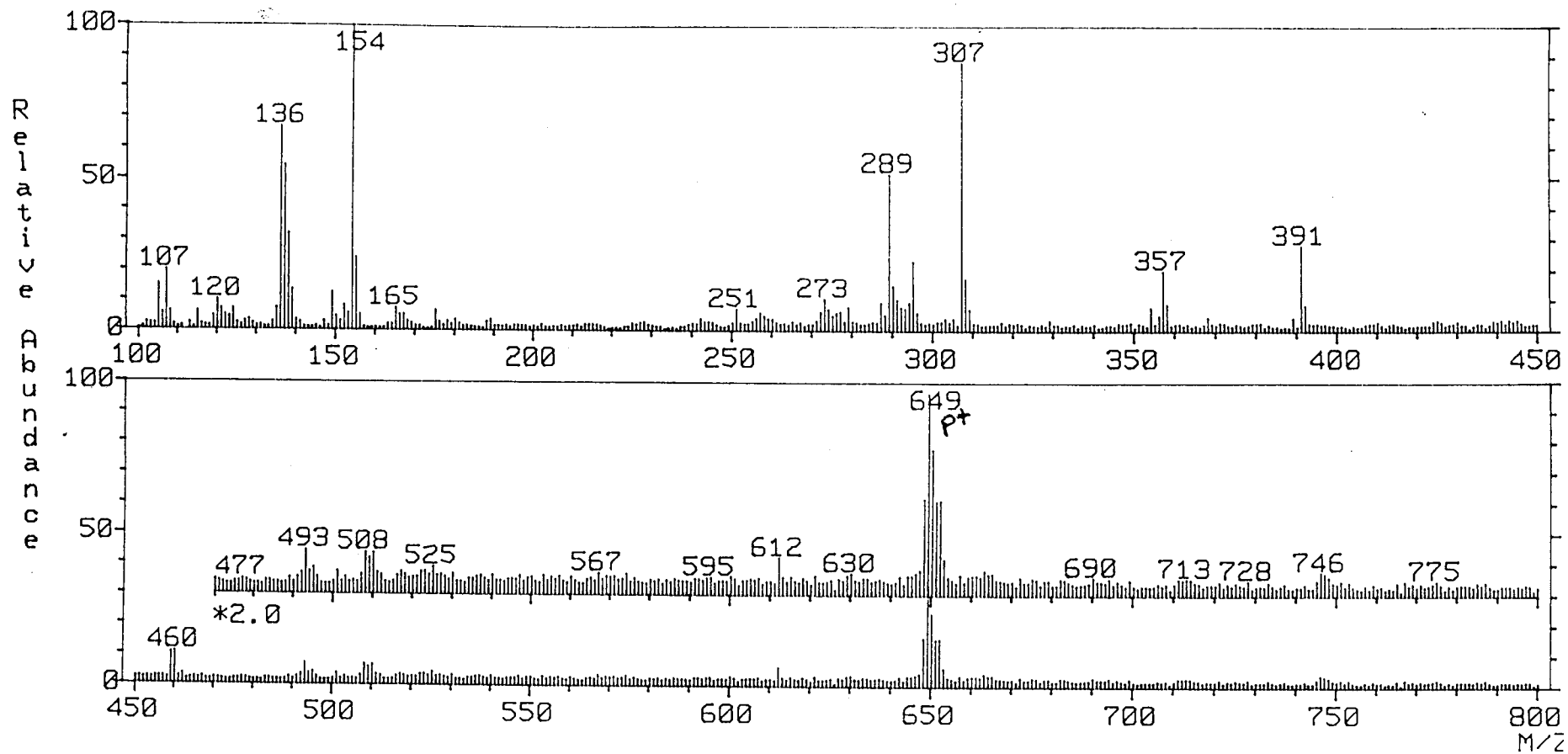
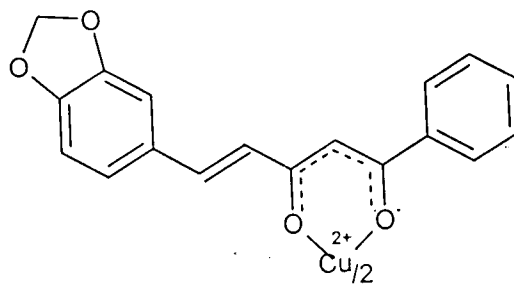


Fig. 4.17. Mass spectrum of copper(II) complex of 4c

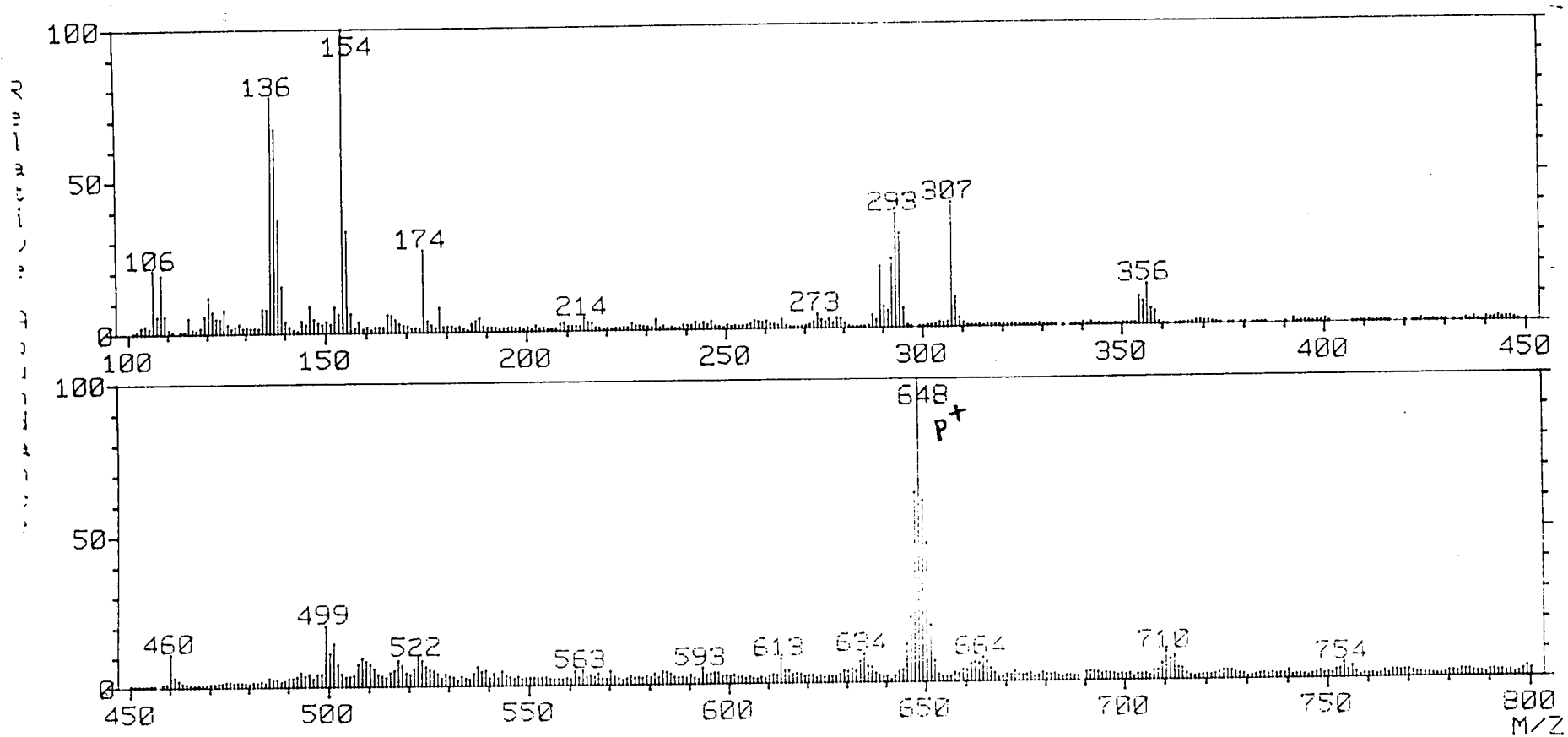
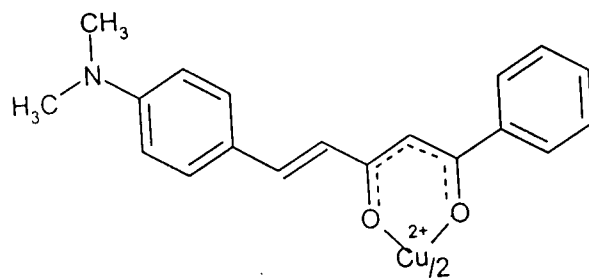


Fig. 4.18. Mass spectrum of copper(II) complex of 4d

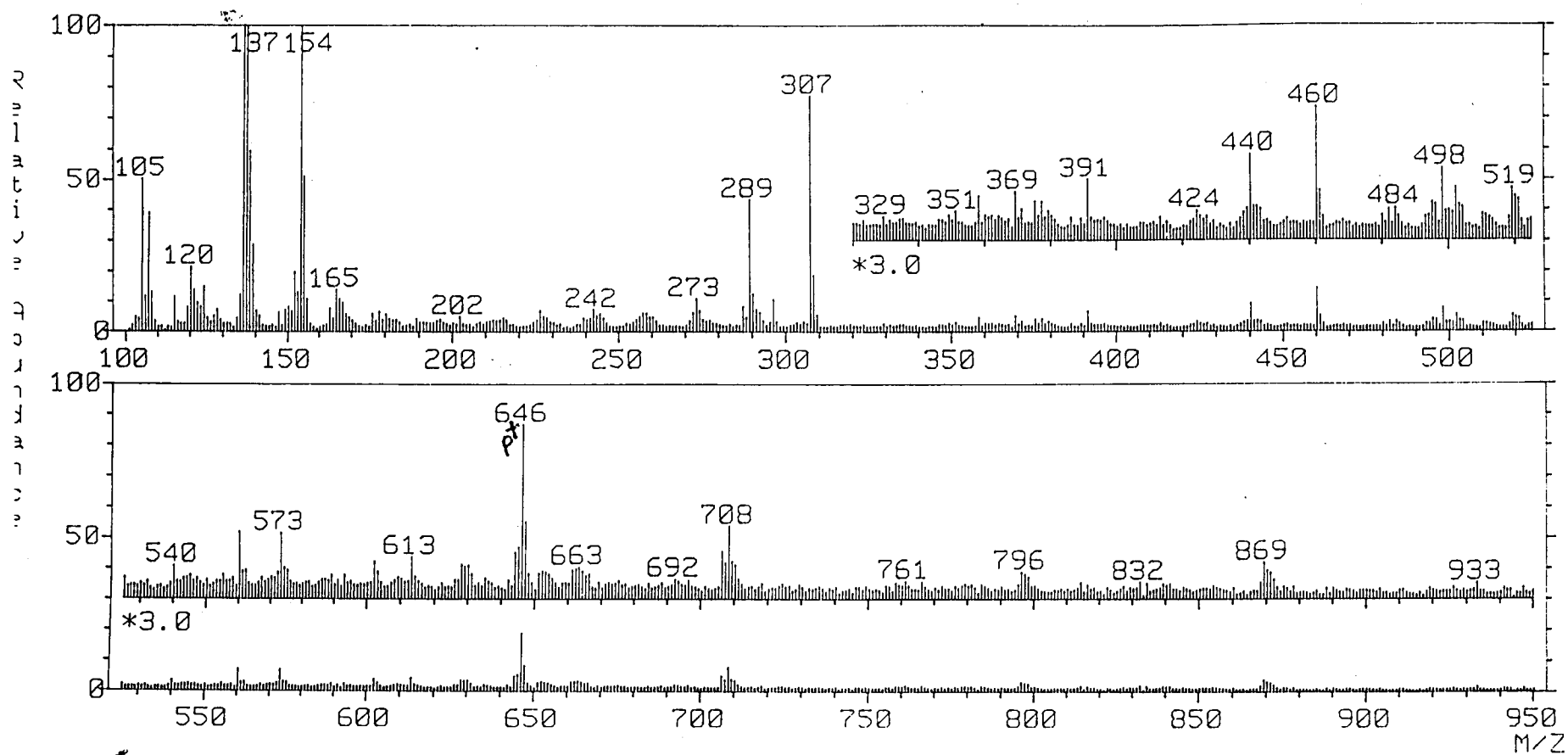
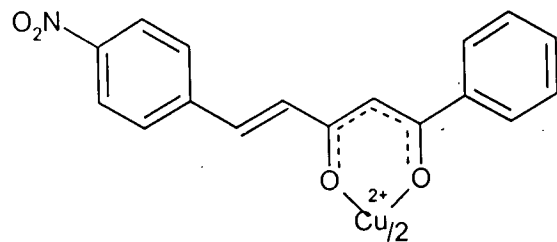


Fig. 4.19. Mass spectrum of copper(II) complex of 4c

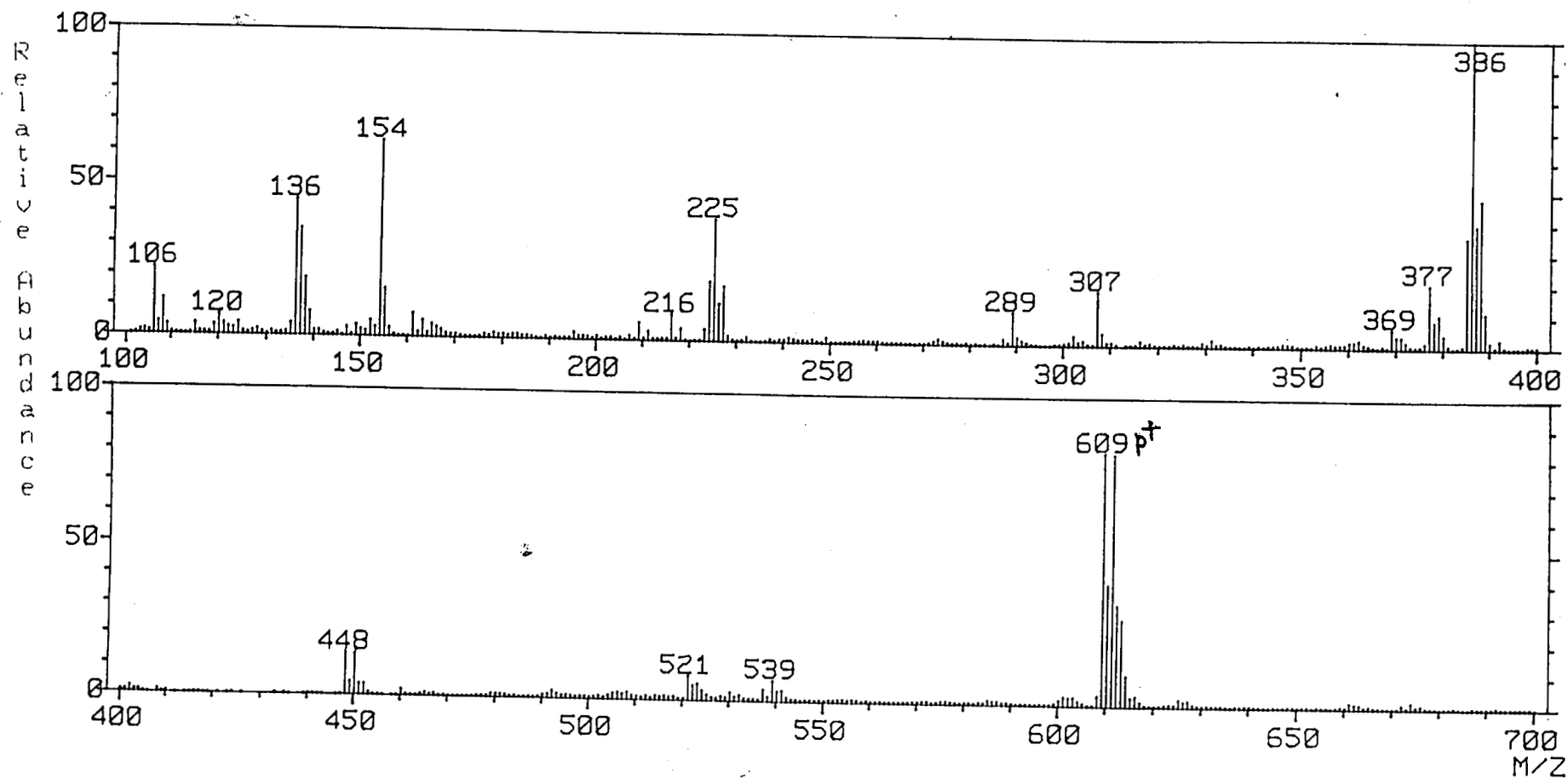
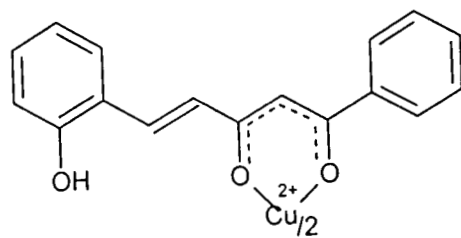
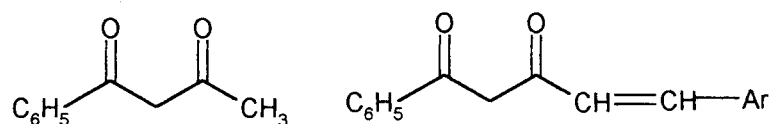


Fig. 4.20. Mass spectrum of copper(II) complex of 4g

by esr spectra^{135,136} and to compare the results with that of benzoylacetone and thereby to gain some information regarding the influence of extended conjugation in the nature of Cu–O bonds.



The esr spectra of typical copper(II) complexes of 5-aryl-1-phenyl pentanoids (**4a**) are given in figure 4.21. The g_{\parallel} and g_{\perp} values calculated are 2.2496 and 2.0484 respectively and the A_{\parallel} and A_{\perp} values are $155 \times 10^4 \text{ cm}^{-1}$ and $22 \times 10^4 \text{ cm}^{-1}$. The g_{\parallel} value is higher than that observed for the corresponding 6-arylhexanoids (chapter 2 Table 2.14). Compared to **2a**, **4a** is more conjugated and hence the g_{\parallel} value should be lower for **2a**. This may probably due to the lack of coplanarity of the system because of the pressure of phenyl groups on both sides that restrict the delocalisation of the π electrons.

Thermal decomposition studies of 5-aryl-1-phenyl-1-pentene 1,3-diones and their metal complexes

Thermogravimetric Analysis **4c** and its Cu(II), Ni(II), Co(II) and Fe(III) complexes were investigated and their datas are given in this part. Thermal decomposition datas are compared and the kinetic parameters for each stage was

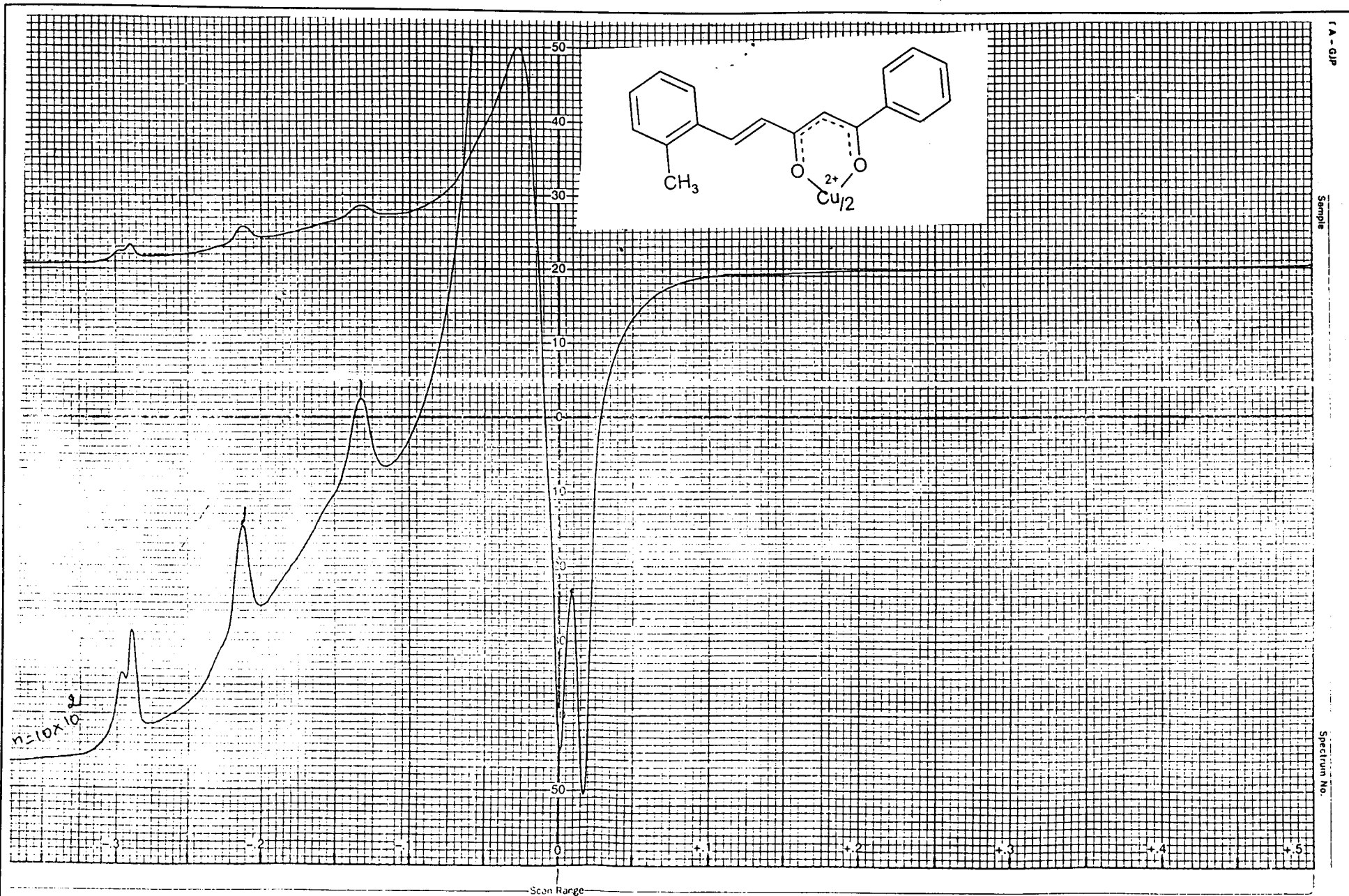
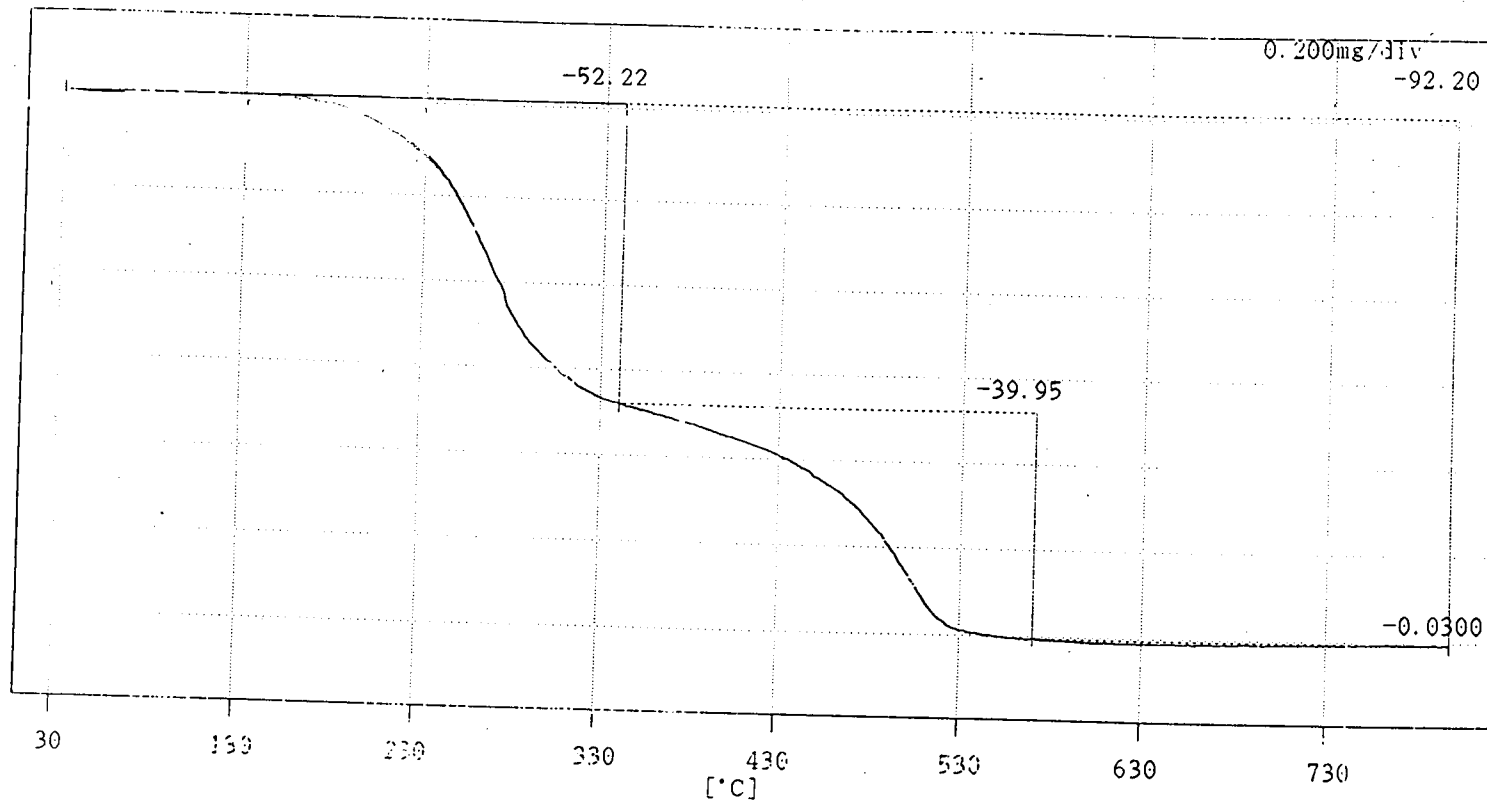
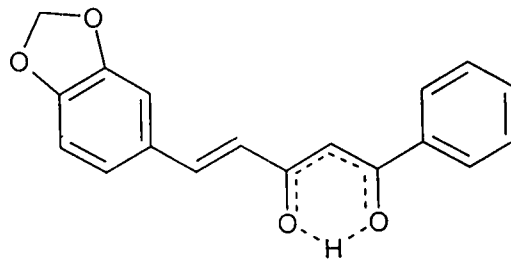


Fig. 4.21. Esr spectra of copper(II) complex of 4a

evaluated based on the three non-mechanistic equations. The order of the reaction was determined. The correlation coefficient (r) were computed by the weighted Least Square Method (LSM) by using these non-mechanistic equations and these are tabulated.

Thermal Analysis: The thermogram (Fig. 4.22) of **4c** shows a two stage decomposition pattern. For 1st stage decomposition the temperature ranges in TG are between 415-613° K with a peak temperature of 543 K. The 2nd stage decomposition range is from 623-853° K with a peak temperature of 783° K. The mass loss from TG and theoretical values are in good agreement (Table 4.14).

The order of the reaction was found to be unity. The kinetic parameters E , A , ΔS and correlation coefficient (r) were calculated for both stages by using the non mechanistic expressions and are given in table 4.15.



[WEIGHT] ---Ti (°C)---Tf (°C)---Wt. Change (%)---

Fig. 4.22, Thermogram of 4c

TABLE 4.14

Thermal decomposition data of the 5-aryl-1-phenyl-4-pentene-1,3-diones and its Cu(II), Ni(II), Co(II) and Fe(III) complexes

Compound/ Complexes (Molecular mass)	Temp. ranges in TG (K)	Peak Temp. (K)	Mass Loss %		Pyrolysis %	Final Product
			TG	Theo- retical		
4c = HL, C ₁₈ H ₄ O ₄ (294)	415-613	543	52.22	54.42	100	--
	623-853	783	39.95	45.15		
CuL ₂ (649.54)	520-1071	583	81.59	87.76	87	CuO
NiL ₂ (680.69)	393-593	543	22.67	23.88	89	NiO
	594-733	673	54.63	64.57		
CoL ₂ (H ₂ O) ₂ 680.93	473-630	523	25.12	26.86	88.22	Co ₃ O ₄
	640-763	703	58.87	58.45		
FeL ₃ (934.85)	473-618	533	21.43	20.11	83	Fe ₂ O ₃
	623-745	683	63.46	62.68		

Thermal Analysis of Metal Complexes

(a) Cu(II) complex of 4c (CuL₂)

Thermograms of the copper(II) complexes shows a single stage decomposition pattern (Figure 4.23). The temperatures ranges in TG is (520-1071° K) with a peak temperature of 583° K. The end product appears to be CuO as the mass loss from the TG curves agree well with the theoretical value (Table 4.14). The kinetic parameters were calculated for the order = 1 and are given in table 4.15.

TABLE 4.15

Kinetic parameters for the decomposition of 4c and their metal complexes

Compound/ Complexes	Equation	E kCal mol ⁻¹	log A s ⁻¹	ΔS kcal deg ⁻¹ mol ⁻¹	Correlation coefficient (r)
4c = HL, C ₁₈ H ₄ O ₄ 1 st Stage	CR	12.54	2.46	-48.44	0.991
	MT	14.26	6.37	-30.55	0.991
	HM	18.01	4.90	-37.28	0.995
2 nd stage	CR	66.1	16.47	14.93	0.986
	MT	67.60	19.72	29.81	0.988
	HM	70.81	17.81	21.04	0.984
(C ₁₈ H ₁₃ O ₄) ₂ Cu Single stage	CR	41.04	13.27	0.857	0.929
	MT	49.23	19.59	29.80	0.923
	HM	54.05	18.43	24.46	0.928
1 st stage (C ₁₈ H ₁₃ O ₄) ₂ Ni	CR	9.21	0.94	-55.43	0.990
	MT	11.60	5.20	-35.90	0.989
	HM	13.66	2.96	-46.17	0.992
2 nd stage	CR	63.30	18.47	24.39	0.963
	MT	64.40	21.59	38.64	0.966
	HM	64.66	18.90	26.35	0.958
1 st stage (C ₁₈ H ₁₃ O ₄) ₂ Co(H ₂ O) ₂	CR	15.46	3.94	-41.60	0.994
	MT	15.61	6.70	-28.97	0.995
	HM	17.33	4.75	-37.89	0.995
2 nd stage	CR	61.31	17.06	17.83	0.998
	MT	92.92	26.37	60.42	0.983
	HM	65.01	18.22	23.15	0.997
(C ₁₈ H ₁₃ O ₄)Fe 1 st stage	CR	13.02	2.80	-46.86	0.989
	MT	13.17	5.60	-34.03	0.992
	HM	15.15	3.73	-42.59	0.990
2 nd stage	CR	70.48	20.46	33.45	0.990
	MT	71.63	23.62	47.92	0.991
	HM	74.33	21.69	39.07	0.989

CR = Coats-Redfern; MT = MacCallum-Tanner; HM – Horowitz Metzger

(b) Ni(II) complex of 4c (NiL₂)

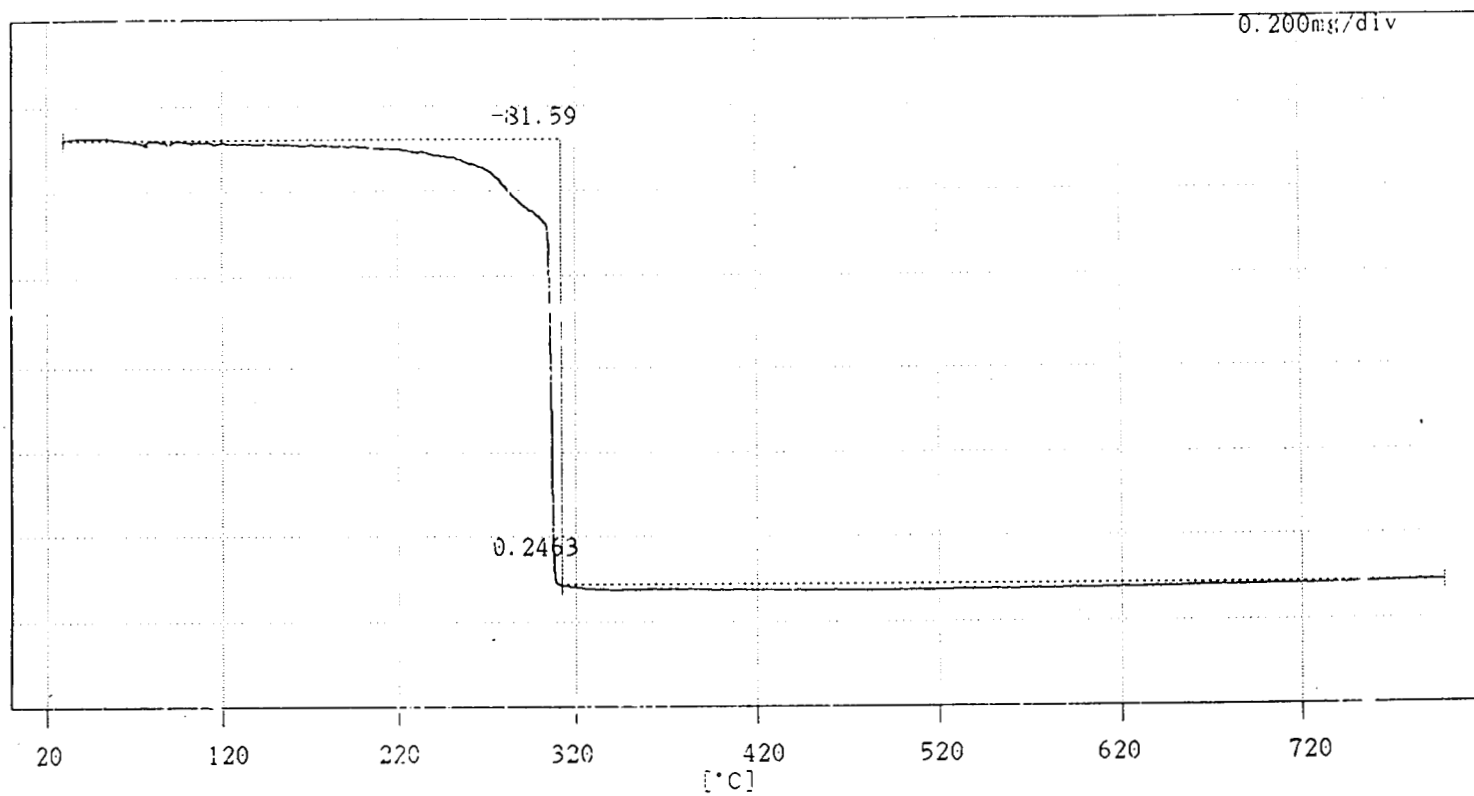
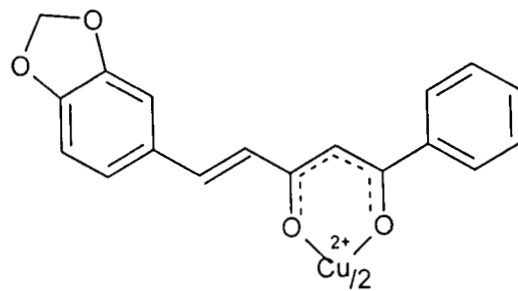
The thermal decomposition of nickel(II) follows a two stage pattern (Figure 4.24). The temperature range in the 1st stage decomposition is (393-593° K) with a peak temperature of 543° K. The 2nd stage decomposition has a range of (594-733° K) with a peak temperature of 673° K. The end product appears to be NiO as the mass loss from TG is in agreement with the theoretical value (Table 4.14). The kinetic parameters were calculated for both stages and given in Table 4.15.

(c) Cobalt(II) complex of 4c [(CoL₂(H₂O)₂]

The thermogram of the cobalt(II) complexes displayed a double stage decomposition pattern (Fig. 4.25). The 1st stage decomposition is from (473-630° K) with a peak temperature of 523° K. The 2nd stage decomposition ranges (640-763° K) with a peak temperature of 703° K. The end product appears to be Co₃O₄ since the mass loss from the TG curve agrees well with the theoretical value. Mass loss corresponding to the elimination of the coordinated water molecule is evident from the observed mass loss in 1st stage (Table 4.14). The kinetic parameters for the two stages of decomposition are given in table 4.15.

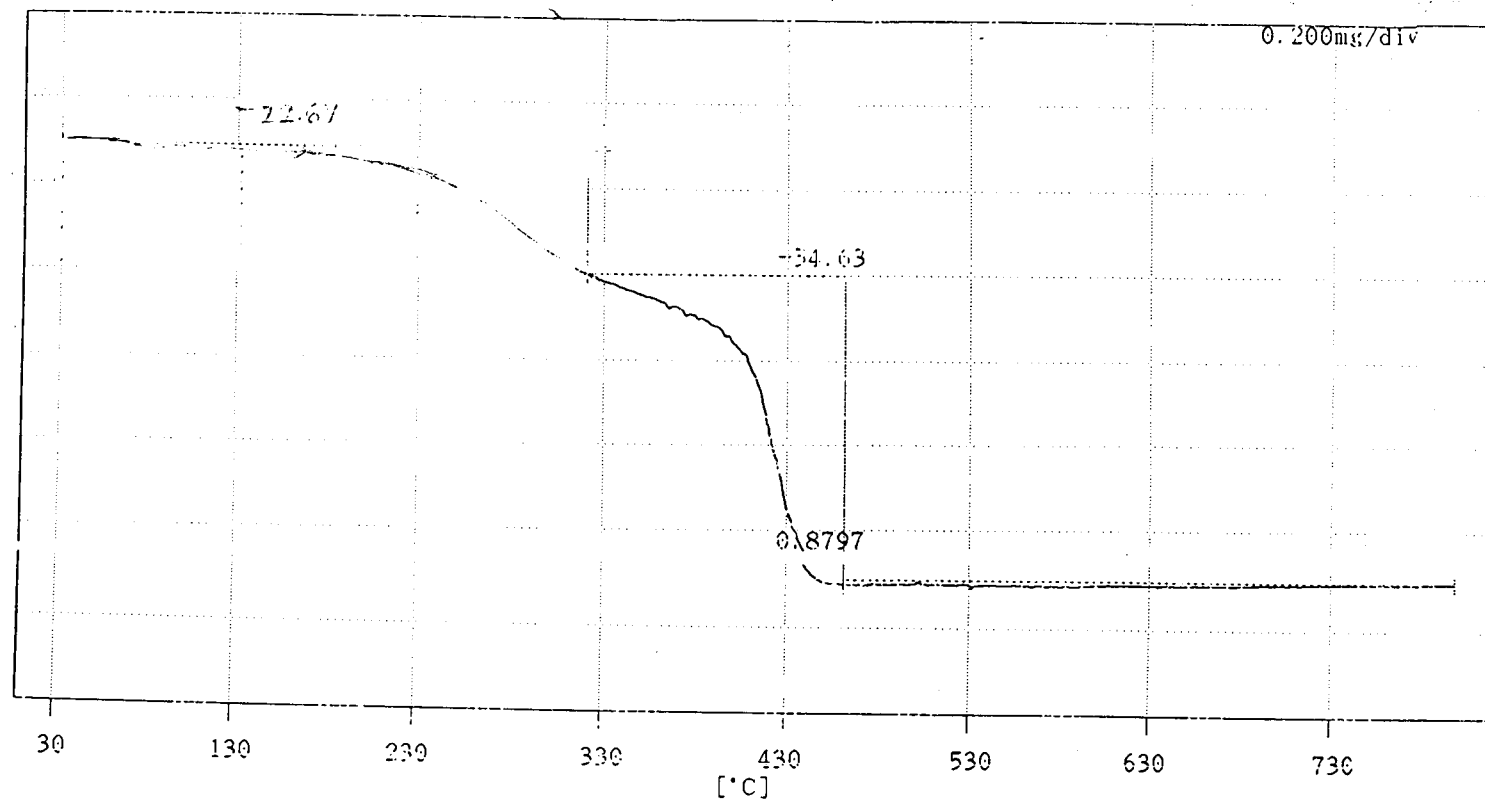
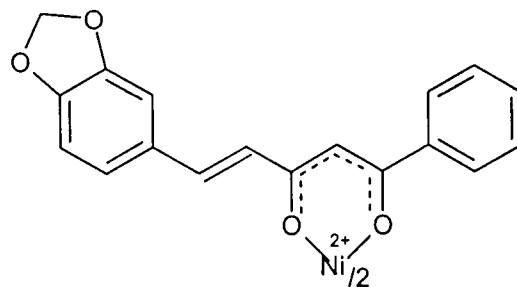
(d) Fe(III) complex of 4c (FeL₃)

The Thermal Analysis curve for FeL₃ complexes are given in figure 4.26. The compound shows a double stage decomposition pattern. The 1st stage ranges



[WEIGHT] -----Ti (°C)-----Tf (°C)-----Wt. Change (%)-----

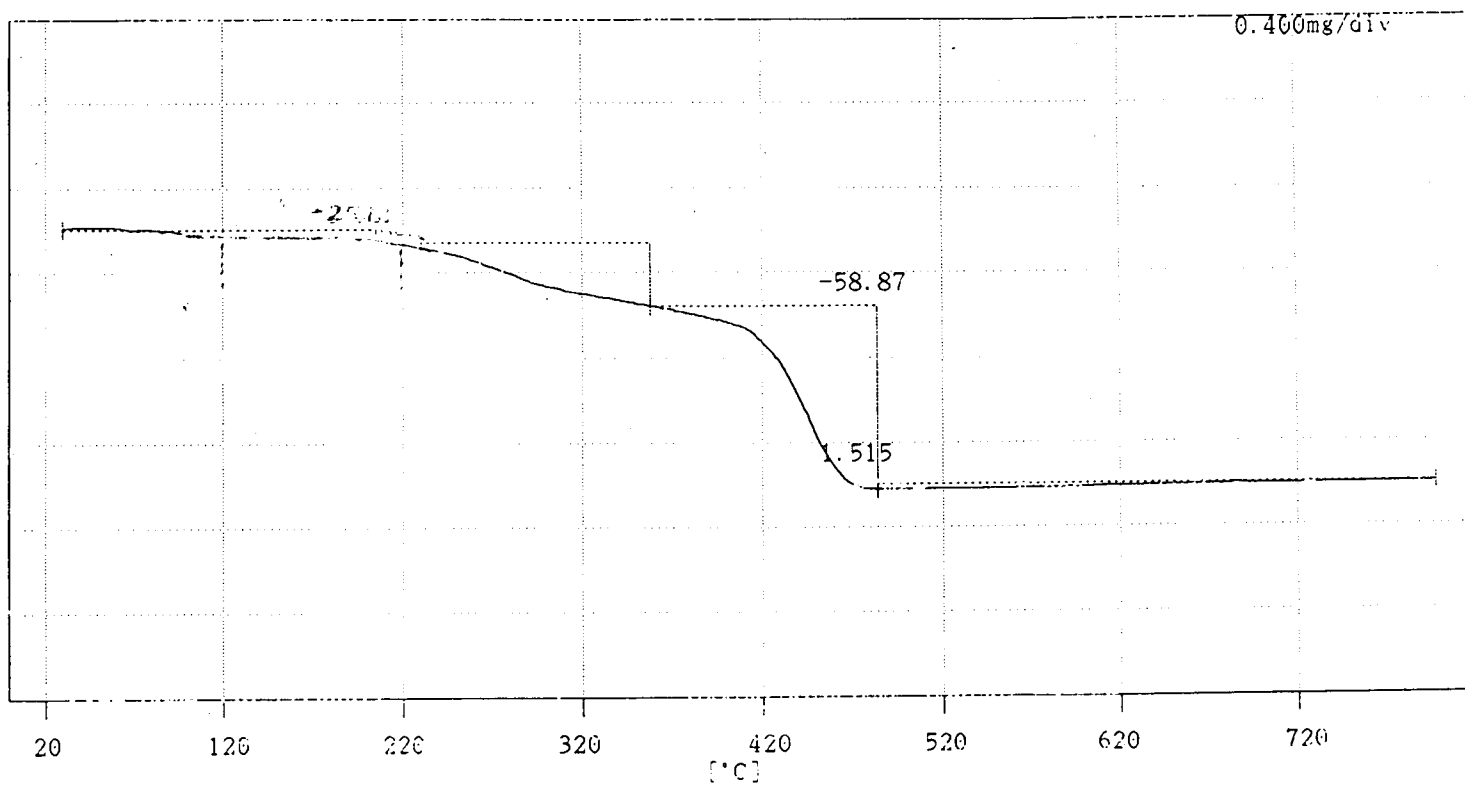
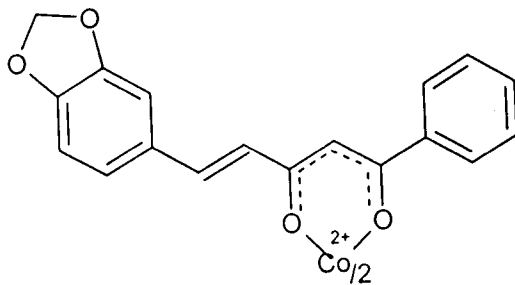
Fig. 4.23. Thermogram of Cu(II) complex of 4c



[WEIGHT] -----Ti (°C)-----Tf (°C)-----Wt. Change (%)-----

Fig. 4.24: Thermogram of Ni(II) complex of 4c

236



[WEIGHT] ---T_i (°C)---T_f (°C)---Wt. Change (%)---

Fig. 4.25 Thermogram of Co(II) complex of 4c

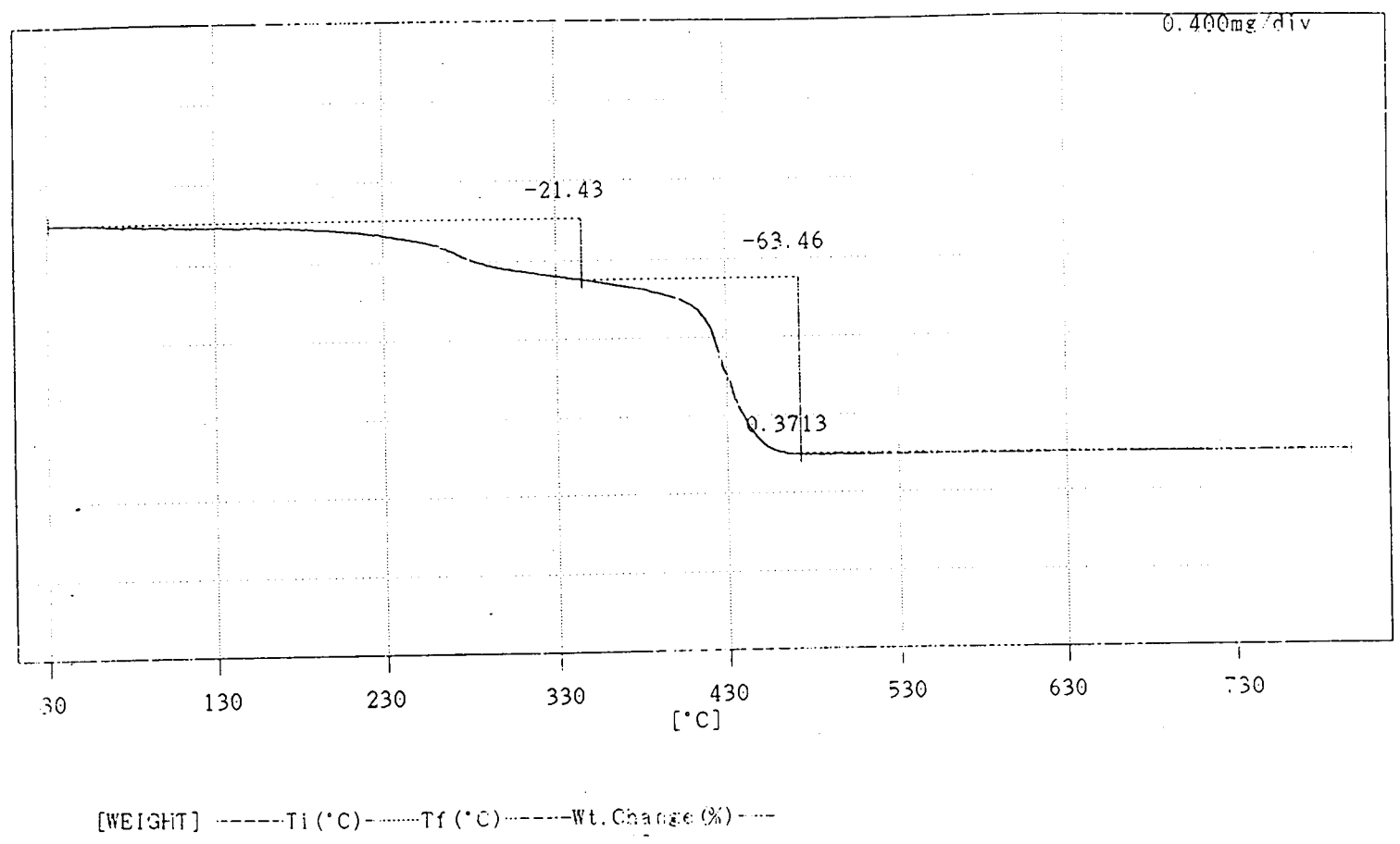
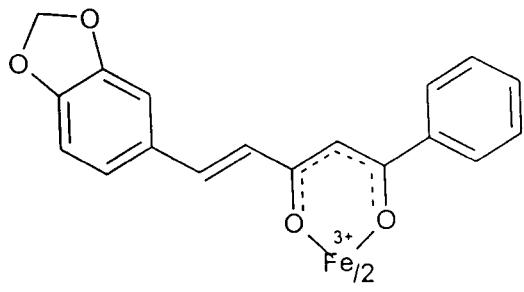


Fig. 4.2.6. Thermogram of Fe(III) complex of 4c

232

between (473-618° K) with a peak temperature of 533° K. The 2nd stage decomposition starts with 628° K and ends by 745° K with a peak maximum of 683°K. The end product seems to be Fe₂O₃ since the mass loss from the TG curve agrees well with the theoretical value (Table 4.14). The kinetic parameters activation were calculated by using non-mechanistic equations and are given in table 4.15.

Biological Studies

As the compounds considered in the present investigation are structurally related to Curcuminoids, some of the biological activities of these compounds were also studied. The results of fungicidal and bactericidal activities of the 5-aryl-1-phenyl-4-pentenoids and their typical metal complexes are discussed below.

The organisms used for studying the antifungal activity are *Aspergillus niger*, *Aspergillus parasiticus*, *Candida albicans* and *Rhizopus oryzae*. The organism selected for antibacterial study was *Staphylococcus aureus*. The cup-plate technique was employed for antifungal activity and 'disk diffusion technique'^{163,164} for antibacterial activity as discussed in chapter 2. The media used, their composition and the method of detecting the antimicrobial activity are same as in chapter 2.

Results and Discussion

The results of antifungal activities of the 5-aryl-1-phenyl-4-pentanoids are given in table 4.16 and their typical metal complexes in table 2. The data revealed that some of the compounds possess antifungal activity comparable to that of the drug "Nistatine". Among the compounds **4f** and **4g** were found to be highly active against all the four fungal strains studied. In both these compounds an OH group is present in the ortho position of the aryl ring. Thus it can be stated that presence of

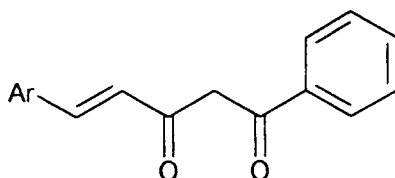
OH group in the aryl ring of these unsaturated 1,3-diketones is a structural requirement for their biological activities.

In the case of 5-aryl-1-phenyl-4-pentanoids, it is found that metal complexation increased the activity (Table 4.17). Copper(II) complexes are found to be highly active, particularly true in the case of **4f** and **4g**. It is to be again pointed out that in these complexes also the OH group of **4f** and **4g** remains free. The OH group on the aryl ring facilitates the antifungal activity of the compounds.

In the case of antibacterial activity preliminary studies on some of the 5-aryl-1-phenyl-4-pentanoids and their complexes revealed that none of them showed significant activity against *Styphylococcus aureus*.

TABLE 4.16

Antifungal Activity of 5-aryl-1-phenyl-4-pentene-1,3-dione compounds

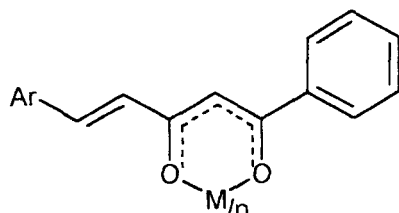


Compound		Diameter of the zone of inhibition (mm)			
No.*	Ar	<i>Aspergillus niger</i>	<i>Aspergillus parasiticus</i>	<i>Rhizopus oryzae</i>	<i>Candida albicans</i>
3b	Cinnamyl	10	10	10	10
3c	naphthyl	10	10	10	10
3d	furyl	12	12	12	12
4a	2-methyl phenyl	10	10	10	10
4b	4-ethoxy phenyl	10	10	10	10
4c	(3,4-dioxymethylene) phenyl	12	10	10	10
4d	(4-dimethylamino) phenyl	11	10	10	10
4e	4-nitrophenyl	15	20	10	10
4f	2-hydroxy naphthyl	18	14	16	20
4g	2-hydroxy phenyl	14	36	14	11

*The numbers are according to name of compounds in respective chapters given before.

TABLE 4.17

**Antifungal Activity of metal complexes of
5-aryl-1-phenyl-4-pentene-1,3-diones**



$n = 2$ for $M = \text{Cu}^{+2}, \text{Ni}^{+2}, \text{Co}^{+2}$
and $n = 3$ for $M = \text{Fe}^{+3}$

Compound			Diameter of the zone of inhibition (mm)			
No.*	Ar	M	<i>Aspergillus niger</i>	<i>Aspergillus parasiticus</i>	<i>Rhizopus oryzae</i>	<i>Candida albicans</i>
3d	furyl	Cu	25	10	10	10
3d	furyl	Ni	14	12	10	10
3d	furyl	Co	14	12	10	10
3d	furyl	Fe	15	11	10	10
4d	(4-dimethyl-amino) phenyl	Cu	33	10	17	10
4d	(4-dimethyl-amino) phenyl	Ni	12	10	10	10
4d	(4-dimethyl-amino) phenyl	Co	14	10	10	10
4d	(4-dimethyl-amino) phenyl	Fe	12	10	10	10
4e	4-nitrophenyl	Cu	31	10	10	10
4e	4-nitrophenyl	Ni	12	10	10	10
4f	2-hydroxy naphthyl	Cu	24	18	16	14
4f	2-hydroxy naphthyl	Ni	18	12	14	14

4f	2-hydroxy naphthyl	Co	18	12	12	14
4f	2-hydroxy naphthyl	Fe	18	12	14	14
4g	2-hydroxy phenyl	Cu	25	12	12	14
4g	2-hydroxy phenyl	Ni	12	11	12	11
4g	2-hydroxy phenyl	Co	14	12	12	11
4g	2-hydroxy phenyl	Fe	14	12	12	14

DMSO	10	10	10	10
Nistatine	12	12	11	12

*The numbers are according to name of compounds in respective chapters given before.

PART III

REFERENCES

1. A Werner, Chem. Ber., **34**, 2584 (1901).
2. Metal 1,3-diketonates and allied derivatives, R.C. Malhotra, D.P. Gaur, R. Bohra, Academic, New York, 1978.
3. J. Emsley, Structure and Bonding, 1984, **57**, 147.
4. G. Allen and R.A. Dwek, J. Chem. Soc., 1966, **B**, 161.
5. C. Reichardt, Angew. Chem., Int. Edn. Engl., 1965, **1**, 29.
6. V. Gutman, Angew. Chem., Int. Edn., Engl., 1970, **9**, 843.
7. A. Combes, Am. Chem., **12**, 199 (1887).
8. G.T. Morgan and F.H. Bustcall, "Inorganic Chemistry – A Survey of Modern Developments", W. Heffer and Sons Ltd., Cambridge, England, 1936.
9. K. Nakamoto and A.E. Martell, J. Chem. Phys., **32**, 588 (1960).
10. M. Mikami, I. Nakagawa and T. Shimanouchi, Spectrochim. Acta, **23A**, 1037 (1967).

11. J.D. Park, H.A. Brown and J.R. Lachen, *J. Am. Chem. Soc.*, **75**, 4753 (1953) and references therein.
12. J.L. Burdett and M.T. Rogers, *J. Am. Chem. Soc.*, **86**, 2105 (1964).
13. H. Koshimura, J. Saito and T. Okunho, *Bull. Chem. Soc., Japan*, **46**, 632 (1923).
14. E. Uhlemann and W.W. Sachan, *I. Anorg. Allg. Chem.*, 342, **41** (1966).
15. G. Klose, Ph. Thomas E. Uhlemann and J. Marki, *Tetrahedron*, **22**, 2695 (1966).
16. G.T. Morgan and H.W. Moss, *Proc. Chem. Soc.*, 1914, **29**, 471.
17. G.T. Morgan and H.W. Moss, *J. Chem. Soc.*, 1914, **105**, 189.
18. N.V. Sidgwick, "The chemical elements and their compounds", Oxford University Press, London, 1950.
19. N.V. Sidgwick and F.M. Brewer, *J. Chem. Soc.*, 1925, **127**, 2389.
20. R.E. Sievers and J.J. Fostman, *Coord. Chem. Rev.*, 1971, **6**, 331.
21. J.P. Facklet Jr., *Progr. Inorg. Chem.* 1966, **7**, 361.
22. John Emsley, "The Composition, Structure and Hydrogen bonding of the β -diketones", p.148.

23. S. Kawaguchi, 'Variety in Coordination Modes of Ligands in Metal Complexes', Springer-Verlag, New York, 1988.
24. L.M. Jackman and B.C. Large, *Tetrahedron*, 1977, **33**, 2737.
25. M. Raban, E. Noe and G. Yamamoto, *J. Am. Chem. Soc.*, 1977, **99**, 657.
26. D.W. Thompson, 'Structure and Bonding', 1970, **9**, 27.
27. K.C. Joshi and V.N. Pathak, *Coord. Chem. Rev.*, 1977, **22**, 37.
28. D. St., C. Black in 'Comprehensive Coordination Chemistry', G. Wilkinson (ed. in chief), Vol. 2. Pergamon, New York, 1987.
29. M. Raban and E. Noe, *J. Am. Chem. Soc.*, 1974, **96**, 6184.
30. S. Kawaguchi, 'Variety in Coordination Modes of Ligands in Metal Complexes', Springer-Verlag, New York, 1988.
31. S. Koda, S. Ooi, H. Kuroya, K. Isobe, Y. Nakamura and S. Kawaguchi, *Chem. Comm.*, 1971, 1321.
32. R.E. Cramer, S.W. Cramer, K.F. Cramer, M.A. Chudyk and K. Seff, *Inorg. Chem.*, 1977, **16**, 219.
33. D. Gibson, *Coord. Chem. Rev.*, 1969, **4**, 225.
34. G.T. Behnke and K. Nakamoto, *Inorg. Chem.*, 1967, **6**, 440.
35. Y. Nakamura and K. Nakamoto, *Inorg. Chem.*, 1975, **14**, 63.

36. A. Robson and M.R. Truter, *J. Chem. Soc.*, 1965, 630.
37. N. Yanase, Y. Nakamura and S. Kawaguchi, *Inorg. Chem.*, 1980, **19**, 1575.
38. S. Okeya, Y. Nakamura, T. Hiromote and S. Kawaguchi, *Bull. Chem. Soc., Japan*, 1982, **55**, 477.
39. Acly and French, *J. Am. Chem. Soc.*, **49** (1927) 847.
40. Morton and Victor, *J. Chem. Soc.*, (1926) 706.
41. French and Lowry, *Proc. R. Soc.*, (1924) 489.
42. Haszeldine, Musgrave, Smith and Turton, *J. Chem. Soc.*, 1951, 609.
43. Marini and Dubois, *C.r. hebd. Seanc. Acad. Sci., Paris*, **236** (1953) 90.
44. Bulford, Martell and Calvin, *J. Inorg. Ind. Chem.*, **2** (1956) 11.
45. Holm and Cotton, *J. Am. Chem. Soc.*, **80** (1958) 5628.
46. Barnum, *J. Inorg. Nucl. Chem.*, **21** (1961) 221.
47. S. Bratoz, D. Hadzi and G. Rossmly, *Trans. Faraday Soc.*, 1956, **52**, 464.
48. A. Novak, 'Structure and Bonding', 1974, **18**, 177.
49. S. Kato, H. Kato and K. Fukni, *J. Am. Chem. Soc.*, 1977, **99**, 684.
50. James U. Lowe, Jr. and Lloyd N. Ferguson, *Journal of Am. Chem. Society*, 3000 (1965).

51. K. Nakamoto and H. Ogueshi, *J. Chem. Phys.* 1966, **45**, 3113.
52. L.J. Bellamy, "The Infrared Spectra of Complex Molecules", Vol. 2, Chapman and Hall, London, 1980.
53. Fackler, J.P., Jr., Cotton F.A., Barnum D.W., *Inorg. Chem.*, **2**, 97 (1963).
54. Forster, L.S., *J. Am. Chem. Soc.*, **86**, 3001 (1964).
55. Holm, R.H., Cotton, F.A., *J. Am. Chem. Soc.*, **79**, 3318 (1957).
56. Collman, J.P., in *Reactions of Coordinated Ligands*, American Chemical Society, Washington D.C., p.78 (1963).
57. Foy, R.C., Piper, T.S., *Inorg. Chem.*, **3**, 348 (1964).
58. Fay, R.C., Piper, T.S., *J. Am. Chem. Soc.*, **84**, 2303 (1962).
59. Mcrady, M.M., Tobias, S.T., *J. Am. Chem. Soc.*, **87**, 1909 (1965).
60. Kennedy, M., Private Communication.
61. Hertner, R.E., *Chem. In. London*, 1397 (1963).
62. J. Emsley, "The Composition, Structure and Hydrogen bonding of the β -diketones", p.160.
63. Nonhebel, D.C., *Tetrahedron* **24**, 1869 (1968).
64. Shapet Ko, N.N., *Org. Mag. Res.*, **5**, 215 (1973).

65. Isaacson, A.D., Morokuma, K., *J. Am. Chem.* 80, **97**, 4453 (1975).
66. Engelbretson, G.R., Rundle, R.E., *J. Am. Chem.*, 80, **86**, 574 (1964).
67. Williams, D.E., Dumke, W.L., Rundle, R.E., *Acta. Cryst.* **15**, 627 (1962).
68. Norrestam, R., Von Glehm, M., Wachtmeister, C.A., *Acta Chem. Scand.* **28B**, 1149 (1974).
69. Chaston, S.H.H., Livingstone, S.E., Lockver, T.N. and Shannon, J.S., *Aust. J. Chem.*, 1965, **18**, 1539.
70. Reid, A.F., Shannon, J.S., Swan, J.M. and Warles P.C., *Aust. J. Chem.*, 1965, **18**, 173.
71. Shannon, J.S. and Swan, J.M. *Chem. Commun.* 1965, No. 3, **33**.
72. Mass spectroscopy and structures of Metal acetylacetonate vapours by C.G. Macdonald and J.S. Shamon, p.1545, 1965.
73. Mc Lafferty, F.W., in "Mass spectroscopy of organic ions" (Ed. F.W. Mc Lafferty), p.309 (Academic Press, London, 1963).
74. C.C. Huickley, *J. Am. Chem. Soc.*, 91, 5160 (1969); *J. Org. Chem.*, **35**, 2834 (1970).
75. A. Lempicki and H. Samelsin, *Phys. Lett.*, **4**, 133 (1963).
76. E.J. Schmitschek, *Appl. Phys. Lett.*, **3**, 117 (1963).

77. G.A. Crosby, R.E. Whan and R.M. Abre, *J. Chem. Phys.*, **32**, 614 (1960).
78. W. Merty, *Physiol., Rev.*, **49**, 163 (1969).
79. V.S. Govindarajan, 'CRC Critical Reviews in Food Science and Nutrition', 1980, **12**, 199.
80. (a) J.J. Wenzel, E.J. Williams, C. Haltiwanger, R. Eservers, *Polyhedron*, **4**(3) (1985) 369; (b) R.E. Seivers, J.E. Saldowska, *Science* **201** (1978) 217.
81. (a) K.E. Laintz, E. Tachikawa, *Anal. Chem.* **66** (1994) 2190; (b) S. Wang, E. Eishwani, C.M. Wai, *Anal. Chem.*, **67** (1995) 919; (c) J. Wang, W.D. Marshall, *Anal. Chem.* **66** (1994) 1658.
82. (a) T.A. Heiner, S.T. D'Arcangelis, F. Farzad, J.M. Stipkala, G.J. Meyer, *Inorg. Chem.* **35** (1996) 5319; (b) B.N. Hansen, B.M. Hybertsen, R.M. Berkley, R.E. Sievers, *Chem. Mater.* **4** (1992) 749; (c) R. M'Hamdi, J.F. Bocquet, K. Chhor, C.J. Pommur, *Supercrit. fluids* **4** (1992) 55; (d) T.T. Kodas, P.B. Comita, *Acc. Chem. Res.* **23** (1990) 188; (e) H. Willushl, J. Wselsum, V. Zumbach, P. Albers, K. Scabold, *J. Phys. Chem.* **370** (1994) 2242.
83. (a) W.R. Cullen, E.B. Wickenheiser, *J. Organomet. Chem.* **370** (1989) 141; (b) C.D. Rao, H.F. Rase, *Ind. Engg. Chem. Prod. Res. Dev.* **20** (1981) 95.
84. F.D. Lewis, A.M. Miller, G.D. Salvi, *Inorg. Chem.* **34** (1995) 3173.

85. S. Peter, US Patent 4892718 (9 Jan. 1990).
86. N.R. Farnsworth in 'Bioactive Compounds from Plants', Wiley, Chinchester, 154.
87. P.N.V. Kurup, "Handbook of Medicinal Plants", Vol. I, Central Council for Research in Indian Medicine and Homoeopathy, New Delhi, 1977, H.P.T. Ammon and M.A. Wahl, *Planta Med.*, 1991, 57, 1.
88. H.H. Tonnesen, Ph.D.Thesis, Institute of Pharmacy, University of Oslo, Oslo, Norway, 1986.
89. O.P. Sharma, *Biochem. Pharmacol.*, 1976, **25**, 1811.
90. Mohd Ali, A. Bagate and J. Gupta, *Indian J. Chem.*, **34B**, 884.
91. A. Banerjee and S.S. Nigam, *Indian J. Med. Res.*, 1978, **68**, 864, 195.
92. R.C. Srimal and B.N. Dhawan, *J. Pharm. Pharmacol.*, 1973, 25, 447.
93. H.H. Tonnesen, M. Arvid and J. Karlsen, *Acta. Chem.Scand.* 1982, **B36**, 475.
94. R.S. Ramsewak, D.L. Dewitt, M.G. Nair, *Phytomedicine* 2000, **7(4)**, 303.
95. C: Ramaprasad and M. Sirsi, *J. Sci. Indust. Res.*, 1956, **156**, 239.
96. A. Mukhopadhyaya, N. Basu, N. Ghatak and P.K. Gujzal, *Agents Actions*, 1982, **12**, 508.

97. A.J. Ruby, G. Kuttan, K.V.D. Babu, K.N.Rajasekharan and R. Kuttan, *Cancer Lett.*, 1995, **94**(1), 79.
98. T. Tanaka, H. Makita, M. Obnishi, Y. Hirose, A. Wang, H. Mori and K.Satoh, *Cancer Res.*, 1994, **54**, 4653.
99. M.T. Hayang, W. Way, R. Lou, T. Ferraso, K. Reuhl, H. New Mark and A.H.Conney, *Proc. Am. Assoc. Cancer Res.*, 1993, **34**, 555.
100. R.J. Anto, J.George, K.V.D. Babu, K.N. Rajasekharan and R. Kuttan, *Mutat. Res.*, 1996, **370**(2), 127.
101. M.T. Huang, Z.Y. Wang, C.A. Geogiadis, J.D. Lasken and A.H. Conney, *Carcinogenesis*, 1992, **13**, 2183.
102. M.T. Haung, R.C. Smart, C.Q. Wong and A.H.Conney, *Cancer Res.*, 1988, **48**, 5941.
103. P. Venugopalan and K. Krishnankutty, *J. Indian Chem. Soc.*, 1998, **75**, 98; *Asian J. Chem.*, 1998, **10**, 453; *Synth. React. Inorg. Met.-Org. Chem.*, 1998, **28**(8), 1313.
104. Arthur I. Vogel, "A Text Book of Practical Organic Chemistry", Longman Group Ltd., London, 3rd Edition, 1975.
105. A. Weissberger, P.S. Proskaner, J.A., Hiddick and B.E. Troops, 'Organic Solvents', Vol. 3, Interscience, New York, 1956.

106. J. Basset, R.C. Denney, G.H. Jeffery and J. Mandhane (eds.), 'Vogel's Text Book of Quantitative Inorganic Analysis', 4th edn., ELBS and Longman, London, 1978.
107. W.J. Geary, *Coord. Chem. Rev.*, 1971, 7, 81.
108. G. Allen and R.A. Dwek. *J. Chem. Soc.*, 1966B, 161.
109. C. Reichardt, *Angew. Chem., Int. Edn. Engl.*, 1965, 1, 29.
110. V. Gutman, *Angew. Chem., Int. Edn. Engl.*, 1970, 9, 843.
111. T.G. Grasselli, 'CRC Atlas of Spectral data and Physical constants of organic compounds', CRC Press, Ohio, 1973.
112. H. Irving and R.J.P. Williams, *J.Chem.Soc.*, 1953, 3192.
113. J.E. Huheey, 'Inorganic Chemistry', 3rd edn., Harper and Row, Cambridge, 1983.
114. R.S. Drago, 'Physical Methods in Inorganic Chemistry', Reinhold, New York, 1965.
115. D. Sutton, 'Electronic Spectra of Transition Metal Complexes', McGraw Hill, New York, 1968.
116. R.L. Luntvedt and H.F. Holttydaw, Jr., *J. Am. Chem. Soc.*, 1966, 88, 2713.
117. R.H. Holm and F.A. Cotton, *J. Am. Chem. Soc.*, 1945, 67, 2003.

118. J. Emsley, Chem. Soc. Rev., 1963, **85**, 1696.
119. L.M. Jackman and S. Sternball, "Application of NMR spectroscopy in organic chemistry", 2nd edn., Pergamon, New York, 1969.
120. J.H. Bowie, D.H. Williams, S.D. Lawerson and G. Schroll, J. Org. Chem., 1966, **31**, 1384.
121. C.G. Macdonald and J.S. Shannon, Ast. J. Chem., 1966, **19**, 1545.
122. B. Bock, K. Flatau, H. Junge, M.K. Lur and H. Musso, Angrew. Chem., Int. Edn. Engl., 1971, **10**, 225.
123. C.N.R. Rao, 'Chemical applications of Infrared spectroscopy', Academic, London, 1963.
124. K. Nakamoto, 'Infra red spectra of Inorganic and Coordination Compounds', 4th edn., Wiley, New York, 1976.
125. H.F. Holtzdan, Jr., R.L. Lintvedt, H.F. Baumgartin, R.G. Parker, M.M. Bursey and P.F. Rogerson, J. Am. Chem. Soc., 1969, **91**, 3774.
126. C. Reichert and J.B. Westmore, Inorg. Chem., 1969, **8**, 1012, Canad. J. Chem., 1970, **48**, 3213.
127. C. Reichert, G.M. Bancroft and J.B. Westmore, Canad. J. Chem., 1970, **48**, 1362.

128. P.J.Ronghley and D.A. Whitins, J. Chem. Soc., Perkins Trans. I, 2379 (1973).
129. V.S. Govindarajan, "CRC Critical Reviews in Food Science and Nutrition", 1980, **12**, 199.
130. Venugopalan, P., Ph.D. Thesis, 1997.
131. H.A. Kuska and M.T. Rogers, J. Chem. Phys., **43**, 1744 (1965).
132. H.A. Kuska, M.T. Rogers and R.E. Drullinger, J. Phys. Chem., **71**, 109 (1967).
133. T.C.Chiany, J.Chem. Phys., **48**, 1814 (1968).
134. T.R. Reddy and R. Srinivasan, Proc. Indian Acad. Sci. Sect. A, **65**, 368 (1967).
135. B.R. Mc Garvey, J. Chem. Phys. 1956, **60**, 71.
136. A. Abragam and B. Bleaney, 'Electron Paramagnetic Resonance of Transition Metal Ions', Oxford University Press, Oxford, 1970.
137. R.C. Mackenzie, Thermochem Acta, 1984, **73**, 249.
138. W. Wendlandt, J. Chem. Educ., 1972, **49**, A571, A623.
139. C. Duval, Inorganic Thermogravimetric Analysis (2nd edn.), Elsevier, Amsterdam, 1963.

140. R.C. Mackenzie, *Talanta*, **16**, 1227 (1969).
141. A.W. Coats and J.P. Redfern, *Nature*, London, 1964, **68**, 201.
142. H.H. Horowitz and G. Metzger, *Anal. Chem.*, **35** (1963) 1464.
143. J.R. Mac Callum and J. Tanner, *Eur. Polym. J.*, 1970, **6**, 1033.
144. Lukaszewski, G.M. and J.P. Redfern, *Lab. Pract.*, **10**, 721 (1961).
145. Peter J. Haines, 'Thermal methods of Analysis, Principles, Application and Problems', Blackie Academic and Professional, an imprint of Chapman and Hall, 1975.
146. W.W. Wendlant, *Thermal methods of Analysis*, 2nd Edn., Elsevier, Amsterdam 1963.
147. K.J. Eisentraut and R.E. Sievers, *J. Inorg. Nucl. Chem.*, **29**, 1931 (1967).
148. P.M. Madhusudanan, P.N. Krishnan Nambisan and C.G. Ramachandran Nair, *Thermochimica Acta*, **9** (1974), 149-155.
149. D.A. Young, *Decomposition of Solids*, Pergamon Press, 1966.
150. J. Sestak, V. Satava and W.W. Wendlandt, *Thermochim Acta*, 1973, **7**, 333.
151. A.K. Galway, "Chemistry of Solids", Science Paperbacks and Chapman and Hall Ltd., London, 1967.
152. Sergio Dilli and Kevin Robards, *Aust. J. Chem.*, 1979, **32**, 277-84.

153. Berg, E.W. and Truemper, J.T., 1960, **64**, 487.
154. M.A. El-Sayed and M.L. Bhaumik, *J. Chem. Phys.*, **39** (1963) 2391.
155. Shigemetsu, M. Matsui and K. Utsonomiya, *Bull. Chem. Soc. Japan*, **41**, 763 (1968).
156. Shigematsu, M. Matsui and K. Utsomiya, *Bull. Chem. Soc. Japan*, **42**, 1278 (1969).
157. K. Utsunomiya, *Bull. Chem. Soc. Japan*, **44**, 2688 (1971).
158. R. Belcher, C.R. Cranley, J.R. Majer, N.I. Stephen and P.C. Uden, *Anal. Chem. Acta*, **50**, 423 (1970).
159. R.E. Siemens and J.W. Cannolly, *Inorg. Synth.* 1272 (1970).
160. *Manual of Clinical Microbiology* (Sixth edn.) Editor in Chief: Patrick R. Murray, ASM Press, Washington DC.
161. C. Viel, P. Hampe, R. Dorme and J.Y. Hernette, *Chem. Abstr.* **70**, 57346 (1969).
162. R. Anantha Narayan and C.K. Jayaram Panikkar, 'A Textbook of Microbiology', 1996, Orient Longman Ltd., Hyderabad.
163. C.H. Collins and P.M. Lyne, 'Microbiological Methods', Butterworths, London, 1970, 414.

164. L.M. Prescott, J.P. Harley and D.A. Klein, 'Microbiology', WCB, Pubuque (USA), 1990, 250.
165. O.P. Sharma, *Biochem. Pharmacol.*, 1976, **25**, 1811.
166. Mohd Ali, A. Bagate and J. Gupta, *Indian J. Chem.*, **34B**, 884.
167. A. Banerjee and S.S. Nigam, *Indian J. Med. Res.*, 1978, **68**, 864, 195.
168. R.C. Srimal and B.N. Dhawan, *J. Pharm. Pharmacol.*, 1973, **25**, 447.
169. H.H. Tonnesen, M. Arvid and J. Karlsen, *Acta. Chem. Scan.* 1982, **B36**, 475.
170. R.S. Ramsewak, D.L. Dewitt, M.G. Nair, *Phytomedicine* 2000, **7(4)**, 303.
171. C. Ramaprasad and M. Sirsi, *J. Sci. Indust. Res.*, 1956, **156**, 239.
172. A. Mukhopadhyay, N. Basu, N. Ghatak and P.K. Gujzal, *Agents Actions*, 1982, **12**, 508.
173. A.J. Ruby, G. Kuttan, K.V.D. Babu, K.N. Rajasekharan and R. Kuttan, *Cancer Lett.*, 195, **94(1)**, 79.
174. T. Tanaka, H. Makita, M. Obnishi, Y. Hisose, A. Wang, H. Mori and K. Satoh, *Cancer Res.*, 1994, **54**, 4653.
175. M.T. Hayng, W. May, R. Lou, T. Ferraro, K. Renhl, H. New Mark and A.H. Conney, *Proc. Am. Assoc. Cancer Res.*, 1993, **34**, 355.

176. R.J. Anto, J. George, K.V.D. Babu, K.N. Rajasekharan and R. Kuttan; Mutat. Res., 1996, 370(2), 127.
177. M.T. Haung, Z.Y. Wang, C.A. Geogiadis, J.D. Lasken and A.H. Conney. Carcinogenesis, 1992, 13, 2183.
178. Y. Shung, H. Shung, T. Shizuko and Kazuo, Yakugaku Zasshi, 1995, 12(4), 269.
179. P. Cleason, P. Tuchinda and V. Rentrakul, J. Indian Chem. Soc., 71, 509 (1994).

NB 2997